# The Involvement of Histone Acetylation and Nuclear Matrix Structure in Gene Expression

By

**Virginia Ann Spencer**

A Thesis Submitted to the Faculty of Graduate Studies
in Partial Fulfillment of the Requirements for the Degree of Doctor of Philosophy
Department of Biochemistry and Medical Genetics
University of Manitoba

THE UNIVERSITY OF MANITOBA

FACULTY OF GRADUATE STUDIES

*****

COPYRIGHT PERMISSION PAGE

**The Involvement of Histone Acetylation and Nuclear Matrix Structure in Gene Expression**

**BY**

**Virginia Ann Spencer**

**A Thesis/Practicum submitted to the Faculty of Graduate Studies of The University of Manitoba in partial fulfillment of the requirements of the degree of**

**DOCTOR OF PHILOSOPHY**

**Acknowledgements**

I would first like to thank my supervisor Dr. Jim Davie. Dr. Davie has been an excellent mentor. Throughout the years he has consistently challenged me in body and soul. He has driven me to work and think hard and, because of this, I feel I am strongly prepared for a career in scientific research. I am truly grateful for all the help and guidance I have received from Dr. Davie and I wish him the best.

Secondly, I would like to thank Dr. Leigh Murphy. Dr. Murphy has been a very supportive, optimistic and encouraging person to me over the years. Her support and encouragement have sustained me through hard times and given me the strength to continue my graduate work.

Thirdly, I would like to thank my mother. She too has offered strong words of encouragement and has supported me throughout my graduate studies. I truly appreciate and will never forget this.

I am also thankful to my advisory committee members Dr. Steven Pind, Dr. Barb Triggs-Raine and Dr. Janice Dodd for their constructive and valuable comments and their encouragement throughout my doctoral studies. I would also like to thank Dr. David Bazett-Jones for enthusiastically accepting to be my external examiner and for assisting in my thesis review and examination process. I would also like to thank the members of Dr. Davie's lab for their help over the past few years.

Lastly, I would like to thank my husband and best-friend, Oscar, for his love and support over the past few years. His passion for life has taught me to enjoy the simplest pleasures of life and to never lose sight of those who matter the most.

## TABLE OF CONTENTS


LIST OF FIGURES ..... VIII

LIST OF TABLES ..... XII

LIST OF ABBREVIATIONS ..... XIII

ABSTRACT ..... XIX

INTRODUCTION ..... 1

THE NUCLEOSOME ..... 4

LINKER HISTONES ..... 6

HISTONE VARIANTS ..... 7

THE EFFECT OF TRANSCRIPTION ON THE NUCLEOSOME ..... 8

THE CHROMATIN FIBER ..... 16

*The Structure of Transcriptionally Active and Inactive Chromatin* ..... *16*

*Function of the Core Histone N terminal Tails in Chromatin Structure* ..... *16*

*The Interaction of the Core Histone N Terminal Histone Tails with Proteins* ..... *18*

*Influence of Salt on Chromatin Structure* ..... *19*

*The Effect of $Mg^{2+}$ vs $Na^{+}$ on Chromatin Structure* ..... *20*

THE HISTONE CODE ..... 21

HISTONE ACETYLATION ..... 26

*Histone Acetyltransferases* ..... *26*

*Histone Deacetylases* ..... *31*

HISTONE ACETYLATION AND CHROMATIN SALT SOLUBILITY ..... 34

HISTONE ACETYLATION AND EPIGENETIC INHERITANCE ..... 36

HISTONE ACETYLATION & NUCLEOSOME STRUCTURE ..... 37

THE EFFECT OF HISTONE ACETYLATION ON INTERACTIONS OF HISTONES WITH NON-NUCLEOSOMAL PROTEINS ..... 37

THE EFFECT OF HISTONE ACETYLTRANSFERASES ON THE PROPERTIES OF TRANSCRIPTION FACTORS ..... 38

THE EFFECT OF HISTONE ACETYLATION ON HIGHER ORDER CHROMATIN STRUCTURE ..... 39

THE EFFECT OF HISTONE ACETYLATION ON H1-MEDIATED CHROMATIN CONDENSATION ..... 40

CLASS I & CLASS II HISTONE ACETYLATION AND TRANSCRIPTION ..... 41

HISTONE ACETYLATION & THE CHROMATIN IMMUNOPRECIPITATION ASSAY (CHIP) ..... 43

GLOBAL HISTONE ACETYLATION ..... 43

PROMOTER LOCALIZED HISTONE ACETYLATION ..... 47

*Promoter-Targeted Histone Acetylation Occurs in Estrogen-Mediated Transcriptional Activation* ..... *49*

*Promoter-Targeted Histone Acetylation Assists Chromatin Remodeling* ..... *54*

*The Function of Promoter-Targeted Histone Acetylation* ..... *56*

HISTONE ACETYLATION ALONG THE CODING REGION ..... 58

*The Function of Histone Acetylation Along the Coding Region* ..... *58*

THE β-GLOBIN LOOP DOMAIN ..... 62

HISTONE ACETYLTRANSFERASES & DEACETYLASES IN CANCER DEVELOPMENT 64

HISTONE DEACETYLASE INHIBITORS ..... 68

*Effect of TSA and Sodium Butyrate on Gene Transcription* ..... *70*

*TSA- and Butyrate-DNA Response Elements* ..... *74*

*TSA and Sodium Butyrate Mediate Transcription Through Sp1 and Sp3* ..... 75
*Histone Deacetylase Inhibitors and Cancer Treatment* ..... 77

THE NUCLEAR MATRIX ..... 81

*Nuclear Matrix Composition* ..... 83
*Nuclear Processes Associated with the Nuclear Matrix* ..... 84
*The Influence of Cell and Nuclear Structure on DNA Organization and Gene Expression* ..... 85
*Alterations in the Structure of DNA in Cancer Cells* ..... 86
*Nuclear Matrix Proteins in Cancer* ..... 87

BREAST CANCER ..... 89

BREAST CANCER PROGRESSION CELL MODELS ..... 90

ESTROGEN ACTION ..... 92

MECHANISM OF ER-ALPHA TRANSCRIPTIONAL ACTIVATION ..... 94

ESTROGEN INDUCES THE TRANSCRIPTIONAL ACTIVATION OF THE pS2 GENE ..... 97

STRUCTURE OF THE pS2 GENE ..... 99

**OBJECTIVES, RATIONALE & HYPOTHESES** ..... 101

**PART I: DYNAMICALLY ACETYLATED HISTONES ARE ASSOCIATED WITH TRANSCRIPTIONALLY ACTIVE AND COMPETENT, BUT NOT INACTIVE, GENES IN THE AVIAN ADULT β-GLOBIN GENE DOMAIN** ..... 106

1.0 METHODS ..... 108

*1.1 Treatment of Adult White Leghorn Chickens with Phenylhydrazine* ..... 108
*1.2 Harvesting of Immature Erythrocytes from Adult White Leghorn Chickens* ..... 108

*1.3 Treatment of Chicken Immature Erythrocytes with 10 mM Sodium Butyrate.. 109*
*1.4 Fractionation of Erythrocyte Chromatin Fractionation ..... 109*
*1.5 DNA Preparation and Hybridization ..... 113*
*1.6 Isolation of Histones ..... 114*
*1.7 Acid-Urea-Triton X-100 Polyacrylamide Gel Electrophoresis ..... 114*
*1.8 Detection of Proteins with Coomassie Brilliant Blue ..... 115*
*1.9 Detection of Acetylated Histones by Immunoblotting ..... 116*
*1.10 Isolation and Fragmentation of PE-Associated Chromatin ..... 118*
*1.11 Assessment of the Efficiency of Formaldehyde-Mediated Chromatin Release from the PE ..... 119*
*1.12 Immunoprecipitation of PE Chromatin Fragments Associated with Acetylated H3 and H4 ..... 120*

**2.0 RESULTS ..... 122**

*2.1 Rate of Deacetylation of Hyperacetylated H2B, H3 and H4 ..... 122*
*2.2 Effect of Histone Deacetylation on 0.15 M NaCl Solubility of Globin Chromatin Fragments ..... 124*
*2.3 Effect of Histone Deacetylation on $MgCl_2$ Solubility of Globin Chromatin Fragments ..... 127*
*2.4 Transcriptionally Active $\beta^A$-globin and Transcriptionally Competent $\varepsilon$-Globin Genes Associated with Fraction PE are Bound to Hyperacetylated Histones H3 and H4 ..... 131*

**3.0 DISCUSSION ..... 135**

**PART II: ASSOCIATION OF DYNAMICALLY HYPERACETYLATED HISTONES WITH THE ESTROGEN-RESPONSIVE PS2 GENE ..... 137**

**1.0 METHODS ..... 139**

*1.1 Cell Maintenance* ..... *139*

*1.2 Cell Treatments* ..... *139*

1.2.1 Formaldehyde Cross-linking of MCF-7 Cells ..... 140

1.2.2 Estradiol Treatment of MCF-7 Cells ..... 141

1.2.3 Sodium Butyrate or Trichostatin A Treatment of MCF-7 Cells ..... 141

1.2.4 DRB Treatment of MCF-7 Cells ..... 142

*1.3 Determination of pS2, GAPDH and Cyclophilin 33 RNA Levels in MCF-7 Cells* ..... *143*

1.3.1 Isolation of Total RNA from MCF-7 Cells ..... 143

1.3.2 Conversion of Total RNA into cDNA Using Reverse Transcriptase (RT) ..... 143

1.3.3 Detection of pS2, GAPDH and Cyclophilin 33 cDNA in MCF-7 ..... 144

*1.4 Extraction and Analysis of Hyperacetylated Histones in MCF-7 Cells* ..... *145*

*1.5 Assessment of ERα, HDAC 1, Sp1 and Sp3 Levels in Sodium Butyrate and TSA-Treated MCF-7 Cells* ..... *146*

1.5.1 Preparation of Total Cell Lysates from MCF-7 Cells ..... 146

1.5.2 SDS-Polyacrylamide Gel Electrophoresis (SDS-PAGE) of Total Cell Lysates from MCF-7 Cells ..... 146

1.5.3 Immunoblot Analysis of ERα, HDAC1, Sp1 and Sp3 Levels in Cell Lysates from Treated MCF-7 Cells ..... 147

*1.6 Isolation of DNA Sequences Associated with Hyperacetylated H3 and H4 Histones and HDAC1 in MCF-7 Cells by the ChIP Assay* ..... *149*

1.6.1 Preparation of MCF-7 Cell Lysate for Immunoprecipitation ..... 149

1.6.2 Immunoprecipitation of DNA sequences Associated with Hyperacetylated H3 and H4 Histones and HDAC1 ..... 150

1.6.3 Quantitative PCR on Input and Immunoprecipitated DNA Sequences... 151

**2.0 RESULTS ..... 153**

*2.1 Sodium Butyrate and TSA Induce Histone Hyperacetylation in MCF-7 Cells 153*

*2.2 Estradiol Increases while DRB, Sodium Butyrate and TSA Decrease pS2 RNA Levels in MCF-7 Cells ..... 155*

*2.3 Sodium Butyrate and TSA do not Alter ERα, HDAC1, HDAC2 or Sp1 Levels in MCF-7 Cells ..... 158*

*2.4 Sodium Butyrate and TSA Decrease HDAC1 Levels Associated with the pS2 Promoter ..... 160*

*2.5 Estradiol, Sodium Butyrate and TSA Induce Histone H3 and H4 Hyperacetylation Along the pS2 Gene in MCF-7 Cells ..... 162*

*2.6 Exposure to Estradiol Induces Histone Hyperacetylation Along the pS2 Promoter and Exon 3 that is Sustained for up to 180 min. ..... 165*

*2.7 Estradiol Induces Histone Acetylation Along the pS2 Promoter and Exon 3 Even When Transcription is Inhibited ..... 168*

*2.8 Estradiol-Induced Histone Acetylation Along the pS2 Promoter and Exon 3 is a Dynamic Process ..... 173*

**3.0 DISCUSSION ..... 177**

**PART III: ANALYSIS OF DNA-ASSOCIATED NUCLEAR MATRIX PROTEIN PROFILES FROM CELL LINES COMPOSING A MODEL OF BREAST CANCER DISEASE DEVELOPMENT ..... 194**

**1.0 METHODS ..... 196**

*1.1 Cell Maintenance ..... 196*

*1.2 Isolation and Analysis of Nuclear Matrix Proteins ..... 196*

*1.3 Isolation and Analysis of Proteins Cross-Linked to DNA in situ. ..... 199*

*1.4 Two-dimensional Gel Electrophoresis of Nuclear Matrix and Cross-linked Proteins.* ..... *200*

**2.0 RESULTS** ..... **202**

*2.1 The Majority of NM and DNA-Cross-linked Proteins are Common Among Cell Lines in a Breast Cancer Cell Line Progression Series* ..... *202*

*2.2 A Small Number of NM and DNA-Cross-Linked Proteins are Differentially Expressed Among Cell Lines in a Breast Cancer Cell Line Progression Series* ..... *204*

**3.0 DISCUSSION** ..... **210**

**SUMMARY** ..... **212**

**FUTURE DIRECTIONS** ..... **217**

**NOVEL FINDINGS** ..... **220**

**REFERENCES** ..... **222**

## List of Figures


| Figure | | Page |
|---|---|---|
| Figure 1. | Diagrammatic Representation of the Several Orders of Chromatin Compaction in an Interphase Cell. | 2 |
| Figure 2. | Diagrammatic Representation of a Chromosome Territory and Transcription Sites in a Thin Section of an Interphase Nucleus. | 3 |
| Figure 3. | Schematic Representation of the Histone Octamer Showing the Positioning of the Core Histones Relative to the Dyad Axis of Symmetry. | 4 |
| Figure 4. | Diagram Showing an Interaction Between the Globular Domains of Two Histones. | 5 |
| Figure 5. | Dr. Studitsky's Hypothetical Model for Transcription by RNA Polymerase II Through a Nucleosome | 9 |
| Figure 6. | Three-Dimensional Reconstruction Calculated from Nucleosomes Associated with Transcriptionally Active Genes. | 12 |
| Figure 7. | Dr. van Holde's Hypothetical Model for Transcription by RNA Polymerase II Through a Nucleosome.. | 15 |
| Figure 8. | Post-Translational Modifications Along the Core Histone N Terminal Tails. | 25 |
| Figure 9. | Proposed Model for the Effect of Estradiol on the Distribution of Histone Acetyltransferases and Histone Deacetylases in Human Breast Cancer Cells. | 51 |
| Figure 10. | Diagram of the Chicken Erythrocyte β-globin Domain Showing Regions of DNase I Sensitivity and Insensitivity. | 63 |

Figure 11. Electron Micrograph Showing the Ultrastructure of the Nuclear Matrix from a CaSki Cell. ..... 82

Figure 12. Schematic Diagram of the pS2 Gene and Promoter. ..... 100

Figure 13. NaCl Chromatin Fractionation Protocol. ..... 110

Figure 14. $MgCl_2$ Chromatin Fractionation Protocol. ..... 112

Figure 15. Immunoblot Analyses of H3, H4 and H2B Deacetylation..... 123

Figure 16. $\beta^A$-globin and ε-globin Chromatin Fragments Lose Solubility in 150 mM NaCl at Similar Rates Following Removal of Sodium Butyrate. ..... 126

Figure 17. Histone Hyperacetylation Influences the $MgCl_2$ Solubility of Transcriptionally Active $\beta^A$-globin and Competent ε-globin Mononucleosomes. ..... 129

Figure 18. $\beta^A$-globin and ε-globin Chromatin Fragments Lose Solubility in 3 mM $MgCl_2$ at Similar Rates Following Removal of Sodium Butyrate..... 130

Figure 19. $\beta^A$-globin and ε-globin Chromatin Fragments Associated with the Low Salt Insoluble Chromatin Fraction are Bound to Hyperacetylated H3 and H4... 134

Figure 20. Diagram of Estradiol (E2), HDAC Inhibitor and DRB Treatment Conditions for MCF-7 Cells. ..... 140

Figure 21. Treatment of MCF-7 Human Breast Cancer Cells with 10 mM Sodium Butyrate for 2 h or 500 ng/ml TSA for 2 h Induces Histone Hyperacetylation. ..... 154

Figure 22. Effect of Estradiol, Sodium Butyrate and TSA on pS2 Total RNA Levels in MCF-7 Cells..... 156

Figure 23. The Effect of Estradiol, Sodium Butyrate and DRB on pS2 Total RNA Levels in MCF-7 Cells..... 157

Figure 24. E2, Sodium Butyrate and TSA do not Significantly Alter ERα, HDAC1, HDAC2 or Sp1 Protein Levels in MCF-7 Cells. ..... 159

Figure 25. The Effect of TSA and Sodium Butyrate on the Association of HDAC1 with the pS2 Promoter, Exon 2 and Exon 3 in MCF-7 Cells..... 161

Figure 26. The Effect of Sodium Butyrate, TSA and Estradiol (E2) on H3 and H4 Acetylation Along the pS2 Promoter, Exon 2 and Exon 3 Gene Sequences in MCF-7 Cells..... 164

Figure 27. The Effects of Estradiol on H3 and H4 Acetylation Along the pS2 Promoter and Exon 3 Gene Sequences.. ..... 167

Figure 28. The Effects of Estradiol and DRB on H3 and H4 Acetylation Along the pS2 Promoter and Exon 3 Gene Sequences. ..... 172

Figure 29. The Effect of Sodium Butyrate (But), Estradiol (E2) and DRB on H3 and H4 Acetylation Along the pS2 Promoter and Exon 3..... 175

Figure 30. Nuclear Matrix Extraction Method. ..... 198

Figure 31. Cisplatin Protein-DNA Cross-linking Protocol. ..... 201

Figure 32. Nuclear Matrix Proteins of MCF-7, MIII, LCC1, and LCC2 Breast Cancer Cell Lines.. ..... 203

Figure 33. Proteins Cross-linked to DNA by Cisplatin *in situ* in MCF-7, MIII, LCC1, and LCC2 Breast Cancer Cell Lines. ..... 206

Figure 34. A Schematic Representation of the Two Dimension Gel Pattern Data of DNA Cross-linked and Non-DNA Cross-linked Proteins from MCF-7, MIII, LCC1, and LCC2 Breast Cancer Cell Lines. ..... 207

Figure 35. Summary Model Describing the Role of Histone Acetylation and Nuclear Matrix Structure in Transcription as they Relate to the Results Presented in this Thesis. ..... 215

## List of Tables


| Table | | Page |
|---|---|---|
| Table 1. | Assessment of the Efficiency of Formaldehyde-Mediated Chromatin Fragment Removal from the PE of Sodium Butyrate-Treated Chicken Immature Erythrocytes as Determined by $A_{260}$ Measurements. | 132 |
| Table 2. | Assessment of the Efficiency of Formaldehyde-Mediated Chromatin Fragment Removal from the PE of Sodium Butyrate-Treated Chicken Immature Erythrocytes as Determined by the Diphenylamine Assay. | 132 |
| Table 3. | Primers Used to Assess pS2, GAPDH and Cyclophilin RNA Levels as well as the Levels of pS2 Promoter and Exon 3 in ChIP DNA. | 145 |
| Table 4. | Relative Levels of DNA Cross-linked Nuclear Matrix Proteins in Two-Dimension Patterns of DNA Cross-linked Protein Preparations. | 208 |
| Table 5. | Relative Levels of Differentially Abundant DNA Cross-linked Proteins in Two-Dimension Patterns of DNA-Cross-linked Protein Preparations. | 209 |

## List of Abbreviations

| | |
|---|---|
| Å | Angstrom |
| $A_{260}$ | Absorbance at 260 nm |
| AUT | Acid-Urea-Triton X-100 |
| AF | Activation Function |
| ATP | Adenosine Triphosphate |
| Act1 | NF-Kappa B Activator 1 |
| Arp | Actin-Related Protein |
| AML | Acute Myeloid Leukemia |
| APL | Acute Promyelocytic Leukemia |
| AIB1 | Amplified in Breast Cancer-1 |
| AP-1 | Activator Protein-1 |
| BbD | Barr Body Deficient |
| bp | Base Pair |
| BCoR | BCL-6 Interacting Corepressor |
| BRG | Brahma-Related Gene |
| Ca | Carbonic Anhydrase |
| CAPS | 3-(Cyclohexylamino)-1-Propanesulfonic Acid |
| CARM1 | Coactivator-Associated Arginine Methyltransferase |
| CBP | CREB-Binding Protein |
| cDNA | Complementary Deoxyribonucleic Acid |
| C/EBP | CCAAT/Enhancer-Binding Protein |
| CENP-A | Centromeric Protein A |
| ChIP | Chromatin Immunoprecipitation |
| CID | Centromere Identifier |
| CK2 | Casein Kinase 2 |
| cpm | Counts Per Minute |
| CREB | cAMP Response Element-Binding Protein |
| CSK | Cytoskeleton |
| CtBP | C-Terminal-Binding Protein |

| | |
|---|---|
| DMEM | Dulbecco's Modified Eagle Medium |
| DNA | Deoxyribonucleic Acid |
| DNase 1 | Deoxyribonuclease 1 |
| dNTP | Deoxyribonucleotide Triphosphate |
| DRB | 5,6-Dichlorobenzimidazole 1-b-D-Ribofuranoside |
| DRIP | Vitamin D(3) Receptor-Interacting Protein |
| DTT | Dithiothreitol |
| E1A | Early region 1A |
| E2 | Estradiol |
| ECL | Enhanced Chemiluminescence |
| ECM | Extracellular Matrix |
| EDTA | (Ethylenedinitrilo) tetraacetic acid |
| EGTA | [Ethylenebis (oxyethylenenitrilo)] tetraacetic acid |
| EGF | Epidermal Growth Factor |
| ERE | Estrogen Response Element |
| ERα | Estrogen Receptor Alpha |
| ERβ | Estrogen Receptor Beta |
| ERK | Extracellular Signal-Regulated Kinase |
| FBS | Fetal Bovine Serum |
| FACT | Facilitates Chromatin Transcription |
| FCS | Fetal Calf Serum |
| G1 | Gap 1 |
| G2 | Gap 2 |
| GCN-5 | General Control Nonderepressible-5 |
| GNAT | Gcn5-Related *N*-Acetyltransferase |
| GRIP-1 | Glucocorticoid Receptor Interacting Protein 1 |
| HAT | Histone Acetyltransferase |
| HAP | Hydroxyapatite |
| HBO | Histone Acetyltransferase Bound to ORC |
| HDA1 | Histone Deacetylase 1 |
| HDAC | Histone Deacetylase |

| | |
|---|---|
| HER2 | Human Epidermal Growth Factor Receptor 2 |
| HIV | Human Immunodeficiency Virus |
| HMG | High Mobility Group |
| hnRNP K | Heterogeneous nuclear ribonucleoprotein K |
| HSP 70 | Heat Shock Protein 70 |
| Htt | Huntingtin |
| ICI | Imperial Chemical Industries |
| INF | Interferon |
| IGFBP-3 | Insulin Growth Factor Binding Protein-3 |
| INO1 | Inositol 1-Phosphate Synthase |
| K8 | Cytokeratin 8 |
| K18 | Cytokeratin 18 |
| K19 | Cytokeratin 19 |
| kbp | Kilo Base Pair |
| kDa | Kilodalton |
| ORC | Origin Recognition Complex |
| M | Mitosis |
| MAP | Mitogen-Activated Protein |
| MAPK | Mitogen-Activated Protein Kinase |
| MAR | Matrix Attachment Region |
| MBD | Methyl-CpG-Binding Domain |
| MCF-7 | Michigan Cancer Foundation- Attempt 7 |
| MDa | Megadalton |
| MeCP | Methyl-CpG Binding Protein |
| Min. | Minutes |
| mM | Millimeter |
| MMLV | Moloney Murine Leukemia Virus |
| MNase | Micrococcal Nuclease |
| MOF | Males-Absent on the First |
| MOZ | Monocytic Leukemia Zinc Finger |
| MTA 1 | Metastatic Associated Protein 1 |

| | |
|---|---|
| MYST | MOZ, Ybf2/Sas3, Sas2, and TIP60 |
| NAD+ | Nicotinamide Adenine Dinucleotide |
| NCoA | Nuclear Receptor Coactivator |
| NCoR | Nuclear Receptor Corepressor |
| NF-Y | Nuclear Factor Y |
| nm | Nanometer |
| NM | Nuclear Matrix |
| NMP | Nuclear Matrix Protein |
| NuA3/4 | Nucleosomal acetyltransferase of histone H3/H4 |
| NuRD | Nucleosome Remodeling and Deacetylase Repressor |
| PAGE | Polyacrylamide Gel Electrophoresis |
| PBS | Phosphate Buffered Saline |
| PCAF | p300/CBP-Associated Factor |
| P/CIP | p300/CBP Interacting Protein |
| PCR | Polymerase Chain Reaction |
| PELP1 | Proline-, Glutamic Acid-, Leucine-Rich Protein 1 |
| PHO5 | Yeast Acid Phosphatase 5 |
| pI | Isoelectric Point |
| PIPES | Piperazine-N,N'-bis (2-ethanesulfonic acid) |
| PKC | Protein Kinase C |
| PLZF | Promyelocytic Leukemia Zinc Finger |
| PML | Promyelocytic Leukemia |
| PMSF | Phenylmethylsulfonyl Fluoride |
| Pol II | RNA polymerase II |
| PP1 | Protein Phosphatase Type 1 |
| PRF | Phenol Red Free |
| RA | Retinoic Acid |
| Rac3 | Retinoic Acid Coactivator 3 |
| RAR | Retinoic Acid Receptor |
| Rb | Retinoblastoma |
| RbAp | Rb-associated protein |

| | |
|---|---|
| RIPA | Radioimmunoprecipitation Buffer |
| RNA | Ribonucleic Acid |
| RNase | Ribonuclease |
| RSB | Reticulocyte Standard Buffer |
| RSC | Nucleosome Remodeling Complex |
| RT | Reverse Transcriptase |
| RXR | Retinoid X Receptor |
| S | Synthesis |
| SAGA | Spt-Ada-Gcn5-Acetyltransferase |
| SBF | Swi4-Swi6 Cell Cycle Box Binding Factor |
| SDC | Sodium Deoxycholate |
| SDS | Sodium Dodecyl Sulfate |
| Set1 | Suppressor of Variegation, Enhancer of Zeste and Trithorax 1 |
| Sir | Silent Information Regulator |
| SMRT | Silencing Mediator for Retinoic Acid and Thyroid Hormone Receptors |
| Snf1 | Sucrose non-fermenting 1 protein kinase |
| Sp1/Sp3 | Specificity Protein 1/3 |
| SRC-1 | Steroid receptor coactivator-1 |
| SRA | Steroid Receptor Co-activator |
| SWI/SNF | Switch/Sucrose Non-Fermentable |
| TAF | TBP Associated Factor |
| TBP | TATA Binding Protein |
| TE | Tris-EDTA |
| TEMED | N,N,N',N-tetramethylethylenediamine |
| TIF-1 | Transcriptional Intermediary Factor-1 |
| TIP60 | Tat-Interactive Protein |
| TGF | Transforming Growth Factor |
| TNM | Tris-NaCl-$MgCl_2$ Buffer |
| TPA | Phorbol 12-tetra-decanoate 13-acetate |
| TRAM | Thyroid Receptor Activator Molecule, |
| TRAP | Thyroid Hormone Receptor-Associated Protein |

| | |
|---|---|
| TRIS | Tris(hydroxylmethyl)aminomethane |
| TSA | Trichostatin A |
| TBS | Tris Buffered Saline |
| TTBS | Tris Buffered Saline with Tween 20 |
| UFD | Ubiquitin Fusion Degradation Protein 3 |
| µg | Microgram |
| µl | Microliter |
| UV | Ultraviolet |
| v | Volume |
| w | Weight |
| W&S | Wray and Stubblefield |
| XIST | X-Inactive Specific Transcript |
| XLP | Cross-Linked Protein |
| YY1 | Yin-Yang 1 |
| ZBP-89 | Zinc Finger Binding Protein-89 |

**Abstract**

The acetylation of specific lysine residues along the N terminal tails of histones H3 and H4 influences chromatin structure and plays an important yet undetermined role in transcription. Furthermore, changes in nuclear matrix composition, the component of the nucleus that influences nuclear shape, are thought to influence DNA organization and gene expression. The nuclear matrix is associated with the transcriptional machinery and is enriched in histone acetyltransferase and deacetylase activity. One of my aims was to determine if rapidly acetylated and deacetylated histones are associated with transcriptionally active, competent and/or inactive genes. By studying the salt solubility of chromatin fragments, we determined that expressed and competent chromatin is associated with rapidly acetylated histones while inactive chromatin is not. We also observed that the coding region of an active and competent gene in a nuclear fraction containing the nuclear matrix is bound to hyperacetylated H3 and H4. We also studied the effect of estrogen, as well as transcription and histone deacetylase inhibitors on H3 and H4 acetylation along the pS2 promoter, exon 2 and exon 3 in MCF-7 human breast cancer cells. We found that estradiol and histone deacetylase inhibitors induce histone acetylation along the promoter and coding regions of the pS2 gene and that dynamic histone acetylation takes place along these gene regions in the presence of a transcriptional inhibitor. This suggests that estrogen-induced histone acetylation occurs in the presence or absence of transcription and that exposure to E2 mediates the recruitment of histone acetyltransferases to the pS2 promoter and coding regions, thereby causing a change in the balance of histone acetyltransferases and deacetylases along these regions. The findings from these two studies suggest that histone acetylation may function in transcription by mediating the rapid and dynamic attachment of active and competent

chromatin to nuclear regions enriched in histone acetyltransferase and histone deacetylase activity such as the nuclear matrix. Lastly, we analysed total and DNA-associated nuclear matrix proteins from a panel of cell lines reflecting different stages of malignant breast cancer progression to determine if changes in DNA organization through changes in nuclear matrix structure are involved in breast cancer development. Specific changes in nuclear matrix proteins bound to nuclear DNA were identified, suggesting that breast cancer progression is accompanied by a reorganization of chromosomal domains which may lead to alterations in gene expression.

## Introduction

Nuclear DNA undergoes considerable levels of organization to ensure that a gene is transcribed in a specific and regulated manner (Figure 1). At the first level of DNA organization, DNA is packaged into chromatin fibers through its association with various proteins. These fibers associate with an insoluble, proteinaceous structure referred to as the nuclear matrix (NM) that organizes them into loop domains containing anywhere from one to several genes [1]. The chromatin fibers also fold up upon themselves in a specific manner and associate with other fibers, creating a complex maze through which transcription factors must travel to reach their target DNA sequence. Finally, during mitosis, the chromatin fiber becomes tightly folded into chromosome structures. On a larger scale, the nucleus organizes chromosomes into territories with the transcriptionally active genes located within regions of the territory that are easily accessible to transcription factors (Figure 2) [2,3].

The exact nature and type of events that influence DNA organization are not well defined. However, DNA is organized into loop domains through its association with the nuclear matrix, suggesting that nuclear matrix composition is one factor important in DNA organization [4-6]. Furthermore, the post-translational modification of specific chromatin proteins alters chromatin structure and, therefore, influences DNA organization. The purpose of this thesis is to present and discuss findings that further explain how alterations in chromatin and NM structure influence gene expression.

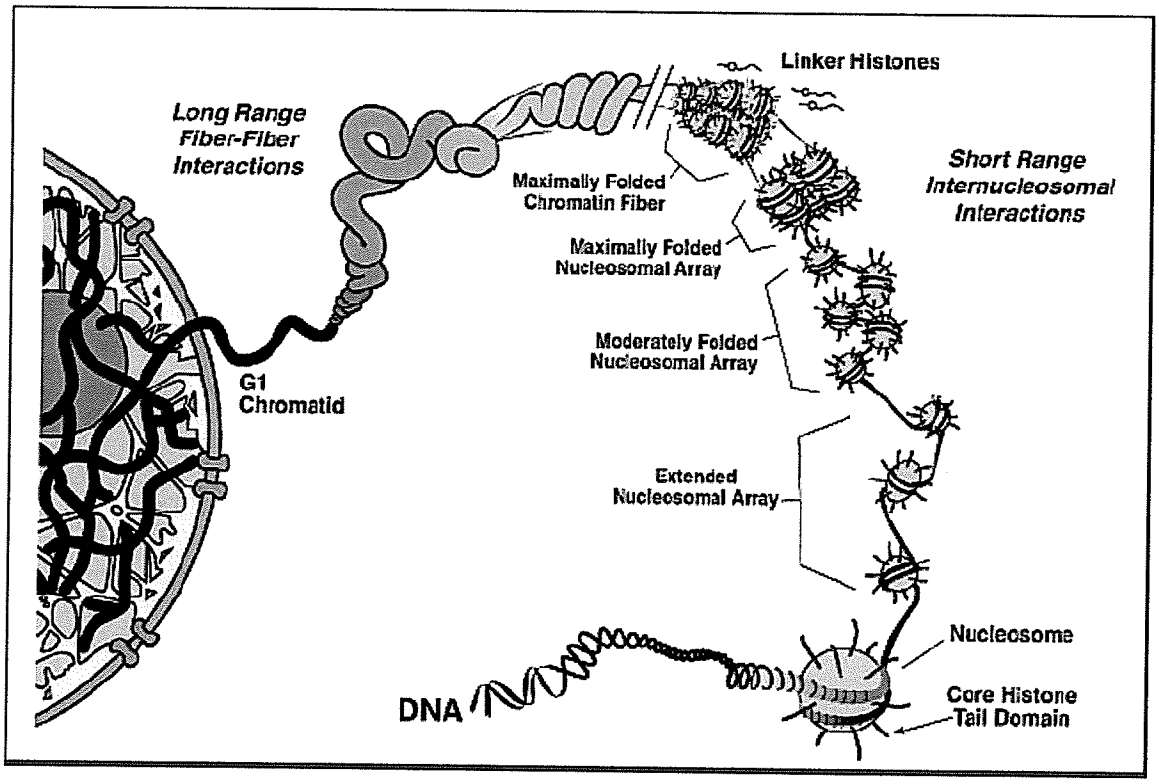


**Figure 1.** **Diagrammatic Representation of the Several Orders of Chromatin Compaction in an Interphase Cell.** DNA is packaged into a 10 nm extended chromatin fiber by associating with histone octamers that bind to 160 bp of DNA. The 10 nm fiber is folded into a more condensed fiber which becomes further compacted into a moderately folded and then maximally folded nucleosomal array through short range intra- and internucleosomal interactions. The binding of linker histone to the chromatin fiber further condenses the fiber into a maximally folded 30 nm fiber that undergoes long range interactions with other chromatin fibers, thus forming a higher order chromatin structure. The chromatin fiber is also organized into loop domains by the nuclear matrix during G1. Figure taken from [7].

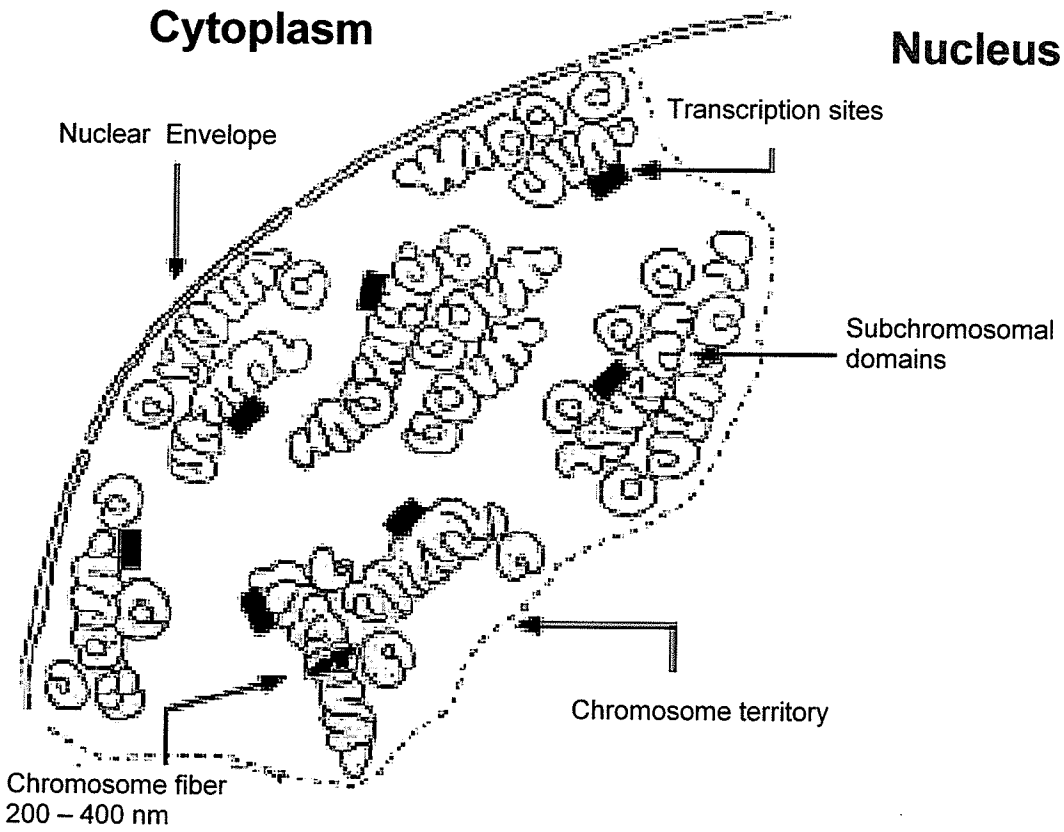


**Figure 2.** **Diagrammatic Representation of a Chromosome Territory and Transcription Sites in a Thin Section of an Interphase Nucleus.** The chromosome fibers follow an irregular path within the territory. Transcriptionally active chromatin is compartmentalized with the active loci (represented as a black box) located predominantly at or near the surface of the compact chromatin fiber domains. Figure taken from [3].

***The Nucleosome***

The basic structural repeating unit of chromatin is the nucleosome which is composed of 146 bp of DNA wrapped 1.65 times around an octamer of two histone H2A-H2B dimers bound to a histone H3-H4 tetramer [8] (Figure 3). The four core histones have a basic N terminal tail, a central globular domain and a C terminal tail. The histone N terminal tails emanate radially from the nucleosome and can interact with linker DNA, as well as other nucleoprotein complexes [9].

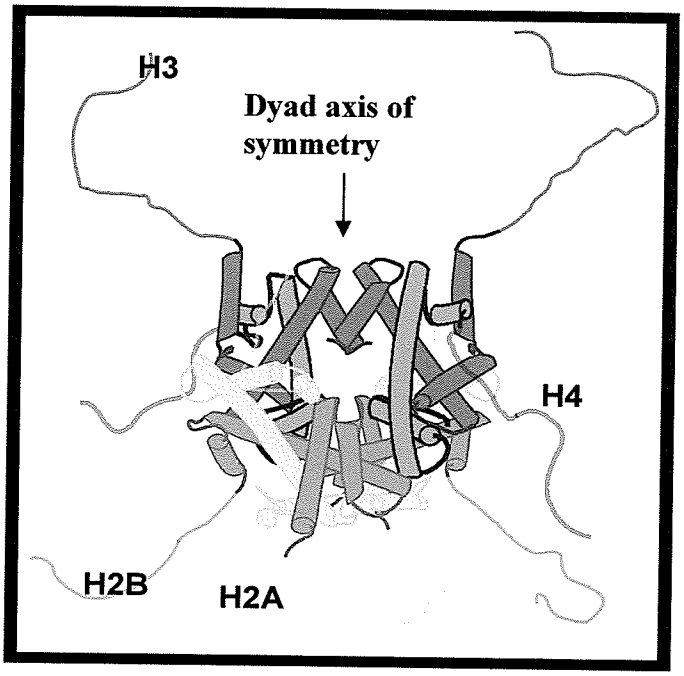


**Figure 3.** **Schematic Representation of the Histone Octamer Showing the Positioning of the Core Histones Relative to the Dyad Axis of Symmetry.** Figure was originally created by Dr. Jacob Waterborg.

The globular domain is organized into three α-helices connected by two loops. This helix-loop-helix structure is referred to as the histone fold (Figure 4) [10]. The long central helix in the histone fold acts as an interface for dimerization to other histone fold motifs, and for histone-DNA interactions [9]. As a result, the histone fold is important in histone octamer and nucleosome formation [8]. The interfaces within H2A-H2B dimers and H3-H4 tetramers are extremely stable [7]. However, salt-solubility studies show that the interactions between the H2A-H2B dimers and the H3-H4 tetramer are considerably more unstable. Raising the concentration of NaCl to above 600 mM causes the H2A-H2B dimers to first dissociate from the nucleosome followed by the H3-H4 tetramer [11,12].

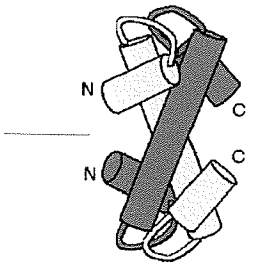


**Figure 4.** **Diagram Showing an Interaction Between the Globular Domains of Two Histones.** Each globular domain is organized into a histone. The dimerization of two histone folds results in the formation of a hand-shake motif.

*Linker Histones*

A fifth type of histone called linker histone H1 is not related to the core histones, but is similar in structure in that it contains a central globular domain surrounded by N and C-terminal tails. In chicken erythrocytes, H1 is partially replaced by histone H5. This histone is an H1 variant that accumulates during the maturation of avian erythrocytes [13]. According to Dr. Bates and Dr. Thomas, mature chicken erythrocyte chromatin contains approximately 0.4 molecules of H1 and 0.9 molecules of H5 per nucleosome [14]. In human chromatin, the ratio of H1 linker histone to nucleosome in bulk chromatin is approximately 1:1 [15]. Histone H1/H5 binds to linker DNA at or near the entry/exit points of the nucleosome core particle [8,16]. As well these linker histones bind to nucleosomal DNA near the dyad axis of symmetry [8,16].

The association of H1 with linker DNA appears to be a dynamic process [17,18]. In a recent study, histone H1 was found to exchange rapidly in both condensed and decondensed chromatin regions [17]. This exchange occurs through a pathway involving the dissociation of H1 from chromatin, diffusion of H1 through the nucleoplasm, and then H1 reassociation with chromatin [17]. In support of this, Dr. Misteli and colleagues also identified a large mobile pool of H1 histone in the nucleus that represented a continuously exchanging H1 fraction [18].

H1 exchange does not require chromatin fiber-fiber interactions [17]. Furthermore, treatment of cells with kinase inhibitors inhibited H1 phosphorylation and increased the duration of H1 binding to chromatin. Similarly, others have observed that H1 phosphorylation diminishes the interaction of H1 with DNA [18-21]. Thus, H1 phosphorylation plays an important role in modulating H1 mobility .

*Histone Variants*

To date, six histone H2A variants have been identified including H2A.1, H2A.2, macroH2A, H2A.Z, H2A.X and H2A-Bbd [22]. The differences in amino acid sequences between these variants and H2A can range from as a little as a few amino acids to as much as several hundred amino acids [22]. Little is known of the function of these variants. One molecule of MacroH2A is present for every 30 nucleosomes in the rat liver [23]. This variant is involved in X chromosome inactivation of female vertebrates possibly through interactions with *XIST* RNA [23-25]. Histone H2A.Z is a minor H2A variant that is ubiquitous to all eukaryotes and essential for cell viability [26-29]. The expression of this variant changes during *Xenopus laevis* development [30]. It has been hypothesized that this variant affects the conformation/stability of nucleosomes, as well as higher levels of chromatin folding, however, the exact function of this variant remains unknown [22]. H2A.X is another minor H2A variant involved in DNA repair [31-33]. The H2A-Bbd variant is deficient in the inactive X chromosome in female cells and colocalizes with acetylated H4, suggesting that this histone may be enriched in nucleosomes from actively transcribing regions within the nucleus [34]. The function of H2A.1 and H2A.2 is unknown. The level of these two H2A variants changes during postnatal development of cortical neurons and their neuroblasts in rats, as well as during the development of Friend tumors in mice [35,36].

Histone H3 variants include H3.1, H3.2, H3.3 and CENP-A. The amino acid sequence differences of H3.1, H3.2 and H3.3 differ from that of H3 by only a few amino acids [22]. CENP-A, however, has a unique N terminal domain and a C terminal histone fold with 60% identity to the H3 histone fold domain. Acetylated H3.1 is a replication-dependent variant that becomes assembled into newly replicated chromatin [37]. Acetylated

H3.2 is assembled into nucleosomes within transcribing chromatin and is frequently lost during subsequent transcription [38]. CENP-A is a centromeric H3 histone variant in eukaryotes [39]. This variant is also found in yeast and *Drosophila* and is referred to as Cse4p and Cid, respectively, in these organisms [40,41].

Several H2B variants have also been identified including H2B.1 and H2B.2. The function of these variants remains unknown. However, H2B.2 along with H2A.Z has been found to stabilize the association of the H2A-H2B dimer in nucleosomes [42]. The levels of H2B.1 and H2B.2 also change with continuing changes in chromatin composition that accompany the development of malignant Friend tumor cells [36].

***The Effect of Transcription on the Nucleosome***

Nucleosomes can act as barriers *in vitro* that prevent RNA polymerase II from transcribing a gene [43,44]. Exactly how the transcriptional process alters or affects nucleosome structure and positioning is unknown. One theory suggests that RNA polymerase II stimulates the release of one H2A-H2B dimer from each nucleosome it encounters (Figure 5) [44,45].

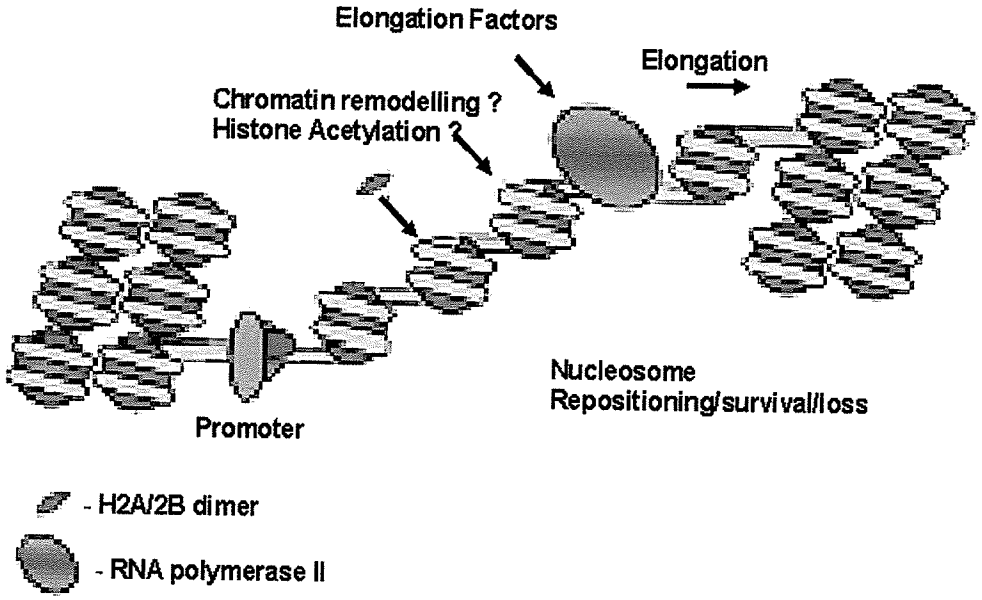


**Figure 5.** **Dr. Studitsky's Hypothetical Model for Transcription by RNA Polymerase II Through a Nucleosome** [44]. As RNA polymerase II encounters a nucleosome in its path, elongation factors in the RNA polymerase II complex facilitate the dissociation of an H2A-H2B dimer which may alter higher order chromatin structure. Nucleosome redistribution and partial nucleosome depletion may also result from the transcription process. The temporal removal of an H2A-H2B dimer provides a window of opportunity for chromatin remodeling factors or DNA-binding proteins to bind to nucleosomal DNA. After an unknown amount of time, an H2A-H2B dimer reassociates with the hexasome, forming a nucleosome.

Chromatin containing transcribed sequences is preferentially bound to RNA polymerase II and depleted in histones H2A and H2B [46]. Dr. Studitsky and colleagues showed that the passage of RNA polymerase II along a mononucleosomal DNA template *in vitro* results in the formation of a subnucleosomal complex containing only one H2A-H2B dimer and a tetramer of H3 and H4 [44]. Dr. Kimura and Dr. Cook have also demonstrated that the majority (>80%) of H3 and H4 molecules do not exchange with other H3 and H4 molecules [45]. Furthermore, approximately 3% of H2B molecules exchange rapidly (within minutes) in a transcription-dependent manner [45]. Dr. Nacheva and colleagues have also shown that the globular domains of H2A and H2B are partially depleted *in vivo* along the highly transcribed hsp 70 gene in *Drosophila* [47].

The release of an H2A-H2B dimer causes nucleosomes to form hexasomes, a histone complex composed of one H3-H4 tetramer and one H2A-H2B dimer [44]. The loss of H2A-H2B dimers from the nucleosome may cause changes in higher order chromatin structure [44]. The nucleosomes remain as hexasomes for a brief window of time before the H2A-H2B dimer reassociates [44]. It has been postulated that the time between H2A-H2B dimer dissociation and re-association may provide the opportunity for additional factors to bind to the nucleosome and destabilize it further [44].

Factors such as FACT that are associated with RNA polymerase II may disrupt the structure of the octamer and cause transient dissociation of an H2A-H2B dimer from the nucleosome as the RNA polymerase II complex enters the nucleosome. Subsequent to transcriptional elongation, the FACT complex alleviates nucleosome-induced blocks in RNA polymerase II-mediated transcriptional elongation [48]. The FACT elongation complex specifically interacts with H2A and H2B and the activity of this complex is

hindered when the histones within a nucleosome are covalently cross-linked [49]. The partially disassembled and unfolded structure of the hexasome may then be maintained by events such as histone acetylation that are mediated by histone acetyltransferases associated with the elongation complex [50-52]. As additional RNA polymerase II complexes traverse the coding region of the same gene, continual cycles of H2A and H2B disruption and reassociation would occur and would most likely contribute towards the dynamic association of the H2A-H2B dimer with transcriptionally active genes.

Additional data that supports the idea of an altered nucleosome structure resulting from the transcription process comes from the studies of the late Dr. Allfrey and colleagues [53,54]. In these studies, mercury affinity chromatography showed that the nucleosomes associated with transcriptionally active genes had exposed H3 cysteine thiol groups near the dyad axis of symmetry while nucleosomes along inactive DNA did not [53,54]. Dr. Bazett-Jones and colleagues have analyzed the structure of these thiol-reactive nucleosomes by electron spectroscopic imaging and have determined that these thiol-reactive nucleosomes are unfolded and shaped into an extended U-shaped particle [55] (Figure 6). This suggests that transcription of a gene involves the unfolding of nucleosomes along this gene and the exposure of H3 cysteine thiol groups located near the nucleosome dyad access of symmetry [53,54]. The process of transcriptional elongation is believed to be responsible for the unfolding of the nucleosome while post-translational events such as histone acetylation maintain the nucleosome in the unfolded conformation [50].

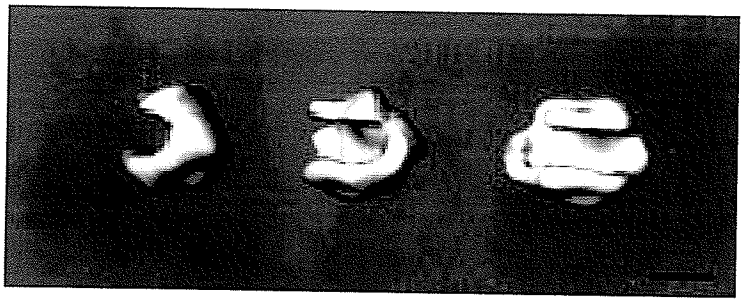

**Figure 6.** **Three-Dimensional Reconstruction Calculated from Nucleosomes Associated with Transcriptionally Active Genes.** Nucleosomes released from human adenocarcinoma cells by a limited MNase digestion were applied to a mercury affinity column. Mercury-bound nucleosomes were eluted with dithiothreitol and analyzed by electron spectroscopic imaging. Image taken from [55].

Another theory suggests that histone octamers are dissociated from DNA as they encounter the RNA polymerase complex [56,57]. In this model, displaced histones may re-bind to their original binding site along the DNA strand; however, this binding would be inefficient. Because of this, a transcriptionally active DNA sequence exposed to subsequent rounds of transcription would be somewhat depleted in nucleosomes. In support of this, Dr. Widmer and colleagues observed in the salivary glands of *Chironomus* larvae that a transcriptionally active salivary protein gene was depleted in nucleosomes when compared to an inactive gene [56]. Similarly, Dr. Karpov and colleagues observed that the central hydrophobic regions of histones could not be cross-linked by the histidine cross-linking method to the coding region of transcriptionally active *hsp* 70

genes when intensely transcribed [47,58]. The moderate transcription of these genes resulted in a partial removal of core histones from the coding region [47].

Using the histidine cross-linking method, Dr. Nacheva et al. also observed an absence of histones along the hsp70 promoter region in *Drosophila* and a decrease in the association of histones H2A and H2B, and to a lesser extent, H3 and H4 globular regions along the coding region of this gene relative to transcriptionally inactive chromatin [47]. However, when the lysine residues of histones were cross-linked to DNA by formaldehyde, the level of core histones associated within 2 Å of the coding region of the hsp70 gene was quantitatively similar to levels along transcriptionally inactive chromatin [47]. Similarly, Dr. Varshavsky and colleagues observed that the level of histone H4 formaldehyde-cross-linked to the transcribed domain and the promoter-proximal region of the *hsp70* gene remained similar in *Drosophila* regardless of heat shock [59]. The histone N terminal tails can also be UV cross-linked to nucleosomal DNA even when they are modified by acetylation [60]. Thus, the process of transcription appears to involve the alteration of nucleosome structure in a manner that permits access of transcriptional machinery to the target DNA sequences of a transcriptionally active gene.

A progressive displacement model has been suggested by Dr. van Holde and colleagues to explain the effect of transcription by RNA polymerases on the nucleosome (Figure 7). In this model, the approach of an RNA polymerase triggers the dissociation of an H2A-H2B dimer from the proximal face of a nucleosome [61]. The dissociation of the dimer may result from positive superhelicity induced by the approaching RNA polymerase complex or by competition between the RNA polymerase and the nucleosome for DNA [61]. Loss of the H2A-H2B dimer facilitates entry of RNA

polymerase into the nucleosome [61]. H2A contacts nucleosomal DNA near the dyad [61]. Dissociation of the H2A-H2B dimer may also destabilize the central part of the nucleosome and facilitate the release of DNA from the H3-H4 pair of the H3-H4 tetramer positioned proximal to the RNA polymerase [61]. The opening of the nucleosome and the release of DNA near the center dyad would allow RNA polymerase to proceed past the nucleosome dyad and displace the distal H3-H4 pair of the H3-H4 tetramer [61]. As this occurs, the proximal H3-H4 dimer binds once again to the nucleosomal DNA [61]. Some time later, the H2A-H2B dimer reattaches to the proximal face of the nucleosome [61]. This event is then followed by reassociation of the distal H3-H4 dimer [61]. At some point during the movement of chromatin through the NM-associated RNA polymerase complex, the distal H2A-H2B pair of each nucleosome along the chromatin fiber will become dissociated to facilitate transcription of the remaining nucleosomal DNA [61]. This dimer will then eventually reassociate with the nucleosome most likely when the RNA polymerase complex has transcribed the entire length of the nucleosomal DNA and subsequent rounds of transcription have ceased to occur. Dr. van Holde's model supports Studitsky's theory of H2A-H2B dissociation from transcriptionally active nucleosomes. This model also supports observations that transcriptionally active chromatin is never completely depleted of histones. Lastly, this model supports Dr. Allfrey's proposed theory of transcriptionally active nucleosomes having an altered structure.

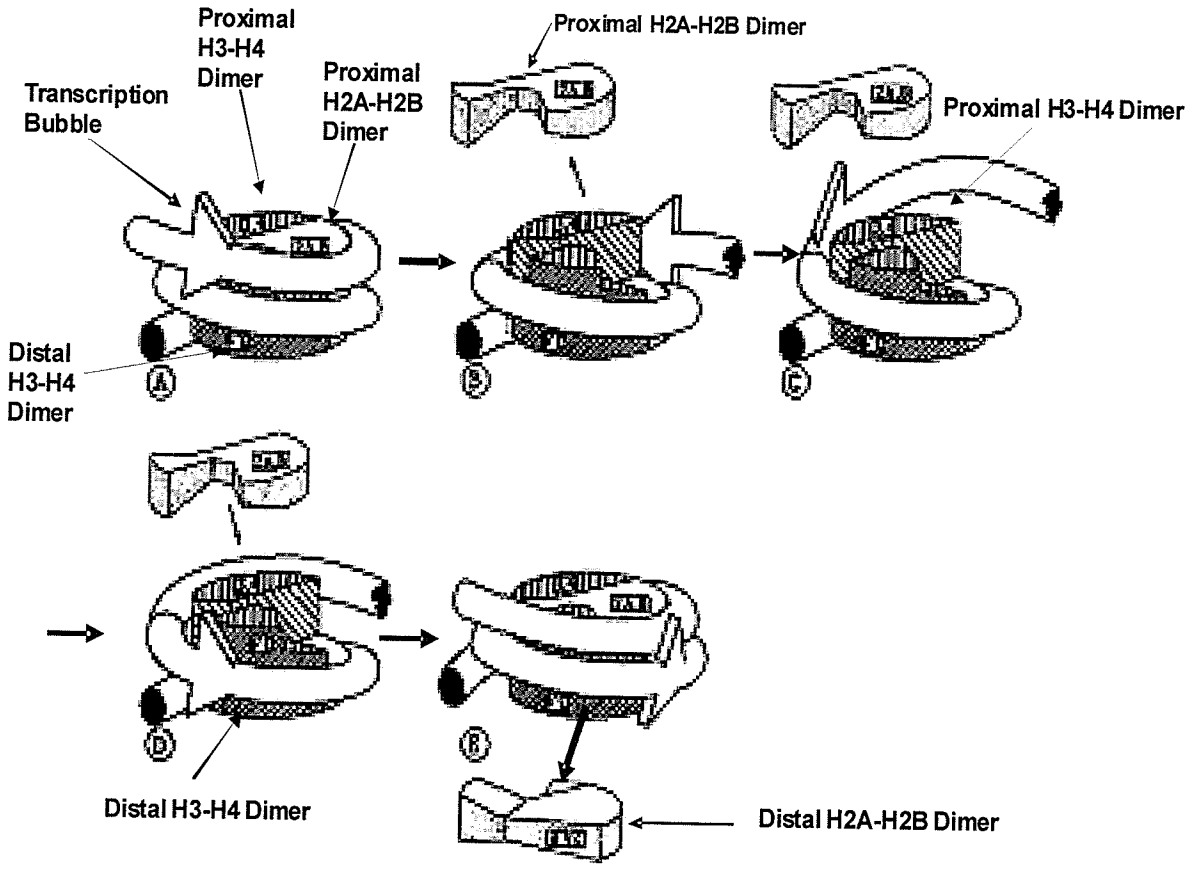


**Figure 7.** **Dr. van Holde's Hypothetical Model for Transcription by RNA Polymerase II Through a Nucleosome [61].** (A). RNA polymerase encounters the nucleosome. (B). RNA polymerase displaces a proximal H2A-H2B dimer and proceeds to a proximal H3-H4 dimer within the H3-H4 tetramer at the dyad axis. (C) RNA polymerase transcribes through the H3-H4 contacts with the dyad axis. (D) RNA polymerase transcribes through the dyad axis and disrupts H2A-H2B contacts while the proximal H3-H4 dimer reassociates with the nucleosome (E) RNA polymerase passes through the distal H3-H4, causing the release of the distal H2A-H2B dimer and association of the proximal H2A-H2B dimer with the proximal side of the H3-H4 tetramer.

*The Chromatin Fiber*

**The Structure of Transcriptionally Active and Inactive Chromatin**

At physiological ionic strength, chromatin assumes a 30 nm fiber and higher order structures [4]. Actively transcribed chromatin is structurally different from bulk inactive chromatin. Chromatin fibers containing active genes are less compact than regions containing inactive genes, have a diameter between 100-200 nm and are referred to as euchromatin [62,63]. Inactive genes are located in heterochromatin which is folded into a compact structure similar to that of chromosomes in metaphase cells [64-66]. The level of chromatin compaction of inactive and active chromatin regions is reflected in the sensitivity of these regions to DNase I. The more open conformation of euchromatin allows DNase I to easily access transcriptionally active DNA sequences, whereas the highly compact nature of heterochromatin prevents DNase I from accessing inactive DNA sequences.

**Function of the Core Histone N terminal Tails in Chromatin Structure**

The chromatin fiber is a dynamic structure that is continually condensing and unfolding. For example, a chromatin fiber composed of nucleosomes spaced at physiological intervals is in equilibrium between an unfolded, moderately folded, highly folded and oligomerized conformation [7,67]. The proteolytic removal of the N terminal domains does not significantly change nucleosome structural integrity, and instead prevents the formation of the 30 nm fiber [68]. Thus, the stability of this 30 nm fiber is maintained by the core histone N terminal tails [68].

The core histone N terminal tails were originally thought to promote chromatin fiber condensation by binding as unstructured coils to nucleosomal DNA and neutralizing the negative charge of the DNA phosphate backbone [69]. Chromatin fiber condensation is a term that describes the ability of a chromatin fiber to fold and oligomerize with itself and other chromatin fibers [67]. However, exposure of nucleosomal arrays lacking core histone N terminal tails to a high concentration of $Mg^{2+}$ salt that will neutralize the negative charge of the nucleosomal DNA phosphate backbone does not promote fiber condensation [70,71]. Thus, charge neutralization does not appear to promote fiber condensation and the core histone N terminal tails most likely promote chromatin fiber condensation by some other means.

Chromatin folding is also dependent on the interaction of the N-terminal tails of the core histones with linker DNA [72]. The core histone N terminal tails are thought to protrude from the nucleosome to distances where they can interact with linker DNA, linker histones, and protein factors involved in transcriptional regulation [72,73]. The N terminal tail of H3 is 44 amino acids long, whereas histones H4, H2B and H2A have N terminal tails that are only 26, 32 and 16 amino acids long, respectively. Thus, the N terminal tail of histone H3 can extend over a significantly larger portion of linker DNA compared to the other core histones [73]. The H3 N terminus is also positioned close to the point where linker DNA enters and exits the nucleosome, and, therefore, it can undergo extensive interactions with the linker DNA [74].

The 30 nm chromatin fiber has an irregular, zig-zagged structure due to the varying lengths of linker DNA, and the varying angles at which this DNA enters and exits the nucleosome [75,76]. The chromatin fiber is stabilized, in part, by histone H1 which

binds to the nucleosome through its globular domain and fixes the trajectory angle of the linker DNA at the points where it enters and exits the nucleosome [77].

The chromatin fibers within a cell interdigitate with neighboring fibers into a higher order fibrous mass that impedes the access of transcription factors to their target sequences, thereby preventing transcription initiation [78]. Fiber-fiber interactions are dependent on the N terminal tails of the H3 and H4 core histones as well as the surrounding concentration of divalent and monovalent cations [78]. These fibrous masses are then further organized into compact chromosome territories within interphase nuclei (Figure 1) [3].

**The Interaction of the Core Histone N Terminal Histone Tails with Proteins**

In addition to binding linker DNA, the core histone N terminal tails are capable of interacting with other histones and non-histone chromosomal proteins. The N terminus of H4 binds to the H2A-H2B dimer of neighboring nucleosomes, and is thought to assist in chromatin folding [79]. In yeast, the transcriptional repressors Sir3, Sir4 and Ssn6/Tup1 interact with the H3 and H4 N terminal domains, causing the associated chromatin to become transcriptionally repressed [80]. Likewise, the *Drosophila* Groucho and its mammalian homologues bind to the N terminal domain of H3 and repress transcription [81,82,82]. These domains also interact with non-histone proteins such as HMG-14 and HMG-17 that promote the unfolding of higher order chromatin structures [83].

**Influence of Salt on Chromatin Structure**

The ionic environment surrounding a chromatin fiber has a significant influence on chromatin structure, and, to date, the ionic milieu within the nucleus has not been accurately determined [7]. The nucleus contains approximately a meter of DNA and the negatively charged phosphate backbone of DNA generates considerable energy as the DNA molecules repel one another [7,66]. Inorganic and organic cations are present within the nucleus to neutralize the negative charge of the DNA molecule and promote chromatin condensation. In fact, condensation of chromatin fibers can occur only in the presence of cations regardless of the presence or absence of linker histones along the chromatin fiber [7]. While chromatin condensation requires the presence of inorganic and organic cations, it also requires the core histone tails. These tails undergo a series of internucleosomal interactions and cause chromatin fibers to assume moderate to maximally folded conformations [7]. However, complete folding and stabilization of chromatin fibers requires the presence of linker histones [7]. The extremely basic C terminal tails of linker histones provide an additional level of charge neutralization that promotes moderately folded chromatin fibers to assume a maximally folded state [7].

Much of our understanding of chromatin structure has come from the biophysical analysis of nucleosomal arrays made from purified histones and a DNA template composed of 208 bp of a nucleosome positioning sequence repeated 12 times in tandem. This array is referred to as a 12-mer. In low salt TE buffer, a 12-mer nucleosomal array will have a sedimentation coefficient of approximately 29S [84,85]. Increasing the salt to more physiological concentrations (150 mM NaCl or 1 mM $MgCl_2$) increases the sedimentation coefficient almost to 40S [7,86]. This indicates that the density and, therefore, the folding of the nucleosomal array have increased [84,85]. The 40S array is

predicted to be folded to the same extent as an open helical structure [84]. The 30 nm chromatin fiber represents a chromatin fiber in its maximally folded state and displays a sedimentation coefficient of approximately 55S [84]. In the presence of 100-250 mM NaCl, structures with sedimentation coefficients between 29S and 40S are formed. As the concentration of NaCl is increased so is the sedimentation coefficient of the various structures. The transition of a nucleosomal array from 29S to 40S is reversible in the absence of salt. A 12-mer nucleosomal array fluctuates between a 29S, fully extended state and a 40S, moderately folded degree of compaction [7]. Formation of the 40S nucleosomal array requires interactions between neighboring nucleosomes. Thus, nucleosomal arrays with a lower number of nucleosomes have less intranucleosomal interactions, and, therefore, a smaller density and sedimentation coefficient.

**The Effect of $Mg^{2+}$ vs $Na^{+}$ on Chromatin Structure**

As was stated previously, the chromatin fiber undergoes both folding and oligomerization. The extent to which a nucleosomal array undergoes intranucleosomal folding is greater in the presence of divalent salts such as 1-2 mM $MgCl_2$ when compared to monovalent salts such as NaCl [7]. As the concentration of $MgCl_2$ increases, nucleosomal arrays start to oligomerize with one another regardless of the extent to which they are folded [78,87]. However, exposure of nucleosomal arrays to monovalent salts such as NaCl does not cause array oligomerization [15,78].

Although salt is important for chromatin condensation, this event also requires the actions of the core histone N terminal tails [7]. In addition, the binding of linker histone to linker DNA additionally neutralizes the negative charge of nuclear DNA and this promotes the transition of chromatin into a maximally folded state [7]. Thus, the presence

of linker histones, the local ionic environment and the internucleosomal interactions of the core histone N terminal tails determine the extent to which a chromatin fiber is folded[7].

***The Histone Code***

The histone N terminal tails undergo several post-translational modifications mediated by a variety of enzymes (Figure 8). Research in the field of gene expression has focused primarily on determining the function of each modification in transcription. However, a new concept has emerged referred to as the "histone code" [88,89]. This term proposes that the different post-translational modifications occurring on one or more histone tails act either together or in sequence to form recognition sites for specific proteins involved in distinct cellular functions.

Dr. Thanos and colleagues have shown that the pattern of acetylation along a specific gene region can serve as a code that is recognized by additional chromatin remodeling factors and transcription factors [90]. Transcriptional activation of the interferon-β gene caused acetylation of histone H4 Lys-8 along the interferon-β promoter and this event mediated SWI/SNF recruitment [90]. However, acetylation of Lys-9 and Lys-14 on H3 along the interferon-β promoter was critical for TFIID recruitment [90].

Evidence from several recent studies suggests that histone phosphorylation and acetylation may function together to promote gene expression. Dynamically acetylated histone H3 is preferentially phosphorylated [91]. H3 phosphorylation occurs along the promoter and within the transcribed region of the c-*fos* and c-*jun* genes before induction of transcription [92]. This modification is thought to be involved in the establishment of

transcriptional competence [92]. The stimulation of mammalian cells by epidermal growth factor causes the sequential phosphorylation of Ser-10 and acetylation of Lys-14 on H3 along the c-*fos* promoter in a MAP kinase-dependent manner [93]. Moreover, the histone acetyltransferase Gcn5 preferentially associates with a Ser-10 phosphorylated form of H3 over a non-phosphorylated form [93]. Several other histone acetyltransferases including CBP, PCAF and SAGA have also been shown to acetylate phosphorylated H3 [92,93]. Recently, the phosphorylation of H3 Ser-10 by the Snf1 kinase was shown to lead to Gcn5-mediated acetylation at the *INO1* promoter [94]. As well, phosphorylation of H3 Ser-10 along the interferon-β promoter precedes Gcn5-dependent H3 acetylation at Lys-14 [90]. Thus, the recruitment of a kinase complex to specific promoters may cause Ser-10 phosphorylation and either increase the affinity of histone acetyltransferase complexes for nucleosomes or increase acetyltransferase catalytic activity [95].

Histone methylation and acetylation may also be important in transcription. Histones H3 and H4 are modified at specific lysine and arginine residues primarily within their N terminal tails [96,97]. The exact function of histone methylation in transcription is unknown. Heterochromatic silencing requires the methylation of Lys-9 on H3 by the lysine methyltransferase Su(var) 39 [98]. The methylation of Lys-9 inhibits phosphorylation of H3 at Ser-10 possibly by hindering the access of kinases to this serine residue [98]. Thus, methylation of H3 Lys-9 may impair transcription by inhibiting phosphorylation events required for transcriptional stimulation [99]. A recent study mapping the distribution of di-methylated Lys-9 on H3 across the chicken β-globin domain during erythropoiesis showed that regions enriched in methylated Lys-9 were depleted of di-acetylated H3 (Lys-9 and Lys-14). However, H3 acetylation correlated

with Lys-4 methylation, suggesting that transcriptional activation is associated with H3 methylated at Lys-4, as well as with acetylated H3 and H4 isoforms [100]. Likewise, in *Tetrahymena,* methylated Lys-4 of H3 is found only in transcriptionally active macronuclei [101].

Di-methylation of Lys-4 on histone H3 along coding regions is also associated with transcriptional activity in yeast [102]. In fact, Lys-4 methylation is more common along coding regions than acetylation. In yeast, Lys-4 methylation along the coding regions of active genes is mediated by Set1 and this modification is required for the maintenance of gene expression [102]. While methylation does not alter the overall charge of the histone tails, it can increase histone basicity and hydrophobicity [96]. Thus, methylation of the histone tails may alter their interaction with DNA and/or chromatin-associated proteins [96].

As was previously stated, Lys-9 methylation is associated with transcriptionally inactive and hypoacetylated genes [103]. The recruitment of RNA polymerase II to the promoter regions of inducible inflammatory genes results in histone demethylation [103]. Furthermore, this event is reversed upon the removal of RNA polymerase II. The histone acetyltransferase Elp3 is associated with RNA polymerase II and may contain histone demethylase activity [104]. Thus, enzymes such as Elp3 may be able to remove methylated Lys-9 without removing methylated Lys-4 and, at the same time, acetylate specific lysine residues along the N terminal tails of H3.

Recently, the CARM1 histone methyltransferase was found to be associated with both CBP and p300 acetyltransferases, as well as the p160 co-activator SRC-2 in cultured mammalian cells [105-107]. In transient transfection studies, the interaction of all three

factors with ERα synergistically enhanced the function of this hormone receptor [105]. Furthermore, this effect was highly dependent on CARM1, and PCAF while other arginine methyltransferases with different substrate specificities could not substitute for CARM1. Treatment of MCF-7 human breast cancer cells with estrogen for 15 min resulted in the initial recruitment of CBP to the promoter region of the pS2 gene which resulted in acetylation of H3 Lys-18 [108] (see Figure 8). After 30 min exposure to estrogen, CARM1 was subsequently recruited to the promoter where it methylated Arg-17 of H3. The acetylation of H3 by CBP stabilized the association of CARM1 with chromatin and enhanced CARM1-mediated Arg-17 methylation. These findings suggest that a crosstalk occurs between CARM1-mediated H3 methylation and CBP-mediated H3 acetylation. The ordered recruitment of different chromatin-modifying factors to the promoter region of the pS2 gene may generate an environment that is recognized by specific proteins [108].

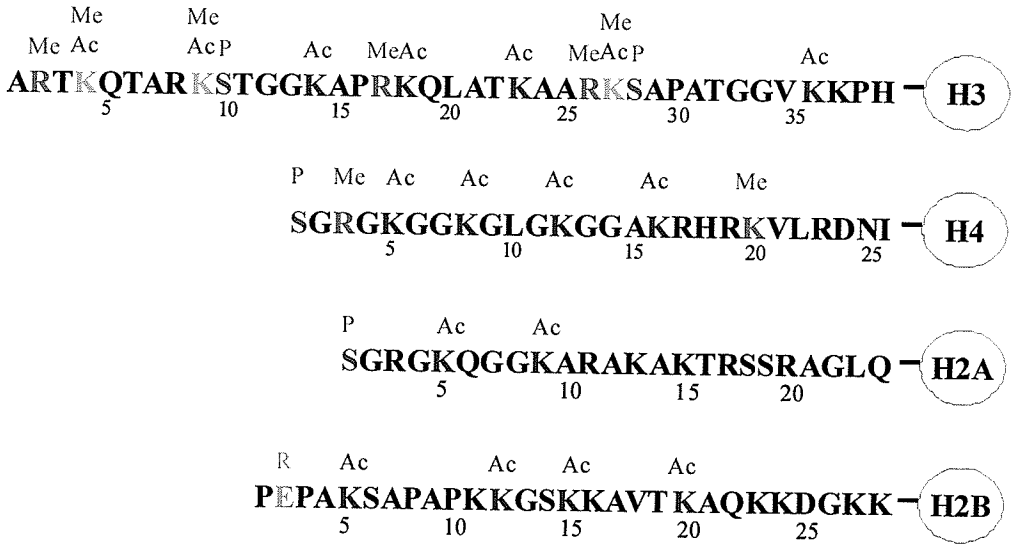


**Figure 8.** **Post-Translational Modifications Along the Core Histone N Terminal Tails.** The central globular domain of each histone is depicted as a circle with the N terminal tail extending towards the left. N terminal tail sequences are from [177]. Me, Ac, P, and R represent methylation, acetylation, phosphorylation and ADP-ribosylation, respectively.

*Histone Acetylation*

To date, over twenty histone acetyltransferase and 10 deacetylase enzymes have been identified and found to be important in normal cell development and proliferation, as well as cancer development.

**Histone Acetyltransferases**

The majority of histone acetyltransferases are categorized into five families based on their sequence similarity with each other [109]. The first histone acetyltransferase family is the GNAT (Gcn5-related *N*-acetyltransferase) superfamily. This family includes proteins involved in transcription initiation (Gcn5 and PCAF), elongation (Elp3), histone deposition and telomeric silencing (Hat1) [110]. GNAT family members function as co-activators for a subset of transcriptional activators and the histone acetyltransferase activity of these proteins is directly involved in transcriptional stimulation [111].

Co-activators are factors that promote transcriptional activity, while co-repressors prevent transcription from occurring [112]. Coactivators modify chromatin structure by promoting either histone acetylation or chromatin remodeling events at the promoter regions of target genes. Thus, a co-activator may alter chromatin structure either by acetylating histones or remodeling chromatin directly or by indirectly recruiting other factors that can perform these functions. For example, the ability of transcription factors such as the ERα to activate gene transcription in the presence of estrogen ligand is dependent on the ability of the estrogen-ERα complex to recruit coactivators either directly or indirectly associated with histone acetyltransferase activity to the promoter region of estrogen-responsive genes [113,114].

Members of the GNAT family of histone acetyltransferases contain a C-terminal bromodomain that is involved in protein-protein interactions [109]. This bromodomain serves as an acetyl-lysine targeting motif [115,116]. The N terminal domain of PCAF also interacts with other co-activators containing intrinsic histone acetyltransferase activity such as CBP/p300 and ACTR [111]. GNAT family members are directly recruited as protein complexes to sites of transcription by several transcription factors including NF-Y, nuclear hormone receptors [estrogen receptor α (ERα), androgen receptor and glucocorticoid receptor], and the E1A viral oncoprotein [111].

A second group of histone acetyltransferases is the CBP/p300 family. CBP and p300 are highly related proteins. The members of this family function as co-activators for multiple transcription factors and are considered to be global regulators of transcription [109]. CBP/p300 proteins contain a bromodomain along with three cysteine-histidine rich domains that mediate protein-protein interactions [109]. The histone acetyltransferase activity of CBP/p300 family members is required for their role in transcription [111]. When bound to the promoter or enhancer region of a gene, transcription factors such as hormone receptors, *fos-jun* (AP-1) and CREB can bind to CBP/p300 either directly or through another co-activator protein [111]. CBP/p300 is required for transcriptional activation by these transcription factors and the levels of CBP are limited within a cell [109,111,113]. Because of this, these transcription factors must compete with one another for available CBP. Thus, a transcription factor will have a greater chance in recruiting CBP/p300 if it is arranged along an enhancer or promoter region with other factors that also bind CBP/p300 [111]. Such is the case for ERα, whose estrogen-induced activation leads to its association with several co-activators including SRC-1, ACTR, and PCAF.

Of these three co-activators, p300 interacts with PCAF while CBP interacts with all three [111,117]. CBP and p300 can also directly bind nuclear receptors in the presence of ligand independently of other co-activators [117].

In addition to interacting with nuclear receptors such as the ER, CBP interacts with RNA polymerase II holoenzyme [52,118,119]. The p300 coactivator also binds to ERα and preferentially acetylates lysines 302 and 303 within the hinge/ligand binding domain of this receptor[120]. Substitution mutation of these two ER lysine residues with arginine or threonine significantly enhances the ability of this receptor to induce the transactivation of an ERE-luciferase reporter construct in the presence of estradiol[120]. This suggests that acetylation of these two lysine residues suppresses the sensitivity of ERα to estrogen ligand [120]. CBP acetylates HMGI(Y) which decreases its DNA binding affinity and causes the disruption of the enhanceosome complex. Thus, coactivators such as CBP are able to bridge the gap between the transcriptional machinery and nuclear receptors, and alter the transcriptional properties of transcription factors.

The third family of histone acetyltransferases is the MYST family. This family includes MOZ, HBO1, Esa1, Ybf2/Sas3, Sas2 and Tip60. Sas3 is the yeast homolog of MOZ and the catalytic subunit of the NuA3 histone acetyltransferase complex. This complex is thought to function in transcriptional elongation and DNA replication, as well as silencing of the yeast HM mating-type loci [121,122]. Esa1 is found in yeast, is homologous to Drosophila MOF and is the catalytic subunit of the NuA3 complex [123]. Esa1 along with Gcn5 induce the widespread acetylation of a 4.25 kb region around the yeast Pho5 gene [123]. This event causes opening of chromatin at the promoter and

enhances the probability that the Pho5 gene will be transcribed [123]. Lastly, HBO1 associates with a protein complex that binds to the origin of replication [124].

The $TAF_{II}250$ histone acetyltransferases comprise the fourth family. The proteins in this family are subunits of the TFIID transcription factor complex. Members of the $TAF_{II}250$ family contain N and C terminal kinase domains, along with a C terminal double bromodomain that binds di-acetylated H4 with high affinity [109].

The fifth and best characterized group of histone acetyltransferases is the p160 family. Three distinct members of the p160 family have been identified as multiple splice variants. These are SRC-1/NCoA-1, SRC-3, TIF2/GRIP1/NCoA-2/SRC-2 and p/CIP/ACTR/RAC3/AIB1/TRAM-1 [113,125-131]. The members of this family function as co-activators of nuclear receptors. The interaction of p160 members with a receptor molecule occurs through the amphipathic LXXLL helical motif of the co-activator protein. Members of the p160 family also interact with CBP through their LXXLL motif[117,132]. The interaction of CBP and SRC-1 with ligand-bound receptor synergistically enhances transcriptional activation. Furthermore, the SRC-2 p160 co-activator was recently shown to interact with the CARM1 histone methyltransferase, as well as both p300 and CBP [105-107]. The interaction of CARM1, SRC-2 and p300 with the ERα synergistically enhanced the function of this hormone receptor [105].

Histone acetyltransferases have different histone substrate specificities and different target genes [110]. For example, the yeast Esa 1 histone acetyltransferase interacts only with the promoter regions of ribosomal protein genes [134]. Likewise, Gcn5 acetylates only a small subset of lysine residues in H3 and H4 during activation of the IFN-β gene

[90]. Mutation of H3 or H4 also significantly decreases p300-dependent transcriptional activation of a Gal4-VP16 reporter construct [135].

Histone acetyltransferases generally exist in large complexes and the proteins within these complexes determine the acetyltransferase target substrate specificity [8,136]. For example, the free full-length form of yeast Gcn5 preferentially acetylates H3 *in vitro* and H3 and H4 *in vivo* [68,110,137]. However, the acetylating efficiency of yeast Gcn5 for nucleosomal histones increases when assembled into high molecular weight, multi-protein complexes referred to as SAGA and Ada [136,137]. In addition, the pattern of histone acetylation for Gcn5 assembled into the SAGA complex is distinct from that exhibited by Gcn5 when assembled into Ada [137]. Similarly, the histone substrate specificity of individual human PCAF and yeast Esa1 acetyltransferases becomes altered when these enzymes are assembled into multi-protein complexes [68]. The phosphorylation of CBP by ERK1 enhances the activity of this acetyltransferase, suggesting that the function of histone acetyltransferases may be regulated by phosphorylation events [138].

To date, every histone acetyltransferase has been shown to exist in multimeric complexes containing other histone acetyltransferases. When a complex contains multiple histone acetyltransferases that target distinct residues on the same protein, these enzymes may work together to enhance transcription factor binding and activation to a level greater than that induced by each acetyltransferase alone. Alternatively, the presence of multiple histone acetyltransferases with different substrate specificities in the same complex may cause proteins such as histones to become acetylated at multiple sites. The resulting pattern of acetylation may act in combination with other post-translational

modifications such as phosphorylation or methylation to form a code that can be recognized by other proteins.

**Histone Deacetylases**

Histone deacetylases are divided into 3 classes defined by their size and sequence homologies to yeast deacetylases. The class I histone deacetylases are approximately 400-500 amino acids in length and include HDACs 1,2,3 and 8. These class I members are nuclear transcriptional co-repressors with homology to the yeast Rpd3 deacetylase. The class II histone deacetylases are larger proteins of approximately 1000 amino acids with structural homology to yeast Hda1 and include HDACs 4,5,6,7,9 and 10 [139,140]. HDAC11 has been recently cloned and characterized [141]. Conserved residues in the catalytic core region of HDAC11 share homology with both class I and class II mammalian histone deacetylases [141]. Class III histone deacetylases are encoded by genes similar to the yeast Sir 2 gene [142,143]. These deacetylases are dependent on NAD+ and have ADP-ribosylase activity [144,145,146].

Class I deacetylases are ubiquitously expressed, while class II deacetylases are tissue-, cell- and differentiation-specific [139]. Both classes of deacetylases can deacetylate the four core histones; however, each deacetylase has a site preference [68]. Similar to histone acetyltransferases, the yeast Rpd3 and Hda1 deacetylases exist in distinct multi-protein complexes. Rpd3, which is usually physically associated with SIN3, represses transcription when organized into a 2 MDa co-repressor complex [147-150]. The histone deacetylase Rpd3 preferentially deacetylates lysine 5 of H4 on only a select number of genes [133].

Like histone acetyltransferases, deacetylases are targeted to specific gene regions through their interactions with other repressor proteins. To date, three complexes containing class I histone deacetylases have been characterized. These are the mSin3, NuRD and NCoR/SMRT deacetylase complexes. Both the NuRD and mSin3 complexes contain HDAC1, HDAC2, RbAp46 and RbAp48 [151-153]. However, each complex also contains distinct factors. The mSin3 complex contains mSin3A/B, SAP30 and SAP18 components [151,152,154-158]. In mammals, Sin3 proteins mediate transcriptional repression caused by transcriptional regulators such as the mammalian heterodimeric repressors Mad/Max [154].

The NuRD complex contains the chromatin remodeling factor Mi-2β, MBD3, a methyl DNA binding protein, and MTA2, a factor that modulates the activity of histone deacetylase [151,154,156,158-160]. The NuRD complex is believed to be recruited to methylated DNA in *Xenopus* for transcriptional silencing [161]. This complex also helps make up the MeCP1, a complex that contains MBD2, HDAC1, HDAC2 and RbAp46/48. MBD2 preferentially binds to methylated DNA and, therefore, recruits the MeCP1 complex to methylated DNA regions [162]. Furthermore, the MeCP1 complex binds to, remodels, and deacetylates methylated nucleosomes, thereby causing transcriptional repression [162]. Thus, in some cases, the repression of gene expression involves the interplay between histone deacetylation, chromatin remodeling and DNA methylation.

In the case of steroid action, SMRT or N-CoR complexes are recruited to unliganded steroid receptors. N-CoR directly associates with HDACs 3, 4 and 5 while SMRT can form a complex with HDACs 5 and 7 or HDAC3 [153,163-166]. These complexes indirectly recruit RPD3/SIN3 complexes and the Sin3 protein, in turn, recruits histone

deacetylase [167-169]. In the presence of receptor ligand, this repressor complex is replaced by a histone acetyltransferase complex [167-169].

The existence of histone deacetylases in unique multi-protein complexes suggests that deacetylases have distinct biological functions. Furthermore, the components of these complexes influence the substrate specificity of these enzymes [139]. For example, the free form of avian HDAC1 preferentially deacetylates free but not nucleosomal H3. When assembled into a multi-protein complex, this deacetylase preferentially deacetylates free H2B and histones assembled into a nucleosome [170].

Class I deacetylases reside in the nucleus [139]. However, the sub-cellular distribution of class II deacetylases is not as straight forward. HDACs 4 and 5 shuttle between the cytoplasm and the nucleus [171]. HDAC7 is predominantly nuclear but binds to the membrane-associated endothelin receptor A and most likely functions in the cytoplasm [172]. HDAC6 is strictly cytoplasmic, and HDAC9 appears to be both nuclear and cytoplasmic [173]. HDACs 4, 5, and 7 are transcriptional co-repressors that interact with MEF2 transcription factors as well as the co-repressors N-CoR, BCoR, and CtBP[171,174]. Similarly, HDAC9 interacts with MEF-2 and represses MEF-2-mediated transcription [173]. HDAC10 resides in the nucleus and the cytoplasm [174]. In the nucleus, this deacetylase functions as a transcriptional repressor when tethered to a promoter [174]. Interestingly, HDAC6 can interact with ubiquitin. As well, the mammalian homologue of UFD3, a yeast protein involved in protein ubiquitination, is part of the cytoplasmic mammalian HDAC6 complex [175].

***Histone Acetylation and Chromatin Salt Solubility***

Histones can be modified by several post-translational modifications including acetylation, phosphorylation, ubiquitination, methylation and ADP ribosylation (Figure 8) [4]. As much as one third of the histone N terminal tails are made up of lysine and/or arginine residues [15]. Specific lysine residues within the N terminal tails of the four core histones are subject to dynamic acetylation, a reversible process catalyzed by histone acetyltransferases, which mediate the transfer of acetyl groups on to the ε-amino group of lysine residues located in the N terminal regions of the core histones, and deacetylases, which catalyze the removal of these acetyl groups [176].

In 1964, Dr. Allfrey and colleagues published a study showing that addition of acetylated histones to a calf thymus RNA polymerase preparation inhibited RNA synthesis by as little as 21%, while addition of non-acetylated histones inhibited RNA synthesis by as much as 75% [178]. The results of this study provided a correlative link between histone acetylation and transcriptional activation. Following these observations, Dr. Nelson and colleagues [179] showed that chromatin regions containing rapidly and highly acetylated histones are preferentially digested by DNase I. As well, micrococcal nuclease can attack the linker DNA region of hyperacetylated chromatin more readily than the linker DNA of hypoacetylated chromatin [180]. Other studies have also shown that $Mg^{2+}$-soluble chromatin fractions released from nuclei by nuclease treatment are enriched in both transcriptionally active genes and hyperacetylated histones [181,182]. Furthermore, treatment of chicken immature erythrocytes with sodium butyrate, an inhibitor of histone deacetylase activity, enhanced the amount of transcriptionally active DNA $\beta^A$-globin sequences and hyperacetylated histones solubilized by $Mg^{2+}$ [182].

To confirm that histone hyperacetylation was indeed responsible for the increased solubilization of hyperacetylated histones and the transcriptionally active $\beta^A$-globin gene in the presence of sodium butyrate, soluble polynucleosomes enriched in $\beta^A$-globin were isolated from chicken immature erythrocytes and used as a substrate for yeast histone deacetylase [183]. In the presence of sodium butyrate, the solubilization of these polynucleosomes by $Mg^{2+}$ was drastically decreased when compared to untreated cells. Furthermore, the transcriptionally inactive gene ovalbumin could not be significantly solubilized in the presence or absence of sodium butyrate [183].

From these results, it appeared that chromatin fragments containing transcriptionally active genes are acetylated more than fragments with inactive genes. In support of this, the distribution of hyperacetylated H4 has been shown to closely follow that of the transcriptionally active histone H5 and $\beta^A$-globin genes in different salt-soluble chromatin fractions isolated from chicken immature erythrocytes [184]. Thus, histone acetylation increases both the sensitivity of transcriptionally active genes to nucleases and chromatin fragment salt-solubility. This suggests that histone acetylation facilitates transcription by altering chromatin structure in a manner that increases transcription factor accessibility to target DNA sequences.

However, not all hyperacetylated and transcriptionally active DNA sequences are readily solubilized by salt after partial nuclease digestion. In fact, as much as 76% of the transcriptionally active histone H5 and $\beta^A$-globin gene sequences and 74% of hyperacetylated H4 are associated with the salt-insoluble nuclear material of chicken immature erythrocytes [184]. The association of the majority of transcriptionally active DNA sequences and hyperacetylated histones with the NM may be a consequence of the

transcription process. Nuclear matrices from trout liver and adult chicken immature erythrocytes contain 60-76% of nuclear histone acetyltransferase activity [184]. As well, 75 - 80% of histone deacetylase activity is located within the insoluble nuclear material of chicken immature erythrocytes and 40 - 50% of this activity is associated with the NM [184,185]. Transcription factors such as AML and YY1 have NM-targeting sequences [186-188], and the transcriptional machinery is associated with the NM [189]. The NM-binding capability of certain transcription factors may allow these factors to recruit target genes to transcription sites within the NM. While positioned at the NM, the histones along the gene would become dynamically hyperacetylated by NM-associated histone acetyltransferases and deacetylases.

***Histone Acetylation and Epigenetic Inheritance***

It has also been suggested that histone acetylation plays a role in marking the state of genetic activity or inactivity from one cell generation to the next, thereby epigenetically determining the heritable transcriptional competence of a gene [190]. However, recent evidence shows that catalytically active histone acetyltransferases and histone deacetylases are unable to acetylate or deacetylate chromatin *in situ* during mitosis [191]. Moreover, these enzymes become spatially reorganized and displaced from condensing chromosomes. Instead, it appears that the spatial organization of these enzymes relative to euchromatin and heterochromatin plays an important role in determining the post-mitotic activation of a gene [191].

***Histone Acetylation & Nucleosome Structure***

Originally acetylation of histones was thought to alter nucleosome structure and weaken the interaction of histone N terminal tails with DNA [192,193]. Dr. Norton and colleagues noted that histone acetylation decreases the extent of negative DNA supercoiling around the nucleosome [193]. Histone acetylation also maintains the open conformation of the transcriptionally active nucleosome [50]. Thus, histone acetylation may neutralize the positive charges on the N terminal lysine residues and loosen the contacts between histones and DNA. A disruption in the contacts between DNA and the nucleosome may alter the path of DNA entry and exit into the nucleosome, which may, in turn, affect the interaction of linker histones with nucleosomal and/or linker DNA.

***The Effect of Histone Acetylation on Interactions of Histones with Non-Nucleosomal Proteins***

In addition to disrupting chromatin fiber-fiber interactions, histone acetylation disrupts interactions between histone N terminal tails and non-nucleosomal proteins. H3 and H4 display α-helical structures in their N terminal domains when assembled into a nucleosome or when bound to DNA [67,69]. This observation has lead to the belief that the histone N terminal tails fold upon contact with proteins or DNA [69]. This α-helical character increases upon acetylation [194]. Histone acetyltransferases may positively influence transcription by altering the structure of the N terminal tails and perturbing the interactions of these tails with proteins that repress transcription. However, histone acetylation may also be associated with transcriptional repression since the heterochromatin of several organisms contains H4 acetylated at lysine 12 [195,196]. As well,

loss of the yeast RPD3 histone deacetylase results in an increase in the silencing of telomeric DNA [197].

***The Effect of Histone Acetyltransferases on the Properties of Transcription Factors***

Histone acetyltransferases can also acetylate transcription factors (p53, ACTR, EKLF, ERα, MyoD, GATA-1, E2F1), non-histone chromosomal proteins (HMG), components of the transcription machinery (TFIIE, TFIIF), the nuclear import protein importin, tubulin, and flap endonuclease-1 (Fen-1), an enzyme involved in DNA metabolism [120,198-208]. Histone acetyltransferases capable of acetylating proteins other than histones are, in fact, protein acetyltransferases with putative histone acetyltransferase activity. However, the content of this thesis focuses on histone acetylation. Thus, proteins capable of acetylating histones will be referred to as histone acetyltransferases regardless of their ability to acetylate substrates other than histones. The acetylation of p53 and MyoD increases their binding affinity for DNA [203,209]. As well, acetylation of E2F1 extends the half-life of this protein [208]. Thus, along with modifying chromatin structure, acetyltransferases may function in transcription by altering the DNA-binding properties of transcription factors or enhancing the stability of transcription factors.

The acetylation of HMGI(Y) plays an important role in viral-induced interferon-β gene activation as well as the inactivation of this event [210]. Upon infection, the enhanceosome assembles at the interferon-β gene promoter with the help of HMGI(Y). At the same time, CBP and PCAF are recruited to the interferon-β gene promoter where they acetylate H3 and H4 and, in combination with the enhanceosome, activate

transcription of the interferon-β gene. Following induction, CBP acetylates HMGI(Y) which decreases its DNA binding affinity and causes the disruption of the enhanceosome complex. In addition, the p300 coactivator preferentially acetylates ERα within the hinge/ligand binding domain of this receptor and this event most likely suppresses the sensitivity of ERα to estrogen ligand [120].

***The Effect of Histone Acetylation on Higher Order Chromatin Structure***

In a study of the effects of histone acetylation on transcriptional activity and higher order chromatin folding, 12-mer nucleosomal arrays with 2 or 6 acetate groups per nucleosome folded into similar structures in the presence of 5 mM $Mg^{2+}$ [211]. Up to 28 lysine residues are capable of being acetylated in a nucleosome. The addition of 12 acetate groups to each nucleosome within the array enhanced transcription 15 fold *in vitro* and prevented folding of the array into a higher order structure, showing that a critical level of histone acetylation must be achieved for disruption of a higher order structure [211]. Dr. Ausio and colleagues also observed that acetylated 12-mer nucleosomal arrays have an extended and unfolded structure at 100 mM NaCl when compared to arrays composed of non-acetylated histones [212]. As a result, acetylation of the core histone N terminal tails is thought to facilitate transcription by disrupting chromatin folding and inter-fiber interactions. Such an event may promote transcriptional initiation by increasing the accessibility of transcription factors to target DNA binding sites and/or facilitate transcriptional elongation by maintaining the open structure of active chromatin[50].

***The Effect of Histone Acetylation on H1-Mediated Chromatin Condensation***

The effect of histone acetylation on higher order chromatin structure may be mediated, in part, by H1 phosphorylation. As was previously mentioned, H1 association with linker DNA appears to be a dynamic process [17,18]. The dynamic exchange of H1 molecules is not an event exclusive to transcriptionally active DNA regions. The residence time between exchange events for a H1-GFP fusion protein on chromatin was several minutes for both euchromatin and heterochromatin [18]. However, heterochromatin appeared to be associated with approximately 25% of the statically bound H1-GFP protein molecules within the nucleus while euchromatin was only associated with approximately 10% [18]. In addition, hyperacetylation of the core histones by Trichostatin A (TSA) treatment increased the rate of exchange between bound and mobile H1-GFP molecules, suggesting that core histone hyperacetylation results in the looser binding of H1-GFP to chromatin [18]. In support of this, acetylation of histones was shown to alter the ability of H1 linker histones to condense transcriptionally active chromatin. Histone acetylation also altered the ability of H1 to condense DNaseI-sensitive but transcriptionally inactive chromatin [70]. This type of chromatin is referred to as transcriptionally competent. Thus, core histone hyperacetylation may influence the transcriptional activity of a gene by loosening H1 binding to transcriptionally active chromatin.

The results of a previous experiment also show that the ability of H1 to condense a chromatin fiber containing transcriptionally active/competent genes is hindered [70]. However, the binding of linker histone to chromatin was not affected by the acetylation status of the core histones [213]. H1 was able to associate with transcriptionally active, hyperacetylated chromatin, but its ability to promote fiber condensation was altered [213].

Histone H1 can be phosphorylated on specific serine and threonine residues along its N and C terminal tails. The phosphorylation of H1 weakens its interactions with linker DNA and destabilizes chromatin structure [18,20,21,111]. H1 phosphorylation occurs throughout the cell cycle and is thought to increase the accessibility of DNA to factors involved in transcription, DNA replication and chromatin condensation during the G1, S and M phases of the cell cycle, respectively. Phosphorylation of the mouse H1(S)-3 subtype depends on ongoing transcription and DNA replication [214] and its ability to decondense chromatin is thought to facilitate subsequent rounds of transcription [215]. Mouse H1 and H1(S)-3 are phosphorylated by the cdk-2 kinase [216,217]. Thus, phosphorylation of H1 and H1(S)-3 by factors in the MAP kinase pathway may be responsible for the continuous exchange of H1 on active chromatin and histone acetylation may increase the rate of this exchange.

***Class I & Class II Histone Acetylation and Transcription***

Histone acetylation typically occurs on up to five lysine residues along the H3 N terminal tail, 4 lysines along the H2B and H4 N terminal tails and 2 lysines along the H2A N terminal tail (Figure 8) [8]. Studies of histone acetylation dynamics indicate that both acetylation and deacetylation occur at more than one rate [218,219,220]. In human fibroblasts and mature avian erythrocytes, there are two populations of acetylated histones. The first population, which accounts for approximately 15% of acetylated core histones in hepatoma tissue culture cells, is rapidly hyperacetylated ($t_{1/2}$= 7 to 15 min for mono-acetylated H4) and rapidly deacetylated ($t_{1/2}$= 3 to 7 min). The second population, which accounts for up to 50% of acetylated histones, is slowly acetylated ($t_{1/2}$= 140 to

300 min for mono-acetylated H4) and then slowly deacetylated (t½= 30 min) [218,219]. Similarly, MCF-7 human breast cancer cells also display two populations of acetylated H3, H4 and H2B histones: a rapidly acetylated one comprising 10% of the total nuclear acetylated histones and a slowly acetylated one that includes approximately 50% of acetylated histones [170].

In chicken immature erythrocytes, approximately 2% of the genome is dynamically acetylated, while the rest is either frozen in a state of mono- or di-acetylation or unacetylated [219]. The acetylated histones in chicken immature erythrocytes are divided into two populations. In contrast to chicken mature erythrocytes, both populations within the immature erythrocytes display the same rate of histone acetylation (t½=12 min for monoacetylated H4). However, in the case of H4, one population is hyperacetylated to tri- or tetra-acetylated isoforms and then rapidly deacetylated (t½= 5 min). This type of histone hyperacetylation is referred to as ***class I acetylation***. Another population of acetylated histones, however, is only mono- or di-acetylated, and subsequently deacetylated at a slower rate (t½=90 min).This type of histone hyperacetylation is referred to as ***class II acetylation***.

Similarly, tri- and tetra-acetylated isoforms of H2B are deacetylated in chicken immature erythrocytes within 5 – 10 min after removal of the sodium butyrate deacetylase inhibitor while mono- and di-acetylated isoforms become deacetylated at a significantly slower rate [219]. Acetylated H3 also appears to be rapidly and dynamically acetylated. Tri-acetylated H3 isoforms in sodium butyrate-treated chicken immature erythrocytes displayed a significant drop in levels 5 min after incubation in the absence of

sodium butyrate, while mono- and di-acetylated isoforms levels remained relatively constant for at least 120 min[219].

***Histone Acetylation & the Chromatin Immunoprecipitation Assay (ChIP)***

The ChIP assay has become an important assay in studying the relationship between histone modifications such as acetylation and transcription. In this assay, chromatin fragmented either by sonication or nuclease treatment is incubated with an antibody to a specifically modified histone isoform or a non-histone DNA-binding protein [62,221-223]. The antibody-antigen complexes are then isolated with either protein A or G sepharose and the DNA associated with the antigen is purified from the immune complex and analyzed by either slot blot analysis or PCR. This assay has provided valuable information in understanding the role of histone acetylation in global-, promoter-targeted and coding-region-targeted histone acetylation.

***Global Histone Acetylation***

The exact role of histone acetylation in transcription has been the subject of debate for several decades. Histone acetylation can occur independently of transcriptional activation [224]. Dr. Workman and colleagues have shown that histone acetyltransferases are capable of altering chromatin structure *in vitro* even in the presence of a transcriptional inhibitor [224]. In addition, Dr. Crane-Robinson and colleagues have observed that acetylated lysines are distributed throughout the entire avian erythrocyte β-globin domain which contains transcriptionally active genes, transcriptionally competent genes and intergenic DNA regions [62].

Histone acetylation can be a global phenomenon. Depletion of yeast Esa1, an acetyltransferase specifically recruited to ribosomal protein and heat shock protein gene promoters, causes a dramatic decrease in H4 acetylation over many regions of the genome without affecting the transcription of many genes [134]. Similarly, acetylation of the yeast PHO5 promoter by Esa1 and Gcn5 and the subsequent deacetylation of this region by HDA1 and Rpd3 results in the widespread histone acetylation and deacetylation of three separate chromosomal regions that make up 22 kb of DNA [123]. These observations and the studies by Dr. Workman and Dr. Crane-Robinson suggest that histone acetylation is not always directly involved in transcription or the immediate preparation of chromatin for transcription [62]. Instead, histone acetylation can cause the chromatin structure of the chicken β-globin domain to assume an open conformation that leaves the genes within this domain accessible to transcription factors [62]. Alternatively, histone acetylation may promote the recruitment of genes to nuclear domains enriched in histone acetyltransferase activity.

The widespread acetylation of histones over several kilobases of DNA or within entire regions of the nucleus is most likely mediated by the localization of transcriptionally active or competent genes to nuclear regions of histone acetyltransferase activity. The nucleus is a highly organized structure. For example, nuclear DNA is organized into discrete chromosome territories during interphase [225-228]. In fibroblasts, heterochromatin, which is depleted in acetylated histones, lines the surface of the nuclear lamina and the nucleolus and defines the boundaries for interchromatin granule clusters (IGCs) [229]. IGCs are clusters of ribonucleoproteins that lie close to transcription sites, contain RNA and are rich in splicing factors [229,230]. These clusters do not contain nascent

transcripts, engaged RNA polymerase II or acetylated histones [231]. Acetylated histones and the histone acetyltransferases $TAF_{II}250$ and CBP are enriched in nuclear regions next to IGCs and excluded from the nuclear periphery and perinucleolar regions [229]. Dynamically acetylated chromatin localized to the periphery of IGC-like chromatin-depleted regions can contain transcriptionally active and competent DNA sequences [229]. However, the localization of active and competent sequences to the periphery of IGCs does not always occur [229]. The histone acetyltransferase CBP is also a dynamic component of promyelocytic leukemia protein (PML) bodies which are ring-shaped nuclear structures composed of PML protein, retinoblastoma protein (Rb), Sp100 and PIC1/SUMO-1 [232,506]. Lastly, histone deacetylases are localized into NM-associated nuclear bodies containing the transcriptional co-repressors SMRT and N-CoR [233].

The majority of studies on histone acetylation have studied only the steady state nature of this event. However, as was previously mentioned, histone acetylation associated with transcription is a dynamic event with a short half-life (several minutes) that is mediated by both histone acetyltransferases and histone deacetylases. Thus, histone acetyltransferases and histone deacetylases are most likely targeted to the same regions of the genome. With this to consider, more attention must be given to understanding how acetyltransferases and deacetylases function together at specific sites along transcriptionally active genes to fully appreciate the role of dynamic histone acetylation in transcription.

Nuclear fractionation studies performed on chicken immature erythrocytes have shown that the nuclear distribution of class I, but not class II, acetylated histones closely follows that of the transcriptionally active $\beta^A$-globin and histone H5 genes [184]. The

majority of histone acetyltransferase and deacetylase activity, class I acetylated histones, and transcriptionally active $\beta^A$-globin and histone H5 DNA sequences are located in the insoluble nuclear material which contains the NM [4,184,189,234].

Similar to the histone acetyltransferases CBP and $TAF_{II}250$, the histone deacetylase HDAC1 is excluded from the immediate nuclear periphery, preferentially localized along the periphery of condensed chromatin regions and enriched in nuclear regions containing IGCs that are depleted in chromatin [229]. The widespread distribution of histone acetyltransferases and histone deacetylases may also maintain a balance between acetylated and deacetylated histones throughout the genome or regions of the genome and this may prevent the histones along genes from becoming transiently or permanently fully acetylated.

Transcriptionally active genes are enriched in the NM [184,235-238]. However, the association of these genes with the NM is dynamic [239]. DNA sequences most frequently attached to the NM are associated with the NM less than 50% of the time [239]. Transcription factors form foci throughout the nucleus and several transcription factors have NM-targeting DNA sequences [65,187,240]. Foci containing transcription factors are positionally stable over short intervals of time and are capable of moving to nearby foci over longer time periods [65]. In the absence of ligand, the CFP-ERα fusion protein is highly mobile [241]. Addition of estrogen slows down CFP-ERα mobility for only a few seconds and CFP-ERα mobility is quickly regained, suggesting that ERα dynamically interacts with insoluble nuclear components in the presence of estrogen. In support of this, ERα can be cross-linked to DNA by cisplatin, an agent that preferentially cross-links NM proteins to DNA and the treatment of MCF-7 breast cancer cells with estradiol

causes ERα and the histone acetyltransferase SRC-1 to associate with the NM [170,242]. IGCs are also continually exchanging some of their components with the surrounding nucleoplasm [65]. Thus, domains of histone acetyltransferases and histone deacetylases may act on chromatin within their proximity, causing the recruitment of a transcriptionally active gene to the NM and to foci enriched in transcription factors. The proximity of a gene to regions of histone acetyltransferase and histone deacetylase activity may influence the acetylation status of histones along specific regions of transcriptionally active genes. Genes located close to regions of high acetyltransferase activity would be more frequently acetylated than deacetylated and regions close to deacetylases would be deacetylated more often than acetylated.

***Promoter Localized Histone Acetylation***

Dynamic histone acetylation is not only a global phenomenon within the nucleus. Nucleosomes bound to a DNA template can inhibit transcription by masking and preventing the access of transcription factors to certain DNA sequences. In a study performed by Dr. Workman and colleagues, the assembly of nucleosomes onto a DNA template repressed transcription *in vitro* and this repression could not be reversed by target transactivators [243]. However, transcription of this nucleosomal array was activated when acetyltransferases were present [243]. H3 acetylation at Lys-14 of the interferon-β promoter also correlates perfectly with TBP recruitment and transcription initiation [90]. As well, severe hypoacetylation of H3 in the coding region of several genes displays a strong correlation with reduced transcription levels in yeast cells deficient in both Gcn5 and Elp-3 histone acetyltransferases [244]. Thus, histone acetylation plays a direct role in transcription or the immediate preparation of chromatin for transcription.

Studies using the ChIP assay have shown that the promoter region of a gene becomes hyperacetylated in response to transcriptional stimulation [167,168,199,210,245-248]. In several cases, histone acetylation was localized only to the promoter region of the transcriptionally active gene and was not induced along regions further downstream. The yeast Sin3-Rpd3 histone deacetylase complex when recruited to a repressed promoter causes histone deacetylation over a 1-2 nucleosome range [247]. Similarly, transcriptional activation of the human interferon-β gene by virus infection was shown by the ChIP assay with anti-acetylated H3 and H4 antibodies to induce histone hyperacetylation over 2-3 nucleosomes within the promoter region [210]. Furthermore, the yeast Gcn5 histone acetyltransferase complex has been shown to acetylate histones H3 and H4 only within a 1 kb region in the *HO* gene promoter [248].

In a recent study, the CpG island of the transcriptionally active chicken carbonic anhydrase gene was found to be associated with higher levels of acetylated histones compared to the near-by promoter region [249]. The acetylation of H3 and H4 along this gene was greatest at the CpG island and showed a drastic drop at approximately 1.5 kilobases into the transcribed region. Similarly, the chicken thymidine kinase gene displayed elevated levels of hyperacetylated histones along its CpG island [250]. High levels of hyperacetylated histones were also mapped to the chicken GAPDH promoter, which is located within a CpG island [249]. The regions downstream of this promoter that do not contain CpG islands displayed a sharp drop in the levels of hyperacetylated H3 and H4. As well, chromatin fragments containing CpG islands are enriched in highly acetylated H3 and H4 isoforms [63]. These findings suggest that histone hyperacetylation is a feature of CpG islands.

The significance of histone acetylation along CpG islands is unknown. In one study, TSA-induced histone acetylation facilitated DNA demethylation of an ectopically methylated pMetCAT fusion construct transfected into HEK 293 cells [251]. Because the interaction of demethylase with DNA is thought to be the limiting step in DNA demethylation, the acetylation of histones associated with CpG islands may increase the accessibility of demethylase to its target DNA sequence [251]. Contrary to these observations, another study showed that DNA demethylation preceded both transcriptional re-activation and histone acetylation of the endogenous hMLH1 promoter in human colorectal cancer cell lines [252]. As well, the methyl DNA-binding protein MeCP2 binds histone deacetylases and recruits these enzymes to methylated DNA where they deacetylate associated histones and generate a repressive chromatin structure [239,253]. However, the promoter DNA sequences of many genes are not methylated [254]. For example, the CpG island of the *Aprt* gene is protected from methylation, presumably by the presence of Sp1 binding sites at the 5' end of the CpG island and the presence of transcription factor(s) that binds to these sites [255].

**Promoter-Targeted Histone Acetylation Occurs in Estrogen-Mediated Transcriptional Activation**

In estrogen-mediated transcriptional activation, the binding of estrogen to ERα causes a conformational change in this receptor molecule that allows the estrogen-ERα complex to bind to estrogen responsive elements (EREs) within the promoter regions of estrogen-responsive genes [199,256,257]. Once bound to the ERE, the estrogen-ER complex

recruits histone acetyltransferases that acetylate histones associated with the promoter[167,168,199].

Dr. Sun and colleagues have shown that exposure to estrogen reduces the rate of histone deacetylation in MCF-7 human breast cancer cells without altering the sub-nuclear location, level or activity of class I and II histone deacetylases [170]. Instead, estrogen alters the distribution of ERα and histone acetyltransferases such as SRC-1 and SRC-3 within these cells by causing both types of factors to become tightly associated with the NM [170,241,258]. Thus, binding of estrogen to the ERα alters the balance between histone acetyltransferases and histone deacetylases sites such that more histone acetyltransferases are recruited to these sites than histone deacetylases. This suggests that estrogen-mediated histone acetylation of estrogen-responsive promoters is a dynamic event that occurs in a background of histone deacetylase activity (Figure 9).

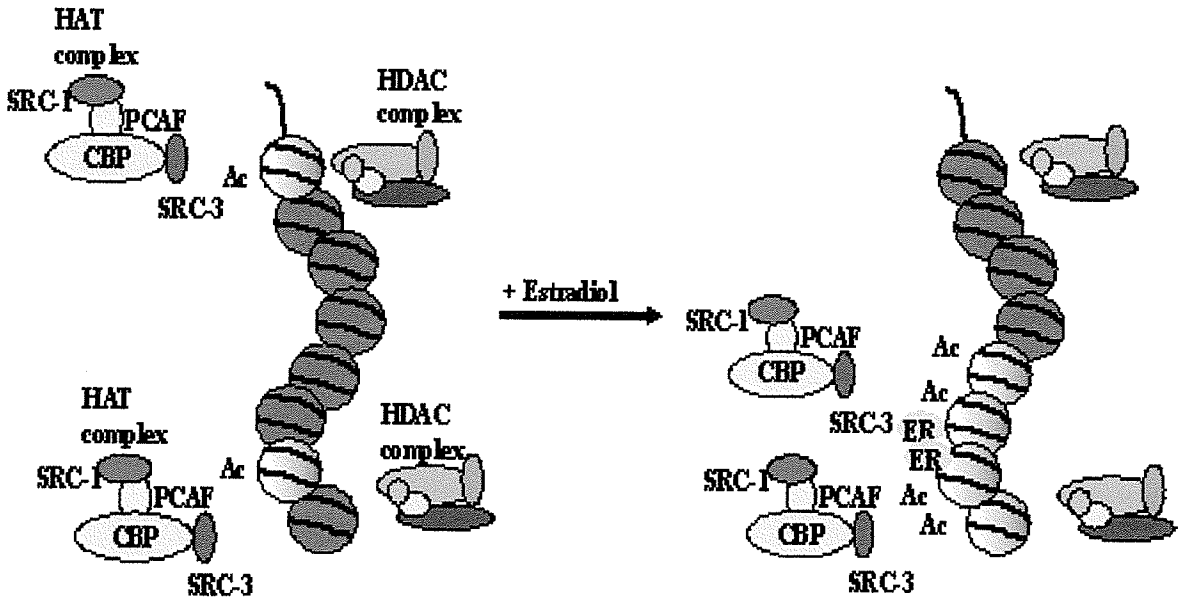


**Figure 9.** **Proposed Model for the Effect of Estradiol on the Distribution of Histone Acetyltransferases and Histone Deacetylases in Human Breast Cancer Cells.** In the absence of estradiol (left), histone acetyltransferases (HAT) such as CBP, SRC-1, SRC-3, and PCAF occupy the same chromatin regions as histone deacetylases (HDACs) such as HDAC1 and HDAC2. Upon addition of estradiol (right), the ER is recruited to NM sites and associates with the ERE in the promoter region of estrogen responsive genes. When bound to estradiol, ERα recruits histone acetyltransferases from other nuclear regions, thereby altering the balance of histone acetyltransferases and deacetylases along specific chromatin regions.

Considerable investigation has been made into the role of histone acetyltransferases in estrogen-mediated transcriptional activation, while little is known of the direct involvement of histone deacetylases. Exposure of MCF-7 human breast to estrogen promotes the temporal and cyclical association of histone acetyltransferases with the promoter region of estrogen-responsive genes [168,245]. Within 15-20 min following estradiol exposure, ERα and the histone acetyltransferases AIB1 and p300 associate with the estrogen-responsive cathepsin D promoter. RNA polymerase associates shortly following this event. This association most likely initiates transcription since significant levels of transcription are observed 45 min after estrogen stimulation. The association of these factors then starts to decline 60 min from the initial time of estrogen treatment. A few minutes before these factors are removed, the levels of CBP and PCAF histone acetyltransferases associated with the cathepsin D promoter start to rise and peak between 60 and 75 min. CBP can acetylate AIB1 and this event has been shown to cause the dissociation of p160 coactivator complexes from the promoter-bound ERα [199]. Thus, the binding of CBP to the cathepsin D promoter after 60 min of estrogen treatment may be responsible for the dissociation of AIB1 from ERα at this time point. In support of this, transcription of the cathepsin D gene is significantly reduced after 75 min of estrogen treatment. After 90 min of estrogen treatment, the levels of CBP and PCAF sharply drop. Then 10 – 15 min later, ERα, AIB1, CBP and PCAF all assemble on the promoter in the same order as before and the rate of transcription once again increases.

In a similar study performed by Dr. Burakov and colleagues [245], the cyclical association of ERα and its p160 coactivators with the pS2 promoter was not as evident[245]. Compared to the observations in the previous study, slight differences in the order and

timing of cofactor association were observed [245]. As well, CBP, AIB1 and p300 did not return to the promoter to any great extent after their initial removal. In this study, the treatment of MCF-7 cells with estrogen resulted in the recruitment of CBP, p300, ERα, SRC-1 and AIB1 to the pS2 promoter after 30 min. The simultaneous recruitment of CBP and AIB1 argues against the theory that acetylation of AIB1 by CBP causes its dissociation from ERα. The level of AIB1 then dropped after 30 min, followed by CBP after 60 min. The level of p300 remained constant for 90 min and began to decrease after 105 min. In addition, the level of ERα remained relatively constant over 150 min of estrogen treatment although a slight decrease was evident between the 105 - 120 min time points [245]. Of interest, however, was the observation that a second coactivator complex composed of DRIP proteins that do not have histone acetyltransferase activity was recruited to the promoter just as the level of p300 started to drop. Thus, instead of the cyclical binding of the same coactivators, transcriptional activation of the pS2 gene appeared to involve the sequential recruitment of different coactivator complexes.

An interesting observation made by Dr. Burakov and colleagues was that ERα, CBP, p300, ACTR, SRC-1 and DRIP 205 are recruited to the pS2 promoter in MCF-7 cells within 2.5 min of estradiol treatment [245]. This recruitment is accompanied by a simultaneous increase in the level of acetylated H4 along the pS2 promoter [245]. Thus, estrogen-induced histone acetylation is a rapidly induced event.

These studies on estrogen-induced histone acetylation provide valuable information about the involvement of histone acetylation in transcription initiation. However, they fail to consider that histone acetylation is a dynamic process mediated by both histone acetyltransferases and histone deacetylases. In a recent study, the treatment

of MCF-7 cells with 100 nM E2 for 45 min caused a decrease in the levels of HDAC2 and HDAC4 associated with the c-*myc* and cathepsin D estrogen-responsive promoters in MCF-7 cells, while ERα, SRC-1, AIB-1, CBP and acetylated H4 levels were increased[167]. However, the dissociation of HDAC2 and HDAC4 was not complete [167]. This agrees with the findings of Dr. Sun et al. [170] and further supports the theory that estrogen treatment promotes the recruitment of histone acetyltransferases to estrogen-responsive promoters without affecting histone deacetylase nuclear localization or activity. Thus estrogen-induced histone acetylation of estrogen-responsive promoters most likely occurs in a background of histone deacetylase activity.

**Promoter-Targeted Histone Acetylation Assists Chromatin Remodeling**

Besides playing a role in transcription factor binding, promoter-directed histone acetylation may also be fundamental for ATP-dependent chromatin remodeling. This type of remodeling uses ATP hydrolysis as a source of energy to alter nucleosome and chromatin structure and enhance transcription factor binding to nucleosomal DNA-binding sites [139]. While chromatin remodeling complexes can alter the chromatin structure of trans-activator binding sites, they are unable to activate transcription alone[259]. The recruitment of the SWI/SNF chromatin remodeling complex to nuclear receptor- and BRCA1-regulated genes is thought to increase nucleosome fluidity and facilitate the subsequent binding of transcription factors to affected regions [260]. ChIP assays have revealed that deletion of the SWI/SNF ATPase subunit, SWI2, results in a decrease in the level of Gcn5-dependent H3 acetylation along the HO TATA box in yeast [248]. In HO gene expression, ChIP assays have shown that binding of the far-upstream transactivator

protein Swi5p to its cognate DNA recognition site is followed by SWI/SNF and then SAGA recruitment to the HO gene promoter [261]. These two factors then facilitate the binding of a second activator called SBF, which is thought to recruit TBP and other components of the pre-initiation complex [260,261].

ATP-dependent chromatin remodeling is also involved in transcription repression[139]. Because of this, ATP-dependent chromatin remodeling complexes are thought to increase the rate at which a chromatin region fluctuates between an active and repressed structure [262]. If factors are present that stabilize chromatin structure and promote transcriptional repression, then the remodeling complex will drive the chromatin into a repressed state by allowing the transcriptional repressors to associate with the chromatin. However, if transcriptional activators are able to bind to the remodeled chromatin, then the remodeling complexes will drive the chromatin structure to a transcriptionally active state. The subsequent binding of histone acetyltransferases and activating complexes to this chromatin structure will then "fix" the chromatin into an active state [262].

However, ChIP assays on the IFN-β promoter in HeLa cells transfected with the Sendai virus show that ATP-dependent chromatin remodeling complexes do not always bind chromatin before histone acetyltransferases [263]. The IFN-β enhanceosome assembles at a nucleosome-free enhancer region of this gene and initially recruits Gcn5 to acetylate the nucleosome positioned over the TATA box and transcription start site [263]. This event is followed by the recruitment of the CBP-Pol II holoenzyme complex which is followed by SWI/SNF recruitment [263]. The BRG1 subunit of the SWI/SNF complex contains a bromodomain that can interact with acetylated histones [264-266]. The presence of

acetylated histones along a promoter may increase the affinity of the SWI/SNF complex to this gene region. The *in vitro* binding affinity of SWI/SNF to a nucleosome array was greater when the array was reconstituted with hyperacetylated histones purified from sodium butyrate-treated cells as opposed to histones from control untreated cells [267]. Furthermore, the acetylation of histones assembled onto nucleosomal arrays by the SAGA and NuA4 histone acetyltransferase complexes increased the *in vitro* binding affinity of SWI/SNF [267]. Acetylation of Lys-8 histone H4 is a prerequisite for enhanceosome-dependent SWI/SNF and TFIID recruitment along the IFN-β promoter [90]. This suggests that site-specific acetylation, and, therefore, the generation of a histone acetylation code along the IFN-β promoter plays an important role in transcriptional initiation of the IFN-β promoter. Lastly, Gcn5-mediated histone acetylation along the PHO5 promoter has also been shown to increase the rate of PHO5 gene induction by accelerating chromatin remodeling [268]. The order of recruitment for chromatin-remodeling activities and the function of these complexes in gene activation or repression are most likely gene-specific and dependent on the combination of transcription factors bound to the promoter.

**The Function of Promoter-Targeted Histone Acetylation**

The exact function of promoter-targeted histone acetylation in transcription is unknown. Some researchers speculate that promoter-targeted histone acetylation alters chromatin structure and increases transcription factor accessibility to cognate recognition sites, while others believe that histone acetylation at specific lysine residues along the core histone N terminal tails acts in concert with additional histone post-translational

modifications at other residues to generate a histone code that can be recognized by specific transcriptional regulatory proteins [88-90,269,270].

Many different acetylated isoforms of the core histones can exist and each isoform can be modified further by the methylation of selected lysine or arginine residues and/or the phosphorylation of serines residues [270]. Many chromatin-associated proteins contain a bromodomain that interacts with acetylated histone N termini [115]. Thus, thousands of histone isoforms containing different combinations of tail modifications can mark the nucleosome surface, creating recognition sites for transcription factors [270]. For example, Gcn5-induced acetylation of H4 at Lys-8 mediates the recruitment of SWI/SNF while acetylation at H3 Lys-9 and Lys-14 is critical for TFIID recruitment [90]. The acetylation of histone H4 Lys-8 is also a prerequisite for enhanceosome-dependent SWI/SNF and TFIID recruitment along the IFN-β promoter [90].

As well, CBP recruitment to the pS2 promoter in MCF-7 cells in response to estrogen treatment causes acetylation at Lys-18 of H3 followed by acetylation at Lys-23 [108]. The acetylation of Lys-23 by CBP tethers recombinant CARM to the N terminal tails of H3 [108]. Thus, CBP-mediated acetylation of H3 at Lys-18 and Lys-23 leads to the recruitment of CARM1 which, in turn, methylates H3 at Arg-17 [108]. CBP also interacts with many histone acetyltransferases, transcription factors and SWI/SNF [105,113,118,129,271]. Thus, the histone code generated by the initial recruitment of histone acetyltransferases, histone methyltransferases and histone phosphatases to the promoter region of specific genes can lead to the subsequent binding of additional regulatory factors and the formation of multi-protein complexes along the promoter regions of transcriptionally stimulated genes [90,113]. The degree to which multiple histone acetyltransferases and

histone deacetylases with different substrate specificities are recruited to a specific gene region will determine the extent of histone acetylation at specific lysine residues along the core histone N terminal tails. This will, in turn, determine whether the histones along a gene region are class I or class II acetylated.

***Histone Acetylation Along the Coding Region***

Histone acetylation is not always localized to the promoter regions of genes. Fine-mapping studies determining the distribution of acetylated histones or acetylated lysine residues have shown that histone acetylation can extend into the coding region of a gene. H4 acetylated at Lys-16 is distributed along the entire length of X-linked genes targeted by the male-specific lethal dosage compensation [272,273]. As well, the chicken $\beta^A$-globin gene displays high levels of widespread H3 and H4 acetylation [249]. Acetylated lysine residues are also located throughout the c-*myc* gene in Raji BL cells [246]. Histones associated with the promoter and coding regions of the c-*jun* and c-*fos* genes are hyperacetylated in quiescent fibroblasts treated with the histone deacetylase inhibitor TSA [92]. Dr. Freedman and colleagues have also shown that both the pS2 promoter and a downstream open reading frame are associated with acetylated H4 in MCF-7 cells treated with estrogen [245].

**The Function of Histone Acetylation Along the Coding Region**

The packaging of DNA into chromatin can hinder the access of RNA polymerase to a gene. Even the presence of a single nucleosome along a DNA sequence can create a strong barrier to RNA polymerase II *in vitro* [44]. Studies have shown that the nucleosomes of a transcribed DNA sequence have an altered shape and/or composition [45,53,55].

Moreover, the chromatin structure of transcriptionally active and competent genes is different. Transcriptionally active and competent genes have an increased sensitivity to DNaseI when compared to inactive genes and the distribution of acetylated histones correlates with that of DNaseI-sensitive regions in the adult chicken β-globin domain [62].

The association of hyperacetylated histones with regions downstream from the promoter suggests that histone acetylation may function in transcriptional elongation. Elp3, a 60-kilodalton subunit of the elongator/RNAPII holoenzyme has histone acetyltransferase activity and is able to acetylate all four core histones *in vitro* [51]. This histone acetyltransferase activity is essential for the elongator function of Elp3 *in vivo* [274]. Furthermore, the removal of Gcn5 and Elp3 acetyltransferase activity from yeast cells causes widespread transcription defects [274]. Gcn5 functions in the transcription of only a subset of genes. Therefore, Elp3 histone acetyltransferase activity must be important for the transcriptional elongation of a significant number of genes.

In a recent study, Gcn5 Elp3 yeast mutants displayed significantly reduced RNA polymerase II levels that were reflected by low STE6 RNA levels and critically low levels of acetylated H3 along the coding region of the STE6 gene [244]. Only severe (4-5 fold) histone H3 hypoacetylation along the STE6 coding region, but not the promoter region, correlated with inhibition of transcription [244]. Moreover, transcriptional inhibition did not correlate with hypoacetylation of any individual N terminal H3 lysine residue along the STE6 coding region but instead correlated with average overall H3 hypoacetylation [244]. Thus, acetylation of gene coding regions by Gcn5-containing (SAGA) and Elp3-containing (Elongator) histone acetyltransferase complexes likely increases the transcriptional elongation efficiency of RNA polymerase II by making the

chromatin structure of regions downstream from a promoter more permissive to the elongation machinery. Elp3 associates with RNA polymerase II [51]. Elp3-induced widespread histone acetylation along the coding region of a gene is most likely accomplished through this association.

As a result, a cell may contain two types of histone acetyltransferases with respect to the transcriptional process: those involved in initiation and those involved in elongation. Histone acetyltransferases required for the initiation process would enhance transcription factor binding to promoter/enhancer target regions, while acetyltransferases required for elongation would maintain the open nucleosome structure and possibly enhance elongation efficiency by increasing the accessibility of elongation factors to coding regions. In support of this theory, the p300 histone acetyltransferase interacts specifically with the initiation-competent form of RNA polymerase II, while PCAF interacts with the elongation-competent form [52].

Transcriptional elongation is also influenced by ATP-remodeling complexes, PCAF, Elongator and FACT [269,275]. The Elongator complex contains the Elp3 histone acetyltransferase [276]. Both the Elongator complex and the PCAF histone acetyltransferase are associated with the elongating, hyperphosphorylated form of RNA polymerase II [52,276]. The FACT complex is also associated with RNA polymerase II [48,276]. This elongation complex may facilitate transcriptional elongation by transiently binding to and dissociating histones H2A and H2B from nucleosomes [49,269]. A subpopulation of SWI/SNF co-immunoprecipitates with RNA polymerase II *in vitro* [52]. ATP-dependent chromatin remodeling proteins most likely disrupt histone-DNA contacts within nucleosomes and increase the accessibility of RNA polymerase II to gene coding regions.

During transcriptional elongation, the FACT complex may disrupt the structure of the octamer and cause transient dissociation of an H2A-H2B dimer from the nucleosome as the RNA polymerase II complex enters the nucleosome. After nucleosome disruption, histone acetylation induced by histone acetyltransferases associated with RNA polymerase II most likely maintains the unfolded and open structure of the transcribed nucleosome [50]. Nucleosomes with an exposed H3 cysteine thiol group are enriched in dynamically acetylated histones and associated with transcriptionally active DNA sequences [50,54,277,278]. Dr. Davie and colleagues observed that thiol-reactive nucleosomes are not found in chromatin fractions containing transcriptionally active nucleosomes that have been isolated from chicken immature erythrocytes treated with an inhibitor of transcription elongation [50]. Moreover, thiol-reactive H3 sulfhydryl groups could not be detected in chicken immature erythrocytes unless they were treated with an inhibitor of histone deacetylase activity [50]. The ability of histone acetylation to maintain the structure of the open nucleosome along gene coding regions most likely facilitates subsequent rounds of transcription.

While much has been learned about the relationship between histone acetylation and transcriptional elongation, little is known about the dynamics of this event. Dr. Mahadevan and colleagues have shown that the promoter and coding regions of the immediate early c-*jun* are associated with dynamically acetylated H3 and H4 histones in quiescent mouse fibroblast cells [92]. Transcriptional stimulation of the c-*jun* gene also results in an increase in the levels of acetylated H3 and H4 associated with these gene regions [92]. This suggests that histone acetyltransferases and histone deacetylases are continually targeted to the promoter and coding regions of the c-*jun* gene in the absence

of transcriptional stimulation. The equilibrium between histone acetyltransferases and histone deacetylases along these gene regions is most likely altered upon transcriptional stimulation such that the level of histone acetyltransferases recruited to these regions exceeds the level of histone deacetylases.

***The β-globin loop domain***

The β-globin loop domain has served as a useful gene model for understanding the relationship between transcriptional activation and changes in chromatin structure. In avian embryonic development there are three generations of erythroid cells: cells made from primitive erythropoiesis in the yolk sac, cells made from definitive erythropoiesis in the yolk sac and cells made from definitive erythropoiesis in the bone marrow [280]. In chicken red blood cell nuclei, the β-globin domain contains four genes (ρ-, ε-, $\beta^{H-}$ and $\beta^{A}$-globin) that are divided into embryonic and adult functional domains (Figure 10) [281]. The embryonic domains containing the ρ- and ε-globin genes are separated by a stretch of adult DNA containing the $\beta^{H-}$ and $\beta^{A}$-globin genes [281]. All genes within the chicken erythroid β-globin domain are independent transcription units [282].

During primitive erythropoiesis, the ρ- and ε-globin genes are expressed in chicken erythroid cells from a primitive lineage that is present at days 2 - 5 of embryo development [282,283]. As the embryo develops, a complete change-over occurs in erythroid cell lineage. Primitive erythroid cells expressing the embryonic ρ- and ε-globin genes are replaced by two cohorts of non-primitive cells that transcribe both embryonic and adult $\beta^{H-}$ and $\beta^{A}$-globin genes between days 6 and 11 [282,284]. By day 12 in embryonic

development, a definitive erythroid cell lineage that expresses only adult globin genes emerges and replaces all previous lineages [284].

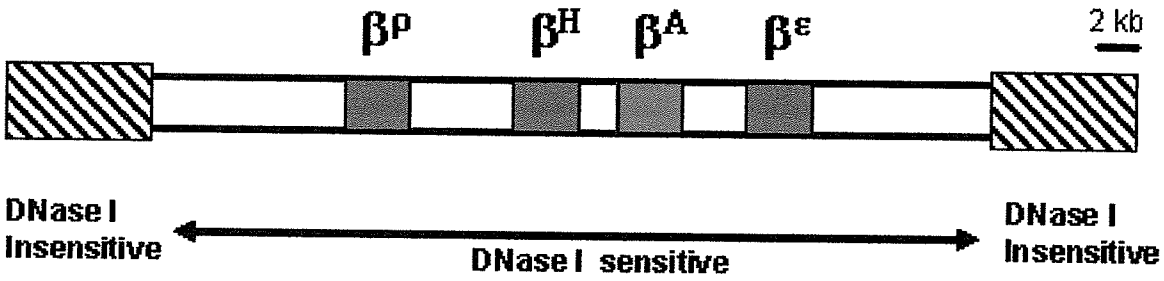


**Figure 10. Diagram of the Chicken Erythrocyte β-globin Domain Showing Regions of DNase I Sensitivity and Insensitivity.** $\beta^{\rho}$, $\beta^{H}$, $\beta^{\varepsilon}$ and $\beta^{A}$ represent the embryonic rho-, hatching-, epsilon- and the adult β-globin genes, respectively.

During definitive erythropoiesis in the blood and bone marrow, the erythroid cells differentiate into erythroblasts which differentiate into early-, mid- and late-polychromatic reticulocytes [280]. These reticulocytes are referred to as immature erythrocytes [280]. The reticulocytes then further differentiate into mature erythrocytes. The amount of RNA in mature erythrocytes decreases 20-100 times below the levels found in early erythroblasts and reticulocytes that still actively synthesize RNA [280,285]. Thus, mature erythrocytes are considerably less transcriptionally active than immature erythrocytes. For this reason, immature erythrocytes are often used instead of mature erythrocytes to study transcription. However, definitive erythropoiesis is a continuous and steady-state process [280]. Therefore, cells at different stages of development are

produced simultaneously. To ensure that the population of cells in a chicken's blood is mostly immature, chickens are treated with phenylhydrazine, an agent that induces anemia [286,287]. The treatment of red blood cells with phenylhydrazine results in the formation of hydrogen peroxide [287]. Hydrogen peroxide oxidizes the sulfhydryl groups of enzymes and peroxidizes membrane lipids [287]. Compared to mature erythrocytes, reticulocytes contain higher levels of enzymes such as glucose-6-phosphate dehydrogenase and catalase that are required to detoxify hydrogen peroxide [286]. Thus, reticulocytes are less susceptible to hydrogen peroxide and the majority of circulating red blood cells remaining in a chicken after phenylhydrazine treatment are immature.

***Histone Acetyltransferases & Deacetylases in Cancer Development***

The role of histone acetyltransferases and deacetylases in cancer development has become more apparent in the past few years. The most obvious case where histone acetylation plays a role in cancer development involves the development of leukemia. In normal immature myeloid cells, retinoic acid (RA) stimulates differentiation through the actions of the retinoic acid receptor (RAR) [288]. In the absence of RA ligand, RAR forms a heterodimer with the retinoid X receptor (RXR). This dimer binds to specific promoters and recruits a co-repressor complex containing N-CoR, SMRT, mSin3A and HDAC1 [289,290]. Thus, in the absence of ligand, RAR target genes are repressed by histone deacetylation. In the presence of ligand, the RAR-RXR heterodimer releases its deacetylase complex and binds to CBP and p300 histone acetyltransferases which in turn recruit PCAF and promote transcriptional events leading to cell differentiation [291-293].

In acute promyelocytic leukemia (APL), the gene encoding RARα is disrupted [288]. In most APL cases, chromosomes 15 and 17 are translocated, forming a fusion protein

containing RARα fused to the N-terminal portion of the promyelocytic leukemia protein[294]. This fusion causes the RARα protein to become unresponsive to physiological levels of RA [288,295,296]. APL can also develop when the RARα protein fuses to the promyelocytic leukemia zinc finger (PLZF) protein [260]. PLZF is required for limb and skeletal development and is a co-repressor protein that binds to histone deacetylases[260,297]. The formation of this RARα-PLZF fusion protein causes the RARα to become resistant to RA [260]. Both forms of APL are treated with RA and TSA [295]. Thus, the development of APL shows that aberrations in histone acetyltransferase and deacetylase recruitment to specific genes can cause abnormalities in cell growth.

Histone deacetylases are also important for normal cell proliferation. The retinoblastoma tumor suppressor gene produces Rb protein. When dephosphorylated, this protein binds to E2F, a transcription factor involved in DNA replication during S phase[298]. This interaction inhibits the function of E2F, thereby causing E2F-target genes to be repressed during G1. Rb also associates with HDAC1 and both proteins have been shown to cooperate with one another in the repression of an E2F-1-driven promoter[298,299]. Exposure to inhibitors of histone deacetylases leads to upregulation of E2F target genes[298]. This observation and the fact that the majority of Rb mutations found in human tumors occur in the domain that interacts with HDAC1 suggests that aberrations in the targeting of histone deacetylases to specific genes can help transform a normal cell into a cancer cell [154].

In a recent study, heregulin-β1 protein levels were shown to be induced by metastatic associated protein 1 (MTA 1), a component of histone deacetylase and nucleosome remodeling complexes [300]. Heregulin-β1 is a protein involved in the

heregulin/HER2 pathway. In ERα positive breast cancer cells, the activation of this pathway suppresses ERE-driven transcription and causes the cell to lose its estrogen responsiveness. Loss of estrogen responsiveness is believed to be a main event in breast cancer disease progression that contributes to the development of a further advanced and invasive cancer cell phenotype. MTA-1 directly interacts with HDAC1, HDAC2 and ERα, and the overexpression of MTA-1 in breast caner cells is correlated with an increase in both invasive behavior and anchorage-independent growth [300]. In addition, treatment of breast cancer cells with the histone deacetylase inhibitor, TSA, blocks MTA-1-mediated repression of ER responsive genes containing EREs. Thus, histone deacetylases are also important in cancer development and the acquisition of an invasive phenotype.

Aberrant expression of histone acetyltransferases can also result in the development of various diseases. The loss of one allele of CBP has also been shown to be responsible for the development of Ruberstein-Taybi syndrome and to leave affected individuals prone to cancer development [68,154]. Somatic translocations involving the CBP gene are found in various forms of leukemia [301]. Furthermore, heterozygous mice mutants for CBP display defects in development and a high incidence of hematological malignancies, suggesting that CBP functions as a tumor suppressor [302,303].

In addition to CBP, the histone acetyltransferase p300 is also important for cell development. P300 double knock-out mice die early after gestation and display abnormalities in cell proliferation and heart development, as well as neurulation [304]. Considerable embryonic lethality can also be observed in single knock-out mice [304].

CBP also appears to be an important factor in breast cancer development. When compared to normal breast tissue, CBP is upregulated in human breast tissue [305]. As well,

the histone acetyltransferases TIF 2 and AIB1 are amplified in human breast tumors [305-307]. Both histone acetyltransferases help mediate estrogen-induced transcriptional activation. Furthermore, evidence exists to suggest that the nuclear receptor corepressor N-CoR is downregulated in invasive breast tumors [305]. In addition to these findings, researchers have also identified an upregulation in the level of ER coactivators such as SRA and PELP1 in human breast tumors [307,308]. Thus, breast cancer development may result, in part, from the upregulation of ER coactivators and the downregulation of ER corepressors.

Based on research findings accumulated to date, it appears that alterations in the equilibrium between histone acetyltransferases and deacetylases are most likely involved in the generation and suppression of various cancers and diseases. In support of this, the development of Huntington's disease is caused by a mutant form of the huntingtin protein, Htt, which binds to and inhibits the activity of the histone acetyltransferases CBP and PCAF through its abnormally expanded polyglutamine-containing domain [309]. Normally, Htt protein with an unexpanded repeat does not localize to the nucleus, and, therefore, is unable to inhibit histone acetyltransferase activity [309].

The effect of hyperacetylation and deacetylation on the expression of a gene varies depending on the gene promoter. Thus, while one event may enhance the transcription of a gene involved in cell growth and transformation, the other event may suppress the expression of this gene and prevent tumorigenesis. Considering this, researchers have attempted to further define the effectiveness and mechanism of action of histone deacetylase inhibitors in disease therapy. As well, attempts are currently being made to identify inhibitory drugs for histone acetyltransferase activity.

*Histone Deacetylase Inhibitors*

As mentioned previously, histone acetylation is a dynamic process mediated by the actions of both histone acetyltransferases and deacetylases. The level of histone acetyltransferase and deacetylase activity surrounding a histone substrate and the proximity of these enzymes to this substrate determines the acetylation status of that histone. Thus, inhibition of histone deacetylase activity by exposure to histone deacetylase inhibitors promotes histone hyperacetylation [310].

To date, several structural classes of histone deacetylase activity inhibitors have been identified including short chain fatty acids (butyrates), hydroxamic acids (TSA, superoylanilide hydroxamic acid (SAHA)), benzamides (MS-27-275) and cyclic peptides (trapoxin A) (reviewed in [311]). These inhibitors, however, are only effective on certain classes of deacetylases. Class I and II histone deacetylases, except HDAC 6, are sensitive to TSA while class III deacetylases are resistant [174,312-314]. Similarly, class I and class II histone deacetylases, except HDAC 6 and 10, are sensitive to sodium butyrate and class III deacetylases are resistant [174,313,314]. The sensitivity of HDAC11 to TSA or sodium butyrate has not yet been determined.

The majority of deacetylase inhibitors prevent the proliferation of numerous types of transformed cell lines by inducing transcription of the cell cycle regulator p21Waf/Cip1 [315-319]. Histone deacetylase inhibitors, however, have differential effects on different cell types, as well as different genes [320]. Thus, the mechanism of action through which deacetylase inhibitors affect a cell varies. Some inhibitors such as TSA are able to specifically and directly inhibit histone deacetylase activity while the effect of other inhibitors is indirect [321]. As well, the effects of some deacetylase inhibitors such as TSA

and sodium butyrate are reversible while other inhibitors such as Trapoxin irreversibly inhibit deacetylase activity [312].

Some deacetylase inhibitors are also more potent in inducing growth arrest than others. For example, sodium butyrate must be present in millimolar concentrations to affect the biological activities of a cell while TSA is effective at nanomolar concentrations [322].These differences in potency may be a consequence of differences in the chain length of the inhibitors since sodium butyrate has a shorter chain length than TSA and the lipid solubility of short chain fatty acids decreases with a decrease in chain length [323].

The most studied class of histone deacetylase inhibitor is the butyrates. These compounds are four-carbon short-chain fatty acids produced by the intestinal microflora as a metabolic by-product of dietary fiber [324]. The physiological concentration of sodium butyrate within the colonic lumen of an individual who consumes a low to moderate fiber diet is 10 mM [325]. The effects of sodium butyrate are reversible due to its short half-life[326]. Sodium butyrate inhibits deacetylase activity and arrests cells in the G1 and G2 phases of the cell cycle [322]. When present at a concentration of 10 mM, this drug is capable of promoting histone hyperacetylation, inducing cellular differentiation and/or apoptosis in transformed cell lines [327-330].

TSA is another well studied deacetylase inhibitor. This compound is considerably more potent than sodium butyrate and is able to induce histone acetylation and cellular differentiation at nanomolar concentrations [322,331]. TSA was initially isolated as an antifungal antibiotic [322]. Like sodium butyrate, TSA inhibits proliferation by arresting cells in G1 and/or G2 [332]. These anti-proliferative effects are mediated by the ability of

TSA to directly inhibit deacetylase activity and promote histone hyperacetylation of specific gene regions [321]. The specificity of TSA for inhibiting histone deacetylase activity is reflected in the fact that this inhibitor has no *in vitro* effect on other enzymes including protein kinases, protein phosphatases, DNA topoisomerases and calmodulin [333].

**Effect of TSA and Sodium Butyrate on Gene Transcription**

The addition of 2 mM sodium butyrate or 0.3 μM TSA to HT-29 colon cancer cells modulated the expression of 23 out of 588 genes (approximately 4%) investigated with the majority of genes displaying an upregulation [315]. Similarly, the expression of a small fraction (2%) of genes was altered in Jurkat and SupT1 cells treated with 400 nM TSA for up to 8 h [331]. Whether TSA and sodium butyrate repress or induce gene transcription varies with gene type.

In general, TSA and sodium butyrate appear to influence the expression of genes important for cell cycle regulation, apoptosis and invasion. Several theories have been postulated to explain the effect of these drugs on transcription. The most popular theory states that sodium butyrate and TSA affect gene transcription by inhibiting histone deacetylase activity which, in turn, promotes histone hyperacetylation [334,335]. The resulting hyperacetylation would then relax chromatin structure and enhances the access of transcription factors to their target DNA regions. In support of this, Archer et al. observed that overexpression of HDAC1 blocked sodium butyrate- and TSA-induced transcription of the p21Waf/Cip1 promoter [336]. TSA also induces transcription of the human immunodeficiency virus-1 (HIV-1) promoter and disrupts the association of a specific nucleosome positioned along this promoter that normally inhibits transcription

[337]. Lastly, TSA-resistant cell lines have an altered histone deacetylase protein, suggesting that histone deacetylase is an important target of TSA [321].

Although sodium butyrate has been shown to affect histone deacetylase activity, the effective concentration of sodium butyrate is high enough that other parts of the cell might be affected by exposure to this drug including the cytoskeleton and enzymes other than histone deacetylases. Whether this inhibitor affects gene expression by directly altering deacetylase activity or by altering the activity of a protein that influences deacetylase function is not clear. Furthermore, sodium butyrate could influence downstream events such as the post-translational modification of various proteins [338]. The effect of sodium butyrate on gene expression is often investigated in cells treated with high (i.e. millimolar) concentrations of sodium butyrate for extensive periods of time (i.e. 24 h or greater) and no study has been performed to date showing the direct effect of short-term (i.e. 1-2 h) sodium butyrate exposure on the activity of various cellular enzymes.

Evidence suggests that exposure to sodium butyrate induces the serine-threonine protein phosphatase type 1, PP1 or another phosphatase belonging to the PP1 family [339]. Therefore, one way sodium butyrate may influence histone deacetylase activity is by altering proteins that affect the phosphorylation/dephosphorylation status of histone deacetylases and other proteins [338]. Changes in phosphorylation state can control the activity of regulatory proteins [339]. For example, HDAC1 is phosphorylated most likely by casein kinase 2 (CK2) and cAMP-dependent kinase [340-342]. In one study by Dr. Schreiber and colleagues, *in vivo* phosphorylation of mammalian HDAC1 fused to a FLAG epitope tag and transfected into T-Ag Jurkat cells reduced both *in vitro* and *in vivo* enzymatic

activity and disrupted HDAC1 complex formation with proteins such as RbAp48 and mSin3A [342].

In another study, Dr. Ahn and colleagues observed that the exposure of cells to the phosphatase inhibitor okadaic acid leads to hyperphosphorylation of HDAC1 and HDAC2 [343]. This effect was accompanied by the disruption of HDAC1-HDAC2 complexes and protein complexes containing HDAC1, mSin3A and YY1 [343]. Complexes containing HDAC1, HDAC2 and RbAp46/48 were not affected [343]. Thus, in these two studies, histone deacetylase phosphorylation disturbed rather than promoted the formation of histone deacetylase complexes. Sodium butyrate-induced PP1 activity may promote HDAC1 and HDAC2 dephosphorylation which may decrease histone deacetylase activity and disrupt HDAC complexes such as Sin3 and NuRD complexes.

Contrary to these findings, Cai et al. observed that the treatment of FLAG-tagged HDAC1 with alkaline phosphatase did not significantly alter the ability of HDAC1 to deacetylate an acetylated histone H4 N terminal peptide *in vitro* [340]. Also, HDAC2 can be phosphorylated by CK2 and this event is important for HDAC2 complex formation[341]. Hypophosphorylation of HDAC2 disrupts the interaction of HDAC2 with mSin3 and Mi2 and phosphorylation of HDAC2 increases its enzymatic activity [341]. Thus, whether sodium butyrate affects gene expression by increasing PP1 activity which, in turn, decreases histone deacetylase phosphorylation and whether this dephosphorylation event is important for histone deacetylase activity and complex formation remains to be determined.

PP1 also dephosphorylates the phosphorylated isoforms of the four core histones[177]. Histone H3 phosphorylation is important in establishing the transcriptional

competence of a gene [177]. Phosphorylation of H3 on Serine 10 weakens the interactions of the H3 N terminal tail with DNA and this event may promote the binding of transcription factors to DNA [344]. Exposure to sodium butyrate may also influence gene expression by promoting histone dephosphorylation which may cause chromatin to assume a more tightly compact structure that hinders transcription factor access to target DNA sequences.

Although an effect of deacetylase inhibitors on protein phosphorylation is a plausible explanation for sodium butyrate- and TSA-induced transcriptional repression, it does not explain the ability of these inhibitors to induce the transcription of certain genes. It is tempting to hypothesize that sodium butyrate and TSA increase the transcription of a gene by promoting histone hyperacetylation that alters chromatin structure and/or maintains the open structure of the active nucleosome. However, work by Dr. Crane-Robinson and colleagues has shown that a hyperacetylated gene is not necessarily transcriptionally active [62,221].

Perhaps the effects of histone deacetylase inhibitors on other cellular proteins may be contributing towards their differential effects on transcription. For example, sodium butyrate is capable of altering the expression levels of the ER in breast cancer cells. A short term treatment of MCF-7 human breast cancer cells with 3 mM sodium butyrate for 3 h decreases ER mRNA levels and decreases the transcription rate of the ER gene [345]. A longer treatment of breast cancer cell lines with 5 mM sodium butyrate for 24 h decreases both unoccupied and total ERα levels in cytosolic and salt-soluble nuclear fractions isolated from human breast cancer cells [346]. Exposure to sodium butyrate also increases insulin growth factor binding protein-3 (IGFBP-3) mRNA and protein levels in prostate

cancer cells [347]. Similarly, exposure of human hepatocarcinoma cells to 480 ng/ml TSA for 6-8 h increases IGFBP-3 mRNA levels [348].

Sodium butyrate also affects the activity of enzymes other than PP1 and histone deacetylase. Sodium butyrate rapidly induces the activity of tyrosine kinases that phosphorylate and activate several proteins including MAP kinase (MAPK) [349]. Sodium butyrate also increases alkaline phosphatase activity in LIM215 colon cancer cells and this event is believed to be regulated by protein kinase C (PKC) [350,351]. Thus, sodium butyrate may affect histone deacetylase activity by inducing PKC activity. In support of this, the histone deacetylase inhibitors sodium butyrate and apicidin induced transcriptional activation of a transiently-transfected p21Waf/Cip1 promoter reporter construct and treatment with the PKC inhibitor, calphostin C, inhibited this induction [352]. Calphostin C-mediated transcriptional inhibition was dependent on the presence of a Sp1/3 site [352]. Sp1 and Sp3 interact with HDAC1 and HDAC2 and apicidin inhibits histone deacetylase activity *in vitro* [353,354]. Thus, histone deacetylase inhibitors may induce PKC and this may alter the activity of histone deacetylases recruited by Sp1/Sp3.

**TSA- and Butyrate-DNA Response Elements**

The direct effect of TSA and sodium butyrate on gene transcription is most likely mediated through one or more TSA or sodium butyrate DNA response elements positioned in the promoter region of a target gene. The calbindin-$D_{28k}$ gene contains a butyrate response element between -175 and -78 and its transcription is upregulated in the presence of sodium butyrate [355]. The HIV type 1 long terminal repeat (LTR) promoter also contains two LTR regions that are inducible by sodium butyrate and a 14 bp region within one of these LTRs is homologous to a portion of the butyrate response element

within the calbindin-$D_{28k}$ gene promoter [356]. A TSA-responsive element has been mapped to a region within the IGFBP-3 that coincides with a Sp1/GC-rich region within the promoter [348]. Similarly, a butyrate response element has also been identified in a 45 bp DNA region along IGFBP-3 in breast cancer cells that contains binding sites for Sp1 and activating protein-2 (AP-2) [357].

**TSA and Sodium Butyrate Mediate Transcription Through Sp1 and Sp3**

The expression of IGFBP-3 is induced by treatment with sodium butyrate [357]. When studying the IGFBP-3 promoter in breast cancer cells, sodium butyrate-induced transcriptional activation requires binding of Sp1 to its target sequence within the promoter and the association of Sp3 with AP-2 [357]. Treatment of breast cancer cells with sodium butyrate did not alter Sp1 or Sp3 total protein levels [357]. Co-immunoprecipitation experiments on MCF-7 nuclear extracts revealed that HDAC1 associates with Sp1 and Sp3 and that sodium butyrate treatment does not alter this association [357]. Instead, these experiments showed that sodium butyrate treatment decreases the association of p300 with Sp1 and Sp3 by 39% and 99%, respectively [357]. DNA affinity precipitation assays showed that sodium butyrate treatment increased the association of the p300 cofactor with the IGFBP-3 promoter by approximately 40%, while the association of Sp1, Sp3 and HDAC1 with this gene region remained unaltered [357]. Thus, p300, HDAC1, Sp1 and Sp3 are most likely assembled into a multi-protein complex along the IGFBP-3 promoter and exposure to sodium butyrate only increases binding of the p300 histone acetyltransferase[357].

Similar to the IGFBP-3 promoter, sodium butyrate-induced thymidine kinase promoter activity also requires a Sp1 binding site [358]. This induction was believed to be a

result of the ability of sodium butyrate to release an inhibitory constraint on Sp1, making it possible for Sp1 to associate with other accessory proteins to regulate transcription of the thymidine kinase gene.

Tsubaki et al. have also observed that both sodium butyrate and TSA increase IGFBP-3 mRNA and protein levels in two human prostate cancer cell lines. However, the butyrate response elements for the IGFBP-3 promoter differed between the two cell lines[347]. One cell line contained a butyrate response element in the IGFBP promoter that closely resembled that found in the IGFBP gene promoter in breast cancer cells. The other cell line contained a butyrate response element within the IGFBP gene promoter that lacked a Sp1 binding site and instead contained p53 and GATA DNA binding sites. Of these two sites, the p53 response element was important for sodium butyrate-induced transactivation [347]. However, neither p53 nor GATA were required for butyrate responsiveness [347]. Thus, in addition to Sp1 binding sites, there are several other response elements important for inducing a butyrate response.

Sodium butyrate has also been shown to induce transcription of p21Waf/Cip1 by a p53-independent mechanism that requires p300 and Sp1 [359]. In the presence of sodium butyrate, the zinc finger transcription factor, ZBP-89, binds to both Sp1 and p300 and mediates the interaction between these two factors [359]. ZBP-89 also recognizes the same p21Waf/Cip1 regulatory sequences as Sp1 [359]. In this case, sodium butyrate is thought to induce p21 Waf/Cip1 transcription by promoting the direct association of ZBP-89 with p300 within a transcriptional complex that contains Sp1 [359].

TSA-induced transcriptional activation of IGFBP-3 also appears to be mediated by Sp1 and Sp3 [348]. TSA induces Sp1 phosphorylation, enhances Sp1 binding to its

consensus DNA sequence, and releases HDAC1 and Sp3 from Sp1 transcription factor complexes [348]. TSA treatment also enhances the binding of Sp3 to its consensus DNA sequence in Hep3B hepatocellular carcinoma cells, however, Sp3 is not able to activate several Sp1-responsive promoters alone [348]. The findings discussed in this section suggest that histone deacetylase inhibitors may perturb transcription by influencing the association of transcription factors such as Sp1, Sp3 and ZBP-89 with specific regulatory DNA sequences, by altering the association of transcription factors bound to Sp1 sites with other transcription factors and/or by inhibiting the activity of Sp1/3-associated histone deacetylases.

**Histone Deacetylase Inhibitors and Cancer Treatment**

Aberrations in cellular differentiation are a hallmark of cancer and inhibitors of histone deacetylases promote cell differentiation and inhibit cell growth. Histone deacetylase inhibitors show considerable promise in the treatment of neurodegenerative diseases such as Huntington's disease and cancer [309,507-509]. The treatment of transgenic flies expressing a mutant form of the Htt protein which is involved in the development of Huntington's disease with the deacetylase inhibitor SAHA increases cell viability by 55% and markedly represses early adult death in a concentration-dependent manner [309]. Histone deacetylase inhibitors are also being studied as chemotherapy agents to be used in combination with conventional cytotoxic drugs, differentiation-inducing agents, demethylating agents, cell cycle modulators and cell survival modulators [508].

Histone deacetylase inhibitors inhibit the proliferation of squamous, breast, ovarian, liver and prostate cancer cell lines in culture [317,320,360]. Furthermore, the injection of sodium butyrate into hepatocellular tumors of nude mice every second day causes an

approximate 50% decrease in tumor size and substantially increases the survival rate [317]. Such findings have prompted researchers to investigate the use of deacetylase inhibitors in cancer patients. However, one significant problem with using sodium butyrate as a treatment drug is its half-life of approximately 6 min. In a recent clinical trial, Tributyrin, a triglyceride containing three sodium butyrate moieties esterified to glycerol, was used to enhance sodium butyrate's short half-life. The oral administration of this drug to patients with solid tumors gives sodium butyrate a half-life long enough to reach an effective concentration of approximately 0.5 mM in 1 day without inducing severe toxicity in the plasma [326].

Sodium butyrate treatment inhibits the growth of breast cancer cells with either an ERα-positive, hormone-dependent or an ERα-negative hormone-independent phenotype[326]. Sodium butyrate treatment is also capable of arresting the ERα-negative, highly invasive and highly metastatic MDA-MB-231 breast cancer cell line in G2/M [326]. A large percentage of breast tumors become resistant to anti-estrogen therapy [112]. Thus, sodium butyrate may be an effective alternative to the drugs currently used in hormone therapy for breast cancer. Also, administration of a moderate to high dose (250-500 mg/kg/day) of phenylbutyrate, a more stable form of butyrate, in BALB/c mice for 7 days has recently been shown to inhibit normal breast epithelial cell cycle progression [361]. Such doses increase the levels of acetylated H3, prevent cyclin D1 expression and significantly reduce the levels of ERα in mouse mammary epithelial cells [361]. In a previous study performed by the same research group, butyrate also increased p21(Waf1/Cip1) expression and hypophosphorylated pRB in normal mammary epithelial cells [362]. Since the presence of ERα is important for early breast cancer development and

cyclin D1, pRb and p21(Waf1/Cip1) are important for cell cycle progression, phenylbutyrate may be a promising drug for breast cancer treatment.

Phenylbutyrate has been shown in a recent clinical trial to cause the complete remission of APL in a 13 year old girl [364]. This treatment elevated the levels of acetylated histones in the mononuclear blood cells of this girl [364]. This remission lasted for 7 months before the girl experienced a relapse and became resistant to phenylbutyrate treatment [364]. However, several other patients with relapsed APL did not experience a remission after this treatment [364].

The histone deacetylase inhibitor SAHA may also be a promising drug for breast cancer treatment. This drug inhibits the proliferation of MCF-7 human breast cancer cells in culture [363]. An accumulation of MCF-7 cells in G1 was shown after exposed to 1.25 and 2.5 μM SAHA for 48 h. Concentrations of SAHA equal to or greater than 5 μM caused cells to arrest in G2/M [363]. Exposure of MCF-7 cells to SAHA also induced the expression of proteins involved in breast epithelial cell differentiation such as milk fat globule protein, milk fat membrane globule protein and lipid droplets [363]. Moreover, SAHA induced the differentiation of other breast cancer cell lines including SKBr-3 (ER-negative) and MDA-468 (retinoblastoma- and ERα-negative) [363]. The effect of SAHA on the differentiation of these other two cell lines was comparable to that seen on MCF-7 cells [363].

Hormonal therapy is a popular treatment for breast cancer. Tumors that require estrogen for proliferation can eventually acquire the ability to grow in the absence of this hormone. Once the tumors have developed this phenotype, they become difficult to treat

by anti-estrogen hormonal therapy. SAHA may therefore be a valuable alternative drug for breast cancers with various phenotypes including hormone-independence.

Histone deacetylase inhibitors have also been shown to cause growth-inhibition and potentiate RA-induced cellular differentiation of an APL cell line derived from a patient with retinoic acid-responsive APL that expresses the PML-RARα fusion protein [365]. Treatment of this cell line with phenylbutyrate, TSA or SAHA increased the fraction of cells in G0/G1 and G2/M and induced apoptosis [365]. Leukemic mice with the PLZF-RARα/RARα-PLZF transgenes also display an increase in their median disease-carrying survival period when treated with RA and a non-toxic dose of SAHA sufficient to induce the accumulation of hyperacetylated H4 in the bone marrow, spleen and peripheral blood [365]. Several histone deacetylase inhibitors in phase I or II clinical trials include FR901228, SAHA and pyroxamide [312].

*The Nuclear Matrix*

The chromatin fiber is organized into loop domains through its association with the NM [4]. These loop domains range in size from 5 kb to 200 kb, with the average size being 70-100 kb [4]. The segment of DNA that attaches to the NM at the base of each loop is referred to as a matrix attachment region (MAR). The NM is defined as the nuclear structure remaining after the treatment of interphase nuclei with nucleases and high salt to remove genomic DNA, chromatin and any loosely bound proteins [366,367]. This structure is also referred to as the nucleoskeleton or the nuclear scaffold depending on the method of isolation. The NM is composed of a nuclear lamina, a fibrogranular ribonucleoprotein network and an internal matrix [368] (Figure 11). The internal matrix occupies the nuclear interior and is connected to the nuclear lamina [368]. This matrix appears as a network of intricately woven fibers built upon an underlying layer of 10 nm fibers [369,370]. The composition of the 10 nm fibers remains unknown.

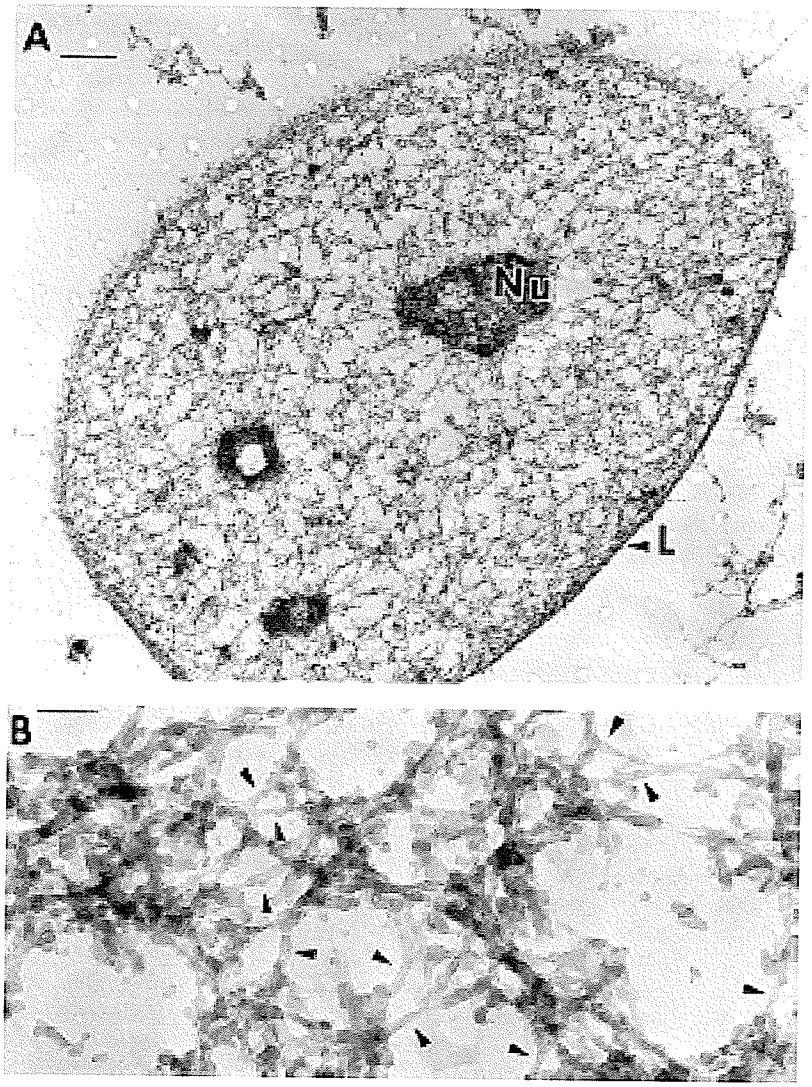


**Figure 11.** **Electron Micrograph Showing the Ultrastructure of the Nuclear Matrix from a CaSki Cell.** (A) The nuclear matrix is composed of the nuclear lamina (L) and a network of interwoven fibers connected to the lamina. This cell section displays 3 remnant nucleoli. (B). Higher magnification of the internal NM fibers showing how they are built on an underlying network of 10 nm filaments [bars = 1 uM (A) and 100 nM (B)]. Image taken from [370].

## Nuclear Matrix Composition

The exact protein composition of the NM varies according to the method of NM protein isolation. The most popular methods use high salt conditions to strip away non-NM proteins (NMPs) from the NM [242,371]. Analysis of NM proteins by two dimension gel electrophoresis indicates that the NM is composed of at least 200 proteins. The majority of these proteins are high molecular weight, nonhistone proteins [372]. Some NM proteins identified to date include lamins A, B and C, nucleolar protein B23, nuclear matrins, the nuclear-mitotic apparatus protein and various heterogeneous nuclear ribonucleoproteins (hnRNPs) including hnRNPK [366,373-377]. HnRNPs are believed to function in RNA metabolism and hnRNPK has been shown to possess all the properties of a transcription factor, suggesting that at least some hnRNPs function in transcription [366,375,382].

Although high salt extraction NM protocols are commonly used, the exposure of nuclei to high salt may strip away some NMPs, leaving behind an underrepresented NM fraction. As well, controversy exists in defining the true nature of a NMP. Some researchers believe that only those proteins detected in a NM fraction can be designated as true NMP, while proteins found both in the NM fraction and other cell fractions are not. However, cytokeratins are some of the more abundant nuclear proteins cross-linked to DNA *in situ* by cisplatin, an agent that predominantly cross-links NM proteins to DNA[379]. As well, a recent study shows that actin is tightly associated with the NM and located within close proximity of DNA [380]. Lastly, vimentin maintains a tight association with lamin B throughout isolation of the NM and, therefore, this protein should be at least referred to as a complementary NMP [381].

The function of these cytoskeletal proteins in the nucleus is unknown. In estrogen-responsive human breast cancer cells, the levels of cytokeratins K8, K18 and K19 associated with nuclear DNA dramatically increase in response to estrogen treatment [379]. Thus, cytokeratins may help mediate estrogen-induced changes in DNA organization and cell structure. In addition, β-actin is a component of the chromatin remodeling SWI/SNF-like Brg-associated factor complex[383]. Actin-related proteins, Arp7 and Arp9, are shared components of the SWI/SNF and RSC chromatin remodeling complexes within yeast *Saccharomyces cerevisiae* [383]. In a previous study, the Act1 actin protein, and the Act3/Act4 actin-related proteins were identified as subunits of the H4/H2A histone acetyltransferase, NuA4 [384]. The integrity of the NuA4 complex relies on the presence of Act3/Act4. Furthermore, Act3/Act4 could bind to nucleosomes *in vitro* through the N terminal domains of histones H3, H4 and H2A [384]. The role of actin in chromatin remodeling and observations that actin is tightly associated with the NM suggest that actin may play a role in transcription by promoting the binding of histone acetyltransferases or other components of chromatin remodeling complexes to the NM[380].

**Nuclear Processes Associated with the Nuclear Matrix**

The NM serves as a platform that is associated with and organizes nuclear processes such as transcription, DNA replication and RNA processing [368]. The NM is enriched in transcriptionally active genes [184,235-238], and RNA polymerase II is fixed at sites along the NM [236,385]. This association suggests that transcriptionally active genes are located at the base of DNA loops where they are positioned close to the transcription machinery. However, the possibility also exists that a gene sequence within a loop

domain may be located at a distal site from the NM and the association of a transcription factor with this sequence promotes its recruitment to the NM. Transcription factors such as AML and YY1 have NM targeting sequences [187]. As well, RbAp48 associates with the NM [386]. Both YY1 and RbAp48 associate with histone acetyltransferases and histone deacetylases [187,387-392]. The binding of estrogen to ERα causes this receptor to bind to its target DNA sequence and become tightly associated with the NM [170]. The NM is also associated with histone acetyltransferases and histone deacetylases as well as ATP-dependent chromatin remodeling factors [184,185,393]. In fact, the majority of histone acetyltransferase and deacetylase activity and most of dynamically hyperacetylated H4 are associated with the NM [184]. Thus, the recruitment of a gene to the NM positions this gene close to factors that promote and initiate transcriptional activation.

## The Influence of Cell and Nuclear Structure on DNA Organization and Gene Expression

The shape of a cell is governed by a dynamic tissue matrix system that links together three-dimensional skeletal networks from the NM, cytoskeleton (CSK) and extracellular matrix (ECM) [394]. The NM is the skeletal framework of the nucleus composed of the nuclear-pore lamina, residual nucleoli and a network of ribonucleoproteins [395]. This structure binds to MAR DNA regions along the chromatin fiber and organizes DNA into loop domains [395].

The tissue matrix system is believed to form a structural and functional connection between the cell periphery and DNA, establishing a mechanical signaling pathway to transmit signals from the cell's exterior to nuclear DNA. In support of this,

disrupting the CSK with cytochalasin D or acrylamide prevents a cell from interacting with the surrounding ECM [396] and pulling a single chromosome out from an interphase cell results in the removal of all subsequent chromosomes along with the CSK [397]. Furthermore, a mechanical tug of the integrins on a cell surface alters the organization of the cytoskeletal filaments, the location of the nucleoli and the shape of the nucleus [394].

Because the tissue matrix connects the cell periphery with nuclear DNA, any changes in the organization of the components of this system may influence gene expression. For example, a change in cell shape induced by the ECM induces the expression of β-casein [398]. As well, a change in cell shape along with the binding of the ECM to the p53 gene leads to changes in the nuclear localization of the p53 gene [398]. Furthermore, the ECM down regulates the expression of TGF-β [399]. Thus, the ECM plays a role in the transcriptional regulation of some genes.

**Alterations in the Structure of DNA in Cancer Cells**

Considering that cell and nuclear structure is intimately related to DNA organization, changes in any of the components affecting cell or nuclear shape may directly or indirectly alter DNA organization. Changes in DNA organization may, in turn, alter the position of particular genes relative to specific transcription factors and subsequently induce the aberrant expression of genes that confer pre-cancer cells with a growth advantage. Such a theory is possible since changes in CSK organization have been observed in Kirsten kidney cells when transformed with the *ras* oncogene [400]. As well, exposure of a cell to the tumor promoter, phorbol 12-tetra-decanoate 13-acetate (TPA) causes gross morphological changes in cell structure and the organization of NM-

associated intermediate filaments [401]. The actin microfilament arrays of the CSK also appear to play an important role in gene expression. Estradiol treatment of the MCF-7 human breast cancer cell line causes rearrangements in the F-actin cytoskeleton that lead to the formation of lamellipodial structures [402].

Studies performed in our laboratory show that exposure of the MCF-7 human breast cancer cell line to estradiol increases the total cellular levels of cytokeratins K8, K18 and K19, as well as the levels of cytokeratins K8, K18 and K19 associated with the NM and with nuclear DNA [395]. Similarly, the treatment of rat vaginal epithelium with estradiol results in an increase in the levels of total cellular cytokeratins [403]. Thus, estrogen appears to induce changes in cytoskeletal structure. Whether these changes are directly involved in or a consequence of estrogen-induced transcriptional initiation remains to be determined.

**Nuclear Matrix Proteins in Cancer**

While some NM proteins are common among different cell types, others are tissue- and cell-type specific with their expression reflecting the stage of differentiation and development [242,366,374,375,378,404,405]. Several studies have also shown that the protein composition of the NM varies between normal and cancer cells [242,406-411]. Breast carcinomas but not normal or benign cells express a 114 kDa matrix attachment region binding protein and the expression of this protein is elevated in poorly differentiated breast ductal carcinomas [412]. Changes in NM composition have also been shown to correlate with the metastatic potential of oncogene-transformed mouse fibroblast cell lines and with the state of differentiation of breast cancer cell lines [242,408]. In addition, the

expression of three NM proteins has been found to correlate with the acquisition of metastatic liver cancer [411].

In a recent study, we identified differences in the levels of proteins associated with DNA in well- and poorly differentiated breast cancer cell lines with hormone-dependent and –independent phenotypes using the agent cisplatin [409]. Cisplatin, otherwise known as *cis*-diamminedichloroplatinum (II), is a particularly useful agent for identifying NM proteins bound to nuclear DNA *in situ* [413,414]. This agent cross-links proteins within a 4 Å distance of DNA and the majority of proteins cross-linked to DNA with cisplatin are NM proteins. As well, the DNA cross-linked to proteins is enriched in MAR sequences [415-424].

In the area of bladder cancer research, scientists have identified NMP22 and BCLA-4 as NM proteins expressed at high levels in bladder cancer cells that are excreted in the urine of cancer patients [425]. Such findings have lead to the development of kits for the detection of these differentially expressed NM proteins from the urine of bladder cancer patients [426]. The development of this non-invasive approach for cancer detection has instigated a widespread effort for identifying NM proteins that are specific for cancer cells and easily detected in the blood or serum of cancer patients. Thus, the use of NM proteins as diagnostic indicators for cancer shows great promise. However, it is important to further elucidate the role of these NM proteins in cancer development since this may reveal new targets for cancer therapy.

*Breast Cancer*

Breast cancer is one of the most common diseases among women in Western countries. Several genetic and environmental factors most likely influence the development of this disease, and, to date, only several risk factors have been established including: age (breast cancer incidence doubles every 10 years), family history of breast cancer and exposure to hormones such as estrogen [427].

The influence of estrogen on breast cancer development has been substantiated by observations that this hormone promotes the development of mammary cancer in rodents and induces the proliferation of human breast cancer cells. Furthermore, the relative risk of a woman in developing breast cancer is dependent on factors influencing the length of exposure to estrogen such as early menarche, late menopause, postmenopausal obesity and hormonal replacement therapy [427].

The breast consists of several different cell types including epithelial, mesenchymal, fat, immune and fibroblast cells. The majority of breast cancers are epithelial in origin. Estrogen action is mediated through the action of the ERα. The ERα is infrequently expressed in normal breast epithelial cells while at least 70% of all invasive breast cancers express the ERα and are termed ER-positive [112]. Breast cancer cells are thought to require estrogen in their initial stages of growth. The majority of breast cancers arise in post-menopausal women. Estrone is the major circulating form of estrogen in these women. This form of estrogen has one-tenth the biological activity of 17β-estradiol [428]. Thus, the estrogenic environment is weak within post-menopausal women. Because of this, it is thought that ER-expressing breast cancer cells acquire a degree of independence from estrogen for proliferation [428].

Another characteristic of late stage disease development is the acquisition of an anti-estrogen resistant phenotype. Endocrine therapy is an important treatment regimen for breast cancer patients. This therapy involves treating patients with anti-estrogenic compounds such as tamoxifen that prevent estrogen-mediated transcriptional activation. However, approximately 50% of ERα-positive breast cancers become resistant to the tamoxifen [428]. Thus, the mechanism of estrogen action and the steps leading to acquisition of an estrogen-independent and anti-estrogen-resistant phenotype must be determined to further understand breast cancer development and to improve disease therapy.

***Breast Cancer Progression Cell Models***

To date, many cells lines have been developed from different tumors and studied to further elucidate the mechanisms responsible for estrogen-induced breast cancer cell proliferation. The data collected from these cell lines have been very useful for understanding early and late stage breast cancer. However, these cell lines have provided little insight into the events involved in the progression of this disease from an early to a late stage of development. Endocrine resistance is an important factor in breast cancer development and treatment. For this reason, Dr. Clarke and colleagues developed a breast cancer progression series composed of cell lines from a common lineage with different stages of estrogen and anti-estrogen responsiveness. For a brief summary of the phenotypes of each cell line, refer to Table 4.

The cell lines in this progression series are MCF-7, MIII, LCC1 and LCC2 [429-431]. The MIII cell line was developed by inoculating the mammary fat pads of an

ovarectomized athymic nude mouse with MCF-7 cells [431]. This inoculation led to the development of a tumor that was harvested and made into the MIII cell line. MIII cells were then injected into each flank of an ovarectomized athymic nude mouse [430]. Proliferating tumors were excised, cultured together and the resulting cell population was designated LCC1. The LCC1 cells were then grown in the presence of increasing concentrations of tamoxifen [429]. Cells able to grow in the presence of $10^{-6}$M tamoxifen were designated LCC2. All four cell lines in this series express ERα to the same extent [429,430]. The MCF-7 cell line is totally dependent on estrogen for growth and tumor formation in nude mice [430]. The MIII, LCC1 and LCC2 cell lines are estrogen-responsive but they do not require estrogen for proliferation [430]. The MIII, LCC1 and LCC2 cell lines form proliferating tumors in untreated ovarectomized nude mice; however the time required for LCC1 cells to form a tumor in these mice is much shorter than that for MIII cells [429,430]. LCC2 cells also have a shorter lag time for tumor formation than MIII cells, but their lag time is slightly longer than that of LCC1 cells [429,430]. All four cell lines are sensitive to ICI (Imperial Chemical Industries) 182,780 [429], an anti-estrogen that decreases cellular levels of ERα by promoting ERα ubiquitination and increasing proteasome-dependent degradation of this receptor molecule[504]. This anti-estrogen also prevents the binding of ERα to DNA [504].

The MCF-7, MIII, and LCC1 cell lines are sensitive to tamoxifen while the LCC2 cell line is tamoxifen-resistant [429]. The binding of tamoxifen to ERα inhibits transcription by promoting the recruitment of transcriptional corepressors such as NCoR, SMRT, HDAC2 and HDAC4 to the promoter region of estrogen-responsive genes [167]. The MCF-7 cell line is non-metastatic and non-invasive while the MIII and LCC1 cell lines are able

to invade locally from solid mammary fat pad tumors and produce metastatic lesions [432]. In addition, the LCC2 cell line is invasive and metastatic [433,434]. The study of this breast cancer progression cell line model may provide insight on the mechanisms responsible for breast cancer development.

***Estrogen Action***

Estrogen is important in the development and function of the reproductive system. Furthermore, estrogen is a key regulator of bone metabolism and may have cardioprotective effects [256]. There are three naturally occurring forms of estrogen: 17β-estradiol (E2), estrone (E1), and estriol (E3). These estrogens are derived from cholesterol.

Estradiol is primarily produced in the ovaries of a woman, while estrone and estriol are primarily formed from estradiol in the liver [435]. During pubescence, a girl will contain 55 to 128 pmol of estradiol per liter of serum. The production of estradiol fluctuates during the menstrual cycle with the highest levels occurring in the pre-ovulatory phase [435]. As a woman enters the peri-menopausal period, a depletion of ovarian follicles occurs and the levels of estradiol in her serum begin to progressively decline [435]. Post-menopausal women display estradiol concentrations as low as 73 pmol per liter of serum. The predominant form of estrogen in these women is estrone and most of the estradiol is produced outside the ovaries [435].

After 17β-estradiol has been synthesized, it is secreted into the bloodstream where it either freely diffuses into target tissues or reversibly binds to sex hormone-binding β-globulin and albumin [435]. When encountering its target cell, estradiol passively diffuses into the cell and binds to ERα.

The ERα is a member of the nuclear receptor superfamily, a family of receptor molecules with similar structural and functional properties. There are two subtypes of the ERα and several isoforms and splice variants of each subtype. The first subtype, ERα, has 6 regions (A-F). The N terminal A/B domain contains a ligand-independent activation function AF-1. Region C is located in the center of the ERα and contains a zinc finger DNA-binding domain. This region is responsible for sequence-specific recognition of DNA response elements. Next to the DNA-binding domain is the hinge region. This region contains elements involved in nuclear localization and may also contain elements involved in ER transactivation function, as well as co-regulator binding[112]. At the C terminal end of the receptor molecule is region E. This region contains a ligand-binding domain, a transcriptional activation domain (AF-2), a dimerization domain, a nuclear localization domain and a co-factor binding domain [112]. AF-2 undergoes conformational changes in the presence of different ligands and creates a hydrophobic surface by co-activators in its agonist-bound conformation [256]. Lastly, region F is a C terminal region of unknown function [114].

The second ER subtype is referred to as ERβ. Compared to ERα, this subtype has a different structure, low sequence homology, and, in most cases, a different tissue distribution. The ligand binding domain of ERβ has only a 55% sequence identity to that of ERα [436]. As a result, the binding affinities of ERα and ERβ vary with different ligands [435]. Despite this difference, both subtypes have the same affinity for 17β-estradiol; however, the manner with which each subtype influences transcription when bound to estradiol differs. Estradiol activates transcription when bound to ERα and represses transcription when bound to ERβ [437]. ERβ can be found in many different tissues

including kidney, intestinal mucosa, bone marrow, bone and endothelial cells, while ERα is found in breast cells, ovarian stroma and endometrium [435].

***Mechanism of ER-Alpha Transcriptional Activation***

The unliganded form of ERα exists in a complex containing chaperone proteins that either stabilize the ERα in an unactivated state or mask the DNA binding domain of the ERα [256,435]. Whether unliganded ERα remains in the cytoplasm or the nucleus remains to be determined. While one theory suggests that unliganded ERα is located predominantly in the nucleus [256], another suggests that unliganded ERα is equally distributed between the cytoplasm and nucleus [256,435]. When free estrogen is present, it binds to the ligand binding domain of the ERα [435], causing helix 12 to alter its position such that it encloses the estrogen molecule in a hydrophobic cavity [438]. These conformational changes in the ERα molecule cause the chaperone proteins associated with ERα to dissociate. The estrogen-ER complex then either diffuses into or relocates itself inside of the nucleus where it binds to an ERE DNA sequence as a homodimer or as a heterodimer with ERβ [256,435,438,505]. The binding of estrogen ligand to ERα and the subsequent binding of this receptor-ligand complex to DNA also enables the interaction of ERα with the LXLL motif of transcription co-activators [439]. These co-activators contain histone acetyltransferase and/or recruit other co-activators with histone acetyltransferase activity[110,111]. In addition, estrogen stimulation of MCF-7 cells leads to the recruitment of the CARM1 arginine methyltransferase to the pS2 promoter. As a result, proteins with histone acetyltransferase and methyltransferase activity become

localized to the ligand-bound receptor, causing the structure of chromatin surrounding this receptor-ligand complex to assume a more permissive environment for transcription.

In its unliganded state, the ERα molecule can also interact with histone acetyltransferases and deacetylases. In a recent study, the histone acetyltransferases AIB-1 and PCAF were associated with the cathepsin D promoter in the absence of estrogen[168,245]. ERα, CBP, SRC-1 and AIB1 are also associated with the pS2 and c-*myc* promoters in the absence of estrogen [245]. However, the levels of histone acetyltransferases along these different promoters are significantly lower compared to levels in estrogen-treated cells. Furthermore, ERα, N-CoR, SMRT, HDAC2 and HDAC4 are associated with the c-*myc* promoter in the absence of estrogen [167]. Such findings suggest that the histones along an estrogen-responsive gene promoter are continually being dynamically acetylated at all times. In support of this, dynamic acetylation has been observed along the *c-fos* and *c-jun* genes in mouse fibroblasts grown in the absence of any transcriptional stimulation or gene transcription [92]. Interestingly, a low level of acetylated H4 is associated with the pS2 and c-*myc* promoters in the absence of estrogen, suggesting that the level of histone acetyltransferase activity recruited to these promoters in the absence of transcriptional stimulation exceeds the level of histone deacetylase activity [167,245]. In the presence of estrogen, the level of histone acetyltransferases associated with the c-*myc*, cathepsin D and pS2 promoters substantially increases. Thus, exposure to estrogen most likely promotes the recruitment of additional histone acetyltransferases to the promoter region of estrogen-responsive genes where they compete with the pre-existing histone deacetylases and sway the balance of histone acetyltransferase and deacetylase activity such that acetylation is the favored reaction.

Several types of EREs exist within the genome. The consensus ERE consists of a palindrome of PuGGTCA motifs separated by 3 bp [256]. Each molecule of the ER dimer binds to its own PuGGTCA motif [256]. The ERα binds with strong affinity to the consensus ERE; however, this sequence is present at a relatively low frequency of approximately one in 4 million base pairs [256]. Recently, it has been proposed that ERE sequences regulate the activity of ERα and other nuclear transcription factors in an allosteric manner. More specifically, the sequence and orientation of EREs may cause changes in the structure of the ERα molecule that influence the association of co-regulatory proteins with this receptor molecule [439,440].

In addition to recognizing the consensus ERE palindrome, ERα binds to imperfect palindromes where at least one of the bases has been mutated [256,441]. In fact, the majority of estrogen target genes contain imperfect palindrome EREs [442]. The ERα dimer binds to these sequences with a much weaker affinity than the consensus sequence; however, the binding affinity of ERα for an ERE does not necessarily reflect the transcriptional response[440]. ERα also binds with weak affinity to sites containing only one PuGGTCA sequence [256,443]. Thus, the ERα has a large number of sites through which it can bind and activate transcription in the presence of estrogen.

The response of a gene to estrogen may also depend on the ability of ERα to cooperate with other transcription factors such as AP1 and Sp1. Many regulatory regions of estrogen responsive genes such as c-*myc* and cathepsin D contain either a half or full ERE palindrome associated with GC boxes (GGGGCGGGG) or GT/CACCC boxes (GGTGTGGGG) [256]. The Sp1 transcription factor binds to these boxes and assists in estrogen-induced transcriptional initiation [444]. In human breast cancer cells, the ER has

even been shown to cooperate with Sp1 in the transcriptional activation of an estrogen-responsive gene lacking an ERE [445-448]. As well, ERα can also regulate estrogen-induced transcription through its association with AP1, a protein heterodimer composed of transcription factors from the Jun/Fos family [444,449]. Such observations show that the ERα does not necessarily bind DNA to initiate transcription. Although the mechanism of Sp1 action is unknown, it appears to be cell type-specific since estrogen is unable to activate Sp1 in HeLa cells expressing ERα [256]. The ability of ERα to interact directly with specific genes through an ERE and/or to interact with other proteins involved in gene regulation may result in "cross-talk", an event where ERα can influence gene expression by activating more than one distinct signaling pathway. Thus, transcriptional regulation by ERα is a very complex event [256].

***Estrogen Induces the Transcriptional Activation of the pS2 Gene***

Approximately 0.4% of the genes within the nucleus are transcriptionally activated in the presence of $10^{-8}$ M estrogen for 3 h [279]. The pS2 gene, otherwise known as Trefoil factor-1, is a well studied, estrogen-responsive gene that has provided considerable information about the mechanism of estrogen action in breast cancer cells. The pS2 gene belongs to the trefoil peptide family, a small family of polypeptides with molecular masses of 6-7 kDa characterized by at least 1 trefoil domain composed of a triple-looped, cysteine-rich region [450]. The Trefoil domain is held together tightly by three disulphide bonds. Because of this, the pS2 protein is resistant to enzymatic digestion [451].

Expression of the pS2 gene was first detected in the MCF-7 human breast cancer cell line during a search for estrogen-induced genes [452,453]. When MCF-7 cells are treated

with 10 nM estradiol, transcription of the pS2 gene begins as early as 15 min and continually increases over a 24 h period [454]. While the pS2 gene is not expressed in normal breast tissue, it is expressed in approximately 68% of breast tumors [455], and its expression correlates strongly with the presence of ERα [455,456]. Only a small portion of the cells within a tumor express pS2 and the percentage of pS2-positive breast cancer cells is lower in tumors from post-menopausal women [455,456]. The expression of pS2 is controlled at the transcriptional level and its expression in human breast tumors is suggestive of a favorable response to therapy with anti-estrogenic compounds that inhibit the growth-promoting effects of estrogen [457].

The pS2 gene is also expressed in other types of carcinomas including stomach, pancreatic, lung, endometrium, prostate, bladder, cervical, ovarian and skin cancer (reviewed in [451]). In these carcinomas, the expression of pS2 is not dependent on the presence of ERα, indicating that the expression of this gene can occur by pathways alternative to those mediated by ERα [458-460]. In support of this, the 5' flanking region of the pS2 gene contains a complex promoter/enhancer region that is responsive to a variety of stimuli including estrogen, EGF, c-*jun*, the c-*Ha-ras* oncoprotein and the tumor promoter, TPA [461]. The ERE within this promoter is an imperfect palindromic sequence consisting of 13 bp (GGTCACGGTGGCC). The efficiency of ERα binding to the pS2 ERE is 5 times lower than that of a perfectly palindromic ERE [462].

Although pS2 is expressed in tumors, it is normally and predominantly expressed in the stomach [451]. In the gastrointestinal tract, pS2 expression is increased around sites of mucosal injury such as peptic ulcers. At these sites, pS2 is thought to assist in mucosal repair by stimulating the migration of surviving cells from the wound edge to over the

exposed lesion [451]. Thus, pS2 is thought to function as a motogen, a factor that promotes cell movement. In support of this, pS2 expression is positively correlated with lymph node metastasis [455].

In the past, it has been speculated that pS2 functions as a mitogen. However, to date, no conclusive evidence has been presented to substantiate this theory. The pS2 protein may also function as a tumor suppressor since pS2-knock out mice display severe hyperplasia and high-grade dysplasia as well as adenoma in the stomach [463].

***Structure of the pS2 Gene***

The pS2 gene consists of 3 exons separated by 2 introns (Figure 12). Response elements to estrogen, EGF, TPA, c-HA-*ras* and c-*jun* are located next to each other in the 5' flanking promoter/enhancer region of the gene [461]. Two nucleosomes are positioned along the pS2 promoter region, one over the TATA box (nucleosome T) and one over the ERE (nucleosome E) [464]. Nucleosome E also covers two Sp1 binding sites and one Ap1 binding site (Figure 12).

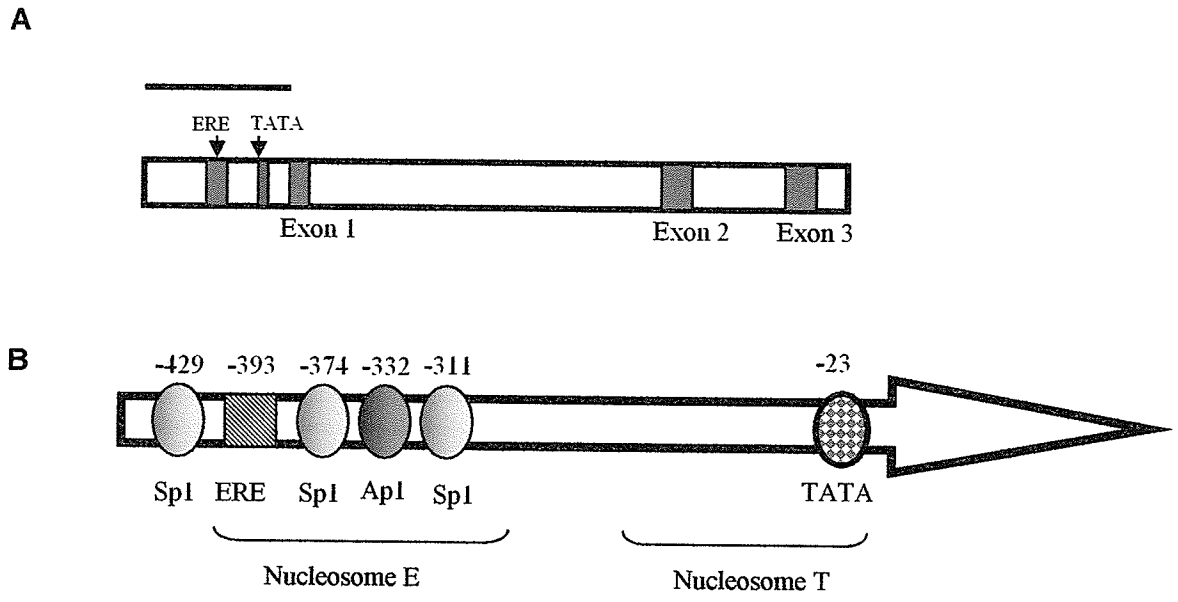


**Figure 12. Schematic Diagram of the pS2 Gene and Promoter. (A)** The pS2 gene is organized into a promoter region and three exons. The bar above the schematic of the pS2 gene represents 1 kb of DNA. **(B)** The pS2 promoter contains an imperfect estrogen response element (ERE), a TATA box, and DNA-binding sites for SP1 and AP1. Nucleosomes E and T display the positioning of nucleosomes over the ERE and TATA DNA sequences.

## Objectives, Rationale & Hypotheses

The overall objective of my studies was to determine the relationship between chromatin structure and gene expression. Since chromatin structure can be influenced directly by factors that alter the properties of histones and indirectly by the NM, my project was divided into two main areas: one focusing on the role of histone acetylation in DNA organization and gene expression and the other focusing on the role of the NM in DNA organization and cancer development.

To further understand the involvement of histone acetylation in transcription, the acetylation dynamics of histones located along a constitutively active ($\beta^A$-globin), competent (ε-globin) and inactive (vitellogenin) gene were studied in chicken immature erythrocytes. While the relationship between histone acetylation and transcription has been well studied, little is known about the dynamic behavior of histone acetylation and how this behavior affects transcription. Populations of histones displaying the same rate of acetylation but different rates of deacetylation have been identified [219,220]. Davie and colleagues have provided correlative evidence suggesting that the histones associated with transcriptionally active genes are rapidly and dynamically acetylated while histones along inactive genes are either slowly acetylated, unacetylated or in a static state of acetylation depending on the transcriptional competence of the gene [184].

The transcriptional machinery and the majority of transcriptionally active DNA sequences are associated with the NM [184,189,234-238]. As well, the majority of histone acetyltransferase and deacetylase activity is associated with the insoluble nuclear skeleton which contains the NM [184]. Thus, the observations of Dr. Davie and colleagues suggest that active genes are located within nuclear regions enriched in histone acetyltransferase

and deacetylase activity and that perhaps the ability of these enzymes to induce a rapid and dynamic state of acetylation assists in the recruitment of transcriptionally active genes to sites of transcription. With this to consider, one of the goals of my research was to determine if the histones along transcriptionally active, competent and inactive genes have the same rate of deacetylation. As well, I determined if the genes bound to the NM are associated with hyperacetylated histones.

We hypothesize that dynamic histone acetylation acts to recruit genes to sites of transcription associated with nuclear substructures such as the NM. Thus, we postulate that transcriptionally active genes are located in nuclear regions enriched in histone acetyltransferase and histone deacetylase activity. The close proximity of these genes to these enzymes causes the histones associated with these active genes to be class I acetylated. Transcriptionally competent genes are most likely located in nuclear regions with lower amounts of histone acetyltransferase and deacetylase activity and are, therefore, associated with histones that are dynamically acetylated at a slower class II rate. Inactive genes remain in a more condensed structure relative to active and competent genes and are not dynamically acetylated.

Another portion of my research focused on studying the involvement of dynamic histone acetylation in estrogen-mediated transcriptional activation. While histone acetylation has been found to occur on the promoter regions of estrogen-responsive genes in the presence of estrogen [168,199], the nature of this acetylation and its exact function in hormone-mediated transcription remains to be determined. To date, the involvement of histone deacetylation in estrogen-mediated transcriptional activation has been largely ignored. Without sufficient proof, many researchers have postulated that exposure to

estrogen causes the replacement of histone deacetylases situated along an estrogen-responsive gene by histone acetyltransferases. However, it is possible that deacetylases are present both in the absence and presence of estrogen and that treatment with estrogen simply disturbs the balance between acetyltransferases and deacetylases, causing an increase in the recruitment of histone acetyltransferases while a background of deacetylase activity persists.

Previous studies suggest that histone acetyltransferases are situated along the promoter region of estrogen-responsive genes in the absence of estrogen [168]. In the presence of estradiol these acetyltransferases cycle on and off the promoter region in a time-dependent manner [168]. Little investigation has been made to determine if dynamic histone acetylation takes place downstream from the promoter regions of estrogen-responsive genes and if this event is dependent on transcription. Therefore, my objectives were: 1) to determine if histone deacetylases are associated with the pS2 gene by using inhibitors of deacetylases that increase histone acetylation levels along gene regions associated with histone deacetylases and by identifying the location of HDAC1 along pS2 promoter and coding regions and 2) to determine if estrogen-induced histone acetylation is a widespread, dynamic and transcription-independent event mediated by histone acetyltransferases and deacetylases that are associated with the entire estrogen-responsive gene.

We hypothesize that in the absence of estrogen, the pS2 estrogen-responsive gene gene is localized to nuclear regions enriched in histone acetyltransferases and histone deacetylases in MCF-7 cells. Exposure to estrogen causes ERα to bind to the pS2 promoter and recruit histone acetyltransferases to this region where they work against the

action of pre-existing histone deacetylases to increase the frequency of histone acetylation. This promoter-targeted event occurs independently of transcriptional initiation and is a cyclical event involving the rapid binding and dissociation of factors to estrogen-responsive promoters. Exposure to estrogen also induces histone acetylation along the pS2 coding regions in the presence or absence of transcription. This event modifies chromatin structure to facilitate transcription. Lastly, treatment of MCF-7 cells with histone deacetylase inhibitors dissociates histone deacetylases from the promoter and coding regions of the pS2 gene without affecting the association of histone acetyltransferases. Thus, exposure to histone deacetylase inhibitors induces histone acetylation along the promoter and coding regions of the pS2 gene.

Lastly, the final objective of my studies was to see if changes in NM organization may be involved in the acquisition of phenotypes important for breast cancer cell invasion, metastasis and resistance to anti-estrogen treatment. In a previous study, differences were observed in the patterns of NM proteins isolated from well- and poorly-differentiated breast cancer cell lines [408] and some of these differences were observed in patterns of NM proteins associated with DNA [409]. This observation was significant because well-differentiated breast cancer cells generally have a more favorable outcome after anti-estrogen treatment when compared to poorly-differentiated cells. The possibility exists that changes in NM composition can alter DNA organization and initiate downstream events that give a cancer cell a more aggressive phenotype. Thus, the final objective of my research was to study the changes that occur in NM composition and DNA-associated proteins in the cell lines from a breast cancer cell line progression series. We hypothesized that cell lines with different phenotypes in a breast cancer

progression series display differences in the expression profiles of specific NM proteins either directly or indirectly involved in DNA organization. Thus, the progression of a breast cancer cell to a more advanced stage in disease development is accompanied by changes in DNA organization mediated in part by the nuclear matrix.

## Part I: Dynamically Acetylated Histones are Associated with Transcriptionally Active and Competent, but not Inactive, Genes in the Avian Adult β-Globin Gene Domain

Both class I and II acetylated histones are acetylated with a $t_{1/2}$ of 12 min; however, class I acetylated histones are deacetylated with a $t_{1/2}$ of 5 min, while class II acetylated histones are deacetylated with a $t_{1/2}$ of 90 min [219]. Davie and colleagues have presented data showing that class I dynamic histone acetylation correlates with transcriptional activity, while class II acetylation correlates with transcriptional competence [184]. This suggests that transcriptionally active DNA sequences may be situated near nuclear regions enriched in histone acetyltransferase and deacetylase activity and, therefore, raises the possibility that dynamic histone acetylation may mediate the attachment of active DNA sequences to regions of the nucleus such as the nuclear matrix.

The objective of this study was characterize the dynamics of histone acetylation along a constitutively active ($\beta^A$-globin), competent (ε-globin) and inactive (vitellogenin) gene in chicken immature erythrocytes. We also determined if dynamically acetylated histones are associated with the insoluble nuclear skeleton since this fraction of the nucleus harbors the majority of transcriptionally active DNA, and histone acetyltransferase and deacetylase activity [184]. As well, no attempts have been made to date to show an association between dynamic histone acetylation and the transcriptionally active and/or competent genes associated with this fraction.

Histones and salt-soluble chromatin fragments were isolated from chicken immature erythrocytes that were pre-treated with sodium butyrate to induce histone

hyperacetylation and then incubated in the absence of this inhibitor for 0-30 min to initiate histone deacetylation. Acetylated chromatin is salt-soluble. Therefore, the rate of histone deacetylation along the $\beta^A$-globin, ε-globin and vitellogenin genes was studied as a function of the rate of loss of salt-solubility of chromatin fragments containing these three DNA sequences. As well, the association of acetylated H3 and H4 with nucleoskeleton-associated chromatin fragments containing the $\beta^A$-globin, ε-globin and vitellogenin DNA sequences was determined using the ChIP assay.

## *1.0 Methods*

### 1.1 Treatment of Adult White Leghorn Chickens with Phenylhydrazine

A solution containing 55% ethanol (v/v) and 0.025 g/ml of acetyl-phenylhydrazine was injected subcutaneously into the breast of adult white leghorn chickens over a six day period. The chickens were injected with 0.7, 0.7, 0.4, 0.6, 0.7, and 0.8 ml of this solution on days 1, 2, 3, 4, 5 and 6, respectively. Such a treatment schedule causes the horn of a chicken to turn from red to light pink and causes the chicken blood to contain 95% reticulocytes and 3% mature erythrocytes [465].

### 1.2 Harvesting of Immature Erythrocytes from Adult White Leghorn Chickens

On the seventh day of treatment, the chickens were anesthetized with a solution containing 3 parts Ketalean, 1 part Rompun, and 2 parts collection buffer. Small birds were injected with 0.2 ml of anesthetic while larger birds were injected with 0.5 ml. The jugular vein of each chicken was then severed and the chicken immature erythrocytes from each chicken were collected into an approximate equal volume of ice-cold collection buffer (pH 7.4) containing 75 mM NaCl, 25 mM EDTA (pH 8.0), and 25 mM Tris-HCl (pH 7.5). The blood was filtered through at least 4 layers of cheese cloth and centrifuged in 30 ml aliquots at 500 x g for 10 min at 4°C. The supernatant and white cell layer were aspirated away from each red cell pellet and the remaining cell pellet was washed with 30 ml of ice-cold Swim's media (pH 7.2) (Sigma-Aldrich). The cells were then centrifuged at 500 x g for 10 min at 4°C, washed a second time in ice-cold Swim's media and centrifuged once again. After the second wash, the supernatant and white cell layer were removed by aspiration and the pellet was either stored at -80°C or resuspended in an equal volume of Swim's media pre-warmed to 37°C.

### 1.3 Treatment of Chicken Immature Erythrocytes with 10 mM Sodium Butyrate

Once suspended in pre-warmed Swim's media, the immature erythrocytes were treated with or without 10 mM sodium butyrate (Sigma-Aldrich) for 60 min at 37°C to induce histone hyperacetylation. The erythrocytes were then washed three times in ice-cold Swim's media, resuspended in fresh Swims media pre-warmed to 37°C and incubated for 0, 5, 10, 15, and 30 min at 37°C. Following treatment, the erythrocytes were immediately resuspended in ice-cold Swim's media, collected by centrifugation and washed one additional time in ice-cold Swim's media. The cells were then centrifuged and stored at -80°C. Three different preparations of erythrocytes were prepared, treated and analyzed.

### 1.4 Fractionation of Erythrocyte Chromatin Fractionation

Chromatin fragments soluble in 150 mM NaCl were isolated from chicken immature erythrocytes as previously described [70] (Figure 13). All buffers contained 1 mM phenylmethylsulfonyl fluoride (PMSF) (Sigma-Aldrich). Nuclei from chicken immature erythrocytes were isolated by suspending the erythrocytes in ice-cold Reticulocyte Standard Buffer (RSB) (10 mM Tris-HCl, pH 7.5, 10 mM NaCl, 3 mM $MgCl_2$) containing 0.25% Triton-X-100 (v/v) and homogenizing the mixture. The cell debris was then separated from the nuclei by centrifugation at 500 xg for 10 min at 4°C. This extraction procedure was performed once again to ensure that the nuclei were well separated from the remaining cell debris.

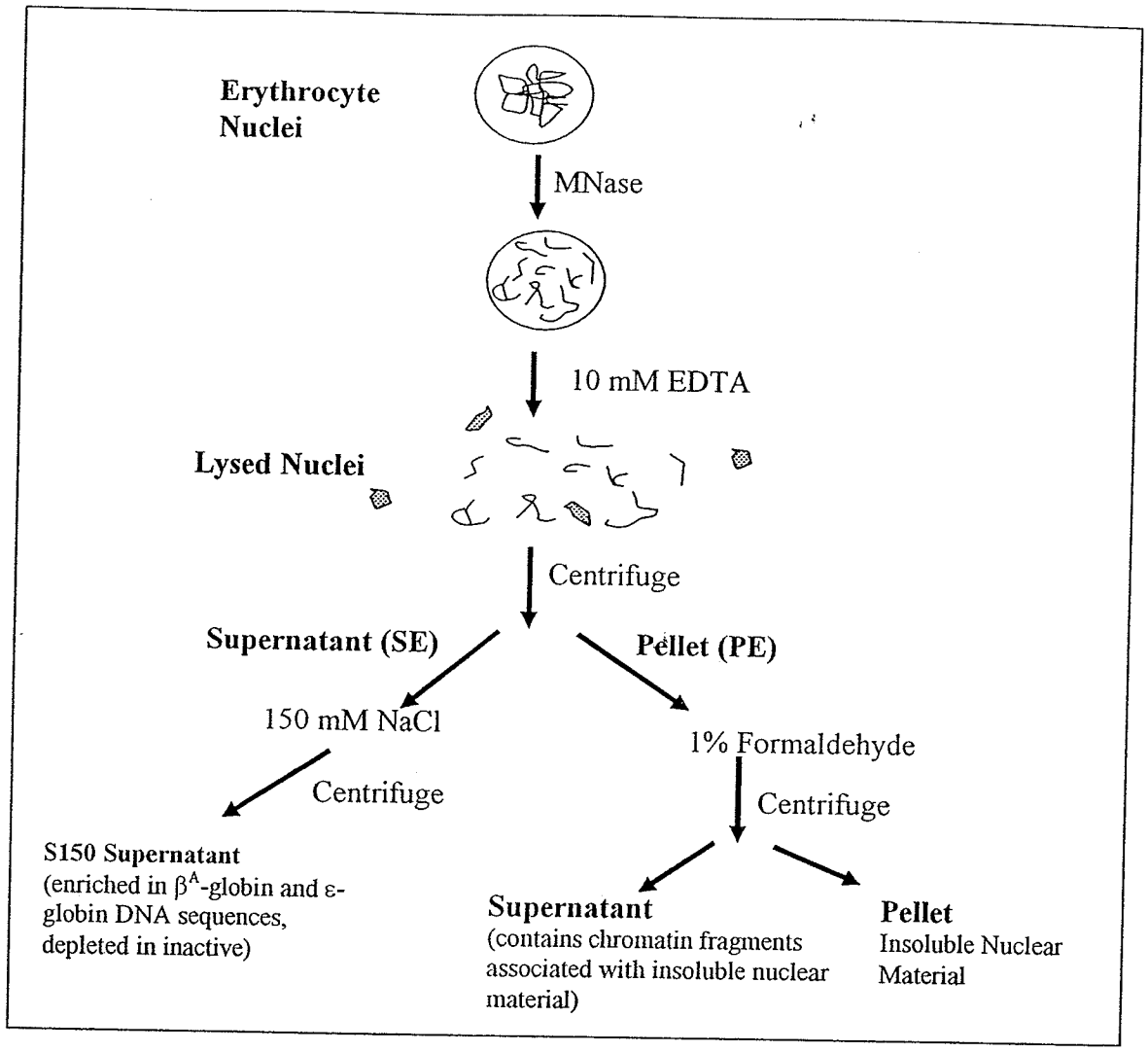


**Figure 13.** **NaCl Chromatin Fractionation Protocol.** Chicken immature erythrocyte nuclei were isolated and treated with MNase. The nuclei were then lysed with EDTA and the nuclear lysate was collected. NaCl was added to the lysate to a final concentration of 150 mM and the salt-soluble chromatin fragments were isolated. The PE pellet was resuspended in cytoskeletal buffer and incubated with 1% formaldehyde for 10 min to remove chromatin fragments associated with the insoluble nuclear material.

Once the nuclei were isolated, they were resuspended to 50 $A_{260}$ units/ml in Wray & Stubblefield (W&S) buffer [1 M hexylene glycol, 10 mM Pipes (Piperazine-N,N'-bis (2-ethanesulfonic acid), pH 7.0, 1% thiodiglycol (v/v), 30 mM sodium butyrate] containing 2 mM $MgCl_2$ and 1 mM $CaCl_2$. The suspension of nuclei was incubated with 15 units of micrococcal nuclease (Worthington Biochemical Corporation, NJ) per mg of total DNA for 5 min at 37°C to partially digest the linker DNA region [180]. EGTA (pH 8.0) was then added to a final concentration of 10 mM to stop the reaction. The nuclei were once again collected by centrifugation (9000 x g, 10 min, 4°C), resuspended in a 10 mM EDTA (pH 8.0) solution, and incubated on ice for 30 min. The suspension was centrifuged at 9000 x g for 10 min at 4°C. The resulting supernatant and the pellet of insoluble nuclear material are referred to as SE and PE, respectively. The SE fraction was then made to 150 mM NaCl and centrifuged (9000 x g, 10 min, 4°C) to remove salt-insoluble chromatin fragments. The supernatant containing NaCl-soluble chromatin fragments (S150) was collected and the DNA sequences within these fragments were isolated and analyzed as described in the following section.

Chromatin fragments soluble in 3 mM $MgCl_2$ were isolated from chicken immature erythrocytes as previously described [466]. All buffers contained 1 mM PMSF. In brief, nuclei from chicken immature erythrocytes were suspended to 70 $A_{260}$ units/ml in a digestion buffer (0.25 M sucrose, 60 mM KCl, 15 mM NaCl, 10 mM sodium butyrate, 15 mM PIPES (pH 6.6)) containing 3 mM $MgCl_2$ and 1 mM $CaCl_2$ (Figure 14). The nuclei were digested with 1 unit of micrococcal nuclease per 50 μg of total DNA for 5 min at 37 °C and centrifuged (9000 x g, 10 min, 4°C). EGTA was then added to the nuclei to a final concentration of 20 mM to terminate the reaction, and the nuclei were centrifuged (9000

x g, 10 min, 4°C). The supernatant fraction containing the $MgCl_2$-soluble chromatin fragments and the pellet fraction containing the insoluble chromatin fragments were collected and the DNA sequences within both fractions were isolated and analyzed as described in the following section.

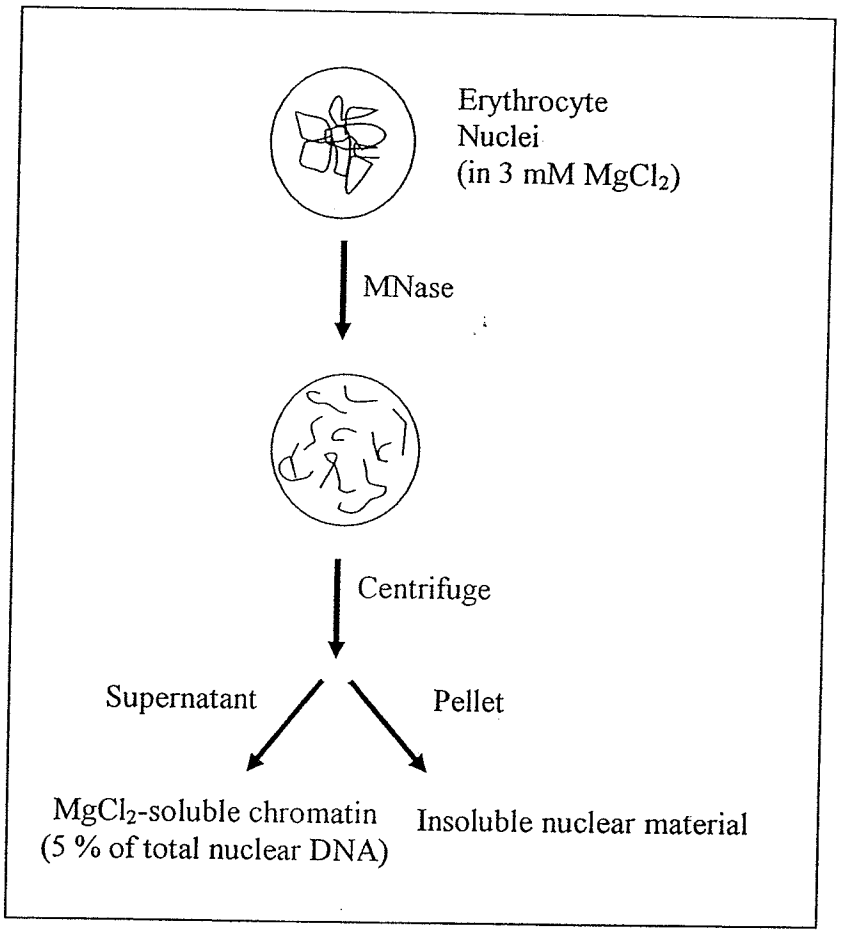


**Figure 14.** **$MgCl_2$ Chromatin Fractionation Protocol.** Immature chicken erythrocyte nuclei were isolated and treated with MNase in the presence of 3 mM $MgCl_2$. The nuclei were then centrifuged and the chromatin fragments released into the supernatant (approximately 5% of total nuclear DNA) were isolated by centrifugation.

## 1.5 DNA Preparation and Hybridization

DNA from S150, $MgCl_2$-soluble and $MgCl_2$-insoluble chromatin fractions was extracted with an equal volume of phenol/chloroform/isoamyl alcohol (25:24:1). The resulting DNA fragments were precipitated with sodium acetate and ethanol, resuspended in Tris-EDTA buffer (pH 8), quantified by UV spectrophotometry, and then either slot blotted using a Schleicher and Schuell slot blotting manifold or Southern blotted onto Hybond N+-charged nylon membrane. For the slot blot analysis, an amount of DNA was applied to each slot such that the relationship between the signal and the amount of DNA slotted was linear. Thus, the signal intensity from each slot was directly proportional to the amount of hybridizable DNA sequence.

The slot or Southern blot was then hybridized overnight at 42°C with $6 \times 10^6$ cpm of $^{32}P$-labelled DNA with a specific activity of approximately $1 \times 10^8$ cpm/μg DNA. DNA probes recognizing the $\beta^A$-globin, ε-globin and vitellogenin genes were used [282,467]. The $\beta^A$-globin and ε-globin DNA probes recognize the second intron of the $\beta^A$- and ε-globin genes, respectively. Both probes are 500 bp long. The $\beta^A$- and ε-globin introns are approximately 800 and 600 bp, respectively, from the transcription start site of their respective gene[468]. The vitellogenin DNA probe is 3.6 kbp in length and recognizes the 5' region of the vitellogenin gene [467]. Following hybridization, the slot or Southern blot was washed to remove non-specifically bound probe. In the Slot blot analysis, the amount of probe hybridized to each slot was quantified by a phosphorimager (Bio-Rad, CA).

## 1.6 Isolation of Histones

To isolate histones from chicken immature erythrocytes, the cells were suspended in RSB buffer containing 0.25% Triton X-100 (v/v) and the nuclei isolated as described in section 1.4. After the final centrifugation step, the nuclei were resuspended in 1 ml of RSB containing 1 mM PMSF. $H_2SO_4$ (250 µl of 4N) was then added to the nuclei and the sample was incubated on ice for 30 min. In cases where histones were extracted from a chromatin preparation, a 1 ml volume of the preparation in digestion buffer (0.25 M sucrose, 60 mM KCl, 15 mM NaCl, 10 mM sodium butyrate, 15 mM PIPES (pH 6.6)) containing 3 mM $MgCl_2$ and 1 mM $CaCl_2$ was supplemented with $H_2SO_4$ to 0.2 N. Acid-insoluble material was removed from the sample by centrifugation at 9000 x g for 10 min at room temperature. The supernatant was then made to 20% trichloroacetic acid (v/v) and centrifuged at 9000 xg for 10 min. The resulting pellet was washed in 1 ml of acetone containing 50 mM HCl and then three times in 1 ml of acetone. The pellet is enriched in histones but also contains other acid-extracted proteins such as HMG proteins. The protein pellet was air-dried, resuspended in double-distilled water and stored at -20°C. Protein concentrations were determined using the Bio-Rad protein microassay (Bio-Rad, CA).

## 1.7 Acid-Urea-Triton X-100 Polyacrylamide Gel Electrophoresis

Twenty µg of acid-extracted proteins were electrophoresed on to an acid-urea-triton 15% polyacrylamide gel as previously described [469] in order to resolve acetylated histone isoforms from each other. The running and stacking gel components were as follows:

| Stock Solution | Resolving Gel (15%) | Stacking Gel (7.5%) |
|---|---|---|
| 29.2% acrylamide/ 0.8% bisacrylamide | 80.0 ml | 20.0 ml |
| 4% TEMED/ 43% acetic acid | 20.0 ml | 0.8 ml |
| Urea | 64.0 g | 32.0 g |
| 0.02% Riboflavin | 3.2 ml | 1.6 ml |
| 100% Triton X-100 | 0.6 ml | 0.3 ml |
| Thiodiglycol | 1.6 ml | 0.8 ml |
| 3M KAc, pH 4 | - | 10 ml |
| Double distilled $H_2O$ | To 160 ml | To 80 ml |

The gels were poured between 2 - 15 cm long glass plates separated by 1.5 mm spacers and polymerized between two light boxes overnight. Two microliters of reducing mix composed of equal volumes of Tris-Acetate, pH 8.8, $H_2O$, and β-mercaptoethanol were added to every 3 µl of protein sample. The sample was then left at room temperature for 10 min. An equal volume of 2 X AUT loading buffer (0.75 M potassium acetate, pH 4.0, 30% (w/v) sucrose, 0.05% (w/v) pyronin y) was added to the sample. The sample was then loaded directly onto the AUT gel and electrophoresed toward the cathode at 200 V for 16-20 h at 4°C. The top and bottom of the AUT gel was emersed in 0.9 N acetic acid during electrophoresis.

## 1.8 Detection of Proteins with Coomassie Brilliant Blue

Gels were stained overnight in a solution of 0.4% (w/v) Serva Blue (Coomassie Brilliant Blue G250 equivalent), 45% (v/v) methanol, 9% (v/v) acetic acid. To remove excess stain, the gels were placed in a strong destaining solution [25% (v/v) methanol,

12.5% (v/v) acetic acid] for 1 h. Gels were then transferred to a milder destaining solution [5% (v/v) methanol, 7.5% (v/v) acetic acid] for several hours to overnight and dried between sheets of gel drying film (Promega Corp., WI) at room temperature.

## 1.9 Detection of Acetylated Histones by Immunoblotting

Before AUT gels were set up for protein transfer, they were soaked in 100 ml of equilibration buffer #1 containing 287.5 µl glacial acetic acid, 5 ml 10% SDS (w/v), and 94.7 ml of double-distilled $H_20$. After 30 min, the old equilibration buffer was replaced with new equilibration buffer and the gel was soaked for another 30 min. The gel was then placed in 100 ml of equilibration buffer #2 composed of 6.25 ml 1 M Tris-HCl, pH 6.8, 5 ml β-mercaptoethanol, 23 ml 10% SDS (w/v), and 65.75 ml of double-distilled $H_20$. The proteins in the equilibrated gel were transferred to nitrocellulose membrane as described previously. The transfer took place overnight at 50 V and 4°C using transfer buffer containing 25 mM CAPS [3-(Cyclohexylamino)-1-Propanesulfonic Acid] and 20% methanol (v/v) [470].

Acetylated isoforms of H2B, H3 and H4 were detected by immunostaining the nitrocellulose membrane with polyclonal antibodies to di-acetylated H2B (Serotec, UK), di-acetylated H3 and penta-acetylated H4 (Upstate Biotech, NY), respectively. When using the acetylated H2B antibody, the nitrocellulose membrane was blocked with 3% (w/v) skimmed milk in 1X TTBS (0.1 M Tris-HCl (pH 8), 0.3 M NaCl, 0.4% (v/v) Tween-20) for 25 min at room temperature on a shaker. The membrane was incubated overnight at 4°C in a 1/400 dilution of the anti-acetylated H2B primary antibody in 1X TTBS. The membrane was then rinsed for 5 min with 1X TTBS and the wash repeated.

The membrane was incubated for 20-30 min at room temperature in a 1/5000 dilution of goat-anti-rabbit horse radish peroxidase secondary antibody in 1X TTBS. The membrane was then washed 2 X 15 min with 1X TTBS and subjected to enhanced chemiluminescence (ECL).

For the acetylated H3 antibody, the nitrocellulose membrane was blocked with 7.5% (w/v) skimmed milk in 1X TTBS for 1 h at room temperature on a shaker. The membrane was incubated overnight at 4°C in a 1/1000 dilution of the anti-acetylated H3 antibody in 1X TTBS. The membrane was then rinsed for 5 min with 1X TTBS and the wash repeated. The membrane was incubated for 20 min at room temperature in a 1/5000 dilution of goat-anti-rabbit horse radish peroxidase secondary antibody in 1X TTBS. The membrane was washed 2 X 15 min with 1X TTBS and subjected to ECL.

Immunoblotting with the penta-acetylated H4 antibody involved blocking the nitrocellulose membrane with 3% (w/v) skimmed milk in 1X TTBS for 15-20 min at room temperature on a shaker. The membrane was then incubated overnight at 4°C in a 1/1000 dilution of the anti-acetylated H4 antibody in 1X TTBS. The membrane was then rinsed for 5 min with 1X TTBS and the wash repeated. The membrane was incubated for 20 min at room temperature in a 1/5000 dilution of goat-anti-rabbit horse radish peroxidase secondary antibody in 1X TTBS. The membrane was washed 2 X 15 min with 1X TTBS and subjected to ECL.

## 1.10 Isolation and Fragmentation of PE-Associated Chromatin

Insoluble nuclear material (PE) was isolated from immature chicken erythrocytes as described in section 1.4 except that the nuclei were digested with 15 units of micrococcal nuclease per mg of total DNA for 10 min at 37°C to more extensively fragment the chromatin (Figure 13). The PE fraction was resuspended in CSK buffer [10 mM Pipes, pH 6.8, 300 mM sucrose, 100 mM KCl, 3 mM $MgCl_2$, 1 mM EGTA, 0.5% thiodiglycol (v/v)] to approximately 10 $A_{260}$ units/ml. Formaldehyde was added to the suspension to a final concentration of 1% for 10 min on ice to release chromatin fragments from the PE fraction [370]. The cross-linking reaction was quenched by the addition of Tris-HCl (pH 8) to a final concentration of 125 mM. The sample was dialyzed overnight at 4°C against double-distilled water and 0.5 mM PMSF, and then concentrated to approximately 4-5 ml using PEG 6000-8000 Carbowax (Fischer Scientific, Ont). Added to the sample was NaCl, Tris-HCl, EDTA, Triton X-100, and SDS to 250 mM, 25 mM (pH 7.5), 5 mM, 1% (v/v), and 0.1% (w/v), respectively (SB250). The DNA within the sample was reduced to 500 bp fragments by sonication on ice for a total time of 4 min at 30% output (Sonifier Cell Disrupter 350, Branson Ultrasonic Corporation, CT). The 4 min period of sonication was divided up into 16 – 15 sec. pulses with 15 sec. waiting intervals on ice in between each pulse. The sonicated PE suspension was then diluted to approximately 9 $A_{260}$ units/ml and centrifuged for 10 min at 9000 x g to remove insoluble material.

## 1.11 Assessment of the Efficiency of Formaldehyde-Mediated Chromatin Release from the PE

To verify that the 1% formaldehyde treatment released the majority of PE-associated chromatin fragments, cross-linked PE was sonicated as described in section 1.10, dialyzed against TE buffer (pH 8) overnight at 4°C, supplemented with NaCl, Tris-HCl, EDTA, Triton X-100, and SDS to 250 mM, 25 mM (pH 7.5), 5 mM, 1%, and 0.1%, respectively. The sample was then diluted to approximately 9 $A_{260}$ units/ml with SB250 buffer and centrifuged (9000 x g, 10 min, 4°C). The amount of DNA associated with this cross-linked PE sample before and after centrifugation was determined by both the diphenylamine assay and $A_{260}$ measurements [471]. For both assays, a 10 µl aliquot was collected from the formaldehyde cross-linked PE in CSK buffer. The cross-linked sample was then centrifuged at 9000 x g for 10 min at 4°C and a 10 µl aliquot was removed from the supernatant.

In the diphenylamine assay, both 10 µl aliquots were diluted to 500 µl with double-distilled water. Perchloric acid [83.33 µl of 60% (v/v)] was then added to the diluted sample to hydrolyze the DNA into nucleotides. Diphenylamine (583.33 µl of a 4% (v/v) solution in glacial acetic acid) was added to the sample to react with the deoxyribose units of the nucleotides and produce a blue-colored product. Lastly, 29.2 µl of 1.6% (v/v) acetaldehyde was added to react with the diphenylamine and potentiate the development of the blue product and the samples were incubated overnight at 30°C. The intensity of the blue product is directly proportional to the concentration of DNA in the sample. The absorbance of each sample and a series of DNA standards were measured at both 595 and 700 nm. The difference between the two absorbance values was

determined. A difference of 0.15 is equal to 10 μg/ml of DNA. Thus, the concentration of DNA in each sample was determined. The concentration of DNA released into the supernatant after formaldehyde cross-linking and centrifugation was divided by the concentration of DNA in the original PE sample.

In the $A_{260}$ assay, both 10 μl aliquots were diluted with 900 μl double distilled $H_2O$. The $A_{260}$ of each diluted sample was measured by spectrophotometry. The $A_{260}$ value for the supernatant was divided by the $A_{260}$ value for the original PE sample to determine the percentage of $A_{260}$ units.

## 1.12 Immunoprecipitation of PE Chromatin Fragments Associated with Acetylated H3 and H4

The suspension of PE-associated chromatin fragments was made up to 1 mM PMSF and 50 μg/ml leupeptin. A volume of 2.5 μl of antibody to di-acetylated H3 or penta-acetylated H4 was added to 500 μl of the suspension and the mixture was incubated overnight at 4°C. The suspension was then incubated for 3 h at 4°C on an orbitron with 20 μl of a 50:50 protein A sepharose slurry (Zymed Laboratories Inc., Ontario) that had been pre-treated overnight at 4°C with 0.1 μg/μl of sonicated salmon sperm DNA and 1 mg/ml of bovine serum albumin (BSA). To control for non-specific binding of DNA to protein A, 500 μl of the suspension was incubated for 3 h at 4°C with 20 μl of the 50:50 protein A slurry in the absence of primary antibody. The protein A sepharose of both samples was then centrifuged at 2200 x g for 30 sec. and washed sequentially with 1 ml of 1X RIPA (Radioimmunoprecipitation) buffer [150 mM NaCl, 50 mM Tris-HCl, pH 8.0, 0.1% SDS (w/v), 0.5% sodium deoxycholate (w/v) (SDC), 1.0% NP-40 (v/v)], 1 ml

of high salt buffer [500 mM NaCl, 1.0% NP-40 (v/v), 0.1% SDS (w/v), 50 mM Tris-HCl, pH 8.0, 1 mM EDTA), 1 ml of LiCl wash buffer [250 mM LiCl, 1.0% NP-40 (v/v), 0.5% SDC (w/v), 1 mM EDTA, 50 mM Tris-HCl, pH 8.0), and two times with 1 ml of TE buffer (pH 8.0). A volume of 100 µl of TE buffer (pH 8.0) was added to the protein A sepharose along with 0.5 mg/ml proteinase K, 0.5% SDS (w/v) and 100 mM NaCl. The mixture was incubated overnight at 37°C and then at 68°C for 6 h. The mixture was centrifuged at 2200 x g for 30 sec and the supernatant was extracted once with an equal volume of phenol/chloroform/isoamyl alcohol (25:24:1). The DNA in the supernatant was precipitated with 20 µg/ml of glycogen carrier, one-tenth the volume of 3 M sodium acetate (pH 5.3), and 3 volumes of absolute ethanol. The DNA was then resuspended in double-distilled water, quantified by fluorometry and slotted on to a Hybond N+-charged nylon membrane using the slot blot manifold described in section 1.5. The slot blot was then hybridized to $\beta^A$-globin, ε-globin, and vitellogenin gene probes previously described in section 1.5.

## *2.0 Results*

### 2.1 Rate of Deacetylation of Hyperacetylated H2B, H3 and H4

Immature erythrocytes were incubated with 10 mM sodium butyrate for 60 min to induce a state of histone hyperacetylation. The erythrocytes were then incubated in the absence of sodium butyrate for 0 to 30 min to deacetylate the hyperacetylated histones. Histones were extracted from the nuclei of cells collected at various time points following sodium butyrate removal and subjected to AUT gel electrophoresis and immunoblotting. The resulting membrane was immunostained with antibodies to highly acetylated H2B, H3 and H4 (Figure 15).

Immunoblot analysis of the total nuclear histone extracts showed a large drop in the levels of penta-acetylated H3 within the first 5 min of incubation in the absence of sodium butyrate. At 10 min the levels of penta-acetylated H3 dropped further, becoming barely detectable at 30 min. A rapid decline in the levels of tetra-acetylated H3 was also observed at 5 min. At 10 min the level of tetra-acetylated H3 declined further, plateauing at a very low level. Levels of tri-acetylated H3 did not change initially but at 10 min a decrease in the levels of this acetylated H3 isoform was observed. At 5, 10, and 15 min following sodium butyrate removal, the levels of mono- and di-acetylated H3 decreased but at a much slower rate than the highly acetylated H3 isoforms.

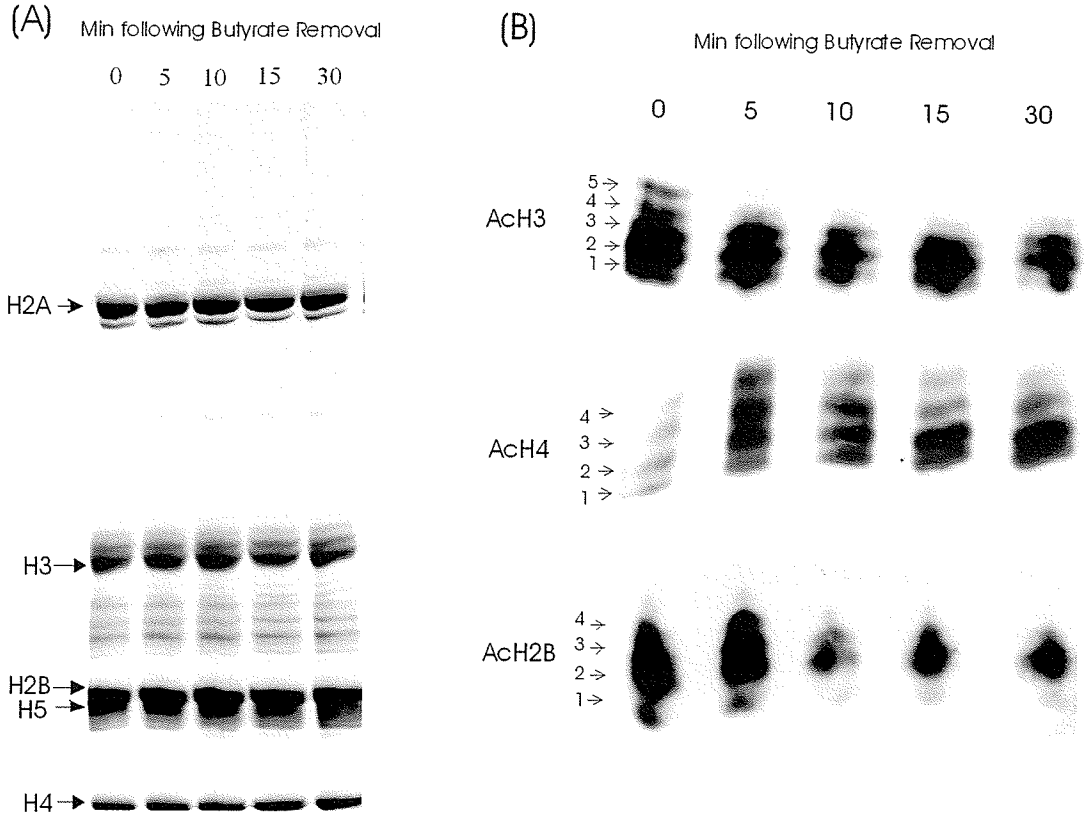


**Figure 15.** **Immunoblot Analyses of H3, H4 and H2B Deacetylation.** Chicken immature erythrocytes were incubated with sodium butyrate for 1 h, followed by incubations for various times in the absence of sodium butyrate. Total nuclear histones were extracted from the nuclei of sodium butyrate-treated chicken immature erythrocytes incubated for 0, 5, 10, 15 and 30 min in the absence of sodium butyrate. Twenty μg of acid-extracted histones were electrophoresed on an Acid-Urea-Triton 15% polyacrylamide gel which was stained with Coomassie Blue (panel A). The proteins were transferred to nitrocellulose and immunostained with antibodies to hyperacetylated H3, H4 or H2B (panel B). 1, 2, 3, 4, and 5 designate mono-, di-, tri-, tetra- and penta-acetylated histone isoforms, respectively.

Immunostaining the blots with anti-penta-acetylated H4 antibody revealed that the levels of tetra-acetylated H4 rapidly declined at 10 min (Figure 15). These levels declined further over the next 20 min. Similarly, the levels of tri-acetylated H4 also decreased at 10 min, although this decrease was not as pronounced as that observed for the tetra-acetylated H4 isoform. The mono- and di-acetylated H4 isoforms accumulated at 15 and 30 min post sodium butyrate removal. In summary the immunoblot analyses show that class 1 highly acetylated H3 and H4 isoforms decline to low levels by 10 min following incubation of cells in media lacking sodium butyrate.

Lastly, immunoblot analysis of the total nuclear histone extracts with an antibody to di-acetylated H2B showed that the level of penta-acetylated H2B drops drastically to undetectable levels when cells were incubated in the absence of sodium butyrate for 10 min. A slight decrease was also observed for di- and tri-acetylated H2B after 10 min. However, the levels of these H2B acetylated isoforms appeared to stay the same when incubated for up to 30 min in the absence of sodium butyrate.

## 2.2 Effect of Histone Deacetylation on 0.15 M NaCl Solubility of Globin Chromatin Fragments

By chromatin fractionation experiments, our research group has determined that chromatin fragments soluble in the presence of 150 mM NaCl are enriched in acetylated histones as well as the transcriptionally active $\beta^A$- and transcriptionally competent ε-globin DNA sequences [184]. In addition, our group has also shown that the solubility of active/competent gene chromatin fragments in 0.15 M NaCl is dependent on the level of acetylated histone species within these fragments [70]. Therefore, the rate of deacetylation of histones associated with transcriptionally active and competent chromatin fragments

can be determined by studying the rate with which these fragments lose their salt solubility in the presence of 0.15 M NaCl.

Soluble chromatin fragments (fraction SE) were isolated from nuclei of cells incubated for various times (0, 5, 10, 15 and 30 min) following the removal of sodium butyrate. Typically 60% of the $A_{260}$ absorbing material was released into this fraction. The SE chromatin fraction was made 0.15 M in NaCl, and the salt-soluble chromatin fragments (fraction S150) isolated. The DNA sequences in these salt-soluble chromatin fragments were analyzed by slot blot hybridization with probes to the $\beta^A$-globin, ε-globin, and vitellogenin DNA sequences. Figure 16 shows that incubation of cells in the absence of sodium butyrate results in a decline in the content of $\beta^A$-globin and ε-globin DNA sequences in the 0.15 M NaCl soluble chromatin fragments. The content of vitellogenin DNA sequences in the salt soluble chromatin fraction was not altered throughout the 30 min. incubation. The parallel drop in the salt solubility of the $\beta^A$-globin and ε-globin chromatin fragments suggests that the deacetylation rates of the histones associated with these chromatin fragments are similar.

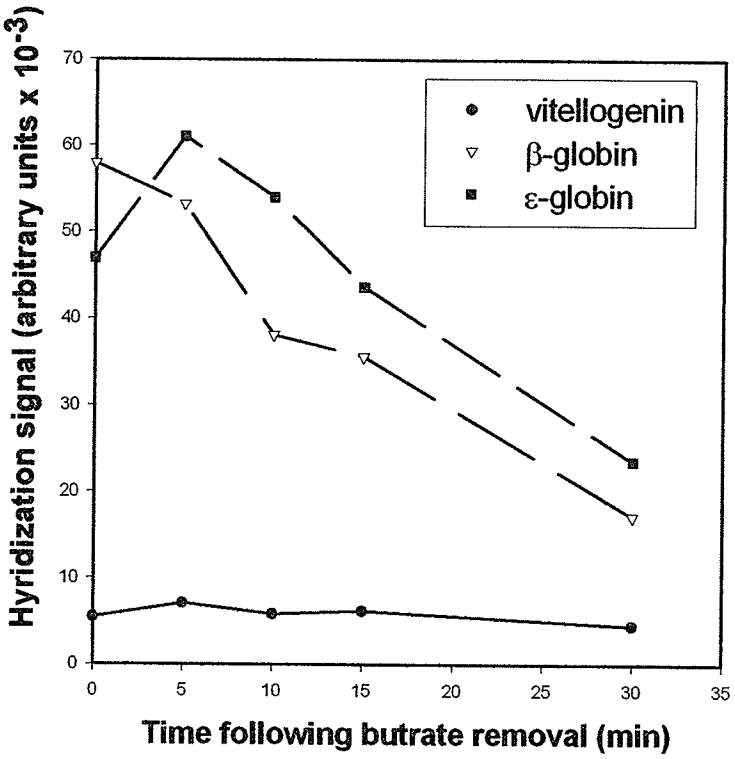


**Figure 16.** **$\beta^A$-globin and ε-globin Chromatin Fragments Lose Solubility in 150 mM NaCl at Similar Rates Following Removal of Sodium Butyrate.** Chicken immature erythrocytes were treated and S150 chromatin was isolated as previously described in Figure 13. Three μg of DNA isolated from NaCl-soluble chromatin fragments were slotted onto nylon membrane and hybridized to DNA probes recognizing intronic regions of the $\beta^A$-globin and ε-globin genes and the 5' region of the vitellogenin gene. The intensity of hybridization to each slot was measured by a phosphorimager and plotted against the time of incubation in the absence of butyrate.

## 2.3 Effect of Histone Deacetylation on $MgCl_2$ Solubility of Globin Chromatin Fragments

Mononucleosomes released from micrococcal nuclease-digested erythrocyte nuclei into buffers containing 3 mM $MgCl_2$ are enriched in the transcriptionally active $\beta^A$-globin DNA sequences and largely depleted in inactive DNA sequences. Inhibiting histone deacetylation increases the enrichment of active mononucleosomes released from the nuclease digested nuclei [472]. Thus, enhanced solubility of transcriptionally active mononucleosomes from nuclease digested nuclei is a direct consequence of induced histone acetylation [183].

To test whether the status of dynamically acetylated histones affected the release of competent ε-globin mononucleosomes from nuclease digested nuclei, nuclei isolated from cells incubated in the absence or presence of sodium butyrate for 60 min were digested with micrococcal nuclease. The chromatin fragments released from the nuclei during digestion and those remaining within the nuclei were collected. The percentage of chromatin released from the nuclease digested nuclei was similar for each preparation (4.4 to 5%). $\beta^A$-globin DNA sequences were enriched in the mononucleosomal fraction released from the nuclease-digested nuclei of sodium butyrate-treated immature erythrocytes (Figure 17). However, this enrichment was not observed with mononucleosomes isolated from cells incubated in the absence of sodium butyrate. These observations are identical to the results of Dr. Nelson and colleagues [219]. The content of ε-globin DNA sequences in the mononucleosome fraction was greater from nuclei isolated from cells incubated in the presence of sodium butyrate compared to that from nuclei of cells incubated in the absence of sodium butyrate (Figure 17). The enrichment

of ε-globin DNA sequences in the 3 mM $MgCl_2$-soluble mononucleosome fraction, however, was less than that attained by the $\beta^A$-globin DNA sequences. In summary, the results show that histone hyperacetylation increases the release of ε-globin mononucleosomes from nuclease digested nuclei.

Since hyperacetylation directly influences the $MgCl_2$ solubility of transcriptionally active and competent mononucleosomes, we monitored the content of these sequences in the mononucleosome fraction as a function of time during which hyperacetylated histones were becoming deacetylated. As with the previous studies, cells were incubated with sodium butyrate to maximize the acetylation state of class 1 histones followed by incubation of the cells for various times in the absence of sodium butyrate to initiate the deacetylation of the hyperacetylated class 1histones. The DNA from the 3 mM $MgCl_2$-soluble mononucleosomes was slotted onto nylon membrane and hybridized to DNA probes recognizing $\beta^A$-globin and ε-globin intronic regions and the 5' region of the vitellogenin gene. A plot of the hybridization signal intensity versus time following removal of sodium butyrate showed that the release of $\beta^A$-globin and ε-globin mononucleosomes was markedly reduced by 5 min followed by a more gradual decline (Figure 18). In contrast to the $\beta^A$-globin and ε-globin mononucleosomes, the deacetylation of hyperacetylated histones did not alter the release of vitellogenin mononucleosomes from the nuclease digested nuclei. The sudden decrease in the release of $\beta^A$-globin and ε-globin mononucleosomes within the first 5 min of incubation in the absence of sodium butyrate closely follows the timing of class 1 hyperacetylated histone deacetylation, particularly that of H3 (see Figure 15). In summary the rapid decline in

the release of $\beta^A$-globin and ε-globin mononucleosomes from nuclease digested nuclei parallels the rapid deacetylation of the hyperacetylated class 1 histones.

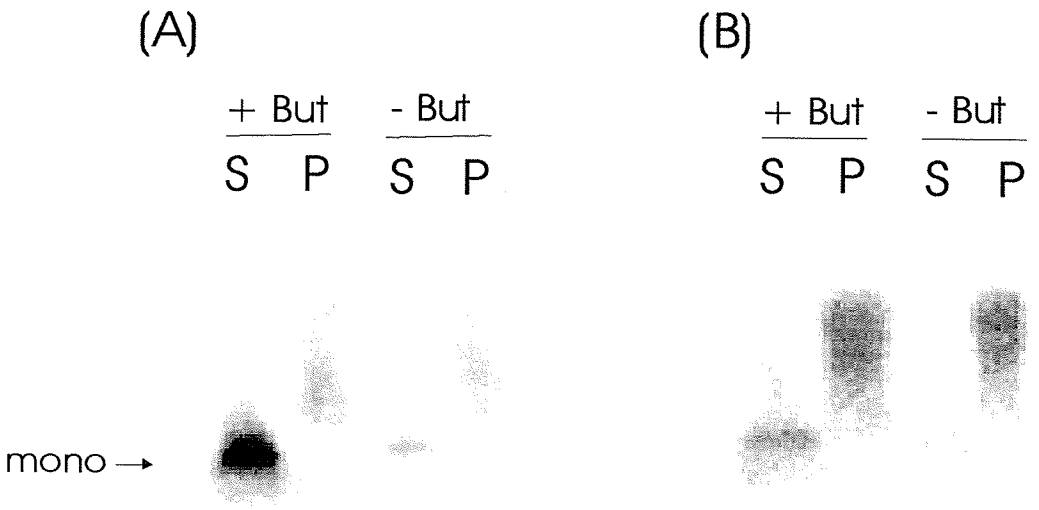


**Figure 17.** **Histone Hyperacetylation Influences the $MgCl_2$ Solubility of Transcriptionally Active $\beta^A$-globin and Competent ε-globin Mononucleosomes.** Eight μg of DNA from $MgCl_2$-soluble and insoluble chromatin fractions of chicken immature erythrocytes treated with or without sodium butyrate (But) for 60 min at 37°C were electrophoresed on to a 0.8% agarose gel. The DNA was transferred to nylon membrane. (A) Hybridization of DNA to a probe containing the intronic sequence from the $\beta^A$-globin gene. (B) Hybridization of DNA to a probe containing the intronic sequence from the ε-globin gene. S and P designate lanes containing $MgCl_2$-soluble and insoluble DNA, respectively. "Mono" designates mononucleosomal-sized DNA fragments.

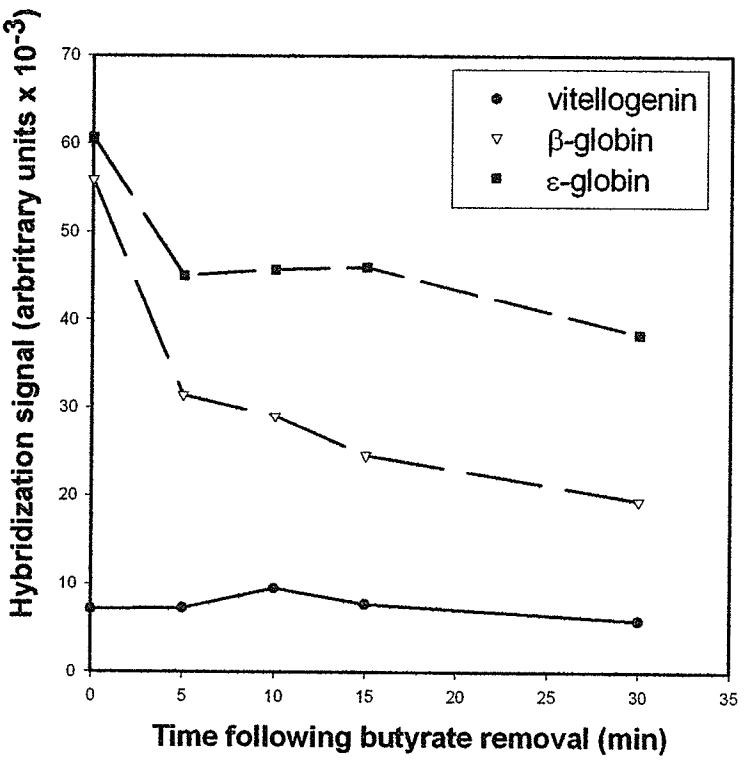


**Figure 18.** **$\beta^A$-globin and ε-globin Chromatin Fragments Lose Solubility in 3 mM MgCl2 at Similar Rates Following Removal of Sodium Butyrate.** Chicken immature erythrocytes were treated and $MgCl_2$–soluble chromatin was isolated as previously described in Figures 14. Three μg of DNA isolated from $MgCl_2$-soluble chromatin fragments were slotted onto nylon membrane and hybridized to DNA probes recognizing intronic regions of the $\beta^A$-globin and ε-globin genes and the 5' region of the vitellogenin gene. The intensity of hybridization to each slot was measured by a phosphorimager and plotted against the time of incubation in the absence of butyrate.

## 2.4 Transcriptionally Active $\beta^A$-globin and Transcriptionally Competent ε-Globin Genes Associated with Fraction PE are Bound to Hyperacetylated Histones H3 and H4

Previous studies have demonstrated directly that acetylated histones are associated with the transcriptionally active $\beta^A$-globin and transcriptionally competent ε-globin genes in avian erythrocytes. However, these ChIP assays used soluble chromatin fragments. Most highly acetylated histones and transcriptionally active $\beta^A$-globin DNA sequences are associated with fraction PE, the low salt insoluble residual nuclear material harboring chromatin associated with the nuclear matrix [184]. To date, no studies have determined if transcriptionally active chromatin bound to the nuclear matrix is associated with highly acetylated histones. To address this question, chromatin fragments associated with the low salt insoluble nuclear material of sodium butyrate-treated chicken immature erythrocytes were briefly incubated with formaldehyde. In addition to cross-linking histones to DNA, formaldehyde incubation releases chromatin fragments from the nuclear matrix [370].

To verify that the formaldehyde treatment conditions could efficiently remove the majority of chromatin fragments associated with the PE, the amount of DNA associated with and released from the PE fraction after formaldehyde treatment was determined using $A_{260}$ measurements and the diphenylamine assay (Tables 1 and 2, respectively). Both assays showed that at least 93% of DNA associated with the PE fraction is released after formaldehyde treatment.

**Table 1.** **Assessment of the Efficiency of Formaldehyde-Mediated Chromatin Fragment Removal from the PE of Sodium Butyrate-Treated Chicken Immature Erythrocytes as Determined by $A_{260}$ Measurements.**

| Replicate | PE ($A_{260}$ units/ml) | Supernatant ($A_{260}$ units/ml) | % $A_{260}$ units released |
|---|---|---|---|
| 1 | 9.5 | 8.5 | 89.5 |
| 2 | 9 | 9 | 100.0 |
| 3 | 9.2 | 9.2 | 100.0 |
| **Average** | **9.2** | **8.9** | **96.5** |

**Table 2.** **Assessment of the Efficiency of Formaldehyde-Mediated Chromatin Fragment Removal from the PE of Sodium Butyrate-Treated Chicken Immature Erythrocytes as Determined by the Diphenylamine Assay.**

| | Replicate | $OD_{595}$ (Units/ml) | $OD_{700}$ (Units/ml) | $OD_{595}$-$OD_{700}$ (Units/ml) | Concentration (µg/ml) |
|---|---|---|---|---|---|
| **PE** | 1 | 8.9 | 2.1 | 6.8 | 453 |
| | 2 | 9.9 | 2.5 | 7.4 | 493 |
| | 3 | 9.8 | 2.6 | 7.2 | 480 |
| | 4 | 9.3 | 2.3 | 7 | 467 |
| | 5 | 10.2 | 2.5 | 7.7 | 513 |
| | **Average** | **9.62** | **2.4** | **7.22** | **481** |
| **Supernatant** | 1 | 24.7 | 17.5 | 7.2 | 480 |
| | 2 | 18.3 | 12.5 | 5.8 | 387 |
| | 3 | 16.3 | 10.7 | 5.6 | 373 |
| | 4 | 17.9 | 11.8 | 6.1 | 407 |
| | 5 | 18.2 | 12 | 6.2 | 413 |
| | **Average** | **13.9** | **7.2** | **6.7** | **450** |

The chromatin fragments bound to hyperacetylated H3 and H4 were isolated by ChIPs. In previous immunoblot experiments and in Figure 15, we demonstrated that the antibodies used in the ChIP assays preferentially recognize highly acetylated isoforms of H3 or H4 [50]. However, the anti-di-acetylated H3 antibody (acetylated K9 and K14) was more discriminating for the highly acetylated H3 isoforms than was the anti-acetylated H4 antibody for the highly acetylated H4 isoforms. The DNA sequences bound to hyperacetylated H3 and H4 were isolated and analyzed by slot blot analysis using DNA probes to the intronic regions of the $\beta^A$-globin and ε-globin genes and to the 5' region of the vitellogenin gene. A comparison of the hybridization signal intensities of the three probes in the input and acetylated H3-immunoprecipitated DNA fractions showed that hyperacetylated H3 was bound to $\beta^A$-globin and ε-globin, but not vitellogenin, DNA (Figure 19). Figure 19 shows that acetylated H4 was bound to $\beta^A$-globin and ε-globin intronic DNA sequences. Vitellogenin DNA was also bound to acetylated H4. Chicken erythrocytes have a population of histones in a static state of mono- and di-acetylation [62]. Thus, we assume that vitellogenin was associated with this histone population. In summary, our results show that hyperacetylated H3 and H4 are bound to the $\beta^A$-globin and ε-globin DNA sequences associated with the insoluble residual nuclear material.

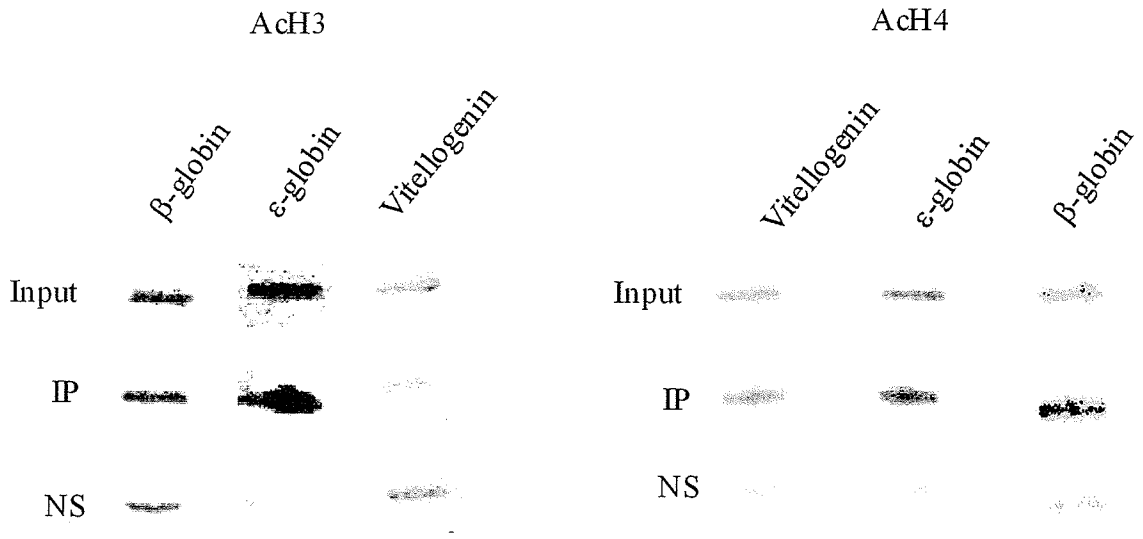


**Figure 19.** **$\beta^A$-globin and ε-globin Chromatin Fragments Associated with the Low Salt Insoluble Chromatin Fraction are Bound to Hyperacetylated H3 and H4.** Input, anti-hyperacetylated H3 (AcH3)-immunoprecipitated, and anti-hyperacetylated H4 (AcH4)-immunoprecipitated DNA were isolated and quantified by fluorometry. Two hundred ng of immunoprecipitated and input DNA were slotted into their respective slots and hybridized to probes recognizing an intronic region of the $\beta^A$-globin and ε-globin genes and the 5' region of the vitellogenin gene. A volume of DNA non-specifically bound to protein A sepharose was slotted that was equivalent to the volume of immunoprecipitated DNA. Input represents the initial total pool of DNA fragments used in the ChIP assay. IP represents DNA immunoprecipitated with anti-acetylated histone antibody. NS represents DNA non-specifically bound to protein A sepharose in the absence of primary antibody.

## *3.0 Discussion*

Rates of histone acetylation and deacetylation are determined in pulse-chase experiments in which protein synthesis is inhibited with cycloheximide [219]. It is possible that some histone acetyltransferases, deacetylases or protein components of these large multi-protein complexes are labile [139]. Thus, when protein synthesis is inhibited, the rapid turnover of these proteins may alter the physiological dynamics of histone acetylation. Our immunoblot analyses with anti-acetylated H2B, H3 and H4 antibodies provide an assessment of the rates of deacetylation of H2B, H3 and H4 without using protein synthesis inhibitors. The rates of deacetylation of the highest acetylated isoforms of H3 were very rapid, in accordance with pulse-chase studies [219]. Similarly, the rates of deacetylation of tri- and tetra-acetylated isoforms of H2B and H4 determined in immunoblot experiments and pulse-chase studies were comparable. We conclude that cycloheximide does not significantly disturb the balance between histone acetyltransferase and histone deacetylase activity in chicken immature erythrocytes.

Our results show that class 1 histones, which are rapidly highly acetylated and deacetylated, are bound to transcriptionally active $\beta^A$-globin and transcriptionally competent ε-globin genes. In parallel $\beta^A$-globin and ε-globin chromatin lost solubility in 150 mM NaCl as deacetylation of the hyperacetylated H3 and H4 isoforms progressed. Further, the rapid deacetylation of hyperacetylated H3 isoforms corresponded to a rapid reduced solubility in 3 mM $MgCl_2$ of $\beta^A$-globin and ε-globin mononucleosomes from nuclease digested nuclei. The loss of the hyperacetylated H3 histones may reverse the disruption of higher order globin chromatin structure, obstructing the release of mononucleosomes from the globin chromatin domain [211,213,473]. However, the extent of

$MgCl_2$ solubility loss of the $\beta^A$-globin mononucleosomes was more acute than that of the ε-globin chromatin fragments. These and other studies show that a greater percentage of $\beta^A$-globin compared to ε-globin chromatin is soluble in 150 mM NaCl or 3 mM $MgCl_2$[235]. We interpret these studies to demonstrate that active coding regions of the $\beta^A$-globin gene are extensively associated with class 1 acetylated histones, while the competent ε-globin gene is a mosaic of class 1 and class 2 acetylated histones. This would explain why in our previous study the partitioning of $\beta^A$-globin DNA sequences precisely matched that of the hyperacetylated H4 isoforms, while competent ε-globin DNA sequences did not [184].

Dr. Crane-Robinson and colleagues have shown that the entire β-globin loop domain is associated with acetylated histones in soluble chromatin fragments [62]. The low salt insoluble chromatin fraction, which contains the bulk of the highly acetylated histones and transcriptionally active DNA, was excluded from their analyses. Our ChIP assays show for the first time that $\beta^A$- and ε-globin intron DNA sequences associated with the residual insoluble nuclear material are bound to highly acetylated H3 and H4. Fraction PE harbors most of the histone acetyltransferase and deacetylase activities. Further, histone acetyltransferase and histone deacetylase activities are associated with the nuclear matrix [235]. Our observations are consistent with a model in which nuclear matrix associated histone acetyltransferases and deacetylases mediate a dynamic attachment between transcriptionally active chromatin domains and the nuclear matrix. In the case of the β-globin domain, these dynamic interactions are not confined to the promoter region but also include the coding regions of expressed and competent genes.

## Part II: Association of Dynamically Hyperacetylated Histones with the Estrogen-Responsive pS2 Gene

While histone acetylation has been found to occur on the promoter regions of estrogen-responsive genes in the presence of estrogen [168,199], the nature of this acetylation and its function in hormone-mediated transcription remains to be determined. To date, the involvement of histone deacetylation in estrogen-mediated transcriptional activation and chromatin remodeling has been largely ignored. Without sufficient proof, many researchers have postulated that exposure to estrogen causes the replacement of histone deacetylases situated along an estrogen-responsive gene with histone acetyltransferases. However, it is possible that deacetylases are present both in the absence and presence of estrogen and that treatment with estrogen simply disturbs the balance between acetyltransferases and deacetylases, causing an increase in the recruitment of histone acetyltransferases while a background of deacetylase activity persists. Little investigation has also been made to determine if dynamic histone acetylation takes place downstream from the promoter regions of estrogen-responsive genes and if this event is dependent on transcription.

In order to further understand the involvement of dynamic histone acetylation in estrogen-mediated chromatin remodelling, the objectives of this study were: 1) to determine if histone deacetylases are associated with the pS2 promoter and coding regions in the absence of transcriptional stimulation by using inhibitors of deacetylases that increase histone acetylation levels along gene regions associated with histone deacetylases and by identifying the location of HDAC1 along the pS2 promoter and coding regions and 2) to determine if estrogen-induced histone acetylation is a

widespread, dynamic and transcription-independent event mediated by histone acetyltransferases and deacetylases that are associated with the pS2 promoter and exon regions. The effects of estrogen, histone deacetylase inhibitors and an inhibitor of transcription on the levels of acetylated H3 and H4 associated with the pS2 promoter and exon regions were determined using the ChIP assay.

## 1.0 Methods

### 1.1 Cell Maintenance

The T5 human breast carcinoma cell line was used. This T5 cell line is a sub-clone of MCF-7 and is referred to as MCF-7 throughout the body of this text. This cell line was maintained in T-185 flasks (Nalge Nunc, NY) and treated on 150 x 20 mm tissue culture dishes (Nalge Nunc) at 37°C (humidified atmosphere, 5% $CO_2$ / 95% Air). The cells were maintained in complete culture medium containing Dulbecco's Modified Eagle Medium (DMEM, Invitrogen Life technologies, CA) supplemented with 1% (v/v) L-glutamine, 1% (v/v) glucose, 1% (v/v) penicillin/streptomycin and 5% (v/v) fetal bovine serum (FBS: Invitrogen).

### 1.2 Cell Treatments

For an overall summary of the different cell treatments, please refer to Figure 20. Prior to treatment, all cells were grown for 4 - 5 days in 5% complete media on 150 x 20 mm tissue culture dishes. At approximately 50 – 60% confluence, the dishes were washed 2 times with 10 ml of 1 X PBS. Fifteen ml of estrogen-depleted phenol red-free (PRF) media (Invitrogen) containing 5% (v/v) twice charcoal-stripped FBS and supplemented as mentioned in the previous section was then added to each plate and the cells were grown for another 3 - 5 days.

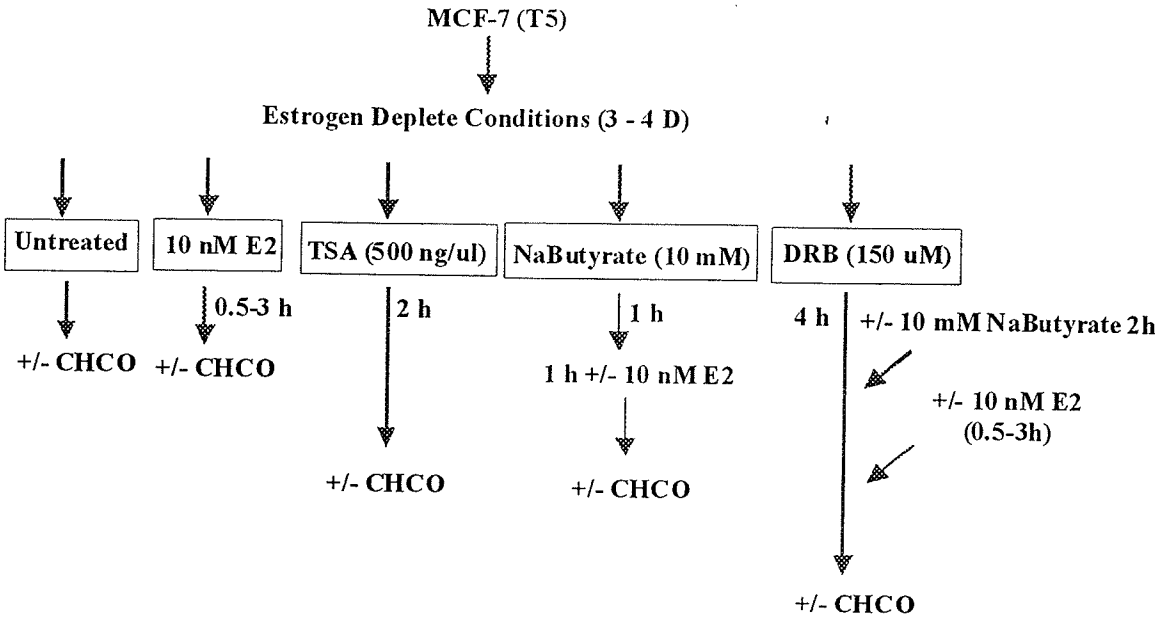


**Figure 20. Diagram of Estradiol (E2), HDAC Inhibitor and DRB Treatment Conditions for MCF-7 Cells.** CHCO signifies treatment with 1% formaldehyde for 10 min. D represents Days.

### 1.2.1 Formaldehyde Cross-linking of MCF-7 Cells

The cross-linking of MCF-7 cells was performed while cells were still attached to tissue culture plates. Immediately after treatment, the media was aspirated from each plate and replaced with 10 ml of a solution containing 1% (v/v) formaldehyde in 1 X PBS. The cells were then incubated at room temperature in the presence of formaldehyde for 10 min. The cross-linking reaction was stopped by adding glycine to a final concentration of 125 mM and/or washing the plates 2 times with approximately 20 ml of ice-cold 1 X PBS. The cross-linked cells were then collected with a rubber policeman and stored at -80°C.

### 1.2.2 Estradiol Treatment of MCF-7 Cells

On the 3rd - 5th day of growth in estrogen-deplete conditions, E2 was added to the media to a final concentration of $10^{-8}$ M from a $10^{-4}$ M stock. The cells were incubated at 37°C in the presence of $10^{-8}$ M E2 for 0, 0.5, 1, 2 or 3 h. At the end of each treatment time, the cells were either immediately collected or cross-linked with 1% (v/v) formaldehyde (see section 1.2.1). In all cases, cells were collected with a rubber policeman, pelleted by centrifugation at 300 x g for 5 min and the media or PBS aspirated. The cell pellets were stored at -80°C.

### 1.2.3 Sodium Butyrate or Trichostatin A Treatment of MCF-7 Cells

On the 3rd - 5th day of growth in estrogen-deplete conditions, sodium butyrate or TSA (Sigma-Aldrich) was added to the media to a final concentration of 10 mM or 500 ng/ml, respectively. The cells were then incubated at 37°C for 2 h. When cells were to be treated with histone deacetylase inhibitor for 2 h plus E2 for 30 min, the inhibitor was added 1.5 h prior to E2 treatment and the media containing the inhibitor was supplemented with E2 for the remaining 30 min. For cells treated with E2 for 1 h, HDAC inhibitor was added to the media 1 h prior to the addition of E2. When cells were to be treated with E2 for more than 1 h, HDAC inhibitor was added in the final 2 h of E2 treatment. Following treatment, the cells were either immediately collected or cross-linked with 1% (v/v) formaldehyde (section 1.2.1). In all cases, cells were collected with a rubber policeman, pelleted by centrifugation at 300 xg for 5 min and the media or PBS aspirated. The cell pellets were stored at -80°C.

### 1.2.4 DRB Treatment of MCF-7 Cells

On the 3rd - 5th day of growth in estrogen-deplete conditions, DRB (5,6-dichlorobenzimidazole 1-b-D-ribofuranoside) was added to a final concentration of 150 μM and the cells were incubated for 4 h to inhibit transcription. DRB blocks transcription by inhibiting CDK7 and CDK9 [494,495]. CDK7 and CDK9 phosphorylate the large subunit of the RNA polymerase II C-terminal domain, an event required to convert RNA polymerase into an elongation mode [495]. When the C terminal domain of RNA polymerase II is underphosphorylated, it can still mediate protein-protein interactions that lead to the assembly of the preinitiation complex, however, it can not initiate transcriptional elongation. If the DRB-treated cells were also to be treated with E2 to study transcription-independent histone acetylation, E2 was added after the initial 4 h DRB treatment as described in section 1.2.2 and the cells were subsequently incubated in the presence of both DRB and E2 for 30 min, 1 h, 2 h or 3 h. In cases where cells were to be treated with DRB, sodium butyrate and E2 together to study transcription-independent dynamic histone acetylation, 150 μM of DRB was added to the cells 4 h prior to the start of the 10 nM E2 treatment, while 10 mM sodium butyrate was added 2 h prior to the completion of the E2 treatment. Following treatment, the cells were either immediately collected or cross-linked with 1% (v/v) formaldehyde (section 1.2.1). In all cases, cells were collected with a rubber policeman, pelleted by centrifugation at 300 x g for 5 min and the media or PBS aspirated. The cell pellets were stored at -80°C.

## 1.3 Determination of pS2, GAPDH and Cyclophilin 33 RNA Levels in MCF-7 Cells

The RNA levels of the estrogen-responsive pS2 gene and the estrogen-non-responsive GAPDH and cyclophilin 33 genes were measured in treated MCF-7 cells to verify that the cells from each treated passage were responding to each treatment in a consistent and similar manner.

### 1.3.1 Isolation of Total RNA from MCF-7 Cells

Total RNA from MCF-7 cells treated with or without $10^{-8}$M E2 and/or transcriptional or HDAC inhibitors was isolated using the Qiagen RNeasy Kit (Qiagen, CA). The concentration of each RNA sample was determined by diluting 3 µl of RNA into a final volume of 50 µl with double-distilled water and reading the $A_{260}$ unit value. The $A_{280}$ units were also determined for each sample to assess the ratio of $A_{260}$: $A_{280}$ values and determine the purity of each RNA sample. Finally, the $A_{260}$ unit value was multiplied by a dilution factor of 16.7 and a conversion factor of 40 to determine the concentration of RNA (µg/ml) in each sample.

### 1.3.2 Conversion of Total RNA into cDNA Using Reverse Transcriptase (RT)

One µg of total RNA from each batch of treated cells was converted into cDNA by the following reaction. One µg of total RNA was transferred into a microcentrifuge tube and diluted to a final volume of 12 µl with double-distilled $H_2O$. The diluted RNA was incubated at 65°C for 5 min, cooled on ice for 5 min and then added to the following Invitrogen products: 6 µl 5 X first strand buffer (250 mM Tris, pH 8.3, 375 mM KCl), 15

mM $MgCl_2$, 0.1 µl 40 U/µl RNase Out, 1.5 µl of a solution containing 10 mM of each dNTP solution, 3 µl 0.1 M DTT, 1 µl of a 50 µM random hexamer solution , 4.9 µl double-distilled $H_20$, and 1.5 µl 200 U/µl Moloney Murine Leukemia Virus (MMLV). The sample was incubated at 37°C for 1 h, boiled for 3 min and then stored at –20°C.

### 1.3.3 Detection of pS2, GAPDH and Cyclophilin 33 cDNA in MCF-7

RNA levels for pS2, GAPDH and Cyclophilin 33 were determined indirectly from the cDNA of each batch of treated cells. Three microliters of cDNA isolated from a 50 µl reverse transcriptase (RT) reaction were added to 5 µl of Invitrogen 10 X PCR buffer (200 mM Tris, pH 8.4, 500 mM KCl), 0.4 µl of 10 mM dNTP (Invitrogen), 1.5 µl 50 mM $MgCl_2$ (Invitrogen), 0.25 µl Platinum Taq (5U/µl) (Invitrogen), 50 µM/2 ng of forward primer, 50 µM/ 2 ng of reverse primer, and 38.85 µl $H_20$. Primers were used to amplify exon 2 of the pS2 gene, as well as exon 7 and exon 2 of the GAPDH and cyclophilin 33 genes, respectively. The sequence of each primer is listed Table 3.

All PCR reactions were placed in a thermocycler (Perkin Elmer, MA) and subjected to 1 cycle of 95°C for 5 min, and then 27 cycles of the following: 95°C for 30 sec, 60°C for 30 sec, and 72°C for 30 sec. Five µl of 10 X DNA loading buffer was then added to the 50 µl PCR reaction and 15-20 µl of the PCR reaction was electrophoresed on a 1% (w/v) agarose gel. The gel was analyzed by scanning densitometry on a Kodak Image Station™ and the density of the amplified PCR product from each treatment was plotted. The fold induction of RNA levels in response to treatment was determined by dividing the net density value of PCR products from treated cells by that of products from

untreated cells. Thus, a fold induction value of less than one represents depletion in the RNA sequence in treated cells relative to untreated cells.

**Table 3.** **Primers Used to Assess pS2, GAPDH and Cyclophilin RNA Levels as well as the Levels of pS2 Promoter and Exon 3 in ChIP DNA.**

| Gene | Gene Region | Primer Sequences |
|---|---|---|
| pS2 | Promoter | 5' CCACCCCGTGAGCCACTGTTG 3'<br>3' GGCCCGGGGATCCTCTGAGAC 5' |
| | Exon 2 | 5' CTGGGGCACCTTGCATTTTCC 3'<br>3' CGGGGGGCCACTGTACACGTC 5' |
| | Exon 3 | 5' GCCACCTCCACCGGACACCTC 3'<br>3' CAGGGTGAAACGCTGCGCTTC 5' |
| GAPDH | Exon 7 | 5' CCAGGAAATGAGCTTGACAAAGTG 3'<br>3' AAGGTCATCCCTGAGCTGAACGGG 5' |
| Cyclophilin 33 | Exon 2 | 5' GCTGCGTTCATTCCTTTTG 3'<br>3' CTCCTGGGTCTCTGCTTTG 5' |

## 1.4 Extraction and Analysis of Hyperacetylated Histones in MCF-7 Cells

Cells were suspended in TNM buffer (10 mM Tris-HCl, pH 8, 100 mM NaCl, 300 mM sucrose, 2 mM $MgCl_2$, 1% (v/v) thiodiglycol, 1 mM PMSF) containing 0.25% (v/v) Triton X-100. The nuclei were then isolated and the histones extracted as previously described in Methods section 1.6 of Part I except TNM buffer was always used instead of RSB buffer. The isolated histones were then separated into their acetylated isoforms by

electrophoresis onto an AUT gel as described in Methods section 1.7 of Part I and the resulting gel was stained with a Coomassie Blue solution as described in Methods section 1.8 of Part I. The intensity of each acetylated histone isoform was quantified by scanning densitometry using a Kodak™ image station.

## 1.5 Assessment of ERα, HDAC 1, Sp1 and Sp3 Levels in Sodium Butyrate and TSA-Treated MCF-7 Cells

### 1.5.1 Preparation of Total Cell Lysates from MCF-7 Cells

MCF-7 cells were lysed in 8 M urea and sonicated for 10 – 20 sec. at 40% output with a Sonifier Cell Disrupter 350 (Branson Ultrasonic Corporation). Protein concentrations were determined using the Bio-Rad protein microassay. Samples were stored at -20°C.

### 1.5.2 SDS-Polyacrylamide Gel Electrophoresis (SDS-PAGE) of Total Cell Lysates from MCF-7 Cells

Proteins from total cell lysate were initially resolved by SDS-PAGE gel electrophoresis. The resolving gel solution consisted of 10% (w/v) acrylamide, 0.1% SDS (w/v), and 375 mM Tris-HCl, pH 8.8. Ammonium persulfate (0.15%, w/v) and TEMED (0.03%, v/v) were added to the gel solution and the gel was allowed to polymerize for 1-2 h. The stacking gel, which consisted of 3% (w/v) acrylamide, 0.1% (w/v) SDS and 125 mM Tris-HCl, pH 6.8, was supplemented with 0.15% (w/v) ammonium sulfate and 0.08% (v/v) TEMED, poured over the resolving gel and allowed to polymerize.

Approximately 10 ml each of resolving and stacking gel solutions were prepared for each gel. The gel thickness was typically 0.75 mm and the gel length was 8 cm high, 6 cm of which belonged to the resolving gel.

Once the stacking gel was polymerized, sample loading buffer [4 X stock: 277 mM SDS, 396 mM Tris-HCl, pH 6.8, 402 mM DTT, 40% (v/v) glycerol, 0.4% (w/v) bromophenol blue] was added to 15 μg of total cell lysate protein from each treatment sample and the sample was boiled for 2-4 min. After boiling, the samples were pulse-centrifuged, loaded into their respective wells and electrophoresed at room temperature for 45 min at 200 V. As well, an aliquot of pre-stained proteins of known molecular weights (Rainbow Marker, Amersham-Pharmacia, ON) was loaded into a well adjacent to the test samples to help assess the molecular mass of unknown proteins. The running buffer consisted of 193 mM glycine, 1% (w/v) SDS, 25 mM Tris-HCl, pH 8.3.

### 1.5.3 Immunoblot Analysis of ERα, HDAC1, Sp1 and Sp3 Levels in Cell Lysates from Treated MCF-7 Cells

The total cell lysate proteins resolved on the SDS-PAGE gels were transferred to nitrocellulose membrane as described in Methods section 1.9 of Part I except no pre-soaking of the gels in equilibration buffer was required.

For Immunoblot analysis of ERα protein, the nitrocellulose membrane was incubated in 5% (w/v) skimmed milk diluted in 1 X TTBS [0.1 M Tris-HCl, pH 8, 0.3 M NaCl, 0.4% (v/v) Tween-20] for 1 h and then washed 2 times with 1 X TTBS, each time for only 2 min. The membrane was incubated in a 1 X TTBS solution containing ERα antibody (Nova Castra, UK) diluted to 1/800 for 1.5 h at room temperature and then

quickly washed twice. The membrane was incubated in a solution of 1 X TTBS containing a 1/3000 dilution of goat-anti-mouse antibody linked to horseradish peroxidase, incubated for 30 min at room temperature and washed twice, each time for 15 min. ECL was performed to detect the interaction of the ERα antibody with its target protein in the MCF-7 cell lysate.

For immunoblot analysis of HDAC1 protein, the nitrocellulose membrane was incubated in 7% (w/v) skimmed milk diluted in 1 X TTBS for 1 h. The membrane was washed 2 times with 1 X TTBS, each time for only 2 min and then placed in a 1 X TTBS solution containing HDAC1 antibody (ABR, NJ) diluted to 1/2000 for 1 h at room temperature. The membrane was quickly washed twice and incubated in a solution of 1 X TTBS containing a 1/10,000 dilution of goat-anti-rabbit antibody linked to horseradish peroxidase for 30 min at room temperature. The membrane was washed twice, each time for 15 min and ECL was performed to detect the interaction of the HDAC1 antibody with its target protein in the MCF-7 cell lysate.

For immunoblot analysis of Sp1 and Sp3 protein, the nitrocellulose membrane was incubated in 7.5% (w/v) skimmed milk diluted in 1 X TTBS for 1 h. The membrane was washed 2 times with 1 X TTBS, each time for only 2 min, placed in 1 X TTBS solution containing Sp1 (Upstate Biotech) or Sp3 (Santa-Cruz Biotechnology, CA) antibody diluted to 1/500, and incubated for 1 h at room temperature. The membrane was then quickly washed twice and incubated in a solution of 1 X TTBS containing a 1/2500 dilution of goat-anti-rabbit antibody linked to horseradish peroxidase for 30 min at room temperature. The membrane was washed twice, each time for 15 min, and ECL was performed to detect the interaction of the Sp1 and Sp3 antibodies with their target

proteins in the MCF-7 cell lysate. The levels of Sp1, Sp3, HDAC1, HDAC2 and ERα were determined for at least two, and, in most cases, three passages of treated MCF-7 cells.

## 1.6 Isolation of DNA Sequences Associated with Hyperacetylated H3 and H4 Histones and HDAC1 in MCF-7 Cells by the ChIP Assay

### 1.6.1 Preparation of MCF-7 Cell Lysate for Immunoprecipitation

The DNA associated with hyperacetylated H3 and H4 antibodies and HDAC1 was isolated using a method based on two previously published protocols [199,474]. Approximately 1x $10^7$ formaldehyde-cross-linked cells were resuspended in 750 µl of lysis buffer [1% SDS (w/v), 10 mM EDTA, 50 mM Tris-HCl, pH 8.1] containing 1 mM PMSF, 50 µM iodoacetamide, 10 µg/ml leupeptin and 1 µg/ml aprotinin. The cell lysate was placed on ice for 5 min and then sonicated at 40% output for 14 - 30 sec. pulses using a sonifier cell disrupter 350 (Branson Ultrasonic Corporation) to reduce the DNA to 300-500 bp fragments. The sonicated lysate was then centrifuged for 10 min at 10,000 rpm in a microcentrifuge at 4°C. The supernatant was transferred to a fresh microcentrifuge tube and diluted to 2 $A_{260}$ units/ml with 1 X RIPA buffer [0.1% (w/v) SDS, 0.1% (w/v) SDC, 1% Triton X-100 (v/v), 1 mM EDTA, 0.5 mM EGTA, 140 mM NaCl, 10 mM Tris-HCl, pH 8] containing the same concentrations of leupeptin, aprotinin, PMSF and iodoacetamide as was in the lysis buffer. The sample at this point is referred to as the input. One hundred µl of input DNA was aliquoted into a clean microcentrifuge tube.

### 1.6.2 Immunoprecipitation of DNA sequences Associated with Hyperacetylated H3 and H4 Histones and HDAC1

Either an anti-HDAC1, anti-acetylated H3, anti-acetylated H4 or anti-integrin α1 (Upstate Biotech) antibody was added to 1 ml of cell lysate to a final dilution of 1/250. The anti-integrin α1 antibody was used as a control for proteins non-specifically immunoprecipitated by non-antibody serum components. The sample was incubated for 2 h at 4°C on an orbitron. BSA and sonicated *E. coli* DNA were then added to the sample to a final concentration of 10 μg/ml and 5 μg/ml, respectively, followed by 50 μl of a 50:50 slurry of protein A sepharose (Amersham-Pharmacia) in 1 X RIPA buffer. The sample was incubated at 4°C for 2 h on an orbitron. Non-specific material bound to the protein A sepharose was removed by washing the sepharose 3 times in 1 ml of ice-cold 1X RIPA, 3 times in 1 ml of ice-cold 1 X RIPA supplemented with 1 M NaCl, 2 times with 1 ml of ice-cold LiCl buffer [0.25 M LiCl, 1% NP-40 (v/v), 1% SDC (w/v), 1 mM EDTA, 10 mM Tris-HCl, pH 8], and then 2 times with 1 ml of ice-cold TE (20 mM Tris-HCl, 1 mM EDTA, pH 8) buffer. Each wash was performed for 4 min on an orbitron.

After the final TE wash, the protein A sepharose was resuspended in 200 μl of 1.5% (w/v) SDS elution buffer and incubated for 15 min at room temperature on an orbitron. The supernatant was transferred to a fresh microcentrifuge tube and 150 μl of 0.5% (w/v) SDS elution buffer was added to the left over beads to elute any complexes still associated with the sepharose. The beads were incubated once again for 15 min at room temperature on an orbitron and the supernatant was combined with the first eluate. EDTA, pH 8, Tris-HCl, pH 6.5, and NaCl were added to the input and the eluted

supernatant to final concentrations of 10 mM, 40 mM, and 200 mM, respectively. The samples were incubated at 68°C overnight to reverse formaldehyde cross-links between the DNA and protein. The following morning, proteinase K was added to the samples to a final concentration of 50 μg/ml and the sample was incubated at 55°C for 2 h to digest away any residual peptides or proteins still associated with the DNA. The samples were extracted once with an equal volume of phenol:chloroform:isoamyl alcohol (25:24:1). Five to ten μg of glycogen carrier (Invitrogen) and 2-3 volumes of absolute ethanol were then added to the samples and the samples were incubated at -80°C overnight to precipitate the immunoprecipitated DNA sequences. The samples were centrifuged for 30 min at 4°C and the resulting pellet of DNA was washed once with 1 ml of ice-cold 70% (v/v) ethanol. The DNA pellet was then resuspended in 20 μl of double-distilled $H_2O$ and stored at 4°C or -20°C.

### 1.6.3 **Quantitative PCR on Input and Immunoprecipitated DNA Sequences**

The immunoprecipitated and input DNA was analyzed for DNA sequences within the pS2 gene by real time PCR. Primers were used to amplify 315, 228 and 196 bp regions from the pS2 promoter, exon 2 and exon 3, respectively (Table 3). The primers for the 315 bp pS2 promoter region amplified most of the promoter region occupied by nucleosome E with the exception of the one Sp1 DNA-binding site upstream from the ERE (see Figure 12). Each PCR reaction was conducted in an iCycler™ (Bio-Rad) in the presence of 1 X Invitrogen PCR buffer, 80 μM dNTP, 1.5 mM $MgCl_2$, 1.25 U Platinum Taq (Invitrogen), 2 μl input or 4 μl immunoprecipitated DNA, and Sybr (Sigma) green diluted to 1/100,000. Amplification conditions were as follows: 1 cycle of 94°C for 5

min, followed by 27-31 cycles of 94°C for 30 sec, 60°C for 30 sec, and 72°C for 30 sec. Bio-Rad iCycler ™ software was used to visualize the intercalation of SyBr green dye into double stranded DNA during the amplification reaction. Initially, PCR reactions were run on input and immunoprecipitated DNA in an iCycler™ for each primer set to determine the number of cycles required for the desired PCR product to reach a linear stage of amplification. All subsequent PCR experiments on input and immunoprecipitated DNA were visualized using the Bio-Rad iCycler™ software to monitor amplification. All PCR reactions were stopped when the PCR product reached a linear stage of amplification.

PCR products were electrophoresed on to a 1% (w/v) agarose gel, stained with ethidium bromide and then quantified using a Kodak Image Station™. The net intensity of each ChIP DNA PCR product from each treatment was divided by the net intensity of the same PCR product from the respective starting input. The resulting normalized value was then divided by the normalized value for untreated samples to determine the fold enrichment of this DNA sequence in treated relative to untreated samples. ChIP assays were performed on at least 3 passages of treated MCF-7 cells.

## *2.0 Results*

### 2.1 Sodium Butyrate and TSA Induce Histone Hyperacetylation in MCF-7 Cells

To determine if the histones associated with the pS2 gene promoter are dynamically acetylated in the absence of estrogen, MCF-7 human breast cancer cells were treated with either 10 mM sodium butyrate or 500 ng/ml TSA for 2 h to inhibit histone deacetylase activity and promote histone hyperacetylation along DNA regions targeted by histone deacetylases. The efficacy of each histone deacetylase inhibitor under these conditions was determined by isolating the histones from treated cells and analyzing their acetylation status by AUT gel electrophoresis. Figure 21 shows that the treatment conditions for both histone deacetylase inhibitors were effective in significantly increasing the levels of acetylated histones. In particular, an increase in the levels of mono-, di-, tri- and tetra-acetylated H2B, H3 and H4 could be easily discerned in lanes containing histones from sodium butyrate- or TSA-treated cells.

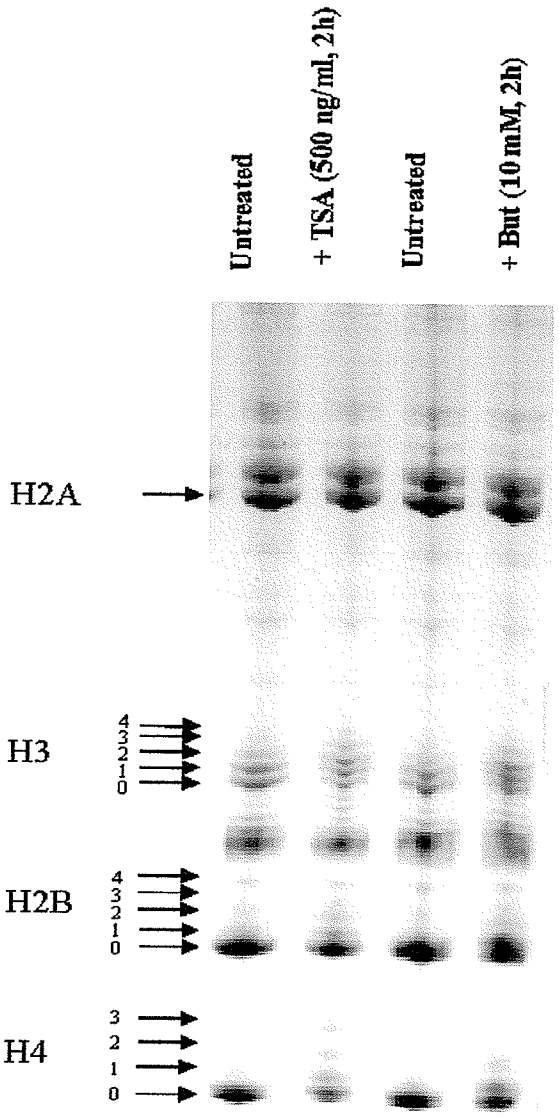


**Figure 21.** **Treatment of MCF-7 Human Breast Cancer Cells with 10 mM Sodium Butyrate for 2 h or 500 ng/ml TSA for 2 h Induces Histone Hyperacetylation.** 20 μg of acid extracted histones was electrophoresed onto a 15% Acid-Urea-Triton gel and the gel was stained with Coomassie Blue. 0, 1, 2, 3, and 4 represent mono-, di-, tri- and tetra-acetylated histone isoforms, respectively.

## 2.2 Estradiol Increases while DRB, Sodium Butyrate and TSA Decrease pS2 RNA Levels in MCF-7 Cells

Next the effect of 10 nM E2 for 1 h, 500 ng/ml TSA for 2 h and 10 mM sodium butyrate for 2 h on pS2, GAPDH and Cyclophilin 33 RNA levels was determined by RT PCR. An E2 concentration of 10 nM was used since E2 present at this concentration fully occupies the ERα and maximally stimulates pS2 gene expression [475]. Analysis of the RT-PCR products revealed that pS2 RNA levels increase 3.2 ± 0.7 fold (n = 7) in MCF-7 cells treated with 10 nM E2 for 60 min when compared to untreated cells, while RNA levels are only 0.6 ± 0.2 (n = 5) and 0.5 ± 0.3 (n = 4) fold in cells treated with 10 mM sodium butyrate (But) for 2 h or 500 ng/ml TSA for 2 h, respectively (Figure 22). GAPDH and Cyclophilin 33 RNA levels did not differ significantly between untreated cells and cells treated with E2, sodium butyrate or TSA.

The effect of treatment with 150 μM DRB alone or in combination with 10 nM E2 and/or 10 mM sodium butyrate on pS2 RNA levels was also determined. The results of this analysis are displayed in Figure 23. Treatment with 10 nM E2 for 1 h induced pS2 RNA levels by 3.2 ± 0.7 fold (n = 7) with respect to untreated cells. Treatment with 10 mM sodium butyrate for 2 h or 150 μM DRB for 4 h decreased pS2 total RNA levels to 0.6 ± 0.2 (n = 6) and 0.5 ± 0.3 fold (n = 4), respectively. Cells treated with both E2 and sodium butyrate or E2 and DRB displayed pS2 levels close to that observed in untreated cells. Lastly, cells treated with E2, DRB and sodium butyrate also displayed no significant change in pS2 RNA levels from that in untreated cells.

**Figure 22. Effect of Estradiol, Sodium Butyrate and TSA on pS2 Total RNA Levels in MCF-7 Cells.** MCF-7 cells were treated with 10 nM E2 for 60 min, 10 mM sodium butyrate for 2 h and 500 ng/ml TSA for 2 h. (A) Treatment with E2 increased pS2 total RNA levels 3.2 ± 0.7 (n = 7) fold, while RNA levels were only 0.6 ± 0.2 (n = 5) and 0.5 ± 0.3 (n = 4) fold after treatment with sodium butyrate (But) or TSA, respectively. (B) Treatment with E2, sodium butyrate or TSA resulted in Cyclophilin 33 RNA levels that were 1.0 ± 0.1 (n = 6), 0.9 ± 0.1 (n = 4) and 0.9 ± 0.1 (n =5) fold, respectively, of levels found in untreated cells. (C) Treatment with E2, sodium butyrate or TSA resulted in GAPDH RNA levels that were 1.0 ± 0.1 (n = 3), 0.8 ± 0.3 (n = 3) and 1.0 ± 0.1 (n = 2) fold, respectively, of levels found in untreated cells. Error bars represent the standard error of the mean.

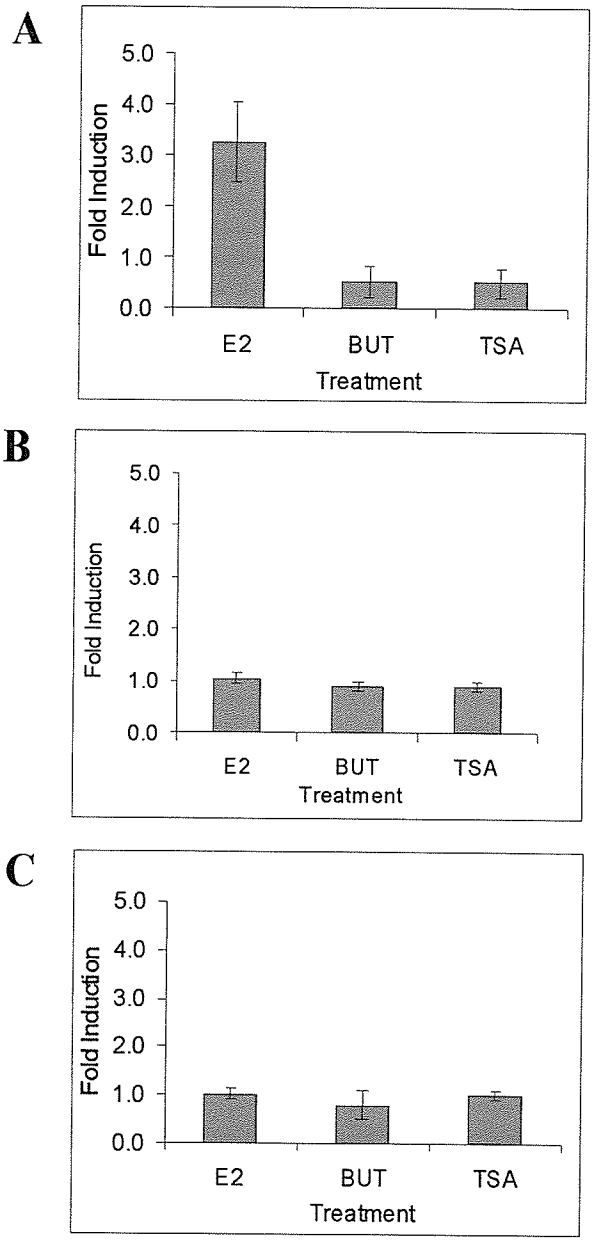

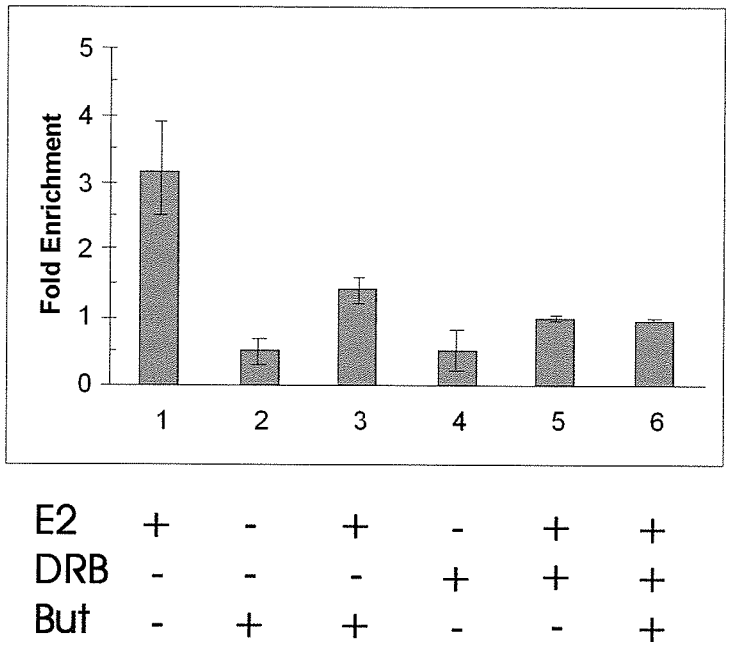


**Figure 23.** **The Effect of Estradiol, Sodium Butyrate and DRB on pS2 Total RNA Levels in MCF-7 Cells.** MCF-7 cells were treated with 150 μM DRB for 4 h and/or 10 mM sodium butyrate (But) for 2 h and/or 10 nM E2 for 1 h. Treatment with E2 increased pS2 total RNA levels 3.2 ± 0.7 (n = 7) fold, while the amount of pS2 RNA was only 0.6 ± 0.2 (n = 5) fold in cells treated with sodium butyrate when compared to untreated cells. Addition of E2 to sodium butyrate-treated cells resulted in a pS2 RNA level that was 1.4 ± 0.2 (n = 4) fold compared to untreated cells and DRB treatment alone yielded pS2 RNA levels that were 0.5 ± 0.3 (n = 4) fold. Cells treated with DRB and E2 displayed pS2 RNA levels that were 1.0 ± 0.04 (n = 2) fold of levels in untreated cells and pS2 RNA levels in cells treated with DRB, sodium butyrate and E2 were only 1.0 ± 0.01 (n = 2) fold. Error bars represent the standard error of the mean.

## 2.3 Sodium Butyrate and TSA do not Alter ERα, HDAC1, HDAC2 or Sp1 Levels in MCF-7 Cells

To further understand the mechanism through which sodium butyrate and TSA affect pS2 gene expression in MCF-7 cells, we measured the total cellular levels of some proteins involved in the estrogen response in untreated and treated MCF-7 cells (Figure 24). These proteins included ERα, HDAC1, HDAC2, Sp1 and Sp3 protein. These results showed that exposure to either 10 mM sodium butyrate or 500 ng/ml TSA for 2 h or 10 nM E2 for 1 h does not significantly alter the levels of ERα, HDAC1, HDAC2 and Sp1 in MCF-7 cells. Treatment with E2 for 1 h also did not significantly alter Sp3 protein levels. Overall, sodium butyrate and TSA did not significantly alter the level of both short forms of Sp3. However, the results of a third experiment showed an increase in both short forms after these treatments. The levels of Sp3 long form protein displayed considerably more variability in response to histone deacetylase inhibitors. In one experiment, sodium butyrate and TSA treatment increased the levels of Sp3 long form. In a second experiment, TSA increased while sodium butyrate did not alter Sp3 long form levels. In a third experiment, TSA decreased Sp3 long form levels while sodium butyrate increased them.

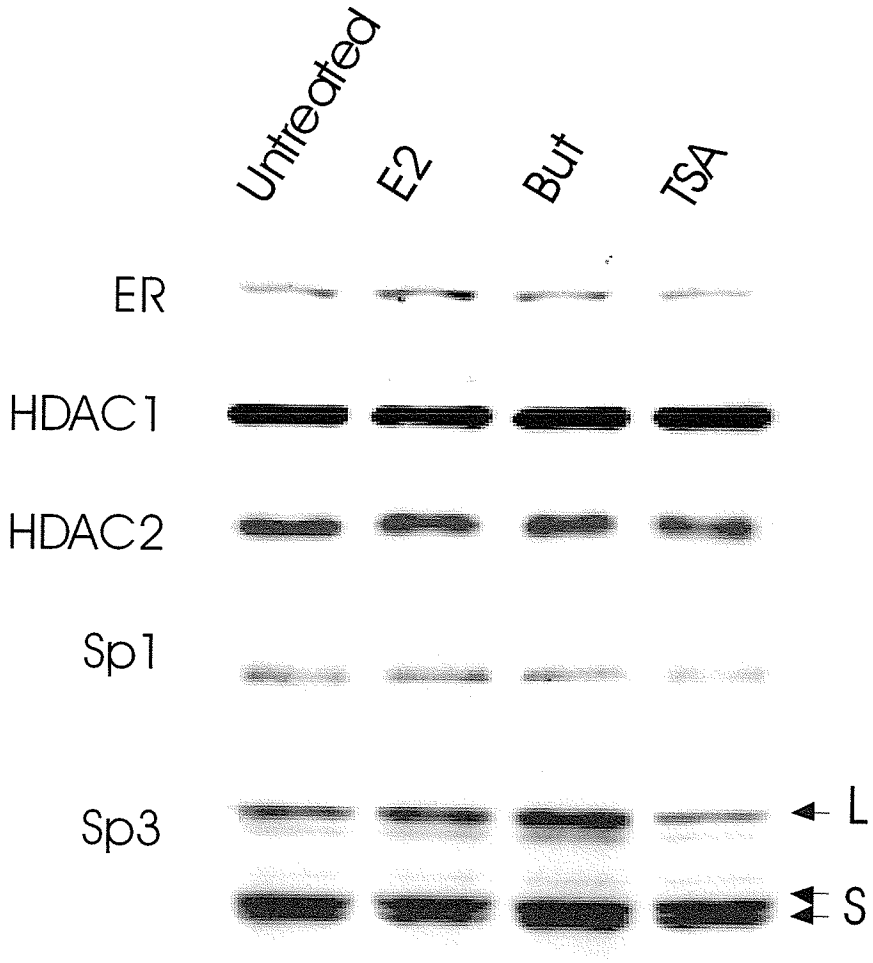


**Figure 24.** **E2, Sodium Butyrate and TSA do not Significantly Alter ERα, HDAC1, HDAC2 or Sp1 Protein Levels in MCF-7 Cells.** MCF-7 cells were treated with 10 mM sodium butyrate (But) or 500 ng/ml TSA for 2 h or 10 nM E2 for 60 min. Fifteen μg of total cell extracts from each treatment sample were electrophoresed on to a 10% SDS-PAGE gel, transferred to nitrocellulose and immunostained with antibodies to ERα, HDAC1, HDAC2, Sp1 or Sp3. L and S designate long and short forms of the Sp3 protein.

## 2.4. Sodium Butyrate and TSA Decrease HDAC1 Levels Associated with the pS2 Promoter

Sodium butyrate has previously been shown to remove HDAC1 from the promoter region of the HER (Human Epidermal Growth Factor Receptor 2) gene and the HIV-1 long terminal repeat [476-478]. Furthermore, the effect of HDAC inhibitors on the association of ERα with estrogen-responsive genes remains to be determined. To see if sodium butyrate and TSA reduce pS2 RNA levels by altering the association of HDAC1 with different regions of the pS2 gene, the DNA sequences associated with HDAC1 were analyzed by quantitative PCR using primers to the pS2 promoter, exon 2 and exon 3 gene regions. PCR analysis was performed on three different passages of sodium butyrate- and TSA–treated cells. With the exception of one MCF-7 passage which displayed no change in HDAC1 levels along the 3 pS2 gene regions in response to TSA treatment, the trend of sodium butyrate and TSA treatment on HDAC1 distribution along each target DNA sequence was similar. A representative PCR data set along with one of the replicate data sets is displayed in Figure 25.

The results of these ChIP assays show that treatment of MCF-7 cells with 10 mM sodium butyrate or 500 ng/ml TSA for 2 h decreases HDAC1 levels along the pS2 promoter. Sodium butyrate treatment also decreased HDAC1 levels along exons 2 and 3, while TSA had no significant effect on HDAC1 association with these two regions. No significant levels of pS2 promoter or coding region DNA sequences were immunoprecipitated non-specifically by the integrin α1 antibody. These results suggest that sodium butyrate inhibits histone deacetylation along the promoter and coding regions of the pS2 gene by disrupting the association between histone deacetylases and these

gene regions. TSA, on the other hand, appears to inhibit the recruitment of histone deacetylases only to the pS2 promoter.

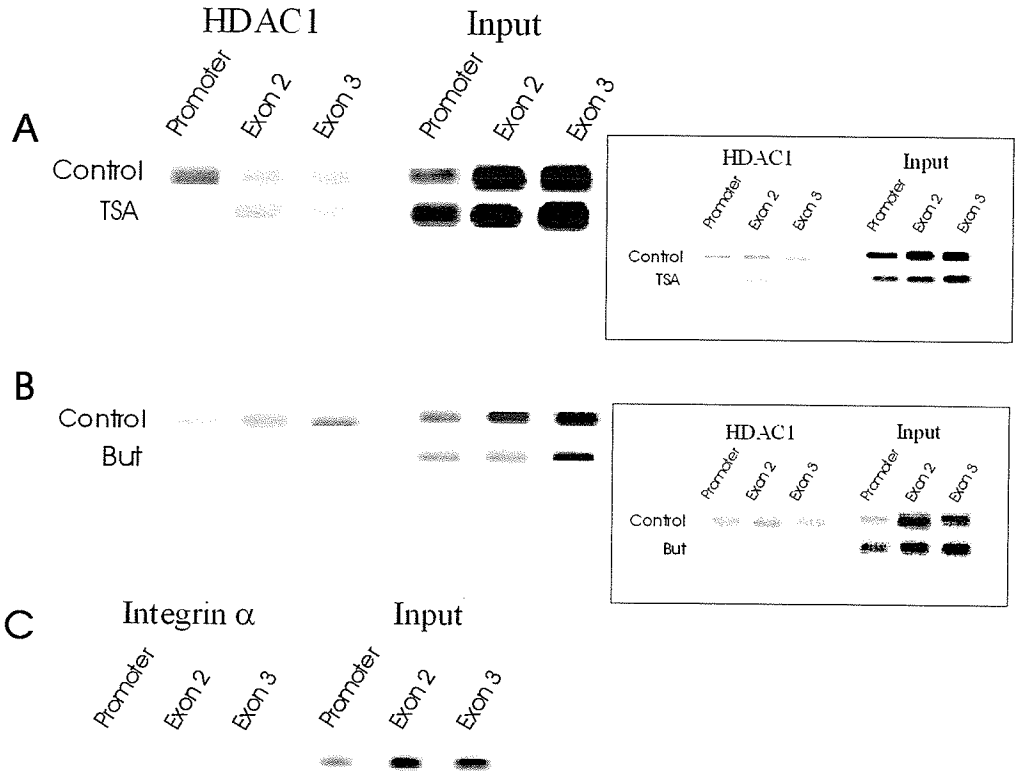


**Figure 25. The Effect of TSA and Sodium Butyrate on the Association of HDAC1 with the pS2 Promoter, Exon 2 and Exon 3 in MCF-7 Cells.** (A) PCR analysis of pS2 promoter, exon 2 and exon 3 DNA sequences associated with HDAC1 in MCF-7 cells treated with 500 ng/ml TSA for 2 h. (B) PCR analysis of pS2 promoter, exon 2 and exon 3 DNA sequences associated with HDAC1 in MCF-7 cells treated with 10 mM butyrate (But) for 2 h. Replicate data for each treatment set are displayed to the right. (C) PCR analysis of pS2 promoter, exon 2 and exon 3 DNA sequences associated with integrin α1 in untreated MCF-7 cells.

## 2.5 Estradiol, Sodium Butyrate and TSA Induce Histone H3 and H4 Hyperacetylation Along the pS2 Gene in MCF-7 Cells

We showed that sodium butyrate and TSA induce histone acetylation in MCF-7 cells (section 2.1). To determine if these histone deacetylase inhibitors induce histone hyperacetylation along the pS2 gene, the ChIP assay was performed on untreated MCF-7 cells as well as MCF-7 cells treated with histone deacetylase inhibitor or 10 nM E2 for 1 h. The DNA sequences associated with hyperacetylated H3 and H4 were analyzed by quantitative PCR using primers to the promoter, exon 2 and exon 3 regions of the pS2 gene. The fold enrichment of each target DNA sequence was then calculated by normalizing the net intensity of each PCR product to its respective starting input and then dividing all normalized values from treated samples by that generated from the untreated sample. PCR analysis was performed on three different passages of E2-, sodium butyrate- and TSA–treated cells. The trend for fold enrichment of acetylated H3 and H4 was similar in all three passages. However, the exact fold enrichment values varied significantly between passages due to variations in the ability of the antibody to immunoprecipitate its target protein. Thus, instead of averaging the three data sets, a representative PCR data set along with a diagrammatic representation of the fold enrichment in acetylated H3 and H4 is displayed in Figure 26. As well, the PCR data from another treated passage is displayed.

The results of these ChIP assays show that treatment of MCF-7 cells with 10 nM E2 for 60 min increases the level of H3 acetylation along the pS2 promoter and exon 2 by approximately 2.6 and 1.9 fold, respectively. The level of acetylated H3 along exon 3, however, was only 1.2 fold of the level along the same gene region in untreated cells. As

well, this E2 treatment increased H4 acetylation levels by a respective 4.6, 2.4 and 4.2 fold along the pS2 promoter, exon 2 and exon 3. Similarly, sodium butyrate treatment also increased acetylated H3 levels along the pS2 promoter and exon 2 by approximately 2.3 and 2.4 fold, respectively. However, acetylated H3 levels along exon 3 in sodium butyrate-treated cells did not vary much from the levels observed in untreated cells since only a 1.2 fold enrichment was observed along this gene region. The levels of acetylated H4 were also increased by approximately 3.8, 2.5 and 3.6 fold along the promoter, exon 2 and exon 3 regions, respectively. Lastly, TSA treatment increased acetylated H3 levels by approximately 1.6, 1.5 and 2.5 fold and acetylated H4 levels by approximately 2.2, 1.9 and 3 fold along the pS2 promoter, exon 2 and exon 3, respectively.

Thus, E2 is able to induce H3 and H4 acetylation along regions downstream from the pS2 promoter. Furthermore, the fact that TSA and sodium butyrate induce histone acetylation along the three pS2 gene regions suggests that both histone acetyltransferases and histone deacetylases are associated with or located close to the pS2 promoter, exon 2 and exon 3 gene regions in the absence of estrogen.

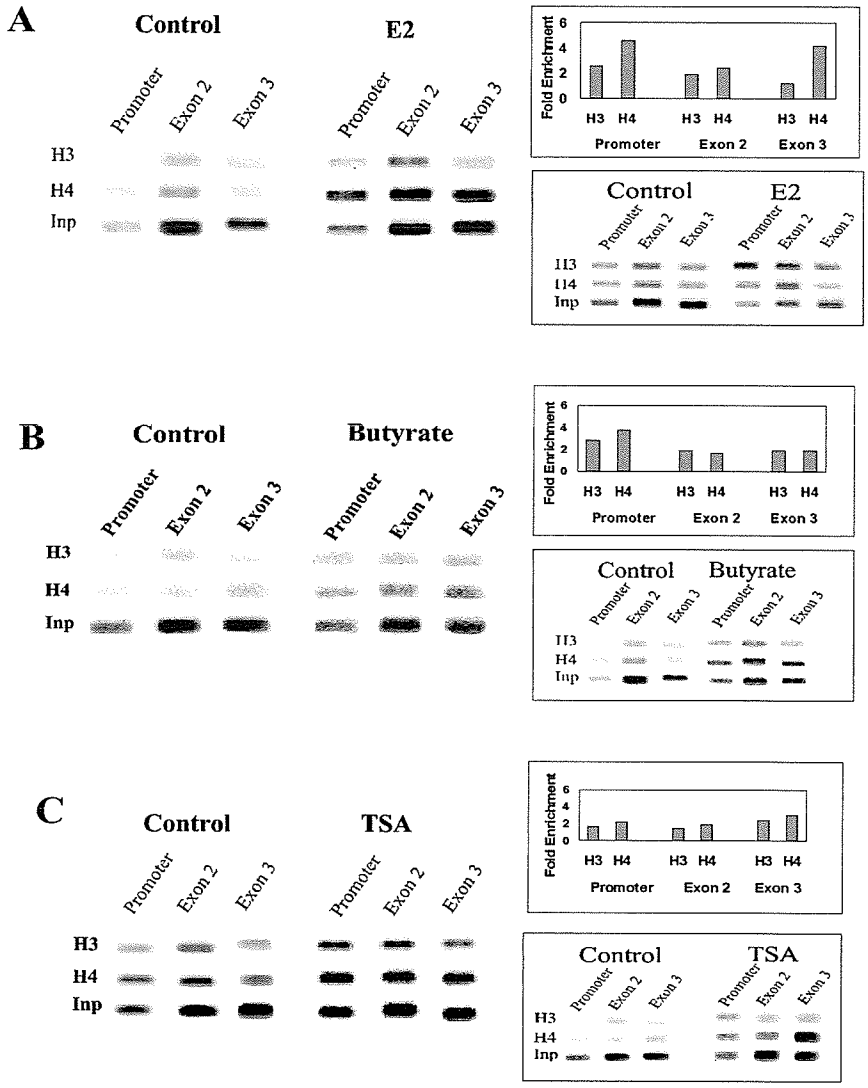


**Figure 26.** **The Effect of Sodium Butyrate, TSA and Estradiol (E2) on H3 and H4 Acetylation Along the pS2 Promoter, Exon 2 and Exon 3 Gene Sequences in MCF-7 Cells .** Representative PCR product data set (left) of H3 - and H4 -associated pS2 promoter, exon 2 and exon 3 DNA sequences in immunoprecipitated DNA accompanied by a replicate data set (Right upper box) and a diagrammatic representation of the fold enrichment of these products in E2- (A), Butyrate (But)- (B), and TSA- (C) treated MCF-7 cells. Inp represents Input.

## 2.6 Exposure to Estradiol Induces Histone Hyperacetylation Along the pS2 Promoter and Exon 3 that is Sustained for up to 180 min.

To determine if the effect of E2 on H3 and H4 acetylation along the pS2 gene is sustained over time, we treated MCF-7 cells with 10 nM E2 for 0 – 180 min. The DNA associated with hyperacetylated H3 and H4 was isolated using the ChIP assay and the fold enrichment of the pS2 promoter and exon 3 DNA sequences in the ChIP DNA was determined as previously described in section 2.5. Once again PCR analysis was performed on three different passages of E2-treated MCF-7 cells. The results of one data set are displayed in Figure 27.

All three passages showed that H3 becomes hyperacetylated along the pS2 promoter at 30 min exposure to E2. In two cell passages, H3 acetylation along the promoter was sustained throughout all treatment time points, while in a third passage H3 acetylation decreased to levels observed in untreated cells when cells were treated with E2 for more than 60 min (data not shown). When compared to untreated cells, the acetylated H3 level was higher than levels in untreated cells along exon 3 at 30 min in two passages and approximately equal to levels in untreated cells in a third passage. Likewise, two passages displayed an increase in acetylated H3 at 60 min, while in a third passage acetylated H3 levels were equal to levels in untreated cells. At 2 h E2 treatment, acetylated H3 levels were equal to levels in untreated cells in two passages, while acetylated H3 levels were increased above control levels in a third passage. The variations observed between acetylated H3 levels on the pS2 promoter and exon 3 regions between passages are most likely due to variations in the immunoprecipitation efficiency of the acetylated H3 antibody between samples. Nevertheless, these results

show that the pS2 promoter and exon 3 are rapidly H3 hyperacetylated in response to E2 treatment by 30 min and that this hyperacetylation lasts for at least 60 min.

Along the pS2 promoter, acetylated H4 levels began to show a significant increase by 60 min, dropped to levels just above untreated control levels at 120 min and then increased again at 180 min. However, in one other passage acetylated H4 levels were still significantly higher than in control cells at 120 min. In one passage, H4 became hyperacetylated as early as 30 min along exon 3 and stayed hyperacetylated for all remaining time points in one cell passage. A similar trend was displayed for two other passages. However, in both of these passages acetylated H4 levels at 120 min of E2 treatment were greater than levels observed before and after this treatment time point. Once again, the variations observed between acetylated H4 levels on the pS2 promoter and exon 3 regions between passages are most likely due to variations in the immunoprecipitation efficiency of the acetylated H4 antibody between samples. These results show that E2 treatment rapidly induces H4 hyperacetylation along the pS2 promoter and exon 3 regions within 30 min and that this hyperacetylation lasts for at least 180 min.

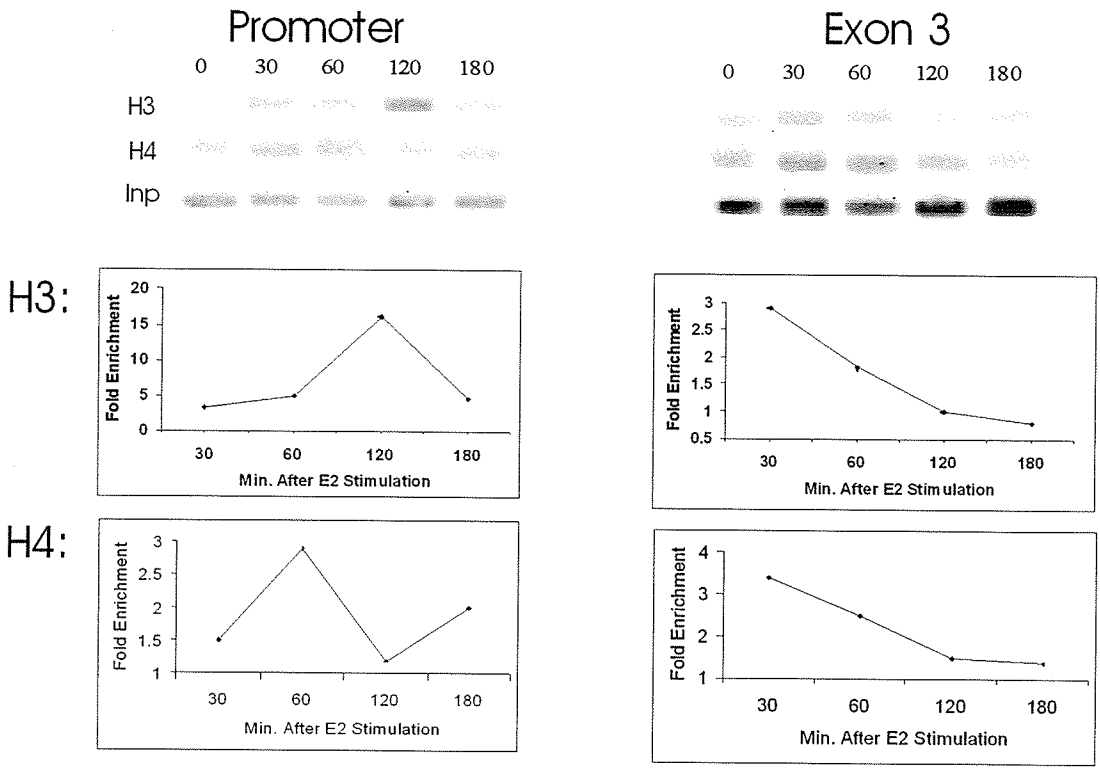


**Figure 27.** **The Effects of Estradiol on H3 and H4 Acetylation Along the pS2 Promoter and Exon 3 Gene Sequences.** PCR analysis of pS2 promoter and exon 3 DNA sequences associated with acetylated H3 and H4 in MCF-7 cells treated with 10 nM E2 for 0 - 180 min. The pS2 promoter and exon 3 PCR products are displayed. Positioned below this display are plots displaying the fold enrichment values of each DNA sequence in acetylated H3 - and H4 -immunoprecipitated DNA samples relative to untreated cells. Inp represents input.

## 2.7 Estradiol Induces Histone Acetylation Along the pS2 Promoter and Exon 3 Even When Transcription is Inhibited

The widespread acetylation of histones along the pS2 gene may function in the recruitment of this active gene to specific nuclear regions such as the NM. Alternatively, this widespread histone acetylation may result from contacts made between regions of the the pS2 gene and the transcriptional initiation and elongation machinery. To determine if transcriptional stimulation was required for estrogen-induced H3 and H4 hyperacetylation along the pS2 gene, MCF-7 cells were treated with 150 μM DRB for 4 h to inhibit transcription. E2 was then added to the DRB-containing media for 0 – 180 min and the DNA sequences associated with hyperacetylated H3 and H4 were isolated and analyzed for pS2 promoter and exon 3 DNA sequences by PCR analysis. This analysis was performed on two passages of treated cells. The results of one data set are displayed in Figure 28.

Both passages displayed a drastic increase in hyperacetylated H3 levels along the promoter when exposed to E2 for 30 min in the presence of DRB. This increase was greater than that observed in DRB-treated cells and cells treated only with E2 for 30 min (Figure 28). Acetylated H3 levels decreased slightly at 60 and 120 min but remained substantially higher than in untreated or DRB-treated cells. Furthermore, at 180 min, acetylated H3 levels were still greater than levels in untreated and DRB-treated cells. In one cell passage, acetylated H3 levels along exon 3 were higher than in untreated or DRB-treated cells at 60, 120 and 180 min of E2 treatment (Figure 28). In another cell passage, DRB-treated MCF-7 cells for all E2 treatment time points displayed the same degree of H3 acetylation along pS2 exon 3 as was seen for untreated cells (data not

shown). However, in this passage, the level of acetylated H3 associated with pS2 exon 3 in response to all E2 treatments did not significantly differ from levels observed in DRB-treated cells.

Exposure of MCF-7 cells to DRB for 5 h led to an increase in H4 histone acetylation along the pS2 promoter in one cell passage (data not shown). This observation, however, could not be repeated since a second DRB-treated passage displayed a slight depletion in acetylated H4 along the pS2 promoter when compared to untreated cells (shown in Figure 28). Both passages of MCF-7 cells treated with E2 for 30 min displayed an increase in acetylated H4 along the pS2 promoter when compared to untreated cells. The level of H4 acetylation along the pS2 promoter in the presence of E2 for 30 min was greater than that observed in one passage of cells treated only with DRB (Figure 28) but not greater than that observed in another passage of DRB-treated cells (data not shown). Acetylated H4 levels along the pS2 promoter still remained high at 60 min E2 treatment when compared to untreated cells. These levels were greater than levels observed in DRB-treated cells from one passage (shown in Figure 28) but not greater than levels observed in a second passage (data not shown). By 120 min E2 treatment, acetylated H4 levels along the pS2 promoter were equivalent to levels observed in DRB-treated cells in one passage (data not shown) and approximately equal to levels observed in the untreated cells of another passage (Figure 28). Acetylated H4 levels then either slightly increased in one passage (Figure 28) or remained steady in a second passage (data not shown) to levels observed in DRB-treated cells at 180 min E2 treatment. The difference in H4 acetylation levels along the pS2 promoter between passages is most likely due to inefficiencies in immunoprecipitation of acetylated H4.

Analysis of pS2 exon 3 revealed that acetylated H4 levels were higher along exon 3 in both cell passages when they were treated with only DRB compared to untreated cells (Figure 28). The addition of E2 to both passages of DRB-treated cells for 30 min increased H4 acetylation levels along exon 3 beyond levels observed in DRB-treated cells. In one passage, H4 acetylation levels were slightly greater than levels observed in DRB-treated cells when cells were treated with E2 for 60 – 180 min (Figure 28). In a second passage, acetylated H4 levels dropped to untreated levels along exon 3 at 60 min E2 treatment, increased a little further to just below levels observed in DRB-treated cells by 120 min E2 treatment and then increased to DRB-treated levels by 180 min E2 treatment (data not shown). However, in a third passage of DRB-treated cells that were exposed to 10 nM E2 for only 60 min, acetylated H4 levels were higher along exon 3 than in untreated cells (data not shown). This suggests that the DRB treatment accompanied by treatment with 10 nM E2 for 60 min induces H4 hyperacetylation along pS2 exon 3 and that the depletion of acetylated H4 in the second passage was most likely a consequence of the inefficient immunoprecipitations of acetylated H4-associated DNA sequences.

Overall, these results show that treatment of MCF-7 cells with 10 nM E2 for 30 – 180 min induces H3 acetylation along the pS2 promoter and possibly increases H3 acetylation along exon 3 in the absence of transcription. DRB treatment most likely induces H4 acetylation along both the pS2 promoter and exon 3 and treatment of MCF-7 cells with 10 nM E2 may mildly induce H4 acetylation levels along the promoter and exon 3 regions of the pS2 gene in the absence of transcription. Of interest was the observation that acetylated H3 and H4 levels were maintained along exon 3 after 30 min

of E2 treatment in the presence of DRB (Figure 28). In MCF-7 cells treated with only E2, H3 and H4 acetylation levels were maximal along exon 3 at 30 min and then started to decline thereafter (Figure 27). Furthermore, a significant amount of H3 and H4 acetylation still occurred along the pS2 promoter when transcription was inhibited. These results suggest that at least some of the histone acetylation that takes place along the pS2 promoter and exon 3 in response to E2 treatment is transcription-independent. However, acetylated H3 levels in E2-treated cells were substantially greater than levels in untreated or DRB plus E2-treated cells along the pS2 promoter and exon 3 at 120 min and 30 min E2 treatment, respectively. Thus, in the case of H3, E2-induced widespread acetylation may also result from contacts made between the pS2 promoter and exon 3 and the transcriptional initiation and elongation machinery.

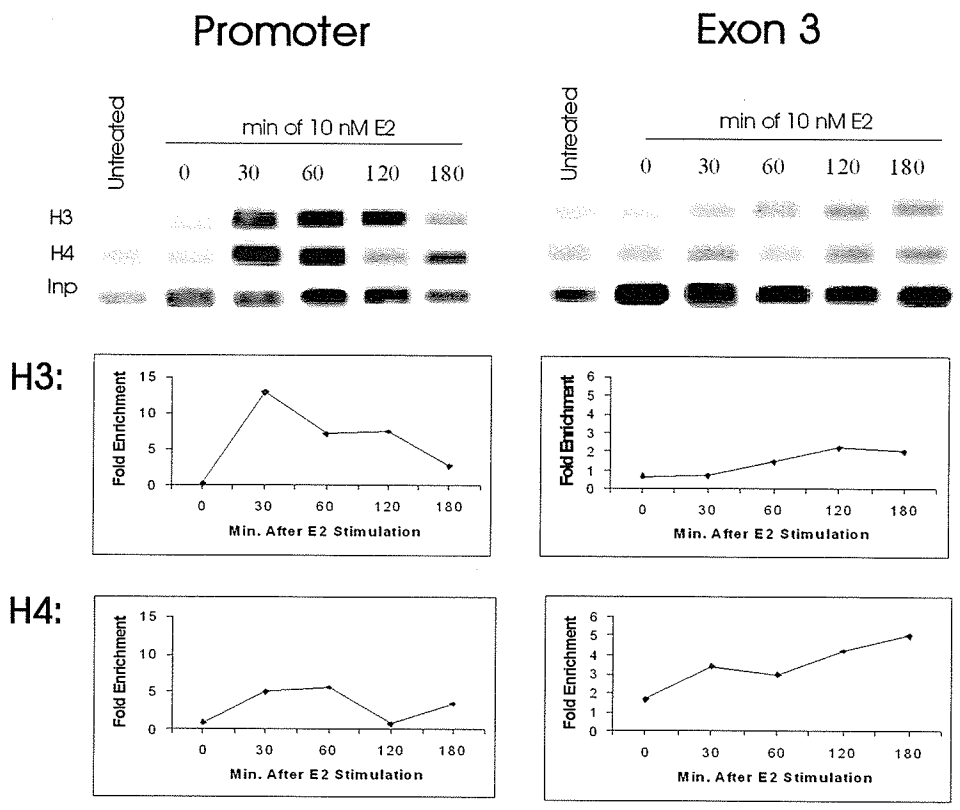


**Figure 28.** **The Effects of Estradiol and DRB on H3 and H4 Acetylation Along the pS2 Promoter and Exon 3 Gene Sequences .** PCR analysis of pS2 promoter and exon 3 DNA sequences associated with acetylated H3 and H4 in MCF-7 cells treated with 10 nM E2 for 0 - 180 min in the presence of 150 μM DRB. The pS2 promoter and exon 3 PCR products are displayed. Positioned below this display are plots of the relative fold enrichment values of each DNA sequence in H3- and H4-immunoprecipitated DNA. Inp represents input.

## 2.8 Estradiol-Induced Histone Acetylation Along the pS2 Promoter and Exon 3 is a Dynamic Process

Histone acetylation is usually a dynamic process mediated by both histone acetyltransferases and histone deacetylases. Therefore, we determined if the E2-induced widespread histone acetylation observed in the presence or absence of DRB is a dynamic event mediated by both these enzymes. MCF-7 cells were treated with DRB and E2 as described in section 2.7 and 10 mM sodium butyrate was added to the E2 plus DRB–containing medium 2 h before completion of the E2 treatment. DNA sequences associated with hyperacetylated H3 and H4 were isolated and analyzed for pS2 promoter and exon 3 DNA sequences by PCR analysis.This analysis was performed on two passages of treated cells. The results of this analysis are presented in Figure 29A. Unfortunately, the PCR analysis for one of the two passages did not produce useful data. Therefore, the results of this section are based on one passage of treated cells and should only be considered preliminary.

The treatment of MCF-7 cells with DRB and sodium butyrate increased H3 and H4 acetylation levels along the pS2 promoter when compared to untreated or DRB-treated cells. Addition of 10 nM E2 to cells treated with both DRB and sodium butyrate drastically increased both acetylated H3 and H4 along the pS2 promoter at 60 min to levels far greater than that observed in E2-, E2 plus DRB– or E2 plus 10 mM sodium butyrate-treated cells. H3 and H4 acetylation levels then started to decline at 120 and 180 min but were still significantly greater than the levels observed in cells treated with E2 or DRB plus E2 for the same time points. These results suggest that, in the absence of transcription, H3 and H4 acetylation along the pS2 promoter is a dynamic process.

Interestingly, both H3 and H4 acetylation levels did not begin to substantially increase until after 30 min E2 exposure. Thus, the presence of sodium butyrate appeared to delay the onset of H3 and H4 acetylation along the pS2 promoter in cells treated with both DRB and E2.

In the absence of E2, sodium butyrate and DRB induced H3 and H4 acetylation along pS2 exon 3. Treatment of DRB- and sodium butyrate–treated cells with 10 nM E2 did not influence H3 and H4 acetylation along this gene region. With the exception of the 30 min E2 time point, DRB and sodium butyrate together in the presence or absence of E2 induced H4 acetylation to a level greater than that observed in cells treated only with DRB or DRB and E2. These results suggest that transcription-independent H3 and, possibly, H4 histone acetylation along pS2 exon 3 is a dynamic event.

The ability of DRB and sodium butyrate to enhance H3 and H4 acetylation levels along the pS2 promoter beyond levels observed in E2- or DRB plus E2–treated cells may result from the ability of sodium butyrate to act additively or synergistically with E2. MCF-7 cells were treated with 10 mM sodium butyrate for 1 h and then 10 mM sodium butyrate plus 10 nM E2 for an additional hour. DNA sequences associated with hyperacetylated H3 and H4 were isolated and analyzed as described in section 2.4. PCR analysis was performed on four passages of treated cells. The results of this analysis are presented in Figure 29B. The treatment of MCF-7 cells with both E2 and butyrate did not increase H3 and H4 acetylation levels along the pS2 promoter and exon 3 when compared to cells treated only with sodium butyrate. Thus, sodium butyrate does not appear to act additively or synergistically with E2 in inducing H3 or H4 hyperacetylation.

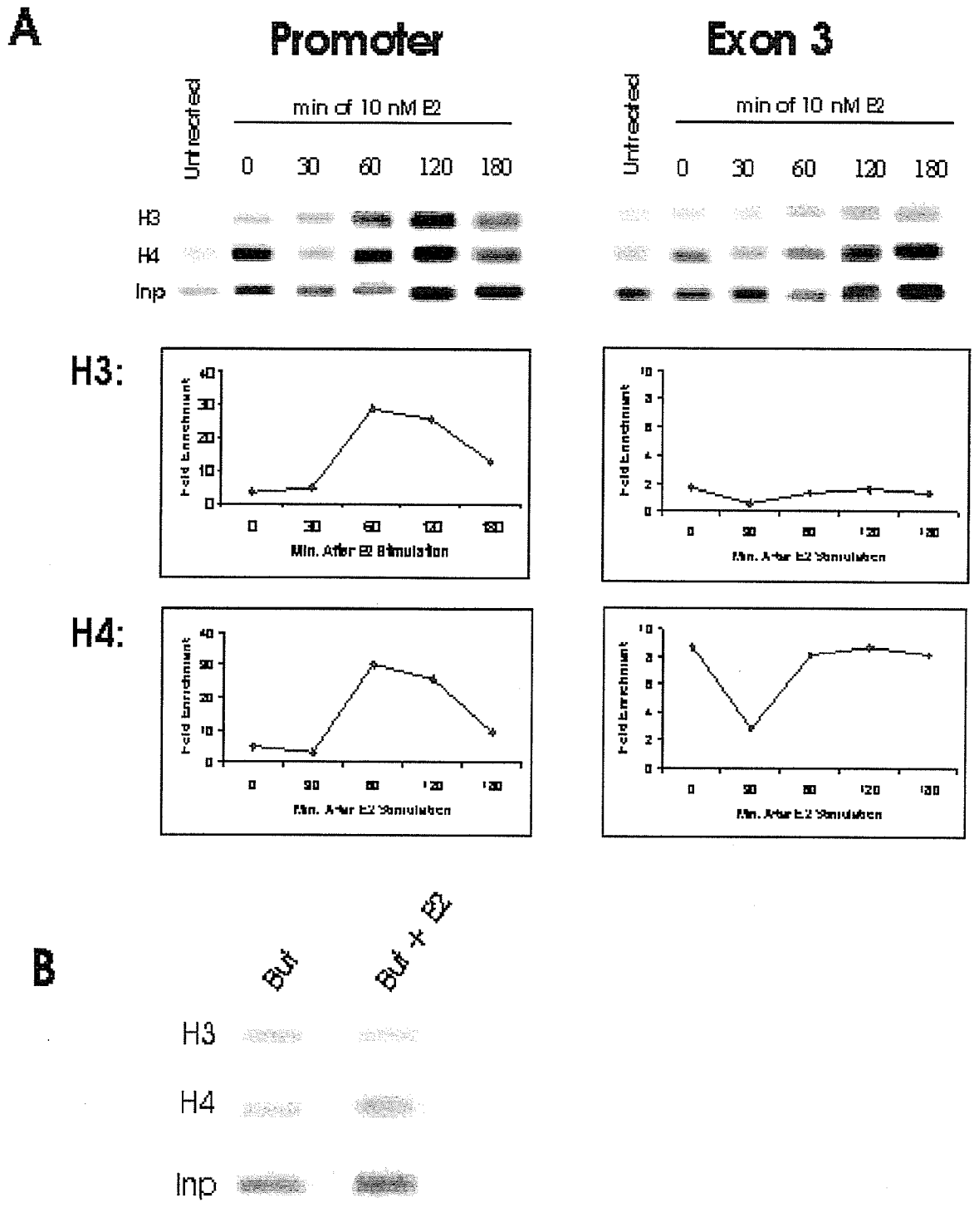


**Figure 29.** **The Effect of Sodium Butyrate (But), Estradiol (E2) and DRB on H3 and H4 Acetylation Along the pS2 Promoter and Exon 3.** (A). PCR analysis of pS2 promoter and exon 3 DNA associated with acetylated H3

and H4 in MCF-7 cells treated with 10 nM E2 for 0-180 min and 10 mM sodium butyrate for 2 h in the presence of 150 mM DRB. Positioned below this display are plots of the relative fold enrichment values of each DNA sequence in H3- and H4-immunoprecipitated DNA. (B). PCR analysis of pS2 promoter and exon 3 DNA sequences associated with acetylated H3 and H4 in MCF-7 cells treated with 10 nM E2 for 60 min and 10 mM sodium butyrate for 2 h. Inp represents input.

## *3.0 Discussion*

The exact function of histone acetylation in transcription has been questioned for decades. To further understand the involvement of this event in transcription, we studied the effect of estrogen on H3 and H4 acetylation along the pS2 promoter, exon 2 and exon 3. To date, estrogen–induced H3 and H4 acetylation has mainly been studied along the promoter regions of the estrogen-responsive pS2, c-*myc*, cathepsin D and EB1 genes[167,168,199]. In a recent study, Dr. Freedman and colleagues showed that exposure of MCF-7 cells to E2 for 15 and 30 min increased acetylated H4 levels along a downstream open reading frame in the pS2 gene [245]. However, whether this acetylation was a dynamic process was not determined. Learning the dynamics of histone acetylation along the different regions of estrogen-responsive genes is important for further elucidating the involvement of this event in estrogen-induced transcription. Furthermore, breast cancer cells proliferate in response to estrogen stimulation. Understanding the events involved in E2-induced transcriptional activation is therefore important for highlighting potential areas of disease therapy.

The first goal in this study was to determine if H3 and H4 are hyperacetylated in response to estrogen stimulation along regions downstream from the pS2 promoter. The treatment of MCF-7 cells with 10 nM E2 for 60 min induced pS2 RNA levels and also induced histone acetylation along the pS2 promoter and exon 2. H3 acetylation appeared not to be increased along exon 3. However, as can be seen in the replicate data set as well as in the E2-time course data set displayed in Figure 27, acetylated H3 levels associated with exon 3 were above levels observed in untreated cells when MCF-7 cells were treated with E2 for 60 min H4, in particular, displayed a larger fold enrichment along the three pS2 gene regions. This was most likely due to the efficiency of the acetylated H3 and H4

antibodies in recognizing their epitopes in the ChIP assay. In fact, even the antibodies themselves produced slight variations between individual immunoprecipitations. For example, the replicate data set in Figure 26 for ChIP assays performed on MCF-7 cells treated with 10 nM E2 for 60 min showed that H4 was hyperacetylated along pS2 exon 3 after E2 treatment. However, the representative data set shows that H4 was not hyperacetylated to the same degree on exon 3 even after considering the weaker intensity of the input exon 3 PCR product. To more accurately determine the effect of E2 on H3 and H4 acetylation along the pS2 promoter and exon 3, we performed ChIP assays on several different passages of E2-treated cells. These additional assays supported the representative data set displayed in Figure 26.

Our finding that estrogen treatment induces widespread H3 and H4 acetylation along the pS2 gene suggests that exposure to E2 either stimulates the recruitment of histone acetyltransferases and/or the removal of histone deacetylases from the pS2 promoter, exon 2 and exon 3. Estrogen-induced histone acetyltransferase recruitment to the pS2 promoter and coding regions is a likely scenario since the treatment of MCF-7 cells with E2 initiates the recruitment of histone acetyltransferases and the subsequent acetylation of histones along the promoter of several estrogen responsive genes including the pS2 gene [167,168,245]. However, E2 treatment promotes the recruitment of the RNA polymerase II complex to estrogen-responsive genes [168] and this complex is associated with histone acetyltransferases such as CBP and ELP3 [51,52]. Thus, the possibility still exists that E2-induced widespread histone acetylation along the pS2 gene resulted from contacts made between the pS2 promoter and exon 3 and the transcriptional initiation and elongation machinery. The induction of H3 and H4 acetylation along the exon regions of

an E2-responsive gene in the presence of E2 has not been shown by another research group.

Whether E2 treatment caused a decrease in the level of histone deacetylases associated with these three pS2 gene regions was not determined. However, in a recent study by Dr. Shang and colleagues, HDAC2 and HDAC4 levels were decreased along the c-*myc* promoter in MCF-7 cells after treatment with 100 nM E2 for 45 min [167]. Thus, histone deacetylase removal from both the promoter and coding regions of estrogen-responsive genes is a likely consequence of estrogen treatment.

Our second goal was to determine if the pS2 promoter, exon2 and exon 3 regions are dynamically or statically acetylated. To accomplish this task, we treated MCF-7 cells with either sodium butyrate or TSA histone deacetylase inhibitors. Our assumption was that if the histones along these gene regions are dynamically acetylated, exposure to an inhibitor of histone deacetylase activity would disturb the balance between the histone acetylation and deacetylation reactions and prolong the histone acetylation reaction. The consequence of this event would be an increase in the levels of acetylated histones in DNA regions situated close to histone acetyltransferases. Thus, observations of an induction in H3 and H4 acetylation levels along a specific gene region in response to histone deacetylases inhibitor treatment would suggest that histone acetyltransferases and histone deacetylases are associated with this gene region.

To address the issue of dynamic histone acetylation along different pS2 gene regions, we first determined the effect of sodium butyrate and TSA on pS2 gene expression. The treatment of MCF-7 cells with 10 mM sodium butyrate or 500 ng/ml TSA for 2 h drastically reduced pS2 RNA levels and therefore inhibited pS2 gene

expression. However, these inhibitors did not alter the expression of GAPDH or cyclophilin 33.

The effect of HDAC inhibitors on transcription is unknown. Butyrate and TSA affect the transcription of only a small fraction of genes within the nucleus [315,331,479] and whether they repress or induce gene transcription varies with gene type. Several studies have presented findings indicating that GAPDH RNA levels remain unaffected by both TSA and sodium butyrate [315,331,480]. Interestingly, pS2 RNA levels were shown to increase upon exposure to 2.5 - 10 ng/ml TSA in the presence of $10^{-11}$ M E2 after a 24 hour incubation. This induction was further increased to 2 fold after 48 h [480]. Although this disagrees with our current findings, it is important to consider that this inducible effect may be a result of the extended TSA and E2 incubation period and the fact that both E2 and TSA have many direct and indirect effects on the cell cycle that may promote pS2 gene expression. As well, we exposed our cells to 50 X the concentration of TSA for only 2 h and 1000 X the concentration of E2 for 1 h. We chose such a high E2 concentration for only 1 h because E2 present at 10 nM will fully occupy the ERα and maximally stimulate pS2 gene expression within an hour without causing significant changes in cell cycle distribution [475]. We also used a higher TSA concentration because this concentration has been used in other studies and shown to effectively induce histone acetylation in as little as 30 min [92]. Furthermore, the fact that exposure to a 10 mM physiological concentration of sodium butyrate for 2 h caused the same degree of inhibition in pS2 gene expression as the TSA treatment suggests that the TSA concentration was not unnecessarily high.

The pS2 protein is thought to function as a motogen, a factor that promotes cell movement and sodium butyrate inhibits the invasive behavior of cancer cells [481]. Exactly how sodium butyrate inhibits pS2 gene expression is unknown. The pS2 gene contains an ERE as well as an AP1-binding site [199,464,482]. Preliminary data obtained by Dr. Sun in our laboratory also indicates that the Sp1 and Sp3 proteins bind to two sites located on either side of the ERE *in vitro* [482-484] (Figure 12). As well, Dr. Sun has presented preliminary data showing that Sp1 and Sp3 bind to the pS2 promoter *in situ*.

The expression of the pS2 gene depends on the formation of multi-protein complexes containing the ERα, histone acetyltransferases and AP-1 [168,245,482]. Also, in transient transfection experiments, Sp1 is required for estrogen-enhanced expression of a reporter construct containing three consensus Sp1 sites [485]. Sp1 is capable of interacting with various transcription factors including p300/CBP, HDAC1 and ERα and the net activity of these factors to promote or hinder transcription most likely depends on their abundance, as well as their binding affinity and residence time along the pS2 promoter[358,486,487].

To determine if butyrate and TSA indirectly inhibit pS2 gene expression by altering the levels of factors important for pS2 transcription, we assessed the levels of Sp1, Sp3, ERα, HDAC1 and HDAC2 in butyrate- and TSA-treated MCF-7 cells. Both inhibitors did not significantly affect the levels of Sp1, ERα, HDAC1 and HDAC2. These inhibitors also did not significantly affect the level of Sp3 short form protein; however, the effect on Sp3 long form protein could not be conclusively determined. In a previous study, Sp1 and Sp3 levels were not altered in sodium butyrate-treated MCF-7 cells [357]. As well, the DNA-binding ability of Sp1 and Sp3 to their target gene was not

affected [357]. Similarly, Sp1, Sp3 or HDAC1 levels were not altered in TSA-treated hepatoma cells [348]. Thus, it seems likely that sodium butyrate and TSA do not exert their effect on pS2 gene transcription in MCF-7 breast cancer cells by altering the levels of these proteins. However, these findings do not exclude the possibility that sodium butyrate and TSA alter the levels of other factors important for pS2 gene expression such as AP-1, CBP, p300, AIB1, SRC-1 or any one of components of the DRIP complex.

Exposure to sodium butyrate increases the levels of the PP1 phosphatase [339]. The transcriptional properties of many of the factors influencing estrogen action are affected by phosphorylation. For example, ERα is phosphorylated by MAPK and this event increases its transcriptional efficiency [488]. The transcription factor Sp1 is also phosphorylated by a DNA-dependent kinase [489]. In addition, the transcriptional activity of AIB1, a ligand-dependent ER coactivator, and the association of this coactivator with p300 is enhanced by estrogen- or growth factor-induced MAPK serine phosphorylation in MCF-7 cells [490]. Similarly, MAPK phosphorylates SRC-1, a histone acetyltransferase that interacts with RNA polymerase II, CBP and ERα [113,482,491,492]. This event enhances the coactivation properties of SRC-1 [492].

Histone deacetylase activity and histone deacetylase complex formation may be regulated by phosphorylation. The *in vivo* phosphorylation of mammalian HDAC1 has been shown to reduce its enzymatic activity and disrupt HDAC1 complex formation with RbAp48 and mSin3A [342]. Similarly, phosphorylation of HDAC1 and HDAC2 disturbs their interactions with one another as well as the interactions between HDAC1 and co-repressors such as mSin3A and YY1 [343]. However, contradictory evidence exists suggesting that HDAC1 phosphorylation does not influence its deacetylase activity [340].

As well, the phosphorylation of HDAC2 activity increases its activity [341]. We showed that sodium butyrate and TSA-treatment increased H3 and H4 acetylation levels and decreased HDAC1 levels along the pS2 promoter. This suggests that both histone deacetylase inhibitors disturb the association of histone deacetylases such as HDAC1 with this gene region; however, the ability of these inhibitors to reduce histone deacetylase activity is also likely. Our results agree with the idea that sodium butyrate induces PP1 activity which disrupts histone deacetylase complexes or decreases histone deacetylase activity.

In addition to altering protein phosphorylation, sodium butyrate and TSA may influence pS2 gene expression by altering the acetylation status of transcription factors. The ubiquitously expressed transcription factor YY1 interacts with the histone acetyltransferases p300 and CBP, as well as the histone deacetylases HDAC1, HDAC2, HDAC3 [391]. Acetylation of YY1 stabilizes its association with histone deacetylases, causing it to act as a transcriptional repressor [391]. In addition, Dr. Pestell and colleagues have reported evidence suggesting that the ability of ERα to induce the transactivation of an ERE-luciferase reporter construct is suppressed by acetylation of two specific lysine residues within the hinge/ligand binding domain of ERα [120]. Sodium butyrate and TSA may inhibit pS2 expression by promoting the acetylation of certain transcription factors which may in some cases stabilize the association of these factors with histone deacetylases and in other cases directly alter the transactivation properties of these factors.

Even though sodium butyrate and TSA inhibited pS2 gene expression, both compounds induced histone acetylation along the pS2 promoter, exon 2 and exon 3 in the

absence of estrogen. We also observed that HDAC1 is associated with all three gene regions in untreated cells. Therefore, in the absence of E2, the pS2 promoter, exon 2 and exon 3 gene regions are dynamically acetylated and most likely situated near regions of histone acetyltransferase and histone deacetylase activity.

These findings are supported by evidence from several studies. Dr. Mahadevan and colleagues recently demonstrated that H3 and H4 are dynamically acetylated along the promoter and two downstream regions of the c-*jun* gene in quiescent mouse fibroblasts [92]. As well, Dr. Freedman and colleagues showed that the pS2 gene promoter is associated with a low level of acetylated H4 in untreated MCF-7 cells [245]. Dr. Brown and colleagues have recently shown that HDAC2 and HDAC4 are associated with the estrogen-responsive c-*myc* promoter in untreated MCF-7 cells [167]. Small levels of ERα and histone acetyltransferases such as SRC-1, AIB-1 and CBP are also associated with the pS2 promoter region in the absence of estrogen [245]. Furthermore, the interaction of ERα with SRC proteins and p300/CBP is sufficient to induce targeted histone acetylation on estrogen-responsive promoters in the absence of transcription [493].

When treated with sodium butyrate, the levels of HDAC1 associated with all three pS2 gene regions significantly decreased while TSA-treated cells displayed a significant decrease only along the promoter. TSA has also been shown to remove HDAC1 and HDAC2 from the HER2 promoter in breast cancer cells [476]. Similarly, TSA treatment removed HDAC1 from the methylated metallothionein gene promoter in mouse lymphosarcoma cells [478]. The differential effect of TSA and sodium butyrate on HDAC1 association along exons 2 and 3 may be a result of TSA having a higher potency and less pleiotropic effects than sodium butyrate on other nuclear proteins [321,322]. Whether these

inhibitors affect the association of other histone deacetylases with the three pS2 gene regions is an area that warrants further investigation.

To determine if estrogen-mediated induction in H3 and H4 acetylation levels is an early immediate or a prolonged response, we treated MCF-7 cells with E2 for 0 to 180 min and analyzed the levels of hyperacetylated H3 and H4 associated with the pS2 promoter and exon 3. Our observations that H3 and H4 acteylation levels were increased along the pS2 promoter for 180 min and along exon 3 regions for up to 120 min suggests that E2-induced H3 and H4 acetylation along the pS2 gene is a prolonged event. In a study by Dr. Evans and colleagues, the levels of acetylated H4 increased along the pS2 promoter between 0 and 60 min E2 treatment [199]. Dr. Freedman and colleagues also observed that acetylated H4 levels along the pS2 promoter were increased by 30 min and were sustained for at least another 135 min in the presence of E2 [245]. This somewhat prolonged estrogen-induced histone acetylation along the pS2 promoter may assist in transcriptional re-initiation events by allowing transcription factors to cycle on and off of the promoter region over time.

Compared to the pS2 promoter region, H3 and H4 acetylation along exon 3 was a relatively short-lived event. Transcription of pS2 occurs within 15 – 30 min of E2 treatment and carries on for at least 6 h in the presence of estrogen [168,454]. Therefore, while the level of histone acetylation along exon 3 decreases to control levels after 120 min, transcription is still an ongoing process.

In a recent study, the overall charge of the H3 histone tail was found to correlate better with transcription than histone acetylation, suggesting that other post-translational modifications of the core histone N terminal tails may be important for transcription [244].

Despite this, histone acetylation is still a necessary event for transcription since the mutation of Gcn5 and Elp3 in yeast caused histone hypoacetylation along the coding regions of several genes and this event correlated with the reduced transcription of these genes [244]. However, other histone modifications such as histone phosphorylation that alter the overall charge of histone N terminal tails could be taking place along exon 3 while histone acetylation starts to decline. Acetylation of H3 by CBP stimulates the tight binding of the CARM1 arginine methyltransferase to chromatin and the subsequent methylation of H3 R17 at 30 min E2 treatment [108]. The presence of CARM1 synergistically enhances the function of ERα [105]. The levels of R17 methylation remain high at 60 and 180 min E2 treatment. Although protein methylation does not alter the overall charge of the histone tails, it does alter the hydrophobicity [96]. The presence of multiple histone modifications along exon 3 may create an environment favored by specific proteins or enzymatic activities. In addition to protein modification, DRIP co-activator proteins are recruited to the pS2 promoter between 105 and 165 min E2 treatment [245]. Thus, as histone acetylation begins to decline along exon 3, other events may take place that continue the transcription process.

MCF-7 cells treated only with DRB displayed a higher level of acetylated H4 along the pS2 promoter and exon 3 than that found in untreated cells while acetylated H3 levels did not display any significant enrichment. As well, the treatment of MCF-7 cells with both DRB and E2 decreased the onset time for H3 and H4 acetylation along the pS2 promoter. The treatment of MCF-7 cells with estrogen causes factors such as histone acetyltransferases and RNA polymerase II to cycle on and off the promoter of estrogen responsive genes [168,245]. This treatment also decreases the levels of histone deacetylases

associated with the promoter regions of estrogen-responsive genes [167]. DRB treatment stabilizes the association of ERα, AIB1 and RNA polymerase II on the promoter of the cathepsin D gene [168]. Different histone acetyltransferases have different target substrate specificities. For example, NuA4 primarily acetylates histone H4 *in vitro* while it does not significantly acetylate H3 [110]. Gcn5 strongly acetylates H3 and weakly acetylates H4 *in vitro* [110]. PCAF also primarily acetylates H3 at Lys-14 and more weakly acetylates H4 at Lys-8 [110]. Thus, in the absence of E2, DRB most likely stabilizes the association of H4-targeting histone acetyltransferases with the pS2 promoter and exon 3.

Alternatively, DRB treatment may promote the disassociation of H4-targeting histone deacetylase complexes from the pS2 promoter and exon 3. DRB inhibits CK2 activity [496]. CK2 phosphorylates HDAC2 and this event is required for HDAC2 complex formation with mSin3 and Mi2 [341]. Therefore, DRB most likely prevents HDAC2 from becoming phosphorylated and this event prevents the recruitment of HDAC2-containing complexes to these gene regions. However, whether DRB actually affects the association or function of HDAC2-containing or other histone deacetylase-containing complexes with the pS2 gene remains to be determined.

The increased speed with which H3 and H4 became acetylated along the pS2 promoter in the presence of E2 and DRB likely resulted from estrogen-mediated recruitment and DRB-induced stabilization of H3- and H4-targeting histone acetyltransferases either associated directly or indirectly with the promoter region through RNA polymerase II [168]. Therefore, treatment with E2 most likely promoted the recruitment of histone acetyltransferases to the pS2 promoter and DRB would have prevented these factors from cycling off this gene region.

DRB-treated MCF-7 cells displayed a delay in estrogen-induced H3 acetylation along exon 3 when compared to levels observed in cells treated with E2 alone. However, this event was prolonged for at least 180 min. H4 acetylation was slightly induced in the presence of DRB alone and E2 treatment further increased acetylated H4 levels for up to 180 min. The ability of DRB to stabilize the association of histone acetyltransferases with downstream regions has not been determined.

Although DRB can stabilize the association of histone acteyltransferases with an estrogen-responsive gene, this transcriptional inhibitor prevents RNA polymerase II from converting into an elongation mode. As well, cells were treated with DRB for 4 h, a time sufficient to ensure that levels of RNA polymerase II remaining on downstream pS2 gene regions were minimal. Thus, E2 treatment induces H3 and H4 acetylation along the pS2 promoter and exon 3 in the absence of transcriptional stimulation.

Acetylated H3 levels in E2-treated cells were substantially greater than levels in untreated or DRB plus E2-treated cells along the pS2 promoter at 120 min E2 treatment and along exon 3 at 30 min of E2 treatment. Therefore, while most of the histone acetylation that took place along the promoter and exon 3 occurred independently of transcription, some histone acetylation was also stimulated by the recruitment of histone acetyltransferases to the pS2 gene during the transcriptional initiation and elongation process.

Lastly, the addition of 10 mM sodium butyrate to cells treated with both DRB and E2 had profound effects on estrogen-induced H3 and H4 histone acetylation along the pS2 promoter and no significant effect on H3 and H4 acetylation levels along exon 3. The drastic induction in H3 and H4 hyperacetylation along the pS2 promoter most likely

resulted from the presence of all three reagents. E2 treatment most likely promotes factor recruitment to and histone deacetylase removal from the pS2 gene, while DRB would most likely stabilize factor association and possibly alter the transcriptional properties of some of the associated factors. Sodium butyrate would then remove any residual histone deacetylases from the pS2 gene and possibly alter the characteristics of various histone acetyltransferases associated with the pS2 gene either by altering their phosphorylation or acetylation status or by altering the components of the multi-protein complex in which they reside. The fact that we observed a large increase in acetylated H3 and H4 levels over time in the presence of all three reagents when compared to levels observed in cells treated only with E2 and DRB suggests that estrogen-induced histone acetylation along the pS2 promoter is a dynamic and prolonged event occurring for at least 180 min.

The majority of E2 treatment time points in MCF-7 cells pre-treated with DRB and sodium butyrate displayed significantly higher levels in histone acetylation along the promoter when compared to cells treated only with E2-, DRB plus E2-, or sodium butyrate. By themselves, E2, DRB and sodium butyrate could not induce H3 and H4 acetylation to the same drastic level as that observed along the pS2 promoter in MCF-7 cells treated with E2 for 60 min in the presence of DRB and sodium butyrate. Likewise, the treatment of MCF-7 cells with E2 plus DRB or DRB plus sodium butyrate also did not drastically induce histone hyperacetylation. Initially, we thought that this drastic induction in H3 and H4 hyperacetylation was a result of the ability of sodium butyrate to act additively or synergistically with E2. However, analysis of histone acetylation along the pS2 promoter in MCF-7 cells treated with butyrate or butyrate plus E2 revealed that

treatment of cells with both sodium butyrate and E2 does not further enhance sodium butyrate-induced H3 and H4 hyperacetylation (Figure 29B).

The addition of E2 to DRB plus sodium butyrate-treated MCF-7 cells did not further increase acetylated H3 levels along exon 3 beyond levels observed in cells treated with DRB plus sodium butyrate, E2 plus DRB, E2 or sodium butyrate. In most cases, treatment of MCF-7 cells with DRB, sodium butyrate and E2 also did not further induce acetylated H4 levels along exon 3 when compared to cells treated with DRB plus E2. However, acetylated H4 levels along this gene region were significantly greater than in cells treated with E2 plus DRB, DRB, sodium butyrate or E2. The substantial increase of acetylated H4 in DRB plus sodium butyrate-treated cells suggests that H4-targeting histone deacetylase complexes are predominantly situated close to exon 3 in the absence of E2.

These observations suggest that E2 is unable to promote the recruitment of additional histone acetyltransferases to exon 3 in the presence of sodium butyrate. We previously showed that acetylated H3 and H4 levels are increased along exon 3 in the presence of DRB and E2. This suggests that DRB does not interfere with histone acetyltransferase recruitment. We aso showed that sodium butyrate and TSA treatment induce H3 and H4 acetylation along exon 3 to approximately the same extent as 60 min of E2 treatment or (Figure 26). Thus, these histone deacetylase inhibitors most likely do not promote the complete removal of histone acetyltransferases.

However, the treatment of MCF-7 cells with sodium butyrate and E2 did not increase H3 and H4 acetylation levels beyond those observed in cells treated only with E2, sodium butyrate or TSA alone (Figure 29B). Perhaps the inability of estrogen to

further increase sodium butyrate-induced H3 and H4 hyperacetylation along exon 3 can be explained by the fact that E2 treatment reduces the association of histone deacetylases with estrogen-responsive genes [167]. Whether E2 completely removes all histone deacetylase activity from an estrogen-responsive gene remains to be determined. With this to consider, we cannot rule out the possibility that at least some dynamic histone acetylation takes place along exon 3 in the presence of E2 and DRB.

Evidence showing that histone acetyltransferases and deacetylases are associated with the pS2 promoter and exon 3 in the absence of E2 suggests that the pS2 gene is located in nuclear regions enriched in histone acetyltransferase and histone deacetylase activity. In the presence of estrogen or sodium butyrate, acetylated H3 and H4 levels are usually greater along the pS2 promoter than along exons 2 or 3 (Figure 26). Our observations that E2 treatment induced H3 and H4 acetylation along the pS2 promoter in the presence of both DRB and sodium butyrate, but not along exon 3, can possibly be explained by the fact that the pS2 promoter is situated within a nuclear region containing more histone acetyltransferase activity than nuclear regions associated with exon 3.

In summary, we showed that dynamic H3 and H4 acetylation takes place along the pS2 promoter, exon 2 and exon 3 in the absence of E2. This suggests that the pS2 gene is localized to nuclear regions associated with histone acetyltransferases and deacetylases in the absence of estrogen. The act of dynamic histone acetylation along the pS2 gene may recruit this gene (and other genes) to the NM or other regions enriched in histone acetyltransferases, deacetylases and transcription factors.

Treatment with E2 induces H3 and H4 acetylation along the pS2 promoter, exon 2 and exon 3 in the presence or absence of transcription. Thus, exposure to E2 most likely mediates the recruitment of additional histone acetyltransferases to the promoter and coding regions of estrogen-responsive genes and these enzymes may function to tighten the association between these genes and nuclear regions such as the NM. In support of this, the binding of ERα to estrogen causes this receptor molecule to become tightly associated with the NM and to recruit histone acetyltransferases to the promoter regions of estrogen-responsive genes [170,241,258].

The fact that higher levels of dynamic H3 and H3 acetylation were often observed along the pS2 promoter compared to coding regions suggests that more histone acetyltransferases are recruited to the promoter in response to E2 treatment compared to downstream regions. The function of these additional acetyltransferases could be to generate a histone code along the core histone N terminal tails associated with the pS2 promoter that can be recognized by additional factors involved in the transcriptional process. As well, the acetylation of core histones in unfolded, transcriptionally active nucleosomes along the pS2 gene may be required to ease the movement of DNA through NM-associated RNA polymerase II molecules. Thus, histone acetylation is important for

the transcription process but can occur independently of this event. The transcriptional activation of the pS2 gene most likely depends on the recruitment of specific transcription factors to the same nuclear region of this gene.

## Part III: Analysis of DNA-associated Nuclear Matrix Protein Profiles from Cell Lines Composing a Model of Breast Cancer Disease Development

The majority of breast cancers initially depend on estrogen for growth and approximately 60% of these tumors respond to anti-estrogen or other endocrine therapies [510,511]. In the malignant progression of breast cancer, breast tumors progress from hormone-dependent growth to a more aggressive phenotype characterized by hormone-independent growth, resistance to endocrine therapy and widespread metastasis [512,513]. As well, over 30% of all breast tumors that express the ERα fail to respond to anti-estrogen therapy, suggesting that loss of hormone dependence in breast cancer cells is an important step in breast cancer development [514]. The NM organizes DNA into loop domains and has a role in determining cell shape [4,515]. This nuclear structure serves as a platform upon which many nuclear processes including transcription, DNA replication and RNA processing are associated [516,517]. The organization and composition of the NM change with nuclear activity [215,518,519]. Alterations in NM organization may, therefore, alter DNA organization and influence gene expression. Changes in the expression patterns of NM proteins between hormone-dependent and hormone-independent human breast cancer cells have been observed [408]. As well, informative NM proteins have been identified for bladder, breast, colon, and cervical cancers [425,520-522]. We have previously shown that the cross-linking agent cisplatin preferentially cross-links NM proteins to DNA *in situ*. Thus, the objective of this study was to determine if changes in NM organization correlate with the acquisition of invasive, metastatic and anti-estrogen resistant phenotypes important for breast cancer cell development.

For this study, we isolated NM and cisplatin DNA-cross-linked NM proteins from various cell lines in a breast cancer progression series [429-431]. This series consists of four cell lines including: MCF-7, MIII, LCC1 and LCC2. All cell lines express ERα and are stimulated to proliferate by estrogen [429,430]. However, the MIII, LCC1 and LCC2 cell lines are able to grow in the absence of estrogen [430]. In addition, all cell lines in this series are sensitive to the anti-estrogen ICI, while only the LCC2 cell line is resistant to the anti-estrogen tamoxifen [429]. The MCF-7 cell line is non-metastatic and non-invasive while the MIII and LCC1 cell lines are able to invade locally from solid mammary fat pad tumors and produce metastatic lesions [432]. In addition, the LCC2 cell line is invasive and metastatic [433,434]. Thus, the MCF-7 cell line has a phenotype more representative of early-stage breast cancer while the MIII and LCC1 cell lines have an intermediate phenotype and the LCC2 cell line displays a phenotype representative of advanced breast cancer. NM and cisplatin DNA-cross-linked proteins were isolated from each cell line and the levels of proteins in each preparation were analyzed by two dimensional electrophoresis.

## *1.0 Methods*

### 1.1 Cell Maintenance

The human breast carcinoma cell lines MCF-7, MIII, LCC1 and LCC2 were used in this study. The MCF-7 cell line was a sub-clone generated by Dr. Rob Clarke and is referred to MCF-7(RC). All cell lines were maintained at 37°C (humidified atmosphere, 5% $CO_2$ / 95% Air) on 150 x 20 mm tissue culture dishes (Nunc). The MCF-7(RC) cell line was cultured in Dulbecco's Modified Eagle Medium (DMEM, Gibco-BRL, Grand Island, New York) supplemented with 1% (v/v) L-glutamine, 1% (v/v) glucose, 1% (v/v) penicillin/streptomycin and 5% (v/v) fetal calf serum (FCS: Gibco, Grand Island, New York). MIII, LCC1 and LCC2 were cultured in Phenol Red Free Dulbecco's Modified Eagle Medium (Sigma), 5% (v/v) twice charcoal stripped fetal calf serum and supplemented as mentioned above. At approximately 90% confluence, cells were scraped from the plates and frozen as pellets containing 1 x $10^7$ cells at -70°C.

### 1.2 Isolation and Analysis of Nuclear Matrix Proteins and Proteins Cross-Linked to DNA *in Situ*.

Nuclear matrices were isolated by Dr. Shanti Samuel from the breast cancer cell lines as previously described (Figure 30) [242]. Cell pellets containing 1 x $10^7$ cells were resuspended in 10 ml of ice-cold TNM buffer (see recipe in Methods section 1.4 of Part II) containing 1 mM PMSF. The cell suspension was homogenized 5 times with a Teflon pestle on ice. Following homogenization, cells were incubated on ice for 5 min. A final concentration of 0.5% (v/v) Triton X-100 was added to release lipids and soluble proteins while nuclei remained intact. The suspension of nuclei was passed three times through an 18 gauge needle and collected by centrifugation at 1000 x g for 10 min at 4°C. The nuclei

were again resuspended in ice-cold TNM buffer with 1 mM PMSF, homogenized and pelleted as before.

The nuclei were resuspended to a concentration of 20 $A_{260}$ units/ml in cold DIG buffer (50 mM NaCl, 300 mM sucrose, 10 mM Tris-HCl, pH 7.4, 3 mM $MgCl_2$, 1% (v/v) thiodiglycol, 0.5% (v/v) Triton X-100) with 1 mM PMSF and digested with DNase I at a concentration of 168 units/ml for 20 min at room temperature. Ammonium sulphate (final concentration of 0.25 M) was added with stirring to facilitate chromatin removal, and the pellet consisting of NM proteins bound to intermediate filament (IF) proteins (NM-IF) was obtained by centrifugation at 9600 x g for 10 min at 4°C. This pellet was resuspended in ice-cold DIG buffer with 1 mM PMSF, extracted by adding 4 M NaCl to a final concentration of 2 M, and incubated on ice for 30 min. The sample was then centrifuged at 9600 x g for 10 min at 4°C. The NaCl-extracted pellet (NM2-IF) was again resuspended in ice-cold DIG buffer, extracted with 2 M NaCl and centrifuged as before.

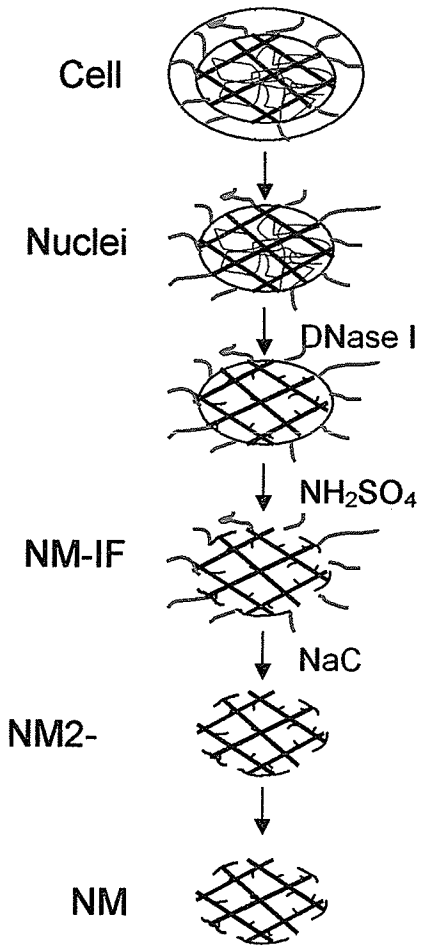


**Figure 30.** **Nuclear Matrix Extraction Method.** Nuclei were isolated from breast cancer cells and treated with DNase I to digest approximately 95% of total nuclear DNA. The nuclei were then treated with $NH_2SO_4$ and centrifuged to remove soluble nuclear proteins, non-histone chromosomal proteins and histones. This resulting pellet contains mostly NM proteins associated with intermediate filament proteins (NM-IF). The NM-IF fraction was treated with NaCl to remove any residual non-nuclear matrix proteins (NM2-IF). The NM2-IF was resuspended in disassembly buffer, dialyzed against assembly buffer and centrifuged to dissociate the intermediate filament proteins from the NM.

The NM2-IF was resuspended in Disassembly buffer (8 M urea, 20 mM 2[N-morpholino] ethane sulfonic acid, pH 6.6, 1 mM EGTA, 1 mM PMSF, 0.1 mM $MgCl_2$, 1% (v/v) β-mercaptoethanol) and dialysed overnight at room temperature against 2 liters of Assembly buffer (0.15 M KCl, 25 mM imidazole, pH 7.1, 5 mM $MgCl_2$, 2 mM DTT, 0.125 M EGTA, 0.2 mM PMSF). Dialysis allowed the urea to be removed and the intermediate filaments (IFs) to reassemble. The IFs were removed by ultracentrifugation at 150,000 x g for 90 min at room temperature. The resulting supernatant containing NM proteins was removed carefully and lyophilized. Lyophilized samples were resuspended in 8 M urea, aliquoted and frozen at -20°C. Protein concentrations were determined using the Bio-Rad assay with BSA as a standard.

### 1.3 Isolation and Analysis of Nuclear Matrix Proteins and Proteins Cross-Linked to DNA *in situ*.

DNA-protein cross-linking was performed as previously described [379] (Figure 31). Approximately 1 x $10^7$ cells were resuspended to a density of 1 x $10^6$ cells/ml in Hanks Buffer containing sodium acetate instead of NaCl at the same concentration. The cells were incubated with 1 mM cisplatin at 37°C for 2 h with gentle shaking. Following this incubation, cells were treated with lysis buffer (5 M urea, 2 M guanidine-HCl, 2 M NaCl and 0.2 M potassium phosphate, pH 7.5). HAP (4 g / $20A_{260}$ units of lysate, Bio-Rad) was then added. The HAP resin was washed with lysis buffer to remove RNA and proteins not cross-linked to DNA. To reverse the cross-linking, the HAP was incubated in lysis buffer containing 1 M thiourea instead of 5 M urea. By doing so, the proteins were released from HAP, while the DNA remained bound. The eluted proteins were

dialyzed against double-distilled $H_2O$, lyophilized and then resuspended in 8 M urea. Protein concentrations were determined using the Bio-Rad Protein Assay with BSA as a standard.

## 1.4 Two-dimensional Gel Electrophoresis of Nuclear Matrix and Cross-linked Proteins.

Two-dimension polyacrylamide gel electrophoresis was performed as described previously [498]. Separation of proteins by their isoelectric point was performed by loading 80 μg of protein sample on to isoelectric focusing tube gels (1.5 mm x 18 cm) containing 2% pre-blended ampholines of isoelectric point (pI) values of 3.5-9.5 and 5-8 (Amersham-Pharmacia). The gels were electrophoresed at 400 V, 400 mA for 16 h and then 800 V, 400 mA for 2 h. After electrophoresis, the gels were placed in a sample reducing buffer containing 3% (w/v) SDS, 1.5% (w/v) DTT, 0.07% (w/v) Tris-HCl, pH 6.7, 0.01% (w/v) bromophenol blue for 20 min at room temperature. Following the incubation, the tube gels were layered on to 8% SDS-PAGE resolving gels.

Electrophoresis was performed at a constant amperage of 50 mA per gel for 2.65 h at room temperature. Gels were stained with silver using the Pharmacia Silver Stain kit (Amersham-Pharmacia) and then dried between sheets of gel drying film (Promega Corp.) at room temperature. Stained gels were scanned using a PDI 325OE densitometer (PDI, Huntington Station, N.Y.), and the data were analyzed with Image Master software (Amersham Pharmacia Biotech). Molecular masses and isoelectric points were determined using two-dimension SDS-PAGE standards (Bio-Rad and Amersham

Pharmacia BioTech) and carbamylated carbonic anhydrase (ca) (Amersham Pharmacia BioTech). All studies were carried out using 3 preparations from each cell line.

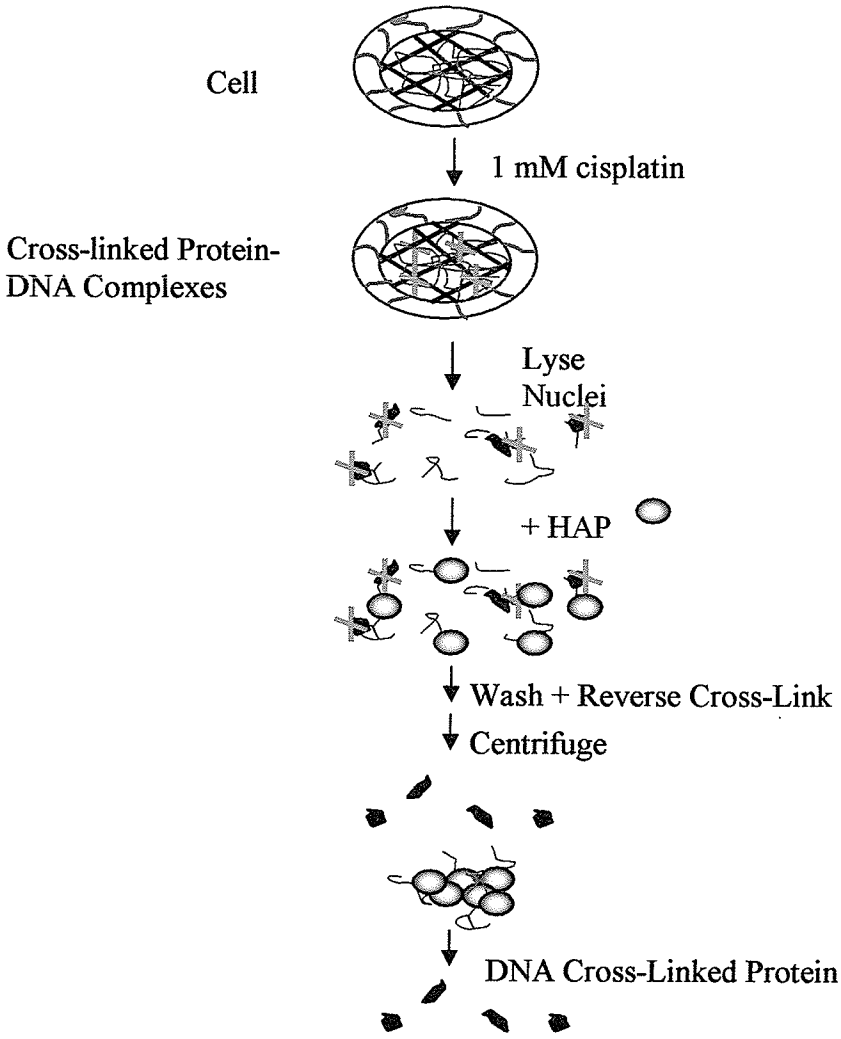


**Figure 31. Cisplatin Protein-DNA Cross-linking Protocol.** Breast cancer cells were treated with 1 mM cisplatin for 2 h and lysed in buffer containing 2 M NaCl, 5 M urea, 2 M GnHCl and 200 mM potassium phosphate. The cell lysate was incubated with hydroxyapatite (HAP) to capture nuclear DNA and DNA-protein complexes. Proteins not cross-linked to DNA and RNA were removed by washing the HAP with lysis buffer. The protein-DNA cross-links were reversed by resuspending the HAP in reverse lysis buffer (2 M NaCl, 1 M thiourea, 2 M GnHCl, 200 mM potassium phosphate) and proteins were isolated from the DNA-HAP complexes by centrifugation.

## *2.0 Results*

### 2.1 The Majority of NM and DNA-Cross-linked Proteins are Common Among Cell Lines in a Breast Cancer Cell Line Progression Series

Nuclear matrix proteins (NMPs) and proteins cross-linked to DNA *in situ* were isolated from MCF-7, MIII, LCC1, and LCC2 cells. The proteins were analysed by two-dimension gel electrophoresis. To compare the proteins in the various gel patterns, several exogenous proteins were used to align protein patterns. Carbamylated carbonic anhydrase (30 kDa, pI 4.8-6.7) served as a reference for determining the molecular mass and isoelectric point of the proteins. Two-dimension SDS-PAGE standards were used to determine the molecular mass of the proteins.

Representative silver-stained two-dimension gel patterns of nuclear matrix proteins (NMP) and proteins cross-linked to DNA *in situ* with cisplatin (XLP) isolated from the various cell lines are shown in Figures 32 and 33, respectively (see Figure 34 for a schematic representation of the two-dimension gel pattern data). Many of the proteins were common to the NMP and XLP preparations both within each cell line and between the four cell lines. For example, hnRNP K, which was identified according to its molecular mass and pI coordinates, was found in all patterns.

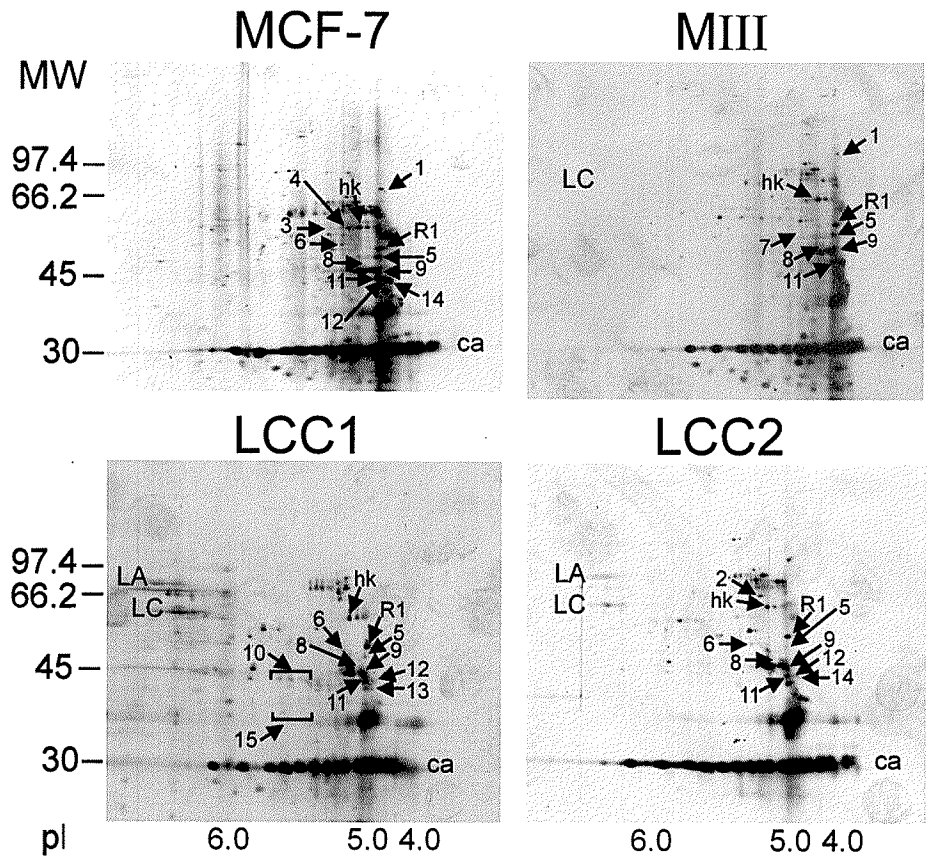


**Figure 32.** **Nuclear Matrix Proteins of MCF-7, MIII, LCC1, and LCC2 Breast Cancer Cell Lines.** Nuclear matrix proteins (90 μg) were electrophoretically resolved on two dimension gels. The gels were stained with silver. The position of the carbamylated forms of carbonic anhydrase is indicated by ca. The position of the molecular mass standards (kDa) is shown to the left of the two dimension gel patterns. LA and LC show the position of lamin A and C, respectively. hK designates the position of transcription factor hnRNP K. R1 designates a protein displaying similar levels among the four cell lines studied.

## 2.2 A Small Number of NM and DNA-Cross-Linked Proteins are Differentially Expressed Among Cell Lines in a Breast Cancer Cell Line Progression Series

Despite the large similarities observed in both NM and DNA-cross-linked protein two-dimension patterns, differences were observed. Proteins displaying different levels in the two-dimension gel patterns were catalogued into three groups: those found in NMP but not in XLP patterns; those detected in NMP and XLP patterns; and those seen in XLP but not NMP patterns. Few NMPs were placed into group 1 as most NMPs were also found in the XLP patterns. The sole group 1 entry NMP1, which has a molecular mass of 79 kDa and pI of 4.85, was present in MCF-7 and MIII but not in LCC1 or LCC2 cells.

Among the group 2 proteins were those showing differences in both NMP and XLP patterns, those displaying differences in NMP but not XLP patterns and those showing variations in the XLP but not NMP patterns. In the nuclear matrix protein fractions, NMP8 was at higher abundance in LCC1 than in MCF-7, MIII or LCC2. However, the abundance of NMP8 did not vary significantly in the XLP patterns (Table 4). NMP5 showed a progressive decrease in abundance in the NMP and XLP preparations from MIII, LCC1 and LCC2, respectively (Table 4).

Among the XLP patterns, NMP10 was found to progressively decline in abundance in the MIII, LCC1 and LCC2 preparations (see Figure 33 and Table 4). NMPs 12, 14 and 15 were at higher concentrations in the XLP preparations from MIII than in those of MCF-7, LCC1 and LCC2. Further, NMP6 and NMP7 displayed a decrease in abundance in the LCC2 pattern when compared to MIII and LCC1 preparations. The levels of NMPs 2, 3 and 4 were greatest in the XLP pattern of LCC2 compared to those of MIII and LCC1. Furthermore, NMP13 showed a progressive increase in abundance over the cell line panel.

The third group of proteins, which were detected in the XLP patterns but not in the NMP patterns, consisted of 5 proteins (Table 5). Figure 33 shows that XLP1 was prominent in the MIII and LCC2 XLP patterns but not in the patterns of the other cells. Likewise, XLP2 was abundant in the MIII pattern compared to the other cell lines. The relative levels of XLP5 progressively decreased in the XLP patterns of MIII, LCC1 and LCC2 cells, respectively. In contrast, the levels of XLP3 and XLP4 gradually increased in the MIII, LCC1 and LCC2 XLP patterns, respectively.

We have previously reported that cytokeratins K8, K18 and K19 were cross-linked to nuclear DNA by cisplatin in breast cancer cells [499]. The abundance of these proteins in the NMP preparation is typically very low since the intermediate filament proteins are removed (see Methods section 2.2). Cytokeratins K8, K18 and K19 were among the more abundant proteins cross-linked to DNA by cisplatin. Although these proteins were seen in the XLP preparations of the four cell lines, their abundance was consistently lower in the MIII preparations (Figure 33). The levels of these three intermediate filament proteins progressively increased in the LCC1 and LCC2 XLP preparations.

When comparing the XLP patterns of MIII, LCC1 and LCC2 preparations, a progressive increase in the levels of lamins A and C was also observed (Figure 33). The levels of lamins A and C were prominent in the XLP patterns of LCC2 cells, while lamin C and to a lesser extent lamin A was observed at lower levels in the LCC1 XLP patterns.

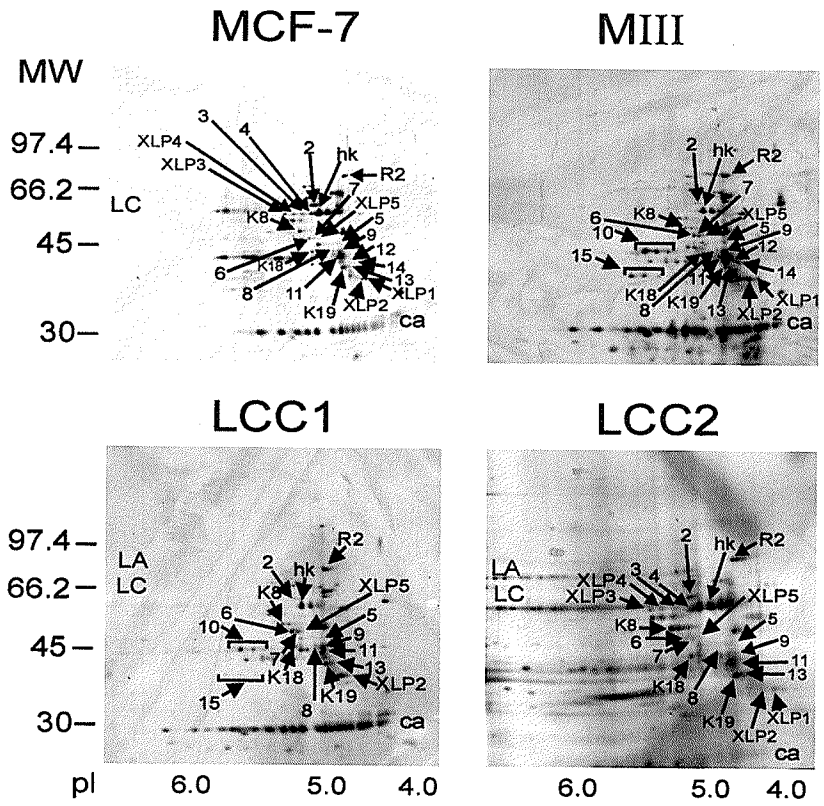


**Figure 33. Proteins Cross-linked to DNA by Cisplatin *in situ* in MCF-7, MIII, LCC1, and LCC2 Breast Cancer Cell Lines.** Eighty μg of DNA cross-linked proteins from cells treated with 1 mM cisplatin were electrophoretically resolved on two dimension gels. The gels were stained with silver. The position of the carbamylated forms of carbonic anhydrase is indicated by ca. The position of the molecular mass standards (kDa) is shown to the left of the two dimension gel patterns. LA and LC represent lamins A and C, respectively. K8, K18 and K19 identify cytokeratins K8, K18 and K19, respectively. hK designates the transcription factor hnRNP K. R2 designates a protein displaying similar levels among the cell lines studied.

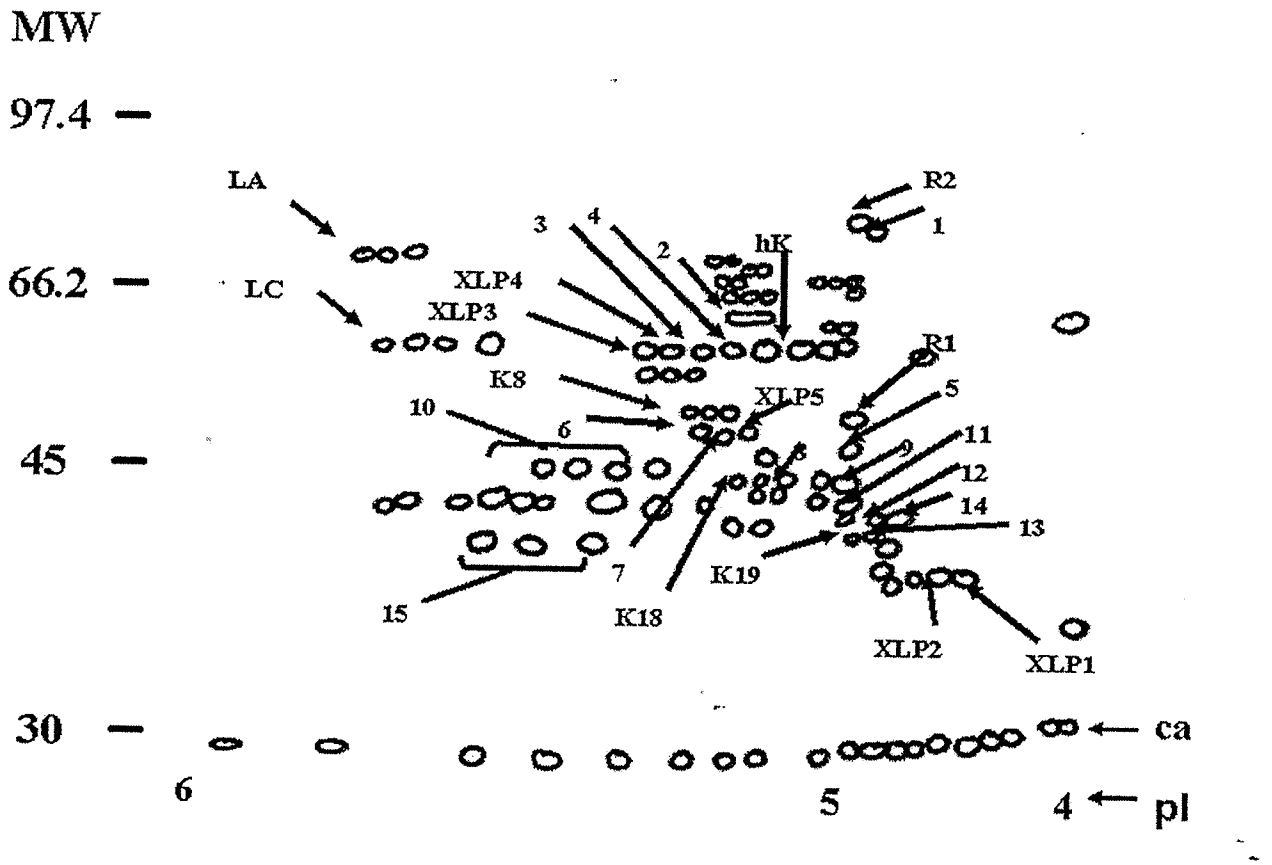


Figure 34. **A Schematic Representation of the Two Dimension Gel Pattern Data of DNA Cross-linked and Non-DNA Cross-linked Proteins from MCF-7, MIII, LCC1, and LCC2 Breast Cancer Cell Lines.** The position of the molecular mass standards (kDa) is shown to the left of the two dimension gel patterns. See legends to figures 32 and 33 for designation of ca, LA, LC, hK, K8, K18, K19, R1 and R2.

**Table 4. Relative Levels of DNA Cross-linked Nuclear Matrix Proteins in Two-Dimension Patterns of DNA Cross-linked Protein Preparations.** Levels of each protein were assessed based on their relative expression to hnRNP K and R2. The level of NMP5 within NMP patterns was assessed based on its relative expression to hnRNP K and R1. "++++", "++", and "+" designate NM proteins present at high, moderate and low levels, respectively. "+/-" represents proteins present at very low levels in one or more preparations, while "-" designates proteins not detected in all preparations.

| Cell Line: | | | MCF-7<br>Estrogen-dependent<br>Estrogen-responsive<br>Anti-estrogen-sensitive | MIII<br>Invasive<br>Metastatic<br>Estrogen-independent<br>Estrogen-responsive<br>Anti-estrogen-sensitive | LCC1<br>Invasive<br>Metastatic<br>Estrogen-independent<br>Estrogen-responsive<br>Anti-estrogen-sensitive | LCC2<br>Invasive<br>Metastatic<br>Estrogen-independent<br>Estrogen-responsive<br>Tamoxifen-resistant<br>ICI-sensitive |
|---|---|---|---|---|---|---|
| | Mass (KDa) | pI | | | | |
| NM Proteins: | | | | | | |
| 2 | 61 | 5.2-5.3 | ++++ | + | + | +++ |
| 3 | 60 | 5.35 | ++ | - | +/- | ++ |
| 4 | 60 | 5.25 | +++ | - | - | +++ |
| 5 | 52 | 5 | +/- | +++ | + | +/- |
| 6 | 50 | 5.3 | ++ | +++ | +++ | + |
| 7 | 50 | 5.25 | ++ | +++ | +++ | + |
| 8 | 46 | 5.2 | + | + | + | +/- |
| 9 | 45 | 5 | +++ | ++++ | ++++ | ++ |
| 10 | 44 | 5.45-5.7 | +/- | ++++ | +++ | +/- |
| 11 | 44 | 5 | ++++ | +++++ | ++++ | ++++ |
| 12 | 42.5 | 4.85 | +/- | +++ | +/- | +/- |
| 13 | 42 | 4.85 | +/- | + | ++ | +++ |
| 14 | 42 | 4.75-4.8 | +/- | ++ | - | +/- |
| 15 | 39 | 5.5-5.75 | +/- | +++ | + | +/- |
| NMP 5 levels in NM: | | | | | | |
| 5 | 52 | 5 | +++++ | +++ | ++ | + |

Table 5. **Relative Levels of Differentially Abundant DNA Cross-linked Proteins in Two-Dimension Patterns of DNA-Cross-linked Protein Preparations.** Levels of DNA-cross-linked proteins were assessed based on their relative expression to hnRNP K and R2. "++++", "++", and "+" designate DNA cross-linked proteins present at high, moderate and low levels, respectively. "+/-" represents proteins present at very low levels in one or more preparations, while "-" designates proteins not detected in all preparations.

| Cell Line: | | | MCF-7 | MIII | LCC1 | LCC2 |
|---|---|---|---|---|---|---|
| | Mass (KDa) | pI | | | | |
| XLP1 | 37 | 4.5 | +/- | ++ | - | ++ |
| XLP2 | 37 | 4.6 | ++ | +++ | + | + |
| XLP3 | 60 | 5.6 | ++ | - | +/- | + |
| XLP4 | 60 | 5.45 | ++ | - | +/- | + |
| XLP5 | 50 | 5.2 | +/- | ++ | + | +/- |

## *3.0 Discussion*

In the progression of breast cancer, ER positive breast epithelial cells no longer require estrogens for growth and gain resistance to anti-estrogens. The cell line series MIII, LCC1 and LCC2 provide a model system to study breast cancer progression. In comparing the MIII, LCC1 and LCC2 NMPs that were cross-linked to nuclear DNA *in situ*, we observed a selective and progressive change in the interaction of NMPs with nuclear DNA. Among this group of NMPs, a loss in cisplatin cross-linking of the NMP to nuclear DNA was found. The loss of cisplatin cross-linking may be a consequence of reduced NMP levels, loss of contact with DNA and/or rearrangement of the NMP relative to DNA such that the NMP is positioned further than 4 Å from nuclear DNA [409].

A parallel change in the abundance of a NMP in the NMP and XLP preparations was noted, but the incidence of this observation was infrequent. For example, NMP5 was less abundant in the LCC1 and LCC2 NMP and XLP preparations compared to the respective MIII preparations. For the remainder of the NMPs exhibiting a change in abundance in the XLP preparations, parallel changes in NMP levels were not found. As examples, NMP10 and NMP15 showed progressive declines in the XLP preparations in the MIII, LCC1 and LCC2 cells, but these changes in NMP10 and NMP15 levels were not observed in the NMP preparations of these cells.

For five XLPs showing variations in abundance in the cell line preparations, the corresponding protein could not be detected in the nuclear matrix preparation. In the preparation of nuclear matrix proteins, intermediate filament proteins and proteins that are able to assemble into insoluble structures are removed [500]. However, this procedure may remove cytoskeletal and perhaps nuclear matrix proteins that are DNA binding proteins.

The cytokeratins are examples of DNA attached proteins that are removed from NMP preparations. Thus, the cisplatin cross-linking procedure complements conventional methods to analyze nuclear matrix proteins [501].

In contrast to decreased cisplatin cross-linking of NMPs to DNA in parallel with progression, lamin A and C and cytokeratin cross-linking to nuclear DNA was enhanced. These observations suggest that rearrangements in chromosomal domains have occurred such that contacts between lamins and cytokeratins at the nuclear periphery and chromosomal domains have been augmented. The chromosomal regions in contact with lamins or cytokeratins are not known. Heterochromatin, which is located at the nuclear periphery, would be expected to make contacts with lamins and cytokeratins [502]. However, transcriptionally active chromatin regions are sometimes located at or near the nuclear periphery and may be in contact with these proteins [503].

In previous studies with oncogene-transformed mouse fibroblasts, we observed a major increase in the abundance of NMPs in cells with high metastatic potential relative to the parental cells [242]. The metastatic potential of MIII, LCC1 and LCC2 is greater than that of MCF-7 parental cells; however, the metastatic potential of these cells has been described as intermediate [432]. In agreement with our previous studies, major changes in nuclear matrix protein profiles are only observed in cells that have acquired high metastatic potential.

## Summary

In summary, we have shown that an intron DNA sequence within the transcriptionally active $\beta^A$-globin gene is associated with a population of very rapidly acetylated and deacetylated H2B, H3 and H4 histones, while an intron within the transcriptionally competent ε-globin gene intron sequence is associated with a mosaic of both rapidly and less rapidly acetylated histones. Moreover, histones associated with the transcriptionally active vitellogenin DNA sequence are not rapidly acetylated or deacetylated. In MCF-7 cells, we showed that the pS2 gene is dynamically acetylated along its promoter, exon 2 and exon 3 regions when it is not exposed to estrogen.

Previous studies have shown that the distribution of very rapidly acetylated and deacetylated (class I) histones follows closely the distribution of transcriptionally active and not inactive or competent DNA sequences [184]. Furthermore, the majority of transcriptionally active DNA sequences and class I acetylated histones are found within the fraction of the nucleus that harbors the NM. We showed that acetylated H3 and H4 are directly associated with DNA in the fraction of the nucleus that harbors the NM. As well, Dr. Davie and colleagues have shown that histone acetyltransferases and histone deacetylases are enriched in this fraction [184,185]. The transcriptional machinery and the majority of transcriptionally active DNA sequences are associated with the NM[4,184,235-238,368,385].

All this evidence supports our hypothesis that dynamic histone acetylation can mediate the recruitment of genes to sites of transcription that are associated with nuclear substructures such as the NM. Therefore, transcriptionally active and competent genes are most likely located in nuclear regions enriched in histone acetyltransferase and histone

deacetylase activity and the close proximity of these genes to these enzymes causes the histones associated with these genes to be dynamically acetylated (Figure 35). Inactive genes, however, remain in a more condensed structure relative to active and competent genes and are not as easily accessible to histone acetyltransferases.

We also observed that the pS2 gene is dynamically acetylated in the absence of transcriptional stimulation and that exposure to E2 further increases the widespread acetylation of histones along this gene. These results support the findings of other studies which have shown an increase in histone acetyltransferase recruitment to estrogen-responsive genes in response to estrogen treatment [167,168,245]. Therefore, the recruitment of additional histone acetyltransferases to a target gene such as pS2 would cause the histone acetyltransferase activity surrounding this gene to overcome the activity of surrounding deacetylases and this would increase the steady state levels of histone acetylation. The function of these additional acetyltransferases could be to generate a histone code along the core histone N terminal tails associated with the target gene promoter that can be recognized by additional factors involved in the transcriptional process. As well, these recruited acetyltransferases could function to maintain the altered conformation of transcriptionally active open nucleosomes along the promoter and coding region of a gene, thereby assisting the subsequent passage of RNA polymerase II molecules along transcriptionally active genes. Thus, whether the pS2 gene becomes transcribed most likely depends on the recruitment of specific transcription factors to the same nuclear region of this gene.

Histone acetylation plays an important role in gene expression. However, the overall structure of DNA is also important in gene expression. DNA is organized into loop

domains through its association with the NM [4]. The composition of the NM varies with cell type and changes with cellular differentiation and transformation [242,366,374,375,378,404,405]. Thus, it is possible that changes in NM composition within a cell could alter gene expression and initiate the expression of genes that contribute towards cancer development.

In an analysis of the NM composition of cell lines that make up a breast cancer progression series, we observed a selective and progressive change in the level of specific NM proteins and the interaction of NM proteins with nuclear DNA. More specifically, we observed changes in NM protein levels and a loss in the cisplatin cross-linking of NM proteins to nuclear DNA. This loss may be a consequence of reduced NM protein levels, loss of contact with DNA and/or rearrangement of the NM protein relative to DNA such that the NM protein becomes positioned further than 4 Å (cisplatin cross-linking distance) from nuclear DNA [409]. The cell line within this breast cancer progression model series having a phenotype most representative of advanced breast tumorigenesis also displayed an increase in lamins A and C and cytokeratin cross-linking to nuclear DNA. Thus, the development of cancer most likely involves augmentations in the contacts between lamins and cytokeratins, as well as alterations in NM protein expression. These changes would then cause rearrangements in chromosomal domains.

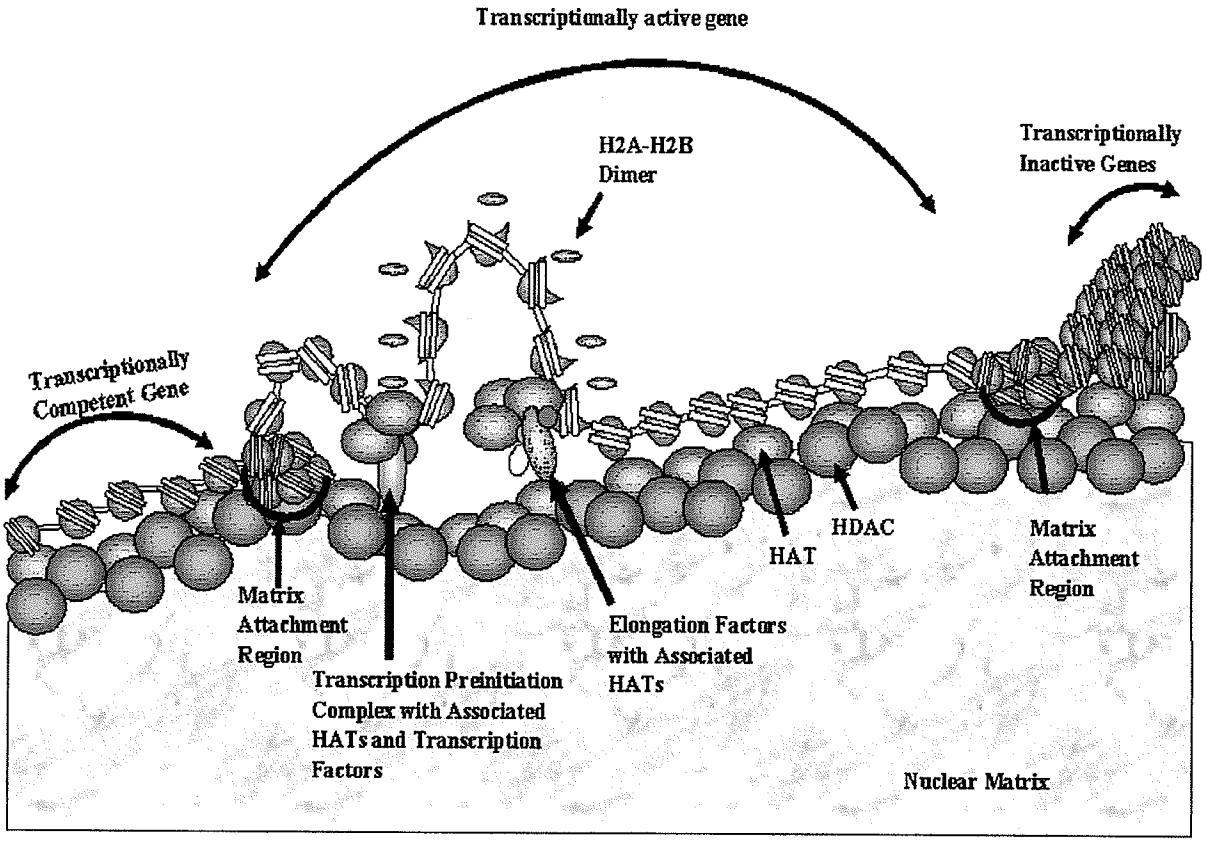


**Figure 35. Summary Model Describing the Role of Histone Acetylation and Nuclear Matrix Structure in Transcription as they Relate to the Results Presented in this Thesis.** DNA binds to the NM at its matrix attachment regions and becomes organized into loop domains. Histone acetyltransferases (HATs) and histone deacetylases (HDACs) concentrated in nuclear regions such as the NM dynamically acetylate histones associated with the promoter and downstream regions of transcriptionally competent and active genes. Transcriptionally inactive genes may also be associated with the NM; however, they exist in a highly compact structure and are relatively inaccessible to histone acetyltransferases. The dynamic histone acetylation of transcriptionally active and competent genes continually mediates their dynamic attachment to the NM. Exposure to transcriptional stimuli causes the recruitment of transcription factors to the promoter region of target

genes. These transcription factors recruit additional histone acetyltransferases that induce dynamic and rapid histone acetylation along the target gene. Competent genes that are not transcriptionally stimulated still remain associated with NM-associated histone acetyltransferases and histone deacetylases. These genes are not targeted by additional histone acetyltransferases, and, therefore, are not acetylated to the same rapid extent. Thus, transcriptionally competent genes are most likely associated with both rapidly and slowly acetylated histones. The rapid and dynamic histone acetylation of transcriptionally active genes may serve to generate a histone code along the N terminal tails of core histones associated with the promoter region. This code can then be recognized by additional factors important in the transcription process. Rapid and dynamic histone acetylation is also most likely important for transcriptional elongation. The movement of a target gene over RNA polymerase II disrupts the structure of nucleosomes along a gene, causing nucleosomes to release an H2A-H2B dimer and unfold. The histones within the unfolded nucleosome then become acetylated by histone acetyltransferases associated with RNA polymerase II to maintain the unfolded structure of transcribed nucleosomes. This acetylation event, however, is short lived and reversed by NM-associated histone deacetylases distributed along the length of the target gene. Transcription factors and chromatin remodeling factors recruited to the gene promoter by transcriptional stimuli eventually cycle off, causing the transcription of the target gene to stop. Processes such as transformation can alter the expression levels of nuclear matrix proteins and/or the contacts between these proteins and DNA. This could alter the organization of DNA loop domains, causing genes that would otherwise be hidden to become situated close to the nuclear matrix and regions of transcriptional activity.

**Future Directions**

The field of chromatin research has advanced considerably in the past decade. In particular, significant advances have been made in further elucidating the role of histone acetylation in transcription. While much has been learned about histone acetylation as a steady state process in transcription, little is known of the dynamics of this event. Researchers have only confirmed the presence of histone acetyltransferases along the promoter regions of transcriptionally active genes, while no attempts have been made to identify the location of histone deacetylases along these regions [167,168,199,210]. As well, very little effort has been made to study histone acetylation along regions downstream from gene promoters.

Our results show that histone acetylation is a dynamic event that takes place along both the promoter and coding regions of a transcriptionally active or competent gene. Our results also show that a histone deacetylase is associated with the promoter and coding region of a transcriptionally competent gene in the absence of transcriptional stimulation. Further efforts need to be made to determine how histone acetyltransferase and histone deacetylase complexes are recruited to the promoter and coding regions of transcriptionally competent genes. Do these enzymes have NM-targeting sequences that aid in their recruitment to nuclear regions such as the NM that are associated with transcriptionally active and competent genes as well as the transcriptional machinery, or are they recruited indirectly to the NM and specific gene regions through multi-protein complexes? Furthermore, are the multi-protein complexes containing histone acetyltransferases and histone deacetylases along a gene promoter the same in composition as those along a gene coding region? Perhaps the Sin3A histone deacetylase complex is recruited only to the

promoter regions but not to the coding regions of a gene. Further understanding the nature of these complexes along transcriptionally active and competent genes will increase our understanding of the events involved in transcriptional initiation and elongation. As well, it will further elucidate the manner with which these complexes are organized within the nucleus.

Histone deacetylase inhibitors show considerable promise in the treatment of many different types of cancer. However, these inhibitors are effective for only short periods of time. As well, cancer patients that are effectively treated with histone deacetylase inhibitors can eventually relapse and become resistant to these inhibitors [364,509]. Increasing our understanding of the nature of histone deacetylase action in gene expression within a normal and cancer cell will allow researchers to develop more effective histone deacetylase inhibitors. For example, our studies show further investigation needs to be made to determine the effect of sodium butyrate and TSA on the association of histone deacetylases with the promoter, exon 2 and exon 3 regions of the pS2 gene, a gene important in the prognosis of breast cancer. Researchers are also currently developing inhibitors for histone acetyltransferases. The production of these acetyltransferase inhibitors will significantly increase our understanding of the role of dynamic histone acetylation in gene expression and tumorigenesis. However, whether these inhibitors will also prove to be anti-tumorigenic remains to be determined.

Studies show that histone methylation and phosphorylation are important events in transcription. The role of these modifications in estrogen-mediated transcription needs to be investigated to further strengthen or diminish the theory of histone code formation by post-translational histone modifications in estrogen-stimulated transcription. This will

allow us to gain a more complete understanding of the transcriptional events responsible for normal and breast cancer cell growth.

Lastly, the role of the NM in gene expression has been largely ignored. Observations that the NM is tightly associated with many nuclear processes and DNA show that this structure most likely has an important structural influence in gene expression. We and others have identified NM proteins that differ in expression levels between normal and cancer cells [408,409,520-522]. As well, we showed that the expression levels of NM proteins associated with DNA change as breast cancer cells acquire more invasive and metastatic phenotypes representative of late stage cancer development. Future work needs to be performed to determine the identity of these differentially expressed NM proteins. Furthermore, we observed an increase in DNA-associated lamin and cytokeratin protein levels among cell lines with more aggressive breast cancer phenotypes. Additional studies need to be conducted to understand the relevance of this increase in breast cancer progression. The solid state chemical-mechanical model of signal transduction which involves the extracellular matrix, cytoskeleton and NM is an area that has great promise for understanding the behaviour and gene expression profile in normal and transformed cells. Furthermore, understanding the changes that occur in the expression of NM proteins, lamins and cytokeratins throughout breast cancer development may introduce new potential diagnostic and prognostic markers of disease development, as well as new potential areas of breast cancer treatment.

**Novel Findings**

- Dr. Davie and colleagues showed that the distribution of acetylated H4 correlated with the distribution of transcriptionally active DNA in different nuclear fractions and that the insoluble nuclear fraction containing the NM also contained the majority of acetylated H4 [184]. No direct evidence was provided by Davie and colleagues showing a direct association between acetylated histones, transcriptionally active and/or competent DNA sequences and the insoluble nuclear material [184]. Our results showed that transcriptionally active and competent DNA sequences with highly acetylated H3 and H4 are directly associated with the insoluble nuclear material that contains the NM.

- We more conclusively determined that transcriptionally active and competent genes are associated with class I acetylated H3, H4 and H2B, suggesting that both types of genes are situated next to or within regions of histone acetyltransferase and histone deacetylase activity. However, transcriptionally competent DNA sequences are associated with a mosaic of class I and class II dynamically acetylated histones, suggesting that competent genes are not associated with histone acetyltransferases and deacetylases to the same extent as active genes.

- Our data showing that the pS2 gene is dynamically acetylated along its exon 2 and 3 regions in the absence of E2 is the first to demonstrate that histone acetyltransferases and deacetylases are associated with the coding regions of an estrogen-responsive gene in the absence of transcriptional stimulation. We are also the first to show that

this dynamic acetylation is a prolonged event that occurs in the absence of transcriptional stimulation.

- Several research groups have only determined the effect of histone deacetylase inhibitors on the association of histone deacetylases with the promoter regions of transcriptionally active genes [476,478]. We are the first to demonstrate that sodium butyrate removes HDAC1 from the promoter, exon 2 and exon 3 regions of an estrogen-responsive gene while TSA only removes HDAC1 from the promoter.

- Many studies have presented evidence showing that the expression levels of NM proteins vary between normal and cancer cells. However, our study is the first to demonstrate that the acquisition of more aggressive phenotypes such as invasion and metastasis in breast cancer cells is accompanied by changes in the subset of NM proteins, nuclear cytokeratins and lamins associated with DNA. This suggests that the development of more aggressive breast cancer phenotypes is accompanied by changes in NM and DNA organization.

**References**


1. Getzenberg, R. H., Pienta, K. J., Ward, W. S., and Coffey, D. S. Nuclear structure and the three-dimensional organization of DNA. J.Cell Biochem., *47*: 289-299, 1991.

2. Mahy, N.L., Perry, P.E., Gilchrist, S., Baldock, R.A., and Bickmore, W.A. Spatial organization of active and inactive genes and noncoding DNA within chromosome territories. J. Cell Biol., *157*: 579-589, 2002.

3. Verschure, P. J., van, D. K., I, Manders, E. M., and van Driel, R. Spatial relationship between transcription sites and chromosome territories. J.Cell Biol., *147*: 13-24, 1999.

4. Davie, J. R. The nuclear matrix and the regulation of chromatin organization and function. Int.Rev.Cytol., *162A* : 191-250, 1995.

5. Adolphs, K. W., Cheng, S. M., Paulson, J. R., and Laemmli, U. K. Isolation of a protein scaffold from mitotic HeLa cell chromosomes. Proc.Natl.Acad.Sci.U.S.A, *74*: 4937-4941, 1977.

6. Cockerill, P. N. and Garrard, W. T. Chromosomal loop anchorage of the kappa immunoglobulin gene occurs next to the enhancer in a region containing topoisomerase II sites. Cell, *44*: 273-282, 1986.

7. Hansen, J. C. Conformational dynamics of the chromatin fiber in solution: determinants, mechanisms, and functions. Annu.Rev.Biophys.Biomol.Struct., *31*: 361-392, 2002.

8. Spencer, V. A. and Davie, J. R. Role of covalent modifications of histones in regulating gene expression. Gene, *240*: 1-12, 1999.

9. Wolffe, A. P. Transcriptional regulation in the context of chromatin structure. Essays Biochem., *37*: 45-57, 2001.

10. Arents, G., Burlingame, R. W., Wang, B. C., Love, W. E., and Moudrianakis, E. N. The nucleosomal core histone octamer at 3.1 Å resolution: a tripartite protein assembly and a left-handed superhelix. Proc.Natl.Acad.Sci.U.S.A, *88*: 10148-10152, 1991.

11. Yager, T. D., McMurray, C. T., and van Holde, K. E. Salt-induced release of DNA from nucleosome core particles. Biochemistry, *28*: 2271-2281, 1989.

12. Hansen, J. C., van Holde, K. E., and Lohr, D. The mechanism of nucleosome assembly onto oligomers of the sea urchin 5 S DNA positioning sequence. J.Biol.Chem., *266*: 4276-4282, 1991.

13. Sinclair, G. D. and Brasch, K. The nucleated erythrocyte: a model of cell differentiation. Rev.Can.Biol., *34*: 287-303, 1975.

14. Bates, D. L. and Thomas, J. O. Histones H1 and H5: one or two molecules per nucleosome? Nucleic Acids Res., *9*: 5883-5894, 1981.

15. van Holde, K. Chromatin.New York: Springer-Verlag, 1988.

16. Zhou, Y. B., Gerchman, S. E., Ramakrishnan, V., Travers, A., and Muyldermans, S. Position and orientation of the globular domain of linker histone H5 on the nucleosome. Nature, *395*: 402-405, 1998.

17. Lever, M. A., Th'ng, J. P., Sun, X., and Hendzel, M. J. Rapid exchange of histone H1.1 on chromatin in living human cells. Nature, *408*: 873-876, 2000.

18. Misteli, T., Gunjan, A., Hock, R., Bustin, M., and Brown, D. T. Dynamic binding of histone H1 to chromatin in living cells. Nature, *408*: 877-881, 2000.

19. Spencer, V. A. and Davie, J. R. Signal transduction pathways and chromatin structure in cancer cells. J.Cell Biochem., *Suppl 35*: 27-35, 2000.

20. Lu, M. J., Mpoke, S. S., Dadd, C. A., and Allis, C. D. Phosphorylated and dephosphorylated linker histone H1 reside in distinct chromatin domains in Tetrahymena macronuclei. Mol.Biol.Cell, *6* : 1077-1087, 1995.

21. Dou, Y., Mizzen, C. A., Abrams, M., Allis, C. D., and Gorovsky, M. A. Phosphorylation of linker histone H1 regulates gene expression *in vivo* by mimicking H1 removal. Mol.Cell, *4*: 641-647, 1999.

22. Ausio, J., Abbott, D. W., Wang, X., and Moore, S. C. Histone variants and histone modifications: a structural perspective. Biochem.Cell Biol., *79*: 693-708, 2001.

23. Pehrson, J. R. and Fried, V. A. MacroH2A, a core histone containing a large nonhistone region. Science, *257*: 1398-1400, 1992.

24. Csankovszki, G., Panning, B., Bates, B., Pehrson, J. R., and Jaenisch, R. Conditional deletion of Xist disrupts histone macroH2A localization but not maintenance of X inactivation. Nat.Genet., *22*: 323-324, 1999.

25. Gilbert, S. L., Pehrson, J. R., and Sharp, P. A. XIST RNA associates with specific regions of the inactive X chromatin. J.Biol.Chem., *275*: 36491-36494, 2000.

26. West, M. H. and Bonner, W. M. Histone 2A, a heteromorphous family of eight protein species. Biochemistry, *19*: 3238-3245, 1980.

27. Liu, X., Bowen, J., and Gorovsky, M. A. Either of the major H2A genes but not an evolutionarily conserved H2A.F/Z variant of Tetrahymena thermophila can function as the sole H2A gene in the yeast *Saccharomyces cerevisiae*. Mol.Cell Biol., *16*: 2878-2887, 1996.

28. van Daal, A. and Elgin, S. C. A histone variant, H2AvD, is essential in Drosophila melanogaster. Mol.Biol.Cell, *3*: 593-602, 1992.

29. Clarkson, M. J., Wells, J. R., Gibson, F., Saint, R., and Tremethick, D. J. Regions of variant histone His2AvD required for Drosophila development. Nature, *399*: 694-697, 1999.

30. Iouzalen, N., Moreau, J., and Mechali, M. H2A.ZI, a new variant histone expressed during Xenopus early development exhibits several distinct features from the core histone H2A. Nucleic Acids Res., *24*: 3947-3952, 1996.

31. Rogakou, E. P., Pilch, D. R., Orr, A. H., Ivanova, V. S., and Bonner, W. M. DNA double-stranded breaks induce histone H2AX phosphorylation on serine 139. J. Biol. Chem., *273*: 5858-5868, 1998.

32. Mahadevaiah, S. K., Turner, J. M., Baudat, F., Rogakou, E. P., de Boer, P., Blanco-Rodriguez, J., Jasin, M., Keeney, S., Bonner, W. M., and Burgoyne, P. S. Recombinational DNA double-strand breaks in mice precede synapsis. Nat. Genet., *27*: 271-276, 2001.

33. Hunter, N., Valentin, B. G., Lichten, M., and Kleckner, N. Gamma-H2AX illuminates meiosis. Nat. Genet., *27*: 236-238, 2001.

34. Chadwick, B. P. and Willard, H. F. A novel chromatin protein, distantly related to histone H2A, is largely excluded from the inactive X chromosome. J. Cell Biol., *152*: 375-384, 2001.

35. Bosch, A. and Suau, P. Changes in core histone variant composition in differentiating neurons: the roles of differential turnover and synthesis rates. Eur. J. Cell Biol., *68*: 220-225, 1995.

36. Leonardson, K. E. and Levy, S. B. Chromatin reorganization during emergence of malignant Friend tumors: early changes in H2A and H2B variants and nucleosome repeat length. Exp.Cell Res., *180* : 209-219, 1989.

37. Kapros, T., Robertson, A. J., and Waterborg, J. H. Histone H3 transcript stability in alfalfa. Plant Mol.Biol., *28*: 901-914, 1995.

38. Waterborg, J. H. Histone synthesis and turnover in alfalfa. Fast loss of highly acetylated replacement histone variant H3.2. J. Biol. Chem., *268*: 4912-4917, 1993.

39. Sullivan, K. F., Hechenberger, M., and Masri, K. Human CENP-A contains a histone H3 related histone fold domain that is required for targeting to the centromere. J. Cell Biol., *127*: 581-592, 1994.

40. Keith, K. C., Baker, R. E., Chen, Y., Harris, K., Stoler, S., and Fitzgerald-Hayes, M. Analysis of primary structural determinants that distinguish the centromere-specific function of histone variant Cse4p from histone H3. Mol. Cell Biol., *19*: 6130-6139, 1999.

41. Henikoff, S., Ahmad, K., Platero, J. S., and van Steensel, B. Heterochromatic deposition of centromeric histone H3-like proteins. Proc. Natl. Acad. Sci. U.S.A, *97*: 716-721, 2000.

42. Li, W., Nagaraja, S., Delcuve, G. P., Hendzel, M. J., and Davie, J. R. Effects of histone acetylation, ubiquitination and variants on nucleosome stability. Biochem. J., *296 ( Pt 3)*: 737-744, 1993.

43. Izban, M. G. and Luse, D. S. Transcription on nucleosomal templates by RNA polymerase II *in vitro*: inhibition of elongation with enhancement of sequence-specific pausing. Genes Dev., *5*: 683-696, 1991.

44. Kireeva, M. L., Walter, W., Tchernajenko, V., Bondarenko, V., Kashlev, M., and Studitsky, V. M. Nucleosome remodeling induced by RNA polymerase II: loss of the H2A/H2B dimer during transcription. Mol Cell, *9*: 541-552, 2002.

45. Kimura, H. and Cook, P. R. Kinetics of core histones in living human cells: little exchange of H3 and H4 and some rapid exchange of H2B. J.Cell Biol., *153*: 1341-1353, 2001.

46. Baer, B. W. and Rhodes, D. Eukaryotic RNA polymerase II binds to nucleosome cores from transcribed genes. Nature, *301*: 482-488, 1983.

47. Nacheva, G. A., Guschin, D. Y., Preobrazhenskaya, O. V., Karpov, V. L., Ebralidse, K. K., and Mirzabekov, A. D. Change in the pattern of histone binding to DNA upon transcriptional activation. Cell, *58*: 27-36, 1989.

48. Shilatifard, A. Factors regulating the transcriptional elongation activity of RNA polymerase II. FASEB J., *12*: 1437-1446, 1998.

49. Orphanides, G., Wu, W. H., Lane, W. S., Hampsey, M., and Reinberg, D. The chromatin-specific transcription elongation factor FACT comprises human SPT16 and SSRP1 proteins. Nature, *400*: 284-288, 1999.

50. Walia, H., Chen, H. Y., Sun, J. M., Holth, L. T., and Davie, J. R. Histone acetylation is required to maintain the unfolded nucleosome structure associated with transcribing DNA. J.Biol.Chem., *273*: 14516-14522, 1998.

51. Wittschieben, B. O., Otero, G., de Bizemont, T., Fellows, J., Erdjument-Bromage, H., Ohba, R., Li, Y., Allis, C. D., Tempst, P., and Svejstrup, J. Q. A novel histone acetyltransferase is an integral subunit of elongating RNA polymerase II holoenzyme. Mol.Cell, *4*: 123-128, 1999.

52. Cho, H., Orphanides, G., Sun, X., Yang, X. J., Ogryzko, V., Lees, E., Nakatani, Y., and Reinberg, D. A human RNA polymerase II complex containing factors that modify chromatin structure. Mol.Cell Biol., *18*: 5355-5363, 1998.

53. Prior, C. P., Cantor, C. R., Johnson, E. M., Littau, V. C., and Allfrey, V. G. Reversible changes in nucleosome structure and histone H3 accessibility in transcriptionally active and inactive states of rDNA chromatin. Cell, *34*: 1033-1042, 1983.

54. Chen, T. A. and Allfrey, V. G. Rapid and reversible changes in nucleosome structure accompany the activation, repression, and superinduction of murine fibroblast protooncogenes c-*fos* and c-*myc*. Proc.Natl.Acad.Sci.U.S.A, *84*: 5252-5256, 1987.

55. Bazett-Jones, D. P., Mendez, E., Czarnota, G. J., Ottensmeyer, F. P., and Allfrey, V. G. Visualization and analysis of unfolded nucleosomes associated with transcribing chromatin. Nucleic Acids Res., *24*: 321-329, 1996.

56. Widmer, R. M., Lucchini, R., Lezzi, M., Meyer, B., Sogo, J. M., Edstrom, J. E., and Koller, T. Chromatin structure of a hyperactive secretory protein gene (in Balbiani ring 2) of Chironomus. EMBO J., *3*: 1635-1641, 1984.

57. van Holde, K. and Zlatanova, J. What determines the folding of the chromatin fiber? Proc.Natl.Acad.Sci.U.S.A, *93*: 10548-10555, 1996.

58. Karpov, V. L., Preobrazhenskaya, O. V., and Mirzabekov, A. D. Chromatin structure of hsp 70 genes, activated by heat shock: selective removal of histones from the coding region and their absence from the 5' region. Cell, *36*: 423-431, 1984.

59. Solomon, M. J., Larsen, P. L., and Varshavsky, A. Mapping protein-DNA interactions *in vivo* with formaldehyde: evidence that histone H4 is retained on a highly transcribed gene. Cell, *53*: 937-947, 1988.

60. Mutskov, V., Gerber, D., Angelov, D., Ausio, J., Workman, J., and Dimitrov, S. Persistent interactions of core histone tails with nucleosomal DNA following acetylation and transcription factor binding. Mol.Cell Biol, *18*: 6293-6304, 1998.

61. van Holde, K. E., Lohr, D. E., and Robert, C. What happens to nucleosomes during transcription? J.Biol.Chem., *267*: 2837-2840, 1992.

62. Hebbes, T. R., Clayton, A. L., Thorne, A. W., and Crane-Robinson, C. Core histone hyperacetylation co-maps with generalized DNase I sensitivity in the chicken beta-globin chromosomal domain. EMBO J., *13*: 1823-1830, 1994.

63. Tazi, J. and Bird, A. Alternative chromatin structure at CpG islands. Cell, *60*: 909-920, 1990.

64. Tumbar, T., Sudlow, G., and Belmont, A. S. Large-scale chromatin unfolding and remodeling induced by VP16 acidic activation domain. J.Cell Biol., *145*: 1341-1354, 1999.

65. Hendzel, M. J., Kruhlak, M. J., MacLean, N. A., Boisvert, F., Lever, M. A., and Bazett-Jones, D. P. Compartmentalization of regulatory proteins in the cell nucleus. J.Steroid Biochem.Mol.Biol., *76*: 9-21, 2001.

66. Horn, P. J. and Peterson, C. L. Molecular biology. Chromatin higher order folding--wrapping up transcription. Science, *297*: 1824-1827, 2002.

67. Annunziato, A. T. and Hansen, J. C. Role of histone acetylation in the assembly and modulation of chromatin structures. Gene Expr., *9*: 37-61, 2000.

68. Davie, J. R. and Spencer, V. A. Signal transduction pathways and the modification of chromatin structure. Prog.Nucleic Acid Res.Mol.Biol., *65*: 299-340, 2001.

69. Hansen, J. C., Tse, C., and Wolffe, A. P. Structure and function of the core histone N-termini: more than meets the eye. Biochemistry, *37*: 17637-17641, 1998.

70. Ridsdale, J. A., Hendzel, M. J., Delcuve, G. P., and Davie, J. R. Histone acetylation alters the capacity of the H1 histones to condense transcriptionally active/competent chromatin. J.Biol.Chem., *265*: 5150-5156, 1990.

71. Tse, C. and Hansen, J. C. Hybrid trypsinized nucleosomal arrays: identification of multiple functional roles of the H2A/H2B and H3/H4 N-termini in chromatin fiber compaction. Biochemistry, *36*: 11381-11388, 1997.

72. Leuba, S. H., Bustamante, C., van Holde, K., and Zlatanova, J. Linker histone tails and N-tails of histone H3 are redundant: scanning force microscopy studies of reconstituted fibers. Biophys.J., *74*: 2830-2839, 1998.

73. Leuba, S. H., Bustamante, C., Zlatanova, J., and van Holde, K. Contributions of linker histones and histone H3 to chromatin structure: scanning force microscopy studies on trypsinized fibers. Biophys.J., *74*: 2823-2829, 1998.

74. Zlatanova, J., Leuba, S. H., and van Holde, K. Chromatin fiber structure: morphology, molecular determinants, structural transitions. Biophys.J., *74*: 2554-2566, 1998.

75. Horowitz, R. A., Agard, D. A., Sedat, J. W., and Woodcock, C. L. The three-dimensional architecture of chromatin in situ: electron tomography reveals fibers composed of a continuously variable zig-zag nucleosomal ribbon. J.Cell Biol, *125*: 1-10, 1994.

76. Woodcock, C. L., Grigoryev, S. A., Horowitz, R. A., and Whitaker, N. A chromatin folding model that incorporates linker variability generates fibers resembling the native structures. Proc.Natl.Acad.Sci.U.S.A, *90*: 9021-9025, 1993.

77. Yang, G., Leuba, S. H., Bustamante, C., Zlatanova, J., and van Holde, K. Role of linker histones in extended chromatin fibre structure. Nat.Struct.Biol, *1*: 761-763, 1994.

78. Schwarz, P. M., Felthauser, A., Fletcher, T. M., and Hansen, J. C. Reversible oligonucleosome self-association: dependence on divalent cations and core histone tail domains. Biochemistry, *35* : 4009-4015, 1996.

79. Luger, K., Mader, A. W., Richmond, R. K., Sargent, D. F., and Richmond, T. J. Crystal structure of the nucleosome core particle at 2.8 Å resolution. Nature, *389*: 251-260, 1997.

80. Grunstein, M. Yeast heterochromatin: regulation of its assembly and inheritance by histones. Cell, *93*: 325-328, 1998.

81. Palaparti, A., Baratz, A., and Stifani, S. The Groucho/transducin-like enhancer of split transcriptional repressors interact with the genetically defined amino-terminal silencing domain of histone H3. J.Biol.Chem., *272*: 26604-26610, 1997.

82. Fisher, A. L. and Caudy, M. Groucho proteins: transcriptional corepressors for specific subsets of DNA-binding transcription factors in vertebrates and invertebrates. Genes Dev., *12*: 1931-1940, 1998.

83. Bustin, M. Regulation of DNA-dependent activities by the functional motifs of the high-mobility-group chromosomal proteins. Mol.Cell Biol., *19*: 5237-5246, 1999.

84. Hansen, J. C., Ausio, J., Stanik, V. H., and van Holde, K. E. Homogeneous reconstituted oligonucleosomes, evidence for salt-dependent folding in the absence of histone H1. Biochemistry, *28*: 9129-9136, 1989.

85. Garcia-Ramirez, M., Dong, F., and Ausio, J. Role of the histone "tails" in the folding of oligonucleosomes depleted of histone H1. J.Biol Chem., *267*: 19587-19595, 1992.

86. Walter, W. and Studitsky, V. M. Facilitated transcription through the nucleosome at high ionic strength occurs via a histone octamer transfer mechanism. J.Biol Chem., *276*: 29104-29110, 2001.

87. Schwarz, P. M. and Hansen, J. C. Formation and stability of higher order chromatin structures. Contributions of the histone octamer. J.Biol.Chem., *269*: 16284-16289, 1994.

88. Strahl, B. D. and Allis, C. D. The language of covalent histone modifications. Nature, *403*: 41-45, 2000.

89. Jenuwein, T. and Allis, C. D. Translating the histone code. Science, *293*: 1074-1080, 2001.

90. Agalioti, T., Chen, G., and Thanos, D. Deciphering the transcriptional histone acetylation code for a human gene. Cell, *111*: 381-392, 2002.

91. Barratt, M. J., Hazzalin, C. A., Cano, E., and Mahadevan, L. C. Mitogen-stimulated phosphorylation of histone H3 is targeted to a small hyperacetylation-sensitive fraction. Proc.Natl.Acad.Sci.U.S.A, *91*: 4781-4785, 1994.

92. Thomson, S., Clayton, A. L., and Mahadevan, L. C. Independent dynamic regulation of histone phosphorylation and acetylation during immediate-early gene induction. Mol.Cell, *8*: 1231-1241, 2001.

93. Cheung, P., Tanner, K. G., Cheung, W. L., Sassone-Corsi, P., Denu, J. M., and Allis, C. D. Synergistic coupling of histone H3 phosphorylation and acetylation in response to epidermal growth factor stimulation. Mol.Cell, *5*: 905-915, 2000.

94. Lo, W. S., Duggan, L., Tolga, N. C., Emre, Belotserkovskya, R., Lane, W. S., Shiekhattar, R., and Berger, S. L. Snf1-a histone kinase that works in concert with the histone acetyltransferase Gcn5 to regulate transcription. Science, *293*: 1142-1146, 2001.

95. Lo, W. S., Trievel, R. C., Rojas, J. R., Duggan, L., Hsu, J. Y., Allis, C. D., Marmorstein, R., and Berger, S. L. Phosphorylation of serine 10 in histone H3 is functionally linked *in vitro* and *in vivo* to Gcn5-mediated acetylation at lysine 14. Mol.Cell, *5*: 917-926, 2000.

96. Rice, J. C. and Allis, C. D. Histone methylation versus histone acetylation: new insights into epigenetic regulation. Curr.Opin.Cell Biol, *13*: 263-273, 2001.

97. Lachner, M. and Jenuwein, T. The many faces of histone lysine methylation. Curr.Opin.Cell Biol, *14*: 286-298, 2002.

98. Rea, S., Eisenhaber, F., O'Carroll, D., Strahl, B. D., Sun, Z. W., Schmid, M., Opravil, S., Mechtler, K., Ponting, C. P., Allis, C. D., and Jenuwein, T. Regulation of chromatin structure by site-specific histone H3 methyltransferases. Nature, *406*: 593-599, 2000.

99. Berger, S. L. An embarrassment of niches: the many covalent modifications of histones in transcriptional regulation. Oncogene, *20*: 3007-3013, 2001.

100. Litt, M. D., Simpson, M., Gaszner, M., Allis, C. D., and Felsenfeld, G. Correlation between histone lysine methylation and developmental changes at the chicken beta-globin locus. Science, *293*: 2453-2455, 2001.

101. Strahl, B. D., Ohba, R., Cook, R. G., and Allis, C. D. Methylation of histone H3 at lysine 4 is highly conserved and correlates with transcriptionally active nuclei in Tetrahymena. Proc.Natl.Acad.Sci.U.S.A, *96*: 14967-14972, 1999.

102. Bernstein, B. E., Humphrey, E. L., Erlich, R. L., Schneider, R., Bouman, P., Liu, J. S., Kouzarides, T., and Schreiber, S. L. Methylation of histone H3 Lys 4 in coding regions of active genes. Proc.Natl.Acad.Sci.U.S.A, *99*: 8695-8700, 2002.

103. Saccani, S. and Natoli, G. Dynamic changes in histone H3 Lys 9 methylation occurring at tightly regulated inducible inflammatory genes. Genes Dev., *16*: 2219-2224, 2002.

104. Chinenov, Y. A second catalytic domain in the Elp3 histone acetyltransferases: a candidate for histone demethylase activity? Trends Biochem.Sci., *27*: 115-117, 2002.

105. Lee, Y. H., Koh, S. S., Zhang, X., Cheng, X., and Stallcup, M. R. Synergy among nuclear receptor coactivators: selective requirement for protein methyltransferase and acetyltransferase activities. Mol.Cell Biol, *22*: 3621-3632, 2002.

106. Chen, D., Ma, H., Hong, H., Koh, S. S., Huang, S. M., Schurter, B. T., Aswad, D. W., and Stallcup, M. R. Regulation of transcription by a protein methyltransferase. Science, *284*: 2174-2177, 1999.

107. Ma, H., Hong, H., Huang, S. M., Irvine, R. A., Webb, P., Kushner, P. J., Coetzee, G. A., and Stallcup, M. R. Multiple signal input and output domains of the 160-kilodalton nuclear receptor coactivator proteins. Mol.Cell Biol, *19*: 6164-6173, 1999.

108. Daujat, S., Bauer, U. M., Shah, V., Turner, B., Berger, S., and Kouzarides, T. Crosstalk between CARM1 methylation and CBP acetylation on histone H3. Curr.Biol, *12*: 2090-2097, 2002.

109. Marmorstein, R. Structure and function of histone acetyltransferases. Cell Mol.Life Sci., *58*: 693-703, 2001.

110. Sterner, D. E. and Berger, S. L. Acetylation of histones and transcription-related factors. Microbiol.Mol.Biol.Rev., *64*: 435-459, 2000.

111. Davie, J. R. and Chadee, D. N. Regulation and regulatory parameters of histone modifications. J.Cell Biochem.Suppl, *30-31*: 203-213, 1998.

112. Murphy, L. C. and Watson, P. Steroid receptors in human breast tumorigenesis and breast cancer progression. Biomed.Pharmacother., *56*: 65-77, 2002.

113. Kamei, Y., Xu, L., Heinzel, T., Torchia, J., Kurokawa, R., Gloss, B., Lin, S. C., Heyman, R. A., Rose, D. W., Glass, C. K., and Rosenfeld, M. G. A CBP integrator complex mediates transcriptional activation and AP-1 inhibition by nuclear receptors. Cell, *85*: 403-414, 1996.

114. Cottone, E., Orso, F., Biglia, N., Sismondi, P., and De Bortoli, M. Role of coactivators and corepressors in steroid and nuclear receptor signaling: potential markers of tumor growth and drug sensitivity. Int.J.Biol.Markers, *16*: 151-166, 2001.

115. Dhalluin, C., Carlson, J. E., Zeng, L., He, C., Aggarwal, A. K., and Zhou, M. M. Structure and ligand of a histone acetyltransferase bromodomain. Nature, *399*: 491-496, 1999.

116. Ornaghi, P., Ballario, P., Lena, A. M., Gonzalez, A., and Filetici, P. The bromodomain of Gcn5p interacts *in vitro* with specific residues in the N terminus of histone H4. J.Mol.Biol, *287*: 1-7, 1999.

117. Collingwood, T. N., Urnov, F. D., and Wolffe, A. P. Nuclear receptors: coactivators, corepressors and chromatin remodeling in the control of transcription. J.Mol.Endocrinol., *23*: 255-275, 1999.

118. Nakajima, T., Uchida, C., Anderson, S. F., Lee, C. G., Hurwitz, J., Parvin, J. D., and Montminy, M. RNA helicase A mediates association of CBP with RNA polymerase II. Cell, *90*: 1107-1112, 1997.

119. Neish, A. S., Anderson, S. F., Schlegel, B. P., Wei, W., and Parvin, J. D. Factors associated with the mammalian RNA polymerase II holoenzyme. Nucleic Acids Res., *26*: 847-853, 1998.

120. Wang, C., Fu, M., Angeletti, R. H., Siconolfi-Baez, L., Reutens, A. T., Albanese, C., Lisanti, M. P., Katzenellenbogen, B. S., Kato, S., Hopp, T., Fuqua, S. A., Lopez, G. N., Kushner, P. J., and Pestell, R. G. Direct acetylation of the estrogen receptor alpha hinge region by p300 regulates transactivation and hormone sensitivity. J.Biol.Chem., *276* : 18375-18383, 2001.

121. John, S., Howe, L., Tafrov, S. T., Grant, P. A., Sternglanz, R., and Workman, J. L. The something about silencing protein, Sas3, is the catalytic subunit of NuA3, a yTAF(II)30-containing HAT complex that interacts with the Spt16 subunit of the yeast CP (Cdc68/Pob3)-FACT complex. Genes Dev., *14*: 1196-1208, 2000.

122. Reifsnyder, C., Lowell, J., Clarke, A., and Pillus, L. Yeast SAS silencing genes and human genes associated with AML and HIV-1 Tat interactions are homologous with acetyltransferases. Nat.Genet., *14*: 42-49, 1996.

123. Vogelauer, M., Wu, J., Suka, N., and Grunstein, M. Global histone acetylation and deacetylation in yeast. Nature, *408*: 495-498, 2000.

124. Iizuka, M. and Stillman, B. Histone acetyltransferase HBO1 interacts with the ORC1 subunit of the human initiator protein. J.Biol.Chem., *274*: 23027-23034, 1999.

125. Onate, S. A., Tsai, S. Y., Tsai, M. J., and O'Malley, B. W. Sequence and characterization of a coactivator for the steroid hormone receptor superfamily. Science, *270*: 1354-1357, 1995.

126. Hong, H., Kohli, K., Trivedi, A., Johnson, D. L., and Stallcup, M. R. GRIP1, a novel mouse protein that serves as a transcriptional coactivator in yeast for the hormone binding domains of steroid receptors. Proc.Natl.Acad.Sci.U.S.A, *93*: 4948-4952, 1996.

127. Voegel, J. J., Heine, M. J., Zechel, C., Chambon, P., and Gronemeyer, H. TIF2, a 160 kDa transcriptional mediator for the ligand-dependent activation function AF-2 of nuclear receptors. EMBO J., *15*: 3667-3675, 1996.

128. Anzick, S. L., Kononen, J., Walker, R. L., Azorsa, D. O., Tanner, M. M., Guan, X. Y., Sauter, G., Kallioniemi, O. P., Trent, J. M., and Meltzer, P. S. AIB1, a steroid receptor coactivator amplified in breast and ovarian cancer. Science, *277*: 965-968, 1997.

129. Chen, H., Lin, R. J., Schiltz, R. L., Chakravarti, D., Nash, A., Nagy, L., Privalsky, M. L., Nakatani, Y., and Evans, R. M. Nuclear receptor coactivator ACTR is a novel histone acetyltransferase and forms a multimeric activation complex with P/CAF and CBP/p300. Cell, *90*: 569-580, 1997.

130. Li, H., Gomes, P. J., and Chen, J. D. RAC3, a steroid/nuclear receptor-associated coactivator that is related to SRC-1 and TIF2. Proc.Natl.Acad.Sci.U.S.A, *94*: 8479-8484, 1997.

131. Takeshita, A., Cardona, G. R., Koibuchi, N., Suen, C. S., and Chin, W. W. TRAM-1, A novel 160-kDa thyroid hormone receptor activator molecule, exhibits distinct properties from steroid receptor coactivator-1. J.Biol.Chem., *272*: 27629-27634, 1997.

132. McInerney, E. M., Rose, D. W., Flynn, S. E., Westin, S., Mullen, T. M., Krones, A., Inostroza, J., Torchia, J., Nolte, R. T., Assa-Munt, N., Milburn, M. V., Glass, C. K., and Rosenfeld, M. G. Determinants of coactivator LXXLL motif specificity in nuclear receptor transcriptional activation. Genes Dev., *12*: 3357-3368, 1998.

133. Rundlett, S. E., Carmen, A. A., Suka, N., Turner, B. M., and Grunstein, M. Transcriptional repression by UME6 involves deacetylation of lysine 5 of histone H4 by RPD3. Nature, *392*: 831-835, 1998.

134. Reid, J. L., Iyer, V. R., Brown, P. O., and Struhl, K. Coordinate regulation of yeast ribosomal protein genes is associated with targeted recruitment of Esa1 histone acetylase. Mol.Cell, *6*: 1297-1307, 2000.

135. An, W., Palhan, V. B., Karymov, M. A., Leuba, S. H., and Roeder, R. G. Selective requirements for histone H3 and H4 N termini in p300- dependent transcriptional activation from chromatin. Mol Cell, *9*: 811-821, 2002.

136. Grant, P. A., Eberharter, A., John, S., Cook, R. G., Turner, B. M., and Workman, J. L. Expanded lysine acetylation specificity of Gcn5 in native complexes. J.Biol.Chem., *274*: 5895-5900, 1999.

137. Zhang, W., Bone, J. R., Edmondson, D. G., Turner, B. M., and Roth, S. Y. Essential and redundant functions of histone acetylation revealed by mutation of target lysines and loss of the Gcn5p acetyltransferase. EMBO J., *17*: 3155-3167, 1998.

138. Liu, Y. Z., Thomas, N. S., and Latchman, D. S. CBP associates with the p42/p44 MAPK enzymes and is phosphorylated following NGF treatment. Neuroreport, *10*: 1239-1243, 1999.

139. Davie, J. R. and Moniwa, M. Control of chromatin remodeling. Crit Rev.Eukaryot.Gene Expr., *10*: 303-325, 2000.

140. Guardiola, A. R. and Yao, T. P. Molecular cloning and characterization of a novel histone deacetylase HDAC10. J.Biol Chem., *277*: 3350-3356, 2002.

141. Gao, L., Cueto, M. A., Asselbergs, F., and Atadja, P. Cloning and functional characterization of HDAC11, a novel member of the human histone deacetylase family. J.Biol Chem., *277*: 25748-25755, 2002.

142. Afshar, G. and Murnane, J. P. Characterization of a human gene with sequence homology to *Saccharomyces cerevisiae* SIR2. Gene, *234*: 161-168, 1999.

143. Frye, R. A. Characterization of five human cDNAs with homology to the yeast SIR2 gene: Sir2-like proteins (sirtuins) metabolize NAD and may have protein ADP-ribosyltransferase activity. Biochem.Biophys.Res.Commun., *260*: 273-279, 1999.

144. Frye, R. A. Phylogenetic classification of prokaryotic and eukaryotic Sir2-like proteins. Biochem.Biophys.Res.Commun., *273*: 793-798, 2000.

145. Imai, S., Armstrong, C. M., Kaeberlein, M., and Guarente, L. Transcriptional silencing and longevity protein Sir2 is an NAD- dependent histone deacetylase. Nature, *403*: 795-800, 2000.

146. Landry, J., Slama, J. T., and Sternglanz, R. Role of NAD(+) in the deacetylase activity of the SIR2-like proteins. Biochem.Biophys.Res.Commun., *278*: 685-690, 2000.

147. Vidal, M. and Gaber, R. F. RPD3 encodes a second factor required to achieve maximum positive and negative transcriptional states in *Saccharomyces cerevisiae*. Mol.Cell Biol, *11*: 6317-6327, 1991.

148. Vidal, M., Strich, R., Esposito, R. E., and Gaber, R. F. RPD1 (SIN3/UME4) is required for maximal activation and repression of diverse yeast genes. Mol.Cell Biol, *11*: 6306-6316, 1991.

149. Pazin, M. J. and Kadonaga, J. T. What's up and down with histone deacetylation and transcription? Cell, *89*: 325-328, 1997.

150. Mahlknecht, U. and Hoelzer, D. Histone acetylation modifiers in the pathogenesis of malignant disease. Mol.Med., *6*: 623-644, 2000.

151. Zhang, Y., Sun, Z. W., Iratni, R., Erdjument-Bromage, H., Tempst, P., Hampsey, M., and Reinberg, D. SAP30, a novel protein conserved between human and yeast, is a component of a histone deacetylase complex. Mol.Cell, *1*: 1021-1031, 1998.

152. Xue, Y., Wong, J., Moreno, G. T., Young, M. K., Cote, J., and Wang, W. NURD, a novel complex with both ATP-dependent chromatin-remodeling and histone deacetylase activities. Mol.Cell, *2*: 851-861, 1998.

153. Li, J., Wang, J., Wang, J., Nawaz, Z., Liu, J. M., Qin, J., and Wong, J. Both corepressor proteins SMRT and N-CoR exist in large protein complexes containing HDAC3. EMBO J., *19*: 4342-4350, 2000.

154. Johnson, C. A. Chromatin modification and disease. J.Med.Genet., *37*: 905-915, 2000.

155. Ayer, D. E. Histone deacetylases: transcriptional repression with SINers and NuRDs. Trends Cell Biol, *9*: 193-198, 1999.

156. Zhang, Y., LeRoy, G., Seelig, H. P., Lane, W. S., and Reinberg, D. The dermatomyositis-specific autoantigen Mi2 is a component of a complex containing histone deacetylase and nucleosome remodeling activities. Cell, *95*: 279-289, 1998.

157. Zhang, Y., Ng, H. H., Erdjument-Bromage, H., Tempst, P., Bird, A., and Reinberg, D. Analysis of the NuRD subunits reveals a histone deacetylase core complex and a connection with DNA methylation. Genes Dev., *13*:1924-1935.

158. Zhang, Y., Iratni, R., Erdjument-Bromage, H., Tempst, P., and Reinberg, D. Histone deacetylases and SAP18, a novel polypeptide, are components of a human Sin3 complex. Cell, *89*: 357-364, 1997.

159. Zhang, Y., Ng, H. H., Erdjument-Bromage, H., Tempst, P., Bird, A., and Reinberg, D. Analysis of the NuRD subunits reveals a histone deacetylase core complex and a connection with DNA methylation. Genes Dev., *13*: 1924-1935, 1999.

160. Ahringer, J. NuRD and SIN3 histone deacetylase complexes in development. Trends Genet., *16*: 351-356, 2000.

161. Wade, P. A., Gegonne, A., Jones, P. L., Ballestar, E., Aubry, F., and Wolffe, A. P. Mi-2 complex couples DNA methylation to chromatin remodelling and histone deacetylation. Nat.Genet., *23*: 62-66, 1999.

162. Feng, Q. and Zhang, Y. The MeCP1 complex represses transcription through preferential binding, remodeling, and deacetylating methylated nucleosomes. Genes Dev., *15*: 827-832, 2001.

163. Wen, Y. D., Perissi, V., Staszewski, L. M., Yang, W. M., Krones, A., Glass, C. K., Rosenfeld, M. G., and Seto, E. The histone deacetylase-3 complex contains nuclear receptor corepressors. Proc.Natl.Acad.Sci.U.S.A, *97*: 7202-7207, 2000.

164. Kao, H. Y., Downes, M., Ordentlich, P., and Evans, R. M. Isolation of a novel histone deacetylase reveals that class I and class II deacetylases promote SMRT-mediated repression. Genes Dev., *14*: 55-66, 2000.

165. Guenther, M. G., Lane, W. S., Fischle, W., Verdin, E., Lazar, M. A., and Shiekhattar, R. A core SMRT corepressor complex containing HDAC3 and TBL1, a WD40-repeat protein linked to deafness. Genes Dev., *14*: 1048-1057, 2000.

166. Huang, E. Y., Zhang, J., Miska, E. A., Guenther, M. G., Kouzarides, T., and Lazar, M. A. Nuclear receptor corepressors partner with class II histone deacetylases in a Sin3-independent repression pathway. Genes Dev., *14*: 45-54, 2000.

167. Shang, Y. and Brown, M. Molecular determinants for the tissue specificity of SERMs. Science, *295*: 2465-2468, 2002.

168. Shang, Y., Hu, X., DiRenzo, J., Lazar, M. A., and Brown, M. Cofactor dynamics and sufficiency in estrogen receptor-regulated transcription. Cell, *103*: 843-852, 2000.

169. Torchia, J., Glass, C., and Rosenfeld, M. G. Co-activators and co-repressors in the integration of transcriptional responses. Curr.Opin.Cell Biol., *10*: 373-383, 1998.

170. Sun, J. M., Chen, H. Y., and Davie, J. R. Effect of Estradiol on histone acetylation dynamics in human breast cancer cells. J.Biol.Chem., 2001.

171. Bertos, N. R., Wang, A. H., and Yang, X. J. Class II histone deacetylases: structure, function, and regulation. Biochem.Cell Biol., *79*: 243-252, 2001.

172. Lee, H. J., Chun, M., and Kandror, K. V. Tip60 and HDAC7 interact with the endothelin receptor α and may be involved in downstream signaling. J.Biol.Chem., *276*: 16597-16600, 2001.

173. Zhou, X., Marks, P. A., Rifkind, R. A., and Richon, V. M. Cloning and characterization of a histone deacetylase, HDAC9. Proc.Natl.Acad.Sci.U.S.A, *98*: 10572-10577, 2001.

174. Guardiola, A. R. and Yao, T. P. Molecular cloning and characterization of a novel histone deacetylase HDAC10. J.Biol.Chem., 2001.

175. Seigneurin-Berny, D., Verdel, A., Curtet, S., Lemercier, C., Garin, J., Rousseaux, S., and Khochbin, S. Identification of components of the murine histone deacetylase 6 complex: Link between acetylation and ubiquitination signaling pathways. Mol.Cell Biol., *21*: 8035-8044, 2001.

176. Kuo, M. H. and Allis, C. D. Roles of histone acetyltransferases and deacetylases in gene regulation. Bioessays, *20*: 615-626, 1998.

177. Davie, J. R. Histone Modifications. *In* S. H. Sanford and J. Zlatanova (eds.), Chromatin structure: State-of-the-art, Netherlands: Publisher Elsevier Science, 2003.

178. Allfrey, V. G. Control mechanisms in ribonucleic acid synthesis. Cancer Res., *26*: 2026-2040, 1966.

179. Nelson, D. A., Perry, M., Sealy, L., and Chalkley, R. DNAse I preferentially digests chromatin containing hyperacetylated histones. Biochem.Biophys.Res.Commun., *82*: 1346-1353, 1978.

180. Libertini, L. J., Ausio, J., van Holde, K. E., and Small, E. W. Histone hyperacetylation. Its effects on nucleosome core particle transitions. Biophys.J., *53*: 477-487, 1988.

181. Davie, J. R. and Candido, E. P. Acetylated histone H4 is preferentially associated with template-active chromatin. Proc.Natl.Acad.Sci.U.S.A, *75*: 3574-3577, 1978.

182. Nelson, D. A., Ferris, R. C., Zhang, D. E., and Ferenz, C. R. The beta-globin domain in immature chicken erythrocytes: enhanced solubility is coincident with histone hyperacetylation. Nucleic Acids Res., *14*: 1667-1682, 1986.

183. Alonso, W. R., Ferris, R. C., Zhang, D. E., and Nelson, D. A. Chicken erythrocyte beta-globin chromatin: enhanced solubility is a direct consequence of induced histone hyperacetylation. Nucleic Acids Res., *15*: 9325-9337, 1987.

184. Hendzel, M. J., Delcuve, G. P., and Davie, J. R. Histone deacetylase is a component of the internal nuclear matrix. J.Biol.Chem., *266*: 21936-21942, 1991.

185. Hendzel, M. J., Sun, J. M., Chen, H. Y., Rattner, J. B., and Davie, J. R. Histone acetyltransferase is associated with the nuclear matrix. J.Biol.Chem., *269*: 22894-22901, 1994.

186. Tang, L., Guo, B., Javed, A., Choi, J. Y., Hiebert, S., Lian, J. B., van Wijnen, A. J., Stein, J. L., Stein, G. S., and Zhou, G. W. Crystal structure of the nuclear matrix targeting signal of the transcription factor acute myelogenous leukemia-1/polyoma enhancer- binding protein 2alphaB/core binding factor alpha2. J.Biol Chem., *274*: 33580-33586, 1999.

187. McNeil, S., Guo, B., Stein, J. L., Lian, J. B., Bushmeyer, S., Seto, E., Atchison, M. L., Penman, S., van Wijnen, A. J., and Stein, G. S. Targeting of the YY1 transcription factor to the nucleolus and the nuclear matrix in situ: the C-terminus is a principal determinant for nuclear trafficking. J.Cell Biochem., *68*: 500-510, 1998.

188. Patturajan, M., Wei, X., Berezney, R., and Corden, J. L. A nuclear matrix protein interacts with the phosphorylated C-terminal domain of RNA polymerase II. Mol.Cell Biol, *18*: 2406-2415, 1998.

189. Jackson, D. A. and Cook, P. R. Transcriptionally active minichromosomes are attached transiently in nuclei through transcription units. J.Cell Sci., *105 ( Pt 4)*: 1143-1150, 1993.

190. Turner, B. M. Histone acetylation as an epigenetic determinant of long-term transcriptional competence. Cell Mol.Life Sci., *54*: 21-31, 1998.

191. Kruhlak, M. J., Hendzel, M. J., Fischle, W., Bertos, N. R., Hameed, S., Yang, X. J., Verdin, E., and Bazett-Jones, D. P. Regulation of global acetylation in mitosis through loss of histone acetyltransferases and deacetylases from chromatin. J.Biol.Chem., *276*: 38307-38319, 2001.

192. Turner, B. M. Histone acetylation and control of gene expression. J.Cell Sci., *99 ( Pt 1)*: 13-20, 1991.

193. Norton, V. G., Imai, B. S., Yau, P., and Bradbury, E. M. Histone acetylation reduces nucleosome core particle linking number change. Cell, *57*: 449-457, 1989.

194. Wang, X., Moore, S. C., Laszckzak, M., and Ausio, J. Acetylation increases the alpha-helical content of the histone tails of the nucleosome. J.Biol Chem., *275*: 35013-35020, 2000.

195. Turner, B. M. Histone acetylation and an epigenetic code. Bioessays, *22*: 836-845, 2000.

196. Turner, B. M., Birley, A. J., and Lavender, J. Histone H4 isoforms acetylated at specific lysine residues define individual chromosomes and chromatin domains in Drosophila polytene nuclei. Cell, *69*: 375-384, 1992.

197. De Rubertis, F., Kadosh, D., Henchoz, S., Pauli, D., Reuter, G., Struhl, K., and Spierer, P. The histone deacetylase RPD3 counteracts genomic silencing in Drosophila and yeast. Nature, *384*: 589-591, 1996.

198. Bannister, A. J., Miska, E. A., Gorlich, D., and Kouzarides, T. Acetylation of importin-alpha nuclear import factors by CBP/p300. Curr.Biol., *10*: 467-470, 2000.

199. Chen, H., Lin, R. J., Xie, W., Wilpitz, D., and Evans, R. M. Regulation of hormone-induced histone hyperacetylation and gene activation via acetylation of an acetylase. Cell, *98*: 675-686, 1999.

200. Imhof, A., Yang, X. J., Ogryzko, V. V., Nakatani, Y., Wolffe, A. P., and Ge, H. Acetylation of general transcription factors by histone acetyltransferases. Curr.Biol., *7*: 689-692, 1997.

201. Munshi, N., Merika, M., Yie, J., Senger, K., Chen, G., and Thanos, D. Acetylation of HMG I(Y) by CBP turns off IFN beta expression by disrupting the enhanceosome. Mol.Cell, *2*: 457-467, 1998.

202. Hasan, S., Stucki, M., Hassa, P. O., Imhof, R., Gehrig, P., Hunziker, P., Hubscher, U., and Hottiger, M. O. Regulation of human flap endonuclease-1 activity by acetylation through the transcriptional coactivator p300. Mol.Cell, *7*: 1221-1231, 2001.

203. Polesskaya, A., Duquet, A., Naguibneva, I., Weise, C., Vervisch, A., Bengal, E., Hucho, F., Robin, P., and Harel-Bellan, A. CREB-binding protein/p300 activates MyoD by acetylation. J.Biol.Chem., *275*: 34359-34364, 2000.

204. Herrera, J. E., Sakaguchi, K., Bergel, M., Trieschmann, L., Nakatani, Y., and Bustin, M. Specific acetylation of chromosomal protein HMG-17 by PCAF alters its interaction with nucleosomes. Mol.Cell Biol., *19*: 3466-3473, 1999.

205. Zhang, W. and Bieker, J. J. Acetylation and modulation of erythroid Kruppel-like factor (EKLF) activity by interaction with histone acetyltransferases. Proc.Natl.Acad.Sci.U.S.A, *95*: 9855-9860, 1998.

206. Hung, H. L., Lau, J., Kim, A. Y., Weiss, M. J., and Blobel, G. A. CREB-Binding protein acetylates hematopoietic transcription factor GATA- 1 at functionally important sites. Mol.Cell Biol., *19*: 3496-3505, 1999.

207. L'Hernault, S. W. and Rosenbaum, J. L. Chlamydomonas alpha-tubulin is posttranslationally modified by acetylation on the epsilon-amino group of a lysine. Biochemistry, *24*: 473-478, 1985.

208. Martinez-Balbas, M. A., Bauer, U. M., Nielsen, S. J., Brehm, A., and Kouzarides, T. Regulation of E2F1 activity by acetylation. EMBO J., *19*: 662-671, 2000.

209. Gu, W. and Roeder, R. G. Activation of p53 sequence-specific DNA binding by acetylation of the p53 C-terminal domain. Cell, *90*: 595-606, 1997.

210. Parekh, B. S. and Maniatis, T. Virus infection leads to localized hyperacetylation of histones H3 and H4 at the IFN-beta promoter. Mol.Cell, *3*: 125-129, 1999.

211. Tse, C., Sera, T., Wolffe, A. P., and Hansen, J. C. Disruption of higher-order folding by core histone acetylation dramatically enhances transcription of nucleosomal arrays by RNA polymerase III. Mol.Cell Biol., *18*: 4629-4638, 1998.

212. Garcia-Ramirez, M., Rocchini, C., and Ausio, J. Modulation of chromatin folding by histone acetylation. J.Biol.Chem., *270*: 17923-17928, 1995.

213. Wang, X., He, C., Moore, S. C., and Ausio, J. Effects of histone acetylation on the solubility and folding of the chromatin fiber. J.Biol.Chem., *276*: 12764-12768, 2001.

214. Chadee, D. N., Allis, C. D., Wright, J. A., and Davie, J. R. Histone H1b phosphorylation is dependent upon ongoing transcription and replication in normal and ras-transformed mouse fibroblasts. J.Biol Chem., *272*: 8113-8116, 1997.

215. Holth, L. T., Chadee, D. N., Spencer, V. A., Samuel, S. K., Safneck, J. R., and Davie, J. R. Chromatin, nuclear matrix and the cytoskeleton: role of cell structure in neoplastic transformation. Int.J.Oncol., *13*: 827-837, 1998.

216. Chadee, D. N., Peltier, C. P., and Davie, J. R. Histone H1(S)-3 phosphorylation in Ha-*ras* oncogene-transformed mouse fibroblasts. Oncogene, *21*: 8397-8403, 2002.

217. Bhattacharjee, R. N., Banks, G. C., Trotter, K. W., Lee, H. L., and Archer, T. K. Histone H1 phosphorylation by Cdk2 selectively modulates mouse mammary tumor virus transcription through chromatin remodeling. Mol Cell Biol, *21*: 5417-5425, 2001.

218. Covault, J. and Chalkley, R. The identification of distinct populations of acetylated histone. J.Biol.Chem., *255*: 9110-9116, 1980.

219. Zhang, D. E. and Nelson, D. A. Histone acetylation in chicken erythrocytes. Rates of deacetylation in immature and mature red blood cells. Biochem.J., *250*: 241-245, 1988.

220. Zhang, D. E. and Nelson, D. A. Histone acetylation in chicken erythrocytes. Rates of acetylation and evidence that histones in both active and potentially active chromatin are rapidly modified. Biochem.J., *250*: 233-240, 1988.

221. Hebbes, T. R., Thorne, A. W., and Crane-Robinson, C. A direct link between core histone acetylation and transcriptionally active chromatin. EMBO J., *7*: 1395-1402, 1988.

222. Weinmann, A. S. and Farnham, P. J. Identification of unknown target genes of human transcription factors using chromatin immunoprecipitation. Methods, *26*: 37-47, 2002.

223. Spencer, V. A., Sun.J.M., Li, L., and Davie, J. R. Chromatin immunoprecipitation: a tool for studying histone acetylation and transcription factor binding. Methods., *in press*: 2003.

224. Steger, D. J., Eberharter, A., John, S., Grant, P. A., and Workman, J. L. Purified histone acetyltransferase complexes stimulate HIV-1 transcription from preassembled nucleosomal arrays. Proc.Natl.Acad.Sci.U.S.A, *95*: 12924-12929, 1998.

225. Lichter, P., Cremer, T., Borden, J., Manuelidis, L., and Ward, D. C. Delineation of individual human chromosomes in metaphase and interphase cells by in situ suppression hybridization using recombinant DNA libraries. Hum.Genet., *80*: 224-234, 1988.

226. Zink, D., Cremer, T., Saffrich, R., Fischer, R., Trendelenburg, M. F., Ansorge, W., and Stelzer, E. H. Structure and dynamics of human interphase chromosome territories *in vivo*. Hum.Genet., *102*: 241-251, 1998.

227. Eils, R., Dietzel, S., Bertin, E., Schrock, E., Speicher, M. R., Ried, T., Robert-Nicoud, M., Cremer, C., and Cremer, T. Three-dimensional reconstruction of painted

human interphase chromosomes: active and inactive X chromosome territories have similar volumes but differ in shape and surface structure. J.Cell Biol, *135*: 1427-1440, 1996.

228. Manuelidis, L. Individual interphase chromosome domains revealed by in situ hybridization. Hum.Genet., *71*: 288-293, 1985.

229. Hendzel, M. J., Kruhlak, M. J., and Bazett-Jones, D. P. Organization of highly acetylated chromatin around sites of heterogeneous nuclear RNA accumulation. Mol Biol Cell, *9*: 2491-2507, 1998.

230. Smith, K. P., Moen, P. T., Wydner, K. L., Coleman, J. R., and Lawrence, J. B. Processing of endogenous pre-mRNAs in association with SC-35 domains is gene specific. J.Cell Biol, *144*: 617-629, 1999.

231. Pombo, A. and Cook, P. R. The localization of sites containing nascent RNA and splicing factors. Exp.Cell Res., *229*: 201-203, 1996.

232. Matera, A. G. Nuclear bodies: multifaceted subdomains of the interchromatin space. Trends Cell Biol, *9*: 302-309, 1999.

233. Downes, M., Ordentlich, P., Kao, H. Y., Alvarez, J. G., and Evans, R. M. Identification of a nuclear domain with deacetylase activity. Proc.Natl.Acad.Sci.U.S.A, *97*: 10330-10335, 2000.

234. Mortillaro, M. J., Blencowe, B. J., Wei, X., Nakayasu, H., Du, L., Warren, S. L., Sharp, P. A., and Berezney, R. A hyperphosphorylated form of the large subunit of

RNA polymerase II is associated with splicing complexes and the nuclear matrix. Proc.Natl.Acad.Sci.U.S.A, *93*: 8253-8257, 1996.

235. Delcuve, G. P. and Davie, J. R. Chromatin structure of erythroid-specific genes of immature and mature chicken erythrocytes. Biochem.J., *263*: 179-186, 1989.

236. Jackson, D. A. and Cook, P. R. Transcription occurs at a nucleoskeleton. EMBO J., *4*: 919-925, 1985.

237. Hentzen, P. C., Rho, J. H., and Bekhor, I. Nuclear matrix DNA from chicken erythrocytes contains beta-globin gene sequences. Proc.Natl.Acad.Sci.U.S.A, *81*: 304-307, 1984.

238. Thorburn, A., Moore, R., and Knowland, J. Attachment of transcriptionally active DNA sequences to the nucleoskeleton under isotonic conditions. Nucleic Acids Res., *16*: 7183, 1988.

239. Pombo, A., Jones, E., Iborra, F. J., Kimura, H., Sugaya, K., Cook, P. R., and Jackson, D. A. Specialized transcription factories within mammalian nuclei. Crit Rev.Eukaryot.Gene Expr., *10*: 21-29, 2000.

240. Stenoien, D. L., Mancini, M. G., Patel, K., Allegretto, E. A., Smith, C. L., and Mancini, M. A. Subnuclear trafficking of estrogen receptor-alpha and steroid receptor coactivator-1. Mol.Endocrinol., *14*: 518-534, 2000.

241. Stenoien, D. L., Patel, K., Mancini, M. G., Dutertre, M., Smith, C. L., O'Malley, B. W., and Mancini, M. A. FRAP reveals that mobility of oestrogen receptor-alpha is li. Nat.Cell Biol., *3*: 15-23, 2001.

242. Samuel, S. K., Minish, T. M., and Davie, J. R. Altered nuclear matrix protein profiles in oncogene-transformed mouse fibroblasts exhibiting high metastatic potential. Cancer Res., *57*: 147-151, 1997.

243. Ikeda, K., Steger, D. J., Eberharter, A., and Workman, J. L. Activation domain-specific and general transcription stimulation by native histone acetyltransferase complexes. Mol Cell Biol, *19*: 855-863, 1999.

244. Kristjuhan, A., Walker, J., Suka, N., Grunstein, M., Roberts, D., Cairns, B. R., and Svejstrup, J. Q. Transcriptional inhibition of genes with severe histone h3 hypoacetylation in the coding region. Mol.Cell, *10*: 925-933, 2002.

245. Burakov, D., Crofts, L. A., Chang, C. P., and Freedman, L. P. Reciprocal recruitment of DRIP/mediator and p160 coactivator complexes *in vivo* by estrogen receptor. J.Biol Chem., *277*: 14359-14362, 2002.

246. Madisen, L., Krumm, A., Hebbes, T. R., and Groudine, M. The immunoglobulin heavy chain locus control region increases histone acetylation along linked c-*myc* genes. Mol.Cell Biol., *18*: 6281-6292, 1998.

247. Kadosh, D. and Struhl, K. Targeted recruitment of the Sin3-Rpd3 histone deacetylase complex generates a highly localized domain of repressed chromatin *in vivo*. Mol.Cell Biol., *18*: 5121-5127, 1998.

248. Krebs, J. E., Kuo, M. H., Allis, C. D., and Peterson, C. L. Cell cycle-regulated histone acetylation required for expression of the yeast HO gene. Genes Dev., *13*: 1412-1421, 1999.

249. Myers, F. A., Evans, D. R., Clayton, A. L., Thorne, A. W., and Crane-Robinson, C. Targeted and extended acetylation of histones H4 and H3 at active and inactive genes in chicken embryo erythrocytes. J.Biol.Chem., *276*: 20197-20205, 2001.

250. Crane-Robinson, C., Myers, F. A., Hebbes, T. R., Clayton, A. L., and Thorne, A. W. Chromatin immunoprecipitation assays in acetylation mapping of higher eukaryotes. Methods Enzymol., *304*: 533-547, 1999.

251. Cervoni, N. and Szyf, M. Demethylase activity is directed by histone acetylation. J.Biol.Chem., *276*: 40778-40787, 2001.

252. Fahrner, J. A., Eguchi, S., Herman, J. G., and Baylin, S. B. Dependence of histone modifications and gene expression on DNA hypermethylation in cancer. Cancer Res., *62*: 7213-7218, 2002.

253. Cameron, E. E., Bachman, K. E., Myohanen, S., Herman, J. G., and Baylin, S. B. Synergy of demethylation and histone deacetylase inhibition in the re- expression of genes silenced in cancer. Nat.Genet., *21*: 103-107, 1999.

254. Rountree, M. R., Bachman, K. E., Herman, J. G., and Baylin, S. B. DNA methylation, chromatin inheritance, and cancer. Oncogene, *20*: 3156-3165, 2001.

255. Macleod, D., Charlton, J., Mullins, J., and Bird, A. P. Sp1 sites in the mouse aprt gene promoter are required to prevent methylation of the CpG island. Genes Dev., *8*: 2282-2292, 1994.

256. Sanchez, R., Nguyen, D., Rocha, W., White, J. H., and Mader, S. Diversity in the mechanisms of gene regulation by estrogen receptors. Bioessays, *24*: 244-254, 2002.

257. Hart, L. L. and Davie, J. R. The estrogen receptor: more than the average transcription factor. Biochem.Cell Biol, *80*: 335-341, 2002.

258. Stenoien, D. L., Nye, A. C., Mancini, M. G., Patel, K., Dutertre, M., O'Malley, B. W., Smith, C. L., Belmont, A. S., and Mancini, M. A. Ligand-mediated assembly and real-time cellular dynamics of estrogen receptor alpha-coactivator complexes in living cells. Mol.Cell Biol., *21*: 4404-4412, 2001.

259. Gregory, P. D., Schmid, A., Zavari, M., Munsterkotter, M., and Horz, W. Chromatin remodelling at the PHO8 promoter requires SWI-SNF and SAGA at a step subsequent to activator binding. EMBO J., *18*: 6407-6414, 1999.

260. Singh, H., Sekinger, E. A., and Gross, D. S. Chromatin and cancer: causes and consequences. J.Cell Biochem., *Suppl 35*: 61-68, 2000.

261. Cosma, M. P., Tanaka, T., and Nasmyth, K. Ordered recruitment of transcription and chromatin remodeling factors to a cell cycle- and developmentally regulated promoter. Cell, *97*: 299-311, 1999.

262. Kingston, R. E. and Narlikar, G. J. ATP-dependent remodeling and acetylation as regulators of chromatin fluidity. Genes Dev., *13*: 2339-2352, 1999.

263. Agalioti, T., Lomvardas, S., Parekh, B., Yie, J., Maniatis, T., and Thanos, D. Ordered recruitment of chromatin modifying and general transcription factors to the IFN-beta promoter. Cell, *103*: 667-678, 2000.

264. Cairns, B. R., Schlichter, A., Erdjument-Bromage, H., Tempst, P., Kornberg, R. D., and Winston, F. Two functionally distinct forms of the RSC nucleosome-remodeling complex, containing essential AT hook, BAH, and bromodomains. Mol.Cell, *4*: 715-723, 1999.

265. Winston, F. and Allis, C. D. The bromodomain: a chromatin-targeting module? Nat.Struct.Biol., *6*: 601-604, 1999.

266. Hassan, A. H., Prochasson, P., Neely, K. E., Galasinski, S. C., Chandy, M., Carrozza, M. J., and Workman, J. L. Function and selectivity of bromodomains in anchoring chromatin- modifying complexes to promoter nucleosomes. Cell, *111*: 369-379, 2002.

267. Hassan, A. H., Neely, K. E., and Workman, J. L. Histone acetyltransferase complexes stabilize swi/snf binding to promoter nucleosomes. Cell, *104*: 817-827, 2001.

268. Barbaric, S., Walker, J., Schmid, A., Svejstrup, J. Q., and Horz, W. Increasing the rate of chromatin remodeling and gene activation--a novel role for the histone acetyltransferase Gcn5. EMBO J., *20*: 4944-4951, 2001.

269. Orphanides, G. and Reinberg, D. RNA polymerase II elongation through chromatin. Nature, *407*: 471-475, 2000.

270. Spotswood, H. T. and Turner, B. M. An increasingly complex code. J. Clin.Invest, *110*: 577-582, 2002.

271. Vandel, L. and Trouche, D. Physical association between the histone acetyl transferase CBP and a histone methyl transferase. EMBO Rep., *2*: 21-26, 2001.

272. Smith, E. R., Allis, C. D., and Lucchesi, J. C. Linking global histone acetylation to the transcription enhancement of X-chromosomal genes in Drosophila males. J.Biol.Chem., *276*: 31483-31486, 2001.

273. Braunstein, M., Sobel, R. E., Allis, C. D., Turner, B. M., and Broach, J. R. Efficient transcriptional silencing in *Saccharomyces cerevisiae* requires a heterochromatin histone acetylation pattern. Mol.Cell Biol., *16*: 4349-4356, 1996.

274. Wittschieben, B. O., Fellows, J., Du, W., Stillman, D. J., and Svejstrup, J. Q. Overlapping roles for the histone acetyltransferase activities of SAGA and elongator *in vivo*. EMBO J., *19*: 3060-3068, 2000.

275. Svejstrup, J. Q. Chromatin elongation factors. Curr.Opin.Genet.Dev., *12*: 156-161, 2002.

276. Otero, G., Fellows, J., Li, Y., de Bizemont, T., Dirac, A. M., Gustafsson, C. M., Erdjument-Bromage, H., Tempst, P., and Svejstrup, J. Q. Elongator, a multisubunit

component of a novel RNA polymerase II holoenzyme for transcriptional elongation. Mol Cell, *3*: 109-118, 1999.

277. Chen-Cleland, T. A., Boffa, L. C., Carpaneto, E. M., Mariani, M. R., Valentin, E., Mendez, E., and Allfrey, V. G. Recovery of transcriptionally active chromatin restriction fragments by binding to organomercurial-agarose magnetic beads. A rapid and sensitive method for monitoring changes in higher order chromatin structure during gene activation and repression. J.Biol Chem., *268*: 23409-23416, 1993.

278. Boffa, L. C., Walker, J., Chen, T. A., Sterner, R., Mariani, M. R., and Allfrey, V. G. Factors affecting nucleosome structure in transcriptionally active chromatin. Histone acetylation, nascent RNA and inhibitors of RNA synthesis. Eur.J.Biochem., *194*: 811-823, 1990.

279. Charpentier, A. H., Bednarek, A. K., Daniel, R. L., Hawkins, K. A., Laflin, K. J., Gaddis, S., MacLeod, M. C., and Aldaz, C. M. Effects of estrogen on global gene expression: identification of novel targets of estrogen action. Cancer Res., *60*: 5977-5983, 2000.

280. Gasaryan, K. G. Genome activity and gene expression in avian erythroid cells. Int.Rev.Cytol., *74*: 95-126, 1982.

281. Brosch, G., Georgieva, E. I., Lopez-Rodas, G., Lindner, H., and Loidl, P. Specificity of Zea mays histone deacetylase is regulated by phosphorylation. J.Biol.Chem., *267*: 20561-20564, 1992.

282. Villeponteau, B., Landes, G. M., Pankratz, M. J., and Martinson, H. G. The chicken beta globin gene region. Delineation of transcription units and developmental regulation of interspersed DNA repeats. J.Biol.Chem., *257*: 11015-11023, 1982.

283. Bruns, G. A. and Ingram, V. M. The erythroid cells and haemoglobins of the chick embryo. Philos.Trans.R.Soc.Lond B Biol.Sci., *266*: 225-305, 1973.

284. Landes, G. M., Villeponteau, B., Pribyl, T. M., and Martinson, H. G. Hemoglobin switching in chickens. Is the switch initiated post- transcriptionally? J. Biol.Chem., *257*: 11008-11014, 1982.

285. Chapman, B. S. and Tobin, A. J. Distribution of developmentally regulated hemoglobins in embryonic erythroid populations. Dev.Biol., *69*: 375-387, 1979.

286. Itano, H. A., Hirota, K., and Hosokawa, K. Mechanism of induction of haemolytic anaemia by phenylhydrazine. Nature, *256*: 665-667, 1975.

287. Jain, S. K. and Subrahmanyam, D. On the mechanism of phenylhydrazine-induced hemolytic anemia. Biochem.Biophys.Res.Commun., *82*: 1320-1324, 1978.

288. Fenrick, R. and Hiebert, S. W. Role of histone deacetylases in acute leukemia. J.Cell Biochem.Suppl, *30-31*: 194-202, 1998.

289. Chen, J. D. and Evans, R. M. A transcriptional co-repressor that interacts with nuclear hormone receptors. Nature, *377*: 454-457, 1995.

290. Kurokawa, R., Soderstrom, M., Horlein, A., Halachmi, S., Brown, M., Rosenfeld, M. G., and Glass, C. K. Polarity-specific activities of retinoic acid receptors determined by a co-repressor. Nature, *377*: 451-454, 1995.

291. Glass, C. K., Rosenfeld, M. G., Rose, D. W., Kurokawa, R., Kamei, Y., Xu, L., Torchia, J., Ogliastro, M. H., and Westin, S. Mechanisms of transcriptional activation by retinoic acid receptors. Biochem.Soc.Trans., *25*: 602-605, 1997.

292. Wade, P. A., Pruss, D., and Wolffe, A. P. Histone acetylation: chromatin in action. Trends Biochem.Sci., *22*: 128-132, 1997.

293. Struhl, K. Histone acetylation and transcriptional regulatory mechanisms. Genes Dev., *12*: 599-606, 1998.

294. Kalantry, S., Delva, L., Gaboli, M., Gandini, D., Giorgio, M., Hawe, N., He, L. Z., Peruzzi, D., Rivi, R., Tribioli, C., Wang, Z. G., Zhang, H., and Pandolfi, P. P. Gene rearrangements in the molecular pathogenesis of acute promyelocytic leukemia. J.Cell Physiol, *173*: 288-296, 1997.

295. He, L. Z., Guidez, F., Tribioli, C., Peruzzi, D., Ruthardt, M., Zelent, A., and Pandolfi, P. P. Distinct interactions of PML-RARalpha and PLZF-RARalpha with co-repressors determine differential responses to RA in APL. Nat.Genet., *18*: 126-135, 1998.

296. Grimwade, D. and Solomon, E. Characterisation of the PML/RAR alpha rearrangement associated with t(15;17) acute promyelocytic leukaemia. Curr.Top.Microbiol.Immunol., *220*: 81-112, 1997.

297. Barna, M., Hawe, N., Niswander, L., and Pandolfi, P. P. Plzf regulates limb and axial skeletal patterning. Nat.Genet., *25*: 166-172, 2000.

298. Luo, R. X., Postigo, A. A., and Dean, D. C. Rb interacts with histone deacetylase to repress transcription. Cell, *92*: 463-473, 1998.

299. Brehm, A., Miska, E. A., McCance, D. J., Reid, J. L., Bannister, A. J., and Kouzarides, T. Retinoblastoma protein recruits histone deacetylase to repress transcription. Nature, *391*: 597-601, 1998.

300. Mazumdar, A., Wang, R. A., Mishra, S. K., Adam, L., Bagheri-Yarmand, R., Mandal, M., Vadlamudi, R. K., and Kumar, R. Transcriptional repression of oestrogen receptor by metastasis- associated protein 1 corepressor. Nat.Cell Biol., *3*: 30-37, 2001.

301. Klochendler-Yeivin, A. and Yaniv, M. Chromatin modifiers and tumor suppression. Biochim.Biophys.Acta, *1551*: M1-10, 2001.

302. Oike, Y., Takakura, N., Hata, A., Kaname, T., Akizuki, M., Yamaguchi, Y., Yasue, H., Araki, K., Yamamura, K., and Suda, T. Mice homozygous for a truncated form of CREB-binding protein exhibit defects in hematopoiesis and vasculo-angiogenesis. Blood, *93*: 2771-2779, 1999.

303. Kung, A. L., Rebel, V. I., Bronson, R. T., Ch'ng, L. E., Sieff, C. A., Livingston, D. M., and Yao, T. P. Gene dose-dependent control of hematopoiesis and hematologic tumor suppression by CBP. Genes Dev., *14*: 272-277, 2000.

304. Yao, T. P., Oh, S. P., Fuchs, M., Zhou, N. D., Ch'ng, L. E., Newsome, D., Bronson, R. T., Li, E., Livingston, D. M., and Eckner, R. Gene dosage-dependent embryonic development and proliferation defects in mice lacking the transcriptional integrator p300. Cell, *93*: 361-372, 1998.

305. Kurebayashi, J., Otsuki, T., Kunisue, H., Tanaka, K., Yamamoto, S., and Sonoo, H. Expression levels of estrogen receptor-alpha, estrogen receptor-beta, coactivators, and corepressors in breast cancer. Clin.Cancer Res., *6*: 512-518, 2000.

306. List, H. J., Reiter, R., Singh, B., Wellstein, A., and Riegel, A. T. Expression of the nuclear coactivator AIB1 in normal and malignant breast tissue. Breast Cancer Res.Treat., *68*: 21-28, 2001.

307. Murphy, L. C., Simon, S. L., Parkes, A., Leygue, E., Dotzlaw, H., Snell, L., Troup, S., Adeyinka, A., and Watson, P. H. Altered expression of estrogen receptor coregulators during human breast tumorigenesis. Cancer Res., *60*: 6266-6271, 2000.

308. Vadlamudi, R. K., Wang, R. A., Mazumdar, A., Kim, Y., Shin, J., Sahin, A., and Kumar, R. Molecular cloning and characterization of PELP1, a novel human coregulator of estrogen receptor alpha. J.Biol.Chem., *276*: 38272-38279, 2001.

309. Steffan, J. S., Bodai, L., Pallos, J., Poelman, M., McCampbell, A., Apostol, B. L., Kazantsev, A., Schmidt, E., Zhu, Y. Z., Greenwald, M., Kurokawa, R., Housman, D. E., Jackson, G. R., Marsh, J. L., and Thompson, L. M. Histone deacetylase inhibitors arrest polyglutamine-dependent neurodegeneration in Drosophila. Nature, *413*: 739-743, 2001.

310. Boffa, L. C., Vidali, G., Mann, R. S., and Allfrey, V. G. Suppression of histone deacetylation *in vivo* and *in vitro* by sodium butyrate. J.Biol.Chem., *253*: 3364-3366, 1978.

311. Marks, P. A., Richon, V. M., and Rifkind, R. A. Histone deacetylase inhibitors: inducers of differentiation or apoptosis of transformed cells. J.Natl.Cancer Inst., *92*: 1210-1216, 2000.

312. Marks, P. A., Richon, V. M., Breslow, R., and Rifkind, R. A. Histone deacetylase inhibitors as new cancer drugs. Curr.Opin.Oncol., *13*: 477-483, 2001.

313. Barlow, A. L., van Drunen, C. M., Johnson, C. A., Tweedie, S., Bird, A., and Turner, B. M. dSIR2 and dHDAC6: Two novel, inhibitor-resistant deacetylases in Drosophila melanogaster. Exp.Cell Res., *265*: 90-103, 2001.

314. Emiliani, S., Fischle, W., Van Lint, C., Al Abed, Y., and Verdin, E. Characterization of a human RPD3 ortholog, HDAC3. Proc.Natl.Acad.Sci.U.S.A, *95*: 2795-2800, 1998.

315. Della, R. F., Criniti, V., Della, P., V, Borriello, A., Oliva, A., Indaco, S., Yamamoto, T., and Zappia, V. Genes modulated by histone acetylation as new effectors of butyrate activity. FEBS Lett., *499*: 199-204, 2001.

316. Lavelle, D., Chen, Y. H., Hankewych, M., and DeSimone, J. Histone deacetylase inhibitors increase p21(WAF1) and induce apoptosis of human myeloma cell lines independent of decreased IL-6 receptor expression. Am.J.Hematol., *68*: 170-178, 2001.

317. Yamamoto, H., Fujimoto, J., Okamoto, E., Furuyama, J., Tamaoki, T., and Hashimoto-Tamaoki, T. Suppression of growth of hepatocellular carcinoma by sodium butyrate *in vitro* and *in vivo*. Int.J.Cancer, *76*: 897-902, 1998.

318. Huang, H., Reed, C. P., Zhang, J. S., Shridhar, V., Wang, L., and Smith, D. I. Carboxypeptidase A3 (CPA3): a novel gene highly induced by histone deacetylase inhibitors during differentiation of prostate epithelial cancer cells. Cancer Res., *59*: 2981-2988, 1999.

319. Lallemand, F., Courilleau, D., Buquet-Fagot, C., Atfi, A., Montagne, M. N., and Mester, J. Sodium butyrate induces G2 arrest in the human breast cancer cells MDA-MB-231 and renders them competent for DNA rereplication. Exp.Cell Res., *247*: 432-440, 1999.

320. Saunders, N., Dicker, A., Popa, C., Jones, S., and Dahler, A. Histone deacetylase inhibitors as potential anti-skin cancer agents. Cancer Res., *59*: 399-404, 1999.

321. Yoshida, M., Kijima, M., Akita, M., and Beppu, T. Potent and specific inhibition of mammalian histone deacetylase both *in vivo* and *in vitro* by trichostatin A. J.Biol.Chem., *265*: 17174-17179, 1990.

322. Yoshida, M., Horinouchi, S., and Beppu, T. Trichostatin A and trapoxin: novel chemical probes for the role of histone acetylation in chromatin structure and function. Bioessays, *17*: 423-430, 1995.

323. van Engelhardt, W. Absorption of short-chain fatty acids from the large intestine. *In* J. H. Cummings, R. L. Rombeau, and S. Takashi (eds.), Physiological and clinical

aspects of short-chain fatty acids, pp. 149-170. Cambridge,UK.: Cambridge University Press, 1995.

324. Sowa, Y. and Sakai, T. Butyrate as a model for "gene-regulating chemoprevention and chemotherapy". Biofactors, *12*: 283-287, 2000.

325. Emenaker, N. J. and Basson, M. D. Short chain fatty acids differentially modulate cellular phenotype and c-*myc* protein levels in primary human nonmalignant and malignant colonocytes. Dig.Dis.Sci., *46*: 96-105, 2001.

326. Conley, B. A., Egorin, M. J., Tait, N., Rosen, D. M., Sausville, E. A., Dover, G., Fram, R. J., and Van Echo, D. A. Phase I study of the orally administered butyrate prodrug, tributyrin, in patients with solid tumors. Clin.Cancer Res., *4*: 629-634, 1998.

327. Staiano-Coico, L., Khandke, L., Krane, J. F., Sharif, S., Gottlieb, A. B., Krueger, J. G., Heim, L., Rigas, B., and Higgins, P. J. TGF-alpha and TGF-beta expression during sodium-N-butyrate-induced differentiation of human keratinocytes: evidence for subpopulation- specific up-regulation of TGF-beta mRNA in suprabasal cells. Exp.Cell Res., *191*: 286-291, 1990.

328. Hague, A., Manning, A. M., Hanlon, K. A., Huschtscha, L. I., Hart, D., and Paraskeva, C. Sodium butyrate induces apoptosis in human colonic tumour cell lines in a p53-independent pathway: implications for the possible role of dietary fibre in the prevention of large-bowel cancer. Int.J.Cancer, *55*: 498-505, 1993.

329. Schwartz, B., Avivi-Green, C., and Polak-Charcon, S. Sodium butyrate induces retinoblastoma protein dephosphorylation, p16 expression and growth arrest of colon cancer cells. Mol.Cell Biochem., *188*: 21-30, 1998.

330. Graham, K. A. and Buick, R. N. Sodium butyrate induces differentiation in breast cancer cell lines expressing the estrogen receptor. J.Cell Physiol, *136*: 63-71, 1988.

331. Van Lint, C., Emiliani, S., and Verdin, E. The expression of a small fraction of cellular genes is changed in response to histone hyperacetylation. Gene Expr., *5*: 245-253, 1996.

332. Yoshida, M. and Beppu, T. Reversible arrest of proliferation of rat 3Y1 fibroblasts in both the G1 and G2 phases by trichostatin A. Exp.Cell Res., *177*: 122-131, 1988.

333. Allfrey, V. G. Histone and nucleohistones.London: Plenum Publishing Corp., 1970.

334. Grunstein, M. Histone acetylation in chromatin structure and transcription. Nature, *389*: 349-352, 1997.

335. Girardot, V., Rabilloud, T., Yoshida, M., Beppu, T., Lawrence, J. J., and Khochbin, S. Relationship between core histone acetylation and histone H1(0) gene activity. Eur.J.Biochem., *224*: 885-892, 1994.

336. Archer, S. Y., Meng, S., Shei, A., and Hodin, R. A. p21(WAF1) is required for butyrate-mediated growth inhibition of human colon cancer cells. Proc.Natl.Acad.Sci.U.S.A, *95*: 6791-6796, 1998.

337. Van Lint, C., Emiliani, S., Ott, M., and Verdin, E. Transcriptional activation and chromatin remodeling of the HIV-1 promoter in response to histone acetylation. EMBO J., *15*: 1112-1120, 1996.

338. Cuisset, L., Tichonicky, L., Jaffray, P., and Delpech, M. The effects of sodium butyrate on transcription are mediated through activation of a protein phosphatase. J.Biol.Chem., *272*: 24148-24153, 1997.

339. Cuisset, L., Tichonicky, L., and Delpech, M. A protein phosphatase is involved in the inhibition of histone deacetylation by sodium butyrate. Biochem.Biophys.Res.Commun., *246*: 760-764, 1998.

340. Cai, R., Kwon, P., Yan-Neale, Y., Sambuccetti, L., Fischer, D., and Cohen, D. Mammalian histone deacetylase 1 protein is posttranslationally modified by phosphorylation. Biochem.Biophys.Res.Commun., *283*: 445-453, 2001.

341. Tsai, S. C. and Seto, E. Regulation of histone deacetylase 2 by protein kinase CK2. J.Biol Chem., *277*: 31826-31833, 2002.

342. Pflum, M. K., Tong, J. K., Lane, W. S., and Schreiber, S. L. Histone deacetylase 1 phosphorylation promotes enzymatic activity and complex formation. J.Biol Chem., *276*: 47733-47741, 2001.

343. Galasinski, S. C., Resing, K. A., Goodrich, J. A., and Ahn, N. G. Phosphatase inhibition leads to histone deacetylases 1 and 2 phosphorylation and disruption of corepressor interactions. J.Biol.Chem., *277*: 19618-19626, 2002.

344. Sauve, D. M., Anderson, H. J., Ray, J. M., James, W. M., and Roberge, M. Phosphorylation-induced rearrangement of the histone H3 $NH_2$-terminal domain during mitotic chromosome condensation. J.Cell Biol, *145*: 225-235, 1999.

345. deFazio, A., Chiew, Y. E., Donoghue, C., Lee, C. S., and Sutherland, R. L. Effect of sodium butyrate on estrogen receptor and epidermal growth factor receptor gene expression in human breast cancer cell lines. J.Biol Chem., *267*: 18008-18012, 1992.

346. Stevens, M. S., Aliabadi, Z., and Moore, M. R. Associated effects of sodium butyrate on histone acetylation and estrogen receptor in the human breast cancer cell line MCF-7. Biochem.Biophys.Res.Commun., *119*: 132-138, 1984.

347. Tsubaki, J., Hwa, V., Twigg, S. M., and Rosenfeld, R. G. Differential activation of the IGF binding protein-3 promoter by butyrate in prostate cancer cells. Endocrinology, *143*: 1778-1788, 2002.

348. Choi, H. S., Lee, J. H., Park, J. G., and Lee, Y. I. Trichostatin A, a histone deacetylase inhibitor, activates the IGFBP-3 promoter by upregulating Sp1 activity in hepatoma cells: alteration of the Sp1/Sp3/HDAC1 multiprotein complex. Biochem.Biophys.Res.Commun., *296*: 1005-1012, 2002.

349. Rivero, J. A. and Adunyah, S. E. Sodium butyrate induces tyrosine phosphorylation and activation of MAP kinase (ERK-1) in human K562 cells. Biochem.Biophys.Res.Commun., *224*: 796-801, 1996.

350. Rickard, K. L., Gibson, P. R., Young, G. P., and Phillips, W. A. Activation of protein kinase C augments butyrate-induced differentiation and turnover in human colonic epithelial cells *in vitro*. Carcinogenesis, *20*: 977-984, 1999.

351. Tran, C. P., Familari, M., Parker, L. M., Whitehead, R. H., and Giraud, A. S. Short-chain fatty acids inhibit intestinal trefoil factor gene expression in colon cancer cells. Am.J.Physiol, *275*: G85-G94, 1998.

352. Han, J. W., Ahn, S. H., Kim, Y. K., Bae, G. U., Yoon, J. W., Hong, S., Lee, H. Y., Lee, Y. W., and Lee, H. W. Activation of p21(WAF1/Cip1) transcription through Sp1 sites by histone deacetylase inhibitor apicidin: involvement of protein kinase C. J.Biol.Chem., *276*: 42084-42090, 2001.

353. Sun, J. M., Chen, H. Y., Moniwa, M., Litchfield, D. W., Seto, E., and Davie, J. R. The transcriptional repressor Sp3 is associated with CK2-phosphorylated histone deacetylase 2. J.Biol Chem., *277*: 35783-35786, 2002.

354. Kim, M. S., Son, M. W., Kim, W. B., In, P. Y., and Moon, A. Apicidin, an inhibitor of histone deacetylase, prevents H-*ras*-induced invasive phenotype. Cancer Lett., *157*: 23-30, 2000.

355. Gill, R. K. and Christakos, S. Identification of sequence elements in mouse calbindin-D28k gene that confer 1,25-dihydroxyvitamin D3- and butyrate-inducible responses. Proc.Natl.Acad.Sci.U.S.A, *90*: 2984-2988, 1993.

356. Bohan, C. A., Robinson, R. A., Luciw, P. A., and Srinivasan, A. Mutational analysis of sodium butyrate inducible elements in the human immunodeficiency virus type I long terminal repeat. Virology, *172*: 573-583, 1989.

357. Walker, G. E., Wilson, E. M., Powell, D., and Oh, Y. Butyrate, a histone deacetylase inhibitor, activates the human IGF binding protein-3 promoter in breast cancer cells: molecular mechanism involves an Sp1/Sp3 multiprotein complex. Endocrinology, *142*: 3817-3827, 2001.

358. Doetzlhofer, A., Rotheneder, H., Lagger, G., Koranda, M., Kurtev, V., Brosch, G., Wintersberger, E., and Seiser, C. Histone deacetylase 1 can repress transcription by binding to Sp1. Mol.Cell Biol., *19*: 5504-5511, 1999.

359. Bai, L. and Merchant, J. L. Transcription factor ZBP-89 cooperates with histone acetyltransferase p300 during butyrate activation of p21wafl transcription in human cells. J.Biol.Chem., *275*: 30725-30733, 2000.

360. Chopin, V., Toillon, R. A., Jouy, N., and Le, B., X Sodium butyrate induces P53-independent, Fas-mediated apoptosis in MCF- 7 human breast cancer cells. Br.J.Pharmacol., *135*: 79-86, 2002.

361. Kennedy, C., Byth, K., Clarke, C. L., and deFazio, A. Cell proliferation in the normal mouse mammary gland and inhibition by phenylbutyrate. Mol.Cancer Ther., *1*: 1025-1033, 2002.

362. Davis, T., Kennedy, C., Chiew, Y. E., Clarke, C. L., and deFazio, A. Histone deacetylase inhibitors decrease proliferation and modulate cell cycle gene expression in normal mammary epithelial cells. Clin.Cancer Res., *6*: 4334-4342, 2000.

363. Munster, P. N., Troso-Sandoval, T., Rosen, N., Rifkind, R., Marks, P. A., and Richon, V. M. The histone deacetylase inhibitor suberoylanilide hydroxamic acid induces differentiation of human breast cancer cells. Cancer Res., *61*: 8492-8497, 2001.

364. Gore, S. D. and Carducci, M. A. Modifying histones to tame cancer: clinical development of sodium phenylbutyrate and other histone deacetylase inhibitors. Expert.Opin.Investig.Drugs, *9*: 2923-2934, 2000.

365. He, L. Z., Tolentino, T., Grayson, P., Zhong, S., Warrell, R. P., Jr., Rifkind, R. A., Marks, P. A., Richon, V. M., and Pandolfi, P. P. Histone deacetylase inhibitors induce remission in transgenic models of therapy-resistant acute promyelocytic leukemia. J.Clin.Invest, *108*: 1321-1330, 2001.

366. Mattern, K. A., Humbel, B. M., Muijsers, A. O., de Jong, L., and van Driel, R. hnRNP proteins and B23 are the major proteins of the internal nuclear matrix of HeLa S3 cells. J.Cell Biochem., *62*: 275-289, 1996.

367. Nickerson, J. A., Blencowe, B. J., and Penman, S. The architectural organization of nuclear metabolism. Int.Rev.Cytol., *162A*: 67-123, 1995.

368. Nickerson, J. Experimental observations of a nuclear matrix. J.Cell Sci., *114*: 463-474, 2001.

369. He, D. C., Nickerson, J. A., and Penman, S. Core filaments of the nuclear matrix. J.Cell Biol., *110*: 569-580, 1990.

370. Nickerson, J. A., Krockmalnic, G., Wan, K. M., and Penman, S. The nuclear matrix revealed by eluting chromatin from a cross-linked nucleus. Proc.Natl.Acad.Sci.U.S.A, *94*: 4446-4450, 1997.

371. Mirkovitch, J., Mirault, M. E., and Laemmli, U. K. Organization of the higher-order chromatin loop: specific DNA attachment sites on nuclear scaffold. Cell, *39*: 223-232, 1984.

372. Berezney, R. and Coffey, D. S. Identification of a nuclear protein matrix. Biochem.Biophys.Res.Commun., *60*: 1410-1417, 1974.

373. Nakayasu, H. and Berezney, R. Nuclear matrins: identification of the major nuclear matrix proteins. Proc.Natl.Acad.Sci.U.S.A, *88*: 10312-10316, 1991.

374. Stuurman, N., Meijne, A. M., van der Pol, A. J., de Jong, L., van Driel, R., and van Renswoude, J. The nuclear matrix from cells of different origin. Evidence for a common set of matrix proteins. J.Biol.Chem., *265*: 5460-5465, 1990.

375. Mattern, K. A., van Goethem, R. E., de Jong, L., and van Driel, R. Major internal nuclear matrix proteins are common to different human cell types. J.Cell Biochem., *65*: 42-52, 1997.

376. Zeng, C., He, D., and Brinkley, B. R. Localization of NuMA protein isoforms in the nuclear matrix of mammalian cells. Cell Motil.Cytoskeleton, *29*: 167-176, 1994.

377. Holzmann, K., Korosec, T., Gerner, C., Grimm, R., and Sauermann, G. Identification of human common nuclear-matrix proteins as heterogeneous nuclear ribonucleoproteins H and H' by sequencing and mass spectrometry. Eur.J.Biochem., *244*: 479-486, 1997.

378. Fey, E. G. and Penman, S. Nuclear matrix proteins reflect cell type of origin in cultured human cells. Proc.Natl.Acad.Sci.U.S.A, *85*: 121-125, 1988.

379. Spencer, V. A., Coutts, A. S., Samuel, S. K., Murphy, L. C., and Davie, J. R. Estrogen regulates the association of intermediate filament proteins with nuclear DNA in human breast cancer cells. J.Biol.Chem., *273*: 29093-29097, 1998.

380. Rando, O. J., Zhao, K., and Crabtree, G. R. Searching for a function for nuclear actin. Trends Cell Biol., *10* : 92-97, 2000.

381. Tolstonog, G. V., Sabasch, M., and Traub, P. Cytoplasmic intermediate filaments are stably associated with nuclear matrices and potentially modulate their DNA-binding function. DNA Cell Biol., *21*: 213-239, 2002.

382. Michelotti, E. F., Michelotti, G. A., Aronsohn, A. I., and Levens, D. Heterogeneous nuclear ribonucleoprotein K is a transcription factor. Mol.Cell Biol., *16*: 2350-2360, 1996.

383. Cairns, B. R., Erdjument-Bromage, H., Tempst, P., Winston, F., and Kornberg, R. D. Two actin-related proteins are shared functional components of the chromatin-remodeling complexes RSC and SWI/SNF. Mol.Cell, *2*: 639-651, 1998.

384. Galarneau, L., Nourani, A., Boudreault, A. A., Zhang, Y., Heliot, L., Allard, S., Savard, J., Lane, W. S., Stillman, D. J., and Cote, J. Multiple links between the NuA4 histone acetyltransferase complex and epigenetic control of transcription. Mol.Cell, *5*: 927-937, 2000.

385. Kimura, H., Tao, Y., Roeder, R. G., and Cook, P. R. Quantitation of RNA polymerase II and its transcription factors in an HeLa cell: little soluble holoenzyme but significant amounts of polymerases attached to the nuclear substructure. Mol.Cell Biol, *19*: 5383-5392, 1999.

386. Gerner, C., Holzmann, K., Meissner, M., Gotzmann, J., Grimm, R., and Sauermann, G. Reassembling proteins and chaperones in human nuclear matrix protein fractions. J.Cell Biochem., *74*: 145-151, 1999.

387. Vermaak, D., Wade, P. A., Jones, P. L., Shi, Y. B., and Wolffe, A. P. Functional analysis of the SIN3-histone deacetylase RPD3-RbAp48-histone H4 connection in the Xenopus oocyte. Mol.Cell Biol, *19*: 5847-5860, 1999.

388. Nicolas, E., Morales, V., Magnaghi-Jaulin, L., Harel-Bellan, A., Richard-Foy, H., and Trouche, D. RbAp48 belongs to the histone deacetylase complex that associates with the retinoblastoma protein. J.Biol Chem., *275*: 9797-9804, 2000.

389. Coull, J. J., Romerio, F., Sun, J. M., Volker, J. L., Galvin, K. M., Davie, J. R., Shi, Y., Hansen, U., and Margolis, D. M. The human factors YY1 and LSF repress the human immunodeficiency virus type 1 long terminal repeat via recruitment of histone deacetylase 1. J.Virol., *74*: 6790-6799, 2000.

390. Zhang, Q., Vo, N., and Goodman, R. H. Histone binding protein RbAp48 interacts with a complex of CREB binding protein and phosphorylated CREB. Mol.Cell Biol, *20*: 4970-4978, 2000.

391. Yao, Y. L., Yang, W. M., and Seto, E. Regulation of transcription factor YY1 by acetylation and deacetylation. Mol.Cell Biol, *21*: 5979-5991, 2001.

392. Ahmad, A., Takami, Y., and Nakayama, T. WD repeats of the p48 subunit of chicken chromatin assembly factor-1 required for *in vitro* interaction with chicken histone deacetylase-2. J.Biol Chem., *274*: 16646-16653, 1999.

393. Reyes, J. C., Muchardt, C., and Yaniv, M. Components of the human SWI/SNF complex are enriched in active chromatin and are associated with the nuclear matrix. J.Cell Biol., *137*: 263-274, 1997.

394. Maniotis, A. J., Chen, C. S., and Ingber, D. E. Demonstration of mechanical connections between integrins, cytoskeletal filaments, and nucleoplasm that stabilize nuclear structure. Proc.Natl.Acad.Sci.U.S.A, *94*: 849-854, 1997.

395. Davie, J. R., Samuel, S. K., Spencer, V. A., Holth, L. T., Chadee, D. N., Peltier, C. P., Sun, J. M., Chen, H. Y., and Wright, J. A. Organization of chromatin in cancer cells: role of signalling pathways. Biochem.Cell Biol., *77*: 265-275, 1999.

396. Haier, J., Nasralla, M., and Nicolson, G. L. Different adhesion properties of highly and poorly metastatic HT-29 colon carcinoma cells with extracellular matrix components: role of integrin expression and cytoskeletal components. Br.J.Cancer, *80*: 1867-1874, 1999.

397. Maniotis, A. J., Bojanowski, K., and Ingber, D. E. Mechanical continuity and reversible chromosome disassembly within intact genomes removed from living cells. J.Cell Biochem., *65*: 114-130, 1997.

398. Bissell, M. J., Weaver, V. M., Lelievre, S. A., Wang, F., Petersen, O. W., and Schmeichel, K. L. Tissue structure, nuclear organization, and gene expression in normal and malignant breast. Cancer Res., *59*: 1757-1763s, 1999.

399. Hansen, R. K. and Bissell, M. J. Tissue architecture and breast cancer: the role of extracellular matrix and steroid hormones. Endocr.Relat Cancer, *7*: 95-113, 2000.

400. Pienta, K. J. and Coffey, D. S. Nuclear-cytoskeletal interactions: evidence for physical connections between the nucleus and cell periphery and their alteration by transformation. J.Cell Biochem., *49*: 357-365, 1992.

401. Fey, E. G. and Penman, S. Tumor promoters induce a specific morphological signature in the nuclear matrix-intermediate filament scaffold of Madin-Darby canine kidney (MDCK) cell colonies. Proc.Natl.Acad.Sci.U.S.A, 1984.

402. DePasquale, J. A. Rearrangement of the F-actin cytoskeleton in estradiol-treated MCF-7 breast carcinoma cells. Histochem.Cell Biol, *112*: 341-350, 1999.

403. Kronenberg, M. S. and Clark, J. H. Changes in keratin expression during the estrogen-mediated differentiation of rat vaginal epithelium. Endocrinology, *117*: 1480-1489, 1985.

404. Dworetzky, S. I., Fey, E. G., Penman, S., Lian, J. B., Stein, J. L., and Stein, G. S. Progressive changes in the protein composition of the nuclear matrix during rat osteoblast differentiation. Proc.Natl.Acad.Sci.U.S.A, *87*: 4605-4609, 1990.

405. Chen, H. Y., Sun, J. M., Hendzel, M. J., Rattner, J. B., and Davie, J. R. Changes in the nuclear matrix of chicken erythrocytes that accompany maturation. Biochem.J., *320 ( Pt 1)*: 257-265, 1996.

406. Leman, E. S., Arlotti, J. A., Dhir, R., Greenberg, N., and Getzenberg, R. H. Characterization of the nuclear matrix proteins in a transgenic mouse model for prostate cancer. J.Cell Biochem., *86*: 203-212, 2002.

407. Brunagel, G., Vietmeier, B. N., Bauer, A. J., Schoen, R. E., and Getzenberg, R. H. Identification of nuclear matrix protein alterations associated with human colon cancer. Cancer Res., *62*: 2437-2442, 2002.

408. Samuel, S. K., Minish, T. M., and Davie, J. R. Nuclear matrix proteins in well and poorly differentiated human breast cancer cell lines. J.Cell Biochem., *66*: 9-15, 1997.

409. Spencer, V. A., Samuel, S. K., and Davie, J. R. Nuclear matrix proteins associated with DNA in situ in hormone- dependent and hormone-independent human breast cancer cell lines. Cancer Res., *60*: 288-292, 2000.

410. Leman, E. S. and Getzenberg, R. H. Nuclear matrix proteins as biomarkers in prostate cancer. J.Cell Biochem., *86*: 213-223, 2002.

411. Brunagel, G., Schoen, R. E., Bauer, A. J., Vietmeier, B. N., and Getzenberg, R. H. Nuclear matrix protein alterations associated with colon cancer metastasis to the liver. Clin.Cancer Res., *8*: 3039-3045, 2002.

412. Galande, S. and Kohwi-Shigematsu, T. Linking chromatin architecture to cellular phenotype: BUR-binding proteins in cancer. J.Cell Biochem.Suppl, *Suppl 35*: 36-45, 2000.

413. Johnson, C. A., O'Neill, L. P., Mitchell, A., and Turner, B. M. Distinctive patterns of histone H4 acetylation are associated with defined sequence elements within both heterochromatic and euchromatic regions of the human genome. Nucleic Acids Res., *26*: 994-1001, 1998.

414. Mattia, E., Eufemi, M., Chichiarelli, S., Ceridono, M., and Ferraro, A. Differentiation-specific nuclear matrix proteins cross-linked to DNA by cis-diammine dichloroplatinum. Exp.Cell Res., *238*: 216-219, 1998.

415. Olinski, R., Wedrychowski, A., Schmidt, W. N., Briggs, R. C., and Hnilica, L. S. *In vivo* DNA-protein cross-linking by *cis*- and *trans*- diamminedichloroplatinum(II). Cancer Res., *47*: 201-205, 1987.

416. Ferraro, A., Grandi, P., Eufemi, M., Altieri, F., and Turano, C. Crosslinking of nuclear proteins to DNA by *cis*-diamminedichloroplatinum in intact cells. Involvement of nuclear matrix proteins. FEBS Lett., *307*: 383-385, 1992.

417. Bubley, G. J., Xu, J., Kupiec, N., Sanders, D., Foss, F., O'Brien, M., Emi, Y., Teicher, B. A., and Patierno, S. R. Effect of DNA conformation on cisplatin adduct formation. Biochem.Pharmacol., *51*: 717-721, 1996.

418. Wedrychowski, A., Bhorjee, J. S., and Briggs, R. C. *In vivo* crosslinking of nuclear proteins to DNA by *cis*- diamminedichloroplatinum (II) in differentiating rat myoblasts. Exp.Cell Res., *183*: 376-387, 1989.

419. Wedrychowski, A., Schmidt, W. N., Ward, W. S., and Hnilica, L. S. Cross-linking of cytokeratins to DNA *in vivo* by chromium salt and cis-diamminedichloroplatinum(II). Biochemistry, *25*: 1-9, 1986.

420. Ferraro, A., Eufemi, M., Cervoni, L., Altieri, F., and Turano, C. DNA-nuclear matrix interactions analyzed by crosslinking reactions in intact nuclei from liver. Acta Biochem.Polonica, *42*: 145-152, 1995.

421. Bubley, G. J., Xu, J., Kupiec, N., Sanders, D., Foss, F., O'Brien, M., Emi, Y., Teicher, B. A., and Patierno, S. R. Effect of DNA conformation on cisplatin adduct formation. Biochem.Pharmacol., *51*: 717-721, 1996.

422. Wedrychowski, A., Bhorjee, J. S., and Briggs, R. C. *In vivo* crosslinking of nuclear proteins to DNA by *cis*- diamminedichloroplatinum (II) in differentiating rat myoblasts. Exp.Cell Res., *183*: 376-387, 1989.

423. Wedrychowski, A., Schmidt, W. N., and Hnilica, L. S. The *in vivo* cross-linking of proteins and DNA by heavy metals. J.Biol.Chem., *261*: 3370-3376, 1986.

424. Olinski, R., Wedrychowski, A., Schmidt, W. N., Briggs, R. C., and Hnilica, L. S. *In vivo* DNA-protein cross-linking by *cis*- and *trans*- diamminedichloroplatinum(II). Cancer Res., *47*: 201-205, 1987.

425. Konety, B. R., Nguyen, T. S., Brenes, G., Sholder, A., Lewis, N., Bastacky, S., Potter, D. M., and Getzenberg, R. H. Clinical usefulness of the novel marker BLCA-4 for the detection of bladder cancer. J.Urol., *164*: 634-639, 2000.

426. Konety, B. R. and Getzenberg, R. H. Nuclear structural proteins as biomarkers of cancer. J.Cell Biochem., *Suppl 32-33*: 183-191, 1999.

427. Baselga, J. and Norton, L. Focus on breast cancer. Cancer Cell, *1*: 319-322, 2002.

428. Clarke, R., Dickson, R. B., and Brunner, N. The process of malignant progression in human breast cancer. Ann.Oncol., *1*: 401-407, 1990.

429. Brunner, N., Frandsen, T. L., Holst-Hansen, C., Bei, M., Thompson, E. W., Wakeling, A. E., Lippman, M. E., and Clarke, R. MCF7/LCC2: a 4-hydroxytamoxifen resistant human breast cancer variant that retains sensitivity to the steroidal antiestrogen ICI 182,780. Cancer Res., *53*: 3229-3232, 1993.

430. Brunner, N., Boulay, V., Fojo, A., Freter, C. E., Lippman, M. E., and Clarke, R. Acquisition of hormone-independent growth in MCF-7 cells is accompanied by increased expression of estrogen-regulated genes but without detectable DNA amplifications. Cancer Res., *53*: 283-290, 1993.

431. Clarke, R., Lippman, M. E., Dickson, R. B., Spang-Thompsen, M., and Brunner, N. *In vivo/ in vitro* selection of hormone independent cells from the hormone dependent MCF-7 human breast cancer cell line. *In* B. Wu and J. Zheng (eds.), Immune-deficient Animals in Experimental Medicine, pp. 190-195. Karger: Basel, 1989.

432. Thompson, E. W., Brunner, N., Torri, J., Johnson, M. D., Boulay, V., Wright, A., Lippman, M. E., Steeg, P. S., and Clarke, R. The invasive and metastatic properties of hormone-independent but hormone-responsive variants of MCF-7 human breast cancer cells. Clin.Exp.Metastasis, *11*: 15-26, 1993.

433. Inoue, T., Cavanaugh, P. G., Steck, P. A., Brunner, N., and Nicolson, G. L. Differences in transferrin response and numbers of transferrin receptors in rat and human mammary carcinoma lines of different metastatic potentials. J.Cell Physiol, *156*: 212-217, 1993.

434. Toh, Y., Pencil, S. D., and Nicolson, G. L. Analysis of the complete sequence of the novel metastasis-associated candidate gene, mta1, differentially expressed in mammary adenocarcinoma and breast cancer cell lines. Gene, *159*: 97-104, 1995.

435. Gruber, C. J., Tschugguel, W., Schneeberger, C., and Huber, J. C. Production and actions of estrogens. N.Engl.J.Med., *346*: 340-352, 2002.

436. Witkowska, H. E., Carlquist, M., Engstrom, O., Carlsson, B., Bonn, T., Gustafsson, J. A., and Shackleton, C. H. Characterization of bacterially expressed rat estrogen receptor beta ligand binding domain by mass spectrometry: structural comparison with estrogen receptor alpha. Steroids, *62*: 621-631, 1997.

437. Paech, K., Webb, P., Kuiper, G. G., Nilsson, S., Gustafsson, J., Kushner, P. J., and Scanlan, T. S. Differential ligand activation of estrogen receptors ER alpha and ERbeta at AP1 sites. Science, *277*: 1508-1510, 1997.

438. Pike, A. C., Brzozowski, A. M., and Hubbard, R. E. A structural biologist's view of the oestrogen receptor. J.Steroid Biochem.Mol.Biol, *74*: 261-268, 2000.

439. Hall, J. M., Couse, J. F., and Korach, K. S. The multifaceted mechanisms of estradiol and estrogen receptor signaling. J.Biol.Chem., *276*: 36869-36872, 2001.

440. Klinge, C. M. Estrogen receptor interaction with estrogen response elements. Nucleic Acids Res., *29*: 2905-2919, 2001.

441. Lannigan, D. A., Koszewski, N. J., and Notides, A. C. Estrogen-responsive elements contain non-B DNA. Mol.Cell Endocrinol., *94*: 47-54, 1993.

442. Anolik, J. H., Klinge, C. M., Hilf, R., and Bambara, R. A. Cooperative binding of estrogen receptor to DNA depends on spacing of binding sites, flanking sequence, and ligand. Biochemistry, *34*: 2511-2520, 1995.

443. Tora, L., Gaub, M. P., Mader, S., Dierich, A., Bellard, M., and Chambon, P. Cell-specific activity of a GGTCA half-palindromic oestrogen-responsive element in the chicken ovalbumin gene promoter. EMBO J., *7*: 3771-3778, 1988.

444. Kim, K., Thu, N., Saville, B., and Safe, S. Domains of estrogen receptor (alpha) (ER alpha) required for ER alpha /Sp1-mediated activation of GC-rich promoters by

estrogens and antiestrogens in breast cancer cells. Mol.Endocrinol., *17*: 804-817, 2003.

445. Wang, W., Dong, L., Saville, B., and Safe, S. Transcriptional activation of E2F1 gene expression by 17 beta-estradiol in MCF-7 cells is regulated by NF-Y-Sp1/estrogen receptor interactions. Mol.Endocrinol., *13*: 1373-1387, 1999.

446. Qin, C., Singh, P., and Safe, S. Transcriptional activation of insulin-like growth factor-binding protein-4 by 17 beta-estradiol in MCF-7 cells: role of estrogen receptor- Sp1 complexes. Endocrinology, *140*: 2501-2508, 1999.

447. Xie, W., Duan, R., and Safe, S. Estrogen induces adenosine deaminase gene expression in MCF-7 human breast cancer cells: role of estrogen receptor-Sp1 interactions. Endocrinology, *140*: 219-227, 1999.

448. Xie, W., Duan, R., Chen, I., Samudio, I., and Safe, S. Transcriptional activation of thymidylate synthase by 17 beta-estradiol in MCF-7 human breast cancer cells. Endocrinology, *141*: 2439-2449, 2000.

449. Gaub, M. P., Bellard, M., Scheuer, I., Chambon, P., and Sassone-Corsi, P. Activation of the ovalbumin gene by the estrogen receptor involves the fos-jun complex. Cell, *63*: 1267-1276, 1990.

450. Thim, L. Trefoil peptides: a new family of gastrointestinal molecules. Digestion, *55*: 353-360, 1994.

451. Wong, W. M., Poulsom, R., and Wright, N. A. Trefoil peptides. Gut, *44*: 890-895, 1999.

452. Jakowlew, S. B., Breathnach, R., Jeltsch, J. M., Masiakowski, P., and Chambon, P. Sequence of the pS2 mRNA induced by estrogen in the human breast cancer cell line MCF-7. Nucleic Acids Res., *12*: 2861-2878, 1984.

453. Masiakowski, P., Breathnach, R., Bloch, J., Gannon, F., Krust, A., and Chambon, P. Cloning of cDNA sequences of hormone-regulated genes from the MCF-7 human breast cancer cell line. Nucleic Acids Res., *10*: 7895-7903, 1982.

454. Brown, A. M., Jeltsch, J. M., Roberts, M., and Chambon, P. Activation of pS2 gene transcription is a primary response to estrogen in the human breast cancer cell line MCF-7. Proc.Natl.Acad.Sci.U.S.A, *81*: 6344-6348, 1984.

455. Henry, J. A., Piggott, N. H., Mallick, U. K., Nicholson, S., Farndon, J. R., Westley, B. R., and May, F. E. pNR-2/pS2 immunohistochemical staining in breast cancer: correlation with prognostic factors and endocrine response. Br.J.Cancer, *63*: 615-622, 1991.

456. Martin, V., Ribieras, S., Song-Wang, X. G., Lasne, Y., Frappart, L., Rio, M. C., and Dante, R. Involvement of DNA methylation in the control of the expression of an estrogen-induced breast-cancer-associated protein (pS2) in human breast cancers. J.Cell Biochem., *65*: 95-106, 1997.

457. Schwartz, L. H., Koerner, F. C., Edgerton, S. M., Sawicka, J. M., Rio, M. C., Bellocq, J. P., Chambon, P., and Thor, A. D. pS2 expression and response to

hormonal therapy in patients with advanced breast cancer. Cancer Res., *51*: 624-628, 1991.

458. Dante, R., Ribieras, S., Baldassini, S., Martin, V., Benzerara, O., Bouteille, C., Bremond, A., Frappart, L., Rio, M. C., and Lasne, Y. Expression of an estrogen-induced breast cancer-associated protein (pS2) in benign and malignant human ovarian cysts. Lab Invest, *71*: 188-192, 1994.

459. Rio, M. C., Bellocq, J. P., Daniel, J. Y., Tomasetto, C., Lathe, R., Chenard, M. P., Batzenschlager, A., and Chambon, P. Breast cancer-associated pS2 protein: synthesis and secretion by normal stomach mucosa. Science, *241*: 705-708, 1988.

460. Welter, C., Theisinger, B., Seitz, G., Tomasetto, C., Rio, M. C., Chambon, P., and Blin, N. Association of the human spasmolytic polypeptide and an estrogen- induced breast cancer protein (pS2) with human pancreatic carcinoma. Lab Invest, *66*: 187-192, 1992.

461. Nunez, A. M., Berry, M., Imler, J. L., and Chambon, P. The 5' flanking region of the pS2 gene contains a complex enhancer region responsive to o estrogens, epidermal growth factor, a tumour promoter (TPA), the c-Ha-*ras* oncoprotein and the c-*jun* protein. EMBO J., *8*: 823-829, 1989.

462. Berry, M., Nunez, A. M., and Chambon, P. Estrogen-responsive element of the human pS2 gene is an imperfectly palindromic sequence. Proc.Natl.Acad.Sci.U.S.A, *86*: 1218-1222, 1989.

463. Lefebvre, O., Chenard, M. P., Masson, R., Linares, J., Dierich, A., LeMeur, M., Wendling, C., Tomasetto, C., Chambon, P., and Rio, M. C. Gastric mucosa abnormalities and tumorigenesis in mice lacking the pS2 trefoil protein. Science, *274*: 259-262, 1996.

464. Sewack, G. F. and Hansen, U. Nucleosome positioning and transcription-associated chromatin alterations on the human estrogen-responsive pS2 promoter. J.Biol Chem., *272*: 31118-31129, 1997.

465. Williams, A. F. The nature of immature avian erythrocytes in severe anaemia induced by phenylhydrazine. J.Cell Sci., *11*: 771-776, 1972.

466. Ferenz, C. R. and Nelson, D. A. N-Butyrate incubation of immature chicken erythrocytes preferentially enhances the solubility of beta A chromatin. Nucleic Acids Res., *13*: 1977-1995, 1985.

467. Burch, J. B. and Weintraub, H. Temporal order of chromatin structural changes associated with activation of the major chicken vitellogenin gene. Cell, *33*: 65-76, 1983.

468. Dolan, M., Dodgson, J. B., and Engel, J. D. Analysis of the adult chicken beta-globin gene. Nucleotide sequence of the locus, microheterogeneity at the 5'-end of beta-globin mRNA, and aberrant nuclear RNA species. J.Biol.Chem., *258*: 3983-3990, 1983.

469. Davie, J. R. Two-dimensional gel systems for rapid histone analysis for use in minislab polyacrylamide gel electrophoresis. Anal.Biochem., *120*: 276-281, 1982.

470. Delcuve, G. P. and Davie, J. R. Western blotting and immunochemical detection of histones electrophoretically resolved on acid-urea-triton- and sodium dodecyl sulfate-polyacrylamide gels. Anal.Biochem., *200*: 339-341, 1992.

471. Burton, K. A study of the conditions and mechanism of the diphenylamine reaction for the colorimetric estimation of deoxyribonucleic acid. Biochem.J., *62*: 315-323, 1956.

472. Ferenz, C. R. and Nelson, D. A. N-Butyrate incubation of immature chicken erythrocytes preferentially enhances the solubility of beta A chromatin. Nucleic Acids Res., *13*: 1977-1995, 1985.

473. Wang, X., He, C., Moore, S. C., and Ausio, J. Effects of histone acetylation on the solubility and folding of the chromatin fiber. J.Biol.Chem., *276*: 12764-12768, 2001.

474. Clayton, A. L., Rose, S., Barratt, M. J., and Mahadevan, L. C. Phosphoacetylation of histone H3 on c-*fos*- and c-*jun*-associated nucleosomes upon gene activation. EMBO J., *19*: 3714-3726, 2000.

475. Weaver, C. A., Springer, P. A., and Katzenellenbogen, B. S. Regulation of pS2 gene expression by affinity labeling and reversibly binding estrogens and antiestrogens: comparison of effects on the native gene and on pS2-chloramphenicol acetyltransferase fusion genes transfected into MCF-7 human breast cancer cells. Mol.Endocrinol., *2*: 936-945, 1988.

476. Mishra, S. K., Mandal, M., Mazumdar, A., and Kumar, R. Dynamic chromatin remodeling on the HER2 promoter in human breast cancer cells. FEBS Lett., *507*: 88-94, 2001.

477. He, G. and Margolis, D. M. Counterregulation of chromatin deacetylation and histone deacetylase occupancy at the integrated promoter of human immunodeficiency virus type 1 (HIV-1) by the HIV-1 repressor YY1 and HIV-1 activator Tat. Mol.Cell Biol., *22*: 2965-2973, 2002.

478. Ghoshal, K., Datta, J., Majumder, S., Bai, S., Dong, X., Parthun, M., and Jacob, S. T. Inhibitors of histone deacetylase and DNA methyltransferase synergistically activate the methylated metallothionein I promoter by activating the transcription factor MTF-1 and forming an open chromatin structure. Mol.Cell Biol., *22*: 8302-8319, 2002.

479. Mariadason, J. M., Corner, G. A., and Augenlicht, L. H. Genetic reprogramming in pathways of colonic cell maturation induced by short chain fatty acids: comparison with trichostatin A, sulindac, and curcumin and implications for chemoprevention of colon cancer. Cancer Res., *60*: 4561-4572, 2000.

480. Ruh, M. F., Tian, S., Cox, L. K., and Ruh, T. S. The effects of histone acetylation on estrogen responsiveness in MCF-7 cells. Endocrine., *11*: 157-164, 1999.

481. Emenaker, N. J., Calaf, G. M., Cox, D., Basson, M. D., and Qureshi, N. Short-chain fatty acids inhibit invasive human colon cancer by modulating uPA, TIMP-1, TIMP-

2, mutant p53, Bcl-2, Bax, p21 and PCNA protein expression in an *in vitro* cell culture model. J.Nutr., *131* : 3041S-3046S, 2001.

482. Barkhem, T., Haldosen, L. A., Gustafsson, J. A., and Nilsson, S. Transcriptional synergism on the pS2 gene promoter between a p160 coactivator and estrogen receptor-alpha depends on the coactivator subtype, the type of estrogen response element, and the promoter context. Mol.Endocrinol., *16*: 2571-2581, 2002.

483. Barkhem, T., Haldosen, L. A., Gustafsson, J. A., and Nilsson, S. pS2 Gene expression in HepG2 cells: complex regulation through crosstalk between the estrogen receptor alpha, an estrogen-responsive element, and the activator protein 1 response element. Mol.Pharmacol., *61*: 1273-1283, 2002.

484. Chinery, R., Poulsom, R., and Cox, H. M. The gene encoding mouse intestinal trefoil factor: structural organization, partial sequence analysis and mapping to murine chromosome 17q. Gene, *171*: 249-253, 1996.

485. Abdelrahim, M., Samudio, I., Smith, R., III, Burghardt, R., and Safe, S. Small inhibitory RNA duplexes for Sp1 mRNA block basal and estrogen- induced gene expression and cell cycle progression in MCF-7 breast cancer cells. J.Biol.Chem., *277*: 28815-28822, 2002.

486. Xiao, H., Hasegawa, T., and Isobe, K. p300 collaborates with Sp1 and Sp3 in p21(waf1/cip1) promoter activation induced by histone deacetylase inhibitor. J.Biol.Chem., *275*: 1371-1376, 2000.

487. Porter, W., Saville, B., Hoivik, D., and Safe, S. Functional synergy between the transcription factor Sp1 and the estrogen receptor. Mol.Endocrinol., *11*: 1569-1580, 1997.

488. Kato, S., Endoh, H., Masuhiro, Y., Kitamoto, T., Uchiyama, S., Sasaki, H., Masushige, S., Gotoh, Y., Nishida, E., Kawashima, H., Metzger, D. and Chambon, P. Activation of the estrogen receptor through phosphorylation by mitogen- activated protein kinase. Science, *270*: 1491-1494, 1995.

489. Jackson, S. P., MacDonald, J. J., Lees-Miller, S., and Tjian, R. GC box binding induces phosphorylation of Sp1 by a DNA-dependent protein kinase. Cell, *63*: 155-165, 1990.

490. Font, d. M. and Brown, M. AIB1 is a conduit for kinase-mediated growth factor signaling to the estrogen receptor. Mol.Cell Biol, *20*: 5041-5047, 2000.

491. Smith, C. L., Onate, S. A., Tsai, M. J., and O'Malley, B. W. CREB binding protein acts synergistically with steroid receptor coactivator-1 to enhance steroid receptor-dependent transcription. Proc.Natl.Acad.Sci.U.S.A, *93*: 8884-8888, 1996.

492. Rowan, B. G., Weigel, N. L., and O'Malley, B. W. Phosphorylation of steroid receptor coactivator-1. Identification of the phosphorylation sites and phosphorylation through the mitogen- activated protein kinase pathway. J.Biol Chem., *275*: 4475-4483, 2000.

493. Kim, M. Y., Hsiao, S. J., and Kraus, W. L. A role for coactivators and histone acetylation in estrogen receptor alpha-mediated transcription initiation. EMBO J., *20*: 6084-6094, 2001.

494. Yankulov, K., Yamashita, K., Roy, R., Egly, J. M., and Bentley, D. L. The transcriptional elongation inhibitor 5,6-dichloro-1-beta-D-ribofuranosylbenzimidazole inhibits transcription factor IIH-associated protein kinase. J.Biol.Chem., *270*: 23922-23925, 1995.

495. Marshall, N. F., Peng, J., Xie, Z., and Price, D. H. Control of RNA polymerase II elongation potential by a novel carboxyl- terminal domain kinase. J.Biol.Chem., *271*: 27176-27183, 1996.

496. Trembley, J. H., Hu, D., Slaughter, C. A., Lahti, J. M., and Kidd, V. J. Casein kinase 2 interacts with cyclin-dependent kinase 11 (CDK11) *in vivo* and phosphorylates both the RNA polymerase II carboxyl-terminal domain and CDK11 *in vitro*. J.Biol Chem., *278*: 2265-2270, 2003.

497. Simmen, R. C., Means, A. R., and Clark, J. H. Estrogen modulation of nuclear matrix-associated steroid hormone binding. Endocrinology, *115*: 1197-1202, 1984.

498. O'Farrell, P. H. High resolution two-dimensional electrophoresis of proteins. J.Biol.Chem., *250*: 4007-4021, 1975.

499. Spencer, V. A., Coutts, A. S., Samuel, S. K., Murphy, L. C., and Davie, J. R. Estrogen regulates the association of intermediate filament proteins with nuclear DNA in human breast cancer cells. J.Biol.Chem., *273*: 29093-29097, 1998.

500. Davie, J. R., Samuel, S., Spencer, V., Bajno, L., Sun, J.-M., Chen, H. Y., and Holth, L. T. Nuclear matrix:application to diagnosis of cancer and role in transcription and modulation of chromatin structure. GeneTher.Mol.Biol, *1*: 509-528, 1998.

501. Hughes, J. H. and Cohen, M. B. Nuclear matrix proteins and their potential applications to diagnostic pathology. Am.J.Clin.Pathol., *111*: 267-274, 1999.

502. Wilson, K. L. The nuclear envelope, muscular dystrophy and gene expression. Trends Cell Biol, *10*: 125-129, 2000.

503. Chan, J. K., Park, P. C., and De Boni, U. Association of DNAse sensitive chromatin domains with the nuclear periphery in 3T3 cells *in vitro*. Biochem.Cell Biol, *78*: 67-78, 2000.

504. Reid, G., Hubner, M.R., Metivier, R., Brand, H., Denger, S., Manu, D., Beaudouin, J., Ellenberg, J., and Gannon, F. Cyclic, proteasome-mediated turnover of unliganded and liganded ERα on responsive promoters is an integral feature of estrogen signaling. Cell, *11*: 695-707, 2003.

505. Cowley, S.M., Hoare, S., Mosselman, S., Parkers, M.G. Estrogen receptors α and β form heterodimers on DNA. J. Cell. Biol., *272*: 19858-19862, 1997.

506. Boisvert FM, Kruhlak MJ, Box AK, Hendzel MJ, and Bazett-Jones DP. The transcription coactivator CBP is a dynamic component of the promyelocytic leukemia nuclear body. J. Cell Biol., *152*: 1099-1106, 2001.

507. Kim, D.H., Kim, M. and Kwon, H.J. Histone deacetylase in carcinogenesis and its inhibitors as anti-cancer agents. J. Biochem. Mol. Biol., *36*:110-119, 2003.

508. Rosato, R.R. and Grant, S. Histone deacetylase inhibitors in cancer therapy. Cancer Biol. Ther., *2*:30-37, 2003.

509. Kouraklis, G. and Theocharis, S. Histone deacetylase inhibitors and anticancer therapy. Curr. Med. Chem.- Anti-Cancer Agents, *2*:477-484, 2002.

510. Vorherr, H. Breast cancer: epidemiology, endocrinology, biochemistry, and pathology. Baltimore: Urban & Schwarzenberg, 1980.

511. Arafah, B.M. and Pearson, O.H. Endocrine treatment of advanced breast cancer. *In*: V.C. Jordan (ed.), Estrogen/antiestrogen action and human breast cancer therapy, pp. 417-429. Wisconsin: University of Wisconsin Press, 1986.

512. Leonessa, F., Boulay, V., Wright, A., Thompson, E.W., Brunner, N., and Clarke, R. The biology of breast tumor progression. Acquisition of hormone independence and resistance to cytotxic drugs. Acta Oncol., *31*:115-123, 1992.

513. Ruiz Cabello, J., Berghmans, K., Kaplan, O., Lippman, M.E., Clarke, R., and Cohen, J.S. Hormone dependence of breast cancer cells and the effects of tamoxifen and estrogen: 31P NMR. Breast Cancer Res. Treat., *33*:209-217, 1995.

514. Clarke, G.M., and McGuire, W.L. Steroid receptors and other prognostic factors in primary breast cancer. Semin. Oncol., *15*:20-25, 1988.

515. Replogle-Schwab, T.S., and Pienta, K.J. Role of the nuclear matrix in breast cancer. *In*: R. Dickson and M. Lippman (eds.), Mammary tumor cell cycle, differentiation, and metastasis, pp. 127-140. Boston: Kluwer Academic Publishers, 1996.

516. Misteli, T. and Spector, D.L. The cellular organization of gene expression. Curr. Opin. Cell Biol., *10*:323-331, 1998.

517. Schul, W, de Jong, L. and van Driel, R. Nuclear neighbors: the spatial and functional organization of genes and nuclear domains. J. Cell Ciochem., *70*:159-171, 1998.

518. Chen, H.Y., Sun, J.M., Hendzel, M.J., Rattner, J.B., and Davie, J.R. Changes in the nuclear matrix of chicken erythrocytes that accompany maturation. Biochem. J., *320*:257-266, 1998.

519. Nickerson, J. A. Nuclear dreams: the malignant alteration of nuclear architecture. J. Cell Biochem., *70*:172-180, 1998.

520. Khanuja, P.S., Lehr, J.E., Soule, H.D., Gehani, S.K., Noto, A.C., Choudhury, S., Chen, R., and Pienta, K.J. Nuclear matrix proteins in normal breast cancer cells. Cancer Res., *53*:3394-3398, 1993.

521. Keesee, S.K., Meneghini, M.D., Szaro, R.P., and Wu, Y.J. Nuclear matrix proteins in human colon cancer. Proc. Natl. Acad. Sci. USA, *91*:1913-1916, 1994.

522. Keesee, S.K., Marchese, J., Meneses, A., Potz, D., Garcia-Cuellar, C., Szaro, R.P., Solorza, G., Osornio-Vargas, A., Mohar, A., de la Garza, J.G., and Wu, Y.J. Human cervical cancer-associated nuclear matrix proteins. Exp. Cell Res., *244*:14-25, 1998.